Investigation of the role of TDP-43 in amyotrophic lateral sclerosis (ALS) using patient derived fibroblasts and zebrafish as models.

by

Dr Channa Adithya Ashubodha Hewamadduma

Submitted for the degree of Doctor of Philosophy (PhD)

Sheffield Institute for Translational Neuroscience
University of Sheffield
September 2014

Supervisors:

Professor Dame Pamela J Shaw

Dr Andrew J Grierson

Dr Tennore Ramesh

Dedication

I dedicate my PhD thesis to my parents, Dharma and Indira, for their selflessness,

togetherness and love, shared and extended unconditionally, throughout the years.

Acknowledgements

A thought

"The important thing is not to stop thinking.
Curiosity has its own reason for existing"

Albert Einstein

Table of contents

Table of figures

17

Table of tables

Abbreviations

%	Percent
$\Delta\Delta CT$	Delta-Delta CT
ΔCT	Delta CT
°C	Degrees Celsius
PBS	Phosphate buffered saline
AD	Alzheimer's Disease
ALS	Amyotrophic Lateral Sclerosis
AMO	Anti-sense Morpholino Oligonucleotides
AMO p53 ^{ATG} /AMOp53	AMO against p53
AMO tardbp^{ATG}	AMO against ATG site of *tardbp*
AMO tardbpl^{ATG}	AMO against ATG site of *tardbpl*
AMO *tardbp^{SpI}*	AMO against splice site I of tardbp gene
AMO *tardbp^{SpII}*	AMO against splice site II of *tardbp gene*
AMO TDPSI	AMO against splice site I of tardbp gene
AMO TDPSII	AMO against splice site II of tardbp gene
AMO-control (CoMo)	AMO scrambled
AMPA receptor	Alpha amino 3 hydroxy 5 methyl 4 isoxazolepropionic acid receptor
ANG	Angiogenin
ANOVA	Analysis of variance
APO II	apolipo protein II
APOA2	apolipo protein II A2 encoding gene
APP	Amyloid precursor protein
APS	Ammonium Persulphate
ARP1	Actin-Related Protein 1
ARF6	ADP-Ribosylation Factor 6
Ars	arsenite
ATG	Translation start site ATG
ATP	Adenosine Triphosphate
ATXN2	Ataxin 2
BAC	Bacterial artificial chromosome
BACE	beta-site APP cleaving enzyme 1
BCA	bicinchoninic acid (protein assay)
BLAST	Basic Local Alignment Search Tool
BN2	temperature-sensitive mutant (ts BN2) of baby hamster kidney cells (BHK21)
bp	base pairs
BSA	Bovine Serum Albumin
C9orf72	Chromosome 9 Open Reading Frame 72
Ca2+	Calcium
CDK6	Cell division protein kinase 6
cDNA	complementary DNA
CFTR	Cystic Fibrosis Trans-membrane Conductance Regulator
ChAT	Choline acetyl transferase
$CHCl_3$	Chloroform
CHMP2B	Chromatin Modifying Protein 2B
CMV	Cytomegalovirus
CNS	Central Nervous System
CoMo	AMO-control (CoMo)
CT/Ct	Threshold cycle

C-terminal	Carboxyl terminal
CTF	C-terminal fragment
Cyclohex.	Cycloheximide
DAB	3,3'-Diaminobenzidine
DAO	D-Amino-acid Oxidase
DAPI	4',6-diamidino-2-phenylindole
DCP1	Decapping Protein 1
DCTN1	Dynactin
DEPC	Diethylpyrocarbonate
dH_2O	Distilled water
DJ1	protein encoded by *PARK7* gene
DMEM	Dulbecco's Modified Eagles Medium
DMSO	Dimethyl Sulfoxide
DN	Dystrophic Neurites
DNA	Deoxyribonucleic Acid
dpf	Days post fertilisation
DsRed	Red fluorescent protein
E3	Zebrafish growth medium
EAAT2	Excitatory Amino Acid Transporter 2
EDTA	Ethylenediaminetetraacetic acid
elF4∝	Elongation factor 4 alpha
ELP3	Elongation Protein 3 Homolog (S. cerevisiae)
EMSA	Electrophoretic Mobility Shift Assay
ENU	N-ethyl-N-nitrosourea
ER	Endoplasmic Reticulum
ERBB4	v-erb-b2 Avian Erythroblastic Leukemia Viral Oncogene Homolog 4
ERK	extracellular signal-regulated kinase
ESE	Exon Splicing Enhancer Sequence
EZ-ECL	Chemiluminescence detection kit for HRP
F1 F2 F5 F6	Founder generation of zebrafish 1-6
F10	Ham's F-10 Nutrient Mixture for cell culture
fALS	familial ALS
FCCP	Trifluorcarbonylcyanide Phenylhydrazone
FCS	Fetal Calf Serum
FHCRC	Fred Hutchinson Cancer Research Center
FIG4	FIG4 homolog, SAC1 lipid phosphatase domain containing (S. cerevisiae)
FMRP	Fragile X Mental Retardation Protein
FTLD	Fronto temporal lobe dementia
FTLD-U	Fronto temporal lobe dementia with ubiquitinated inclusion
FUS	Fused in Sarcoma
FUS1	Fused in sarcoma 1
g	gram
G1 phase	Growth-1 phase
G3BP	Ras-GAP SH3 domain binding protein
GABA	Gamma amino butyric acid
GAL4/UAS	GAL4- yeast transcription activator protein GAL4, UAS-Upstream Activation Sequence
GCI	Glial Cytoplasmic Inclusions
GEM Body	Gemini of Cajal body
GFP	Green Fluorescent protein
Glu	Glutamate
GRD	Glycine Rich Domain

GRR	Glycine Rich Region
GST	Glutathione S-transferase
GTP	Guanosine triphosphate
h	hour(s)
h.TDP-43 Ab1	human anti TDP-43 antibody 1
h.TDP-43 Ab2	human anti TDP-43 antibody 2
H_2O_2	Hydrogen Peroxide
HAP	hnRNP A1 interacting protein
HB9	Homeobox protein 9
HCl	Hydrochloric Acid
HDAC	Histone Deacetylase
HEK293T	Human embryonic kidney cells line 293T
HeLa	Henrietta Lacks immortal cancer cell line
HEPES	4-(2-hydroxyethyl)-1-piperazineethanesulfonic acid
HET	Heterozygous
HIV1	Human Immunodeficiency 1 Virus
hNFL	human neuro filament
hnRNP	Heterogeneous Nuclear Ribonucleoproteins
HOM	Homozgous
HOM_{CT}	Homozgous thermal cycle
hpf	hours post fertilisation
HRP	Horseradish peroxidase
HRP1	yeat hnRNP like protein 1
HSF1	Heat Shock Factor 1
hsp	Heat Shock Proteins
Htt	huntingtin protein
HuR	Hu antigen R
IBM	inclusion body myositis
IBMPFD	inclusion body myositis, Paget's disease, and fronto temporal dementia
IGHMBP2	Immunoglobulin Mu binding Protein 2
iPSC	induced pluripotent stem cells
JNK	c-Jun N-terminal kinases
KCl	Postassium Chloride
kDa	kilo Dalton
KH_2PO_4	Monopotassium dihydrogen phosphate
LB	Luria-Bertani
LMN	Lower Motor Neuron
LMNB1	Lamin B1
LRRK2	Leucine-rich repeat kinase 2
M	Molar
mA	mili Ampere
mAb	mouse antibody
MAP	Microtubule associated protein
MATR3	Matrin 3
mg	miligram(s)
MG132	carbobenzoxy-Leu-Leu-leucinal is a peptide aldehyde
Mg^{2+}	Magnesium
min	minute(s)
miRNA	micro Ribonucleic Acid
ml	mililitre(s)
mM	millimolar(s)

MND	Motor Neuron Disease
mPrP	mouse prion protein
mRNA	messenger RNA
ms	millisecond(s)
mSOD1	Mutant Superoxide Dismutase 1
mTDP-43	mouse TDP-43
mur-Thy1	mouse Thy1 promoter
MVB	multi-vesicular body
N- terminal	Amino terminal
N+Cy	Nuclear + cytoplasmic (staining)
Na_2HPO_4	Disodium hydrogen phosphate
NaCl	Sodium Chloride
NCI	Neuro-Cytoplasmic Inclusions
NEFH	neurofilament heavy polypeptide
NES	Nuclear Export Signal
NFkB	Nuclear Factor Kappa B
NFL	Neurofilament light chain
ng	Nanogram(s)
NGS	Normal Goat Serum
NHS	National Health Service
NII	Neuronal Intra-nuclear Inclusions
nl	nanolitres
NLS	Nuclear Localisation Signal
nm	nanometre
NMJ	Neuromuscular junction
nmol	nanomoles
NO	Nitrous Oxide
NONO	non-POU domain contain- ing, octamer-binding
NRES	National Research Ethics Service
nSB	Nuclear Stress Body
NSC34	Neuroblastoma spinal cord (NSC) hybrid cell line 34
NSFL1C	N-ethylmaleimide-sensitive factor (NSF)L1C encoding gene
NSR1	yeast nuclear localization sequence-binding protein
OPTN	Optineurin
PAPB1	poly(A)-binding protein
PARK2	Parkin gene (RBR E3 ubiquitin protein ligase)
PARP1	Poly ADP Ribose Polymerase-1
PBDT	PBS+DMSO+ 0.1% Tween20
PSP	Progressive bulbar palsy
PBS	Phosphate buffered saline
PBST	Phosphate buffered saline+tween
PBT	PBS+1% Triton X 100
PCR	Polymerase Chain Reaction
PFA	Paraformaldehyde
PFN1	Profilin 1
pTDP-43	phosphorylated-TDP-43
PINK1	PTEN induced putative kinase
PLS	Primary lateral sclerosis
PMA	Progressive muscular atrophy
PML	Promyelocytic Leukemia (PML) Nuclear Bodies
PMSF	phenylmethylsulfonyl fluoride

POD	Promyeloctic leukaemia body
pRb	Retinoblastoma Protein
PrP	Prion Protein
PRPH	Peripherin
PSF	splicing factor proline/ glutamine-rich (SFPQ)
pTDP-43	phospho-TDP-43
PTU	1-Phenyl 2-Thiourea
Ran-GTP	GTP-binding nuclear protein Ran
RBM14	RNA binding motif protein 14
RBP	RNA binding proteins
RCC1	Regulator of Chromosome Condensation 1
REEP1	Receptor expression enhancing protein 1
RIPA	Radioimmunoprecipitation assay buffer
RNA	Ribonucleic Acid
RNP	Ribonucleoprotein
rpm	Revolutions per Minute
RRM	RNA Recognition Motif
RRM1	RNA Recognition Motif 1
RRM2	RNA Recognition Motif 2
rRNA	ribosomal Ribonucleic Acid
RT-PCR	Real time, polymerase chain reaction
RT-qPCR	Real time, quantitative polymerase chain reaction
S phase	Synthesis phase
Saf-B	Scaffold attachment factor B
sALS	Sporadic ALS
SC35	Splicing factor 35
SDS	Sodium Dodecyl Sulphate
SDS20	Sodium Dodecyl Sulfate (SDS), 20%
SETDB1	Encodes Histone-lysine N-methyltransferase
SETX	Senataxin
SG	Stress granules
SHSY-5Y	A neuroblast-like subclone of SK-N-SH
SIGMAR1	Sigma Non-Opioid Intracellular Receptor 1
SILAC	multiplex stable isoptope labeling with amino acids in culture
siRNA	Small interfering RNA
SL	Standard Length
SMA	Spinal Muscular Atrophy
SMARD1	Spinal muscular atrophy with respiratory distress type 1
SMI31	Neurofilaments, Phosphorylated antibody
SMI32	Neurofilaments, Phosphorylated antibody
SMN	Survival of Motor Neurons gene
snRNPs	small nuclear ribonucleoproteins
SOD1	Superoxide Dismutase 1
SP10	sperm intra-acrosomal protein 10
SPAST	Spastin
SPG11	Spastic Paraplegia 11
SQSTM1	Sequestosome 1
SUMO	Small Ubiquitin-like Modifier
SUMO-2	Small Ubiquitin-like Modifier 2
SUMO-3	Small Ubiquitin-like Modifier 3
SV2	synaptic vesicle protein 2
TAF15	Encodes TATA-binding protein-associated factor 2N

TARDBP	Encodes Transactive response-DNA binding protein
tardbp$^{+/+}$	wild type *tardbp* alleles
tardbp$^{fh301/+}$	heterozygous Y220X mutant allele
tardbp$^{fh301/fh301}$	homozygous for Y220X mutation
tardbpl	tardbp-like
tardbpl-FL	tardbp-like: full length
TB	TDP Bodies
TBP	TATA box binding protein
TBPH	Drosophila orthologue of TDP-43
TDP	Trans active DNA binding protein
TDP-43	Trans active DNA binding protein 43
TDPS1	AMO against splice site I of tardbp gene
TDPS2	AMO against splice site II of tardbp gene
TEMED	Tetramethylethylenediamine
Thaps.	Thapsigargin
Thy-1	thy1 promoter
TIA	T Cell Induced Antigen
TIA-1	T Cell Induced Antigen 1
TIAR	TIA-1 related protein
TIFF	Tagged Image File Format
TILLING	Targeting induced local lesions in the genome
TLS1	Translocated in Liposarcoma 1
TNFα	Tumour Necrosis Factor Alpha
tRNA	transfer Ribonucleic Acid
TUNEL	Terminal deoxynucleotidyl transferase dUTP nick end labeling
U2OS	human osteosarcoma cell line expressing wild type p53 and Rb
UBAD	Ubiquilin association domain
UBQLN	Ubiquilin
UBQLN2	Ubiquilin 2
UGn	(Uracil, Guanine) multiple repeats (n)
UK	United Kingdom
UMN	Upper Motor Neuron
UN	Uninjected
UNC13A	UNC-13 Homolog A (C. elegans)
UNSTR	Unstressed control fibroblasts
UPP	Ubiquitin Proteasomal Pathway
UPS	Ubiquitin Proteasome System
USA	United States of America
UTR	Untranslated Region
V	Volts
v/v	Volume to volume ratio
VAPB	Vesicle-Associated Membrane Protein-Associated Protein B
VCP	Valosin-containing Protein
VEGF	Vascular Endothelial Growth Factor
w/v	Weight by volume
WGS	Whole Genome Sequencing
WT	Wild Type
WT-HOM	Wild Type Homozygous
wtTDP-43	wild type TDP-43
X63	63 times objective lens
XRN2	5'-3' Exoribonuclease 2

YH2AX	assay for detecting DNA double strand breaks
ZHX1	Zinc Fingers and Homeoboxes 1
ZIRC	Zebrafish International Resource Center
ZnP1	anti-synaptotagmin 2 antibody
μg	microgram(s)
μl	microlitre(s)

Chapter 01: Introduction

1.0 Background

1.1 History

Motor neuron disease (MND) or Lou Gehrig's disease as it is known in the USA, is a devastating and relentlessly progressive group of neurodegenerative conditions, which are incurable and usually result in death about 2-5 years after the onset of symptoms (Shaw and Eggett, 2000, Strong and Rosenfeld, 2003, Chio et al., 2008). MND is the commonest degenerative condition of the motor neurons and one of the three most common neurodegenerative conditions (Talbot, 2002, Shaw, 2005). J.M Charcot and Joffroy in 1869 coined the term Amyotrophic Lateral Sclerosis (ALS) (Charcot JM, 1869). About 20 years prior to Charcot another French doctor named Aran described seven families with 'Progressive muscular atrophy' of which one family had had an extensive family history. Charcot ignored the extensive family history and incorrectly claimed that ALS was never inherited (Charcot JM, 1869). Although this statement was widely believed until recently, with the spate of descriptions of familial forms of ALS and mutations in various genes associated with ALS, it is well established that there is an inherited form of ALS (Shaw et al., 2007) (Shaw, 2005).

1.2 Epidemiology

Although the terms MND and ALS are used interchangeably, in the UK the broad group of MND is further classified into amyotrophic lateral sclerosis (ALS), progressive muscular atrophy (PMA), progressive bulbar palsy and primary lateral sclerosis (PLS). Approximately 90-95% of ALS cases are sporadic in nature (Sporadic ALS- sALS), whereas 0.8 to 13.5% of ALS cases have a family history of ALS, familial ALS (fALS). Incidence rates for MND are similar throughout the world at 0.86-2.5 per 100,000 per year (Brooks, 1996, Traynor et al., 1999, Beghi et al., 2006, Bonvicini et al., 2008), except in certain high incidence foci such as the Western Pacific island of Guam, two villages in the Kii peninsula of Japan and the Irian Jaya of Western New Guinea, where an interesting interaction of environmental, dietary and genetic causes result in a 50-100 fold increased

incidence of MND (Reed and Brody, 1975, Roman, 1996, Kuzuhara, 2007). The prevalence rate of MND at any given date is estimated to be around 6-8 per 100,000. Men are significantly more likely to have a younger age of onset of symptoms compare to women, especially when the symptom onset is before 45 years of age. On average the male to female ratio in ALS cases is 1.4:1. The incidence of ALS increases with age. Only about 5% of ALS cases have an age of onset below the age of 30 and 10% below 40 years, the mean age of onset is about 50-60 years (Nelson, 1995, Brooks, 1996, Ascherio, 2005, Logroscino et al., 2008). Apart from MND in the Guam population there is no clear convincing evidence to support an exogenous environmental risk factor as causative in sALS. Because of the reports of an increased incidence of ALS in professional sportsmen and sports women, it is hypothesised that excessive physical activity is a risk factor for ALS, although the evidence for this is inconclusive and requires properly constructed large-scale epidemiological studies (Longstreth et al., 1991, Ascherio, 2005). In fALS and some sALS cases the association of genetic defects in several pathogenic genes has been described. Therefore, to date the, most widely accepted hypothesis of the aetio pathogenesis of ALS is a genetic-environmental interaction (Majoor-Krakauer et al., 2003, Beleza-Meireles and Al-Chalabi, 2009, Harwood et al., 2009).

1.3 Diagnosis

The diagnosis of MND is based largely on clinical and to some extent on neurophysiological evidence of both upper and lower motor neuron signs. In the US, MND and ALS are used interchangeably but in the El Escorial criteria, first described in 1994, ALS, Primary Lateral Sclerosis (PLS), Progressive Muscular Atrophy (PMA) and Progressive Bulbar Palsy (PBP) are grouped as "suspected ALS". The El Escorial criteria have created uniformity in the diagnosis of MND, especially for the recruitment of cases for research, to monitor disease progression and to assess the therapeutic benefit of pharmacological interventions. MND is categorised into possible, probable and definite MND according to the El Escorial criteria. Although these criteria have flaws they are helpful in highlighting the level of certainty of the diagnosis (Brooks, 1994, Brooks et al., 2000).

1.4 Clinical features

1.4.1 Subtypes

1.4.1.1 Amyotrophic lateral sclerosis (ALS)

ALS is clinically defined by the presence of both upper and lower motor neuron signs and symptoms, which cannot be explained by any other cause. Lower motor neuron signs (LMN) are muscle weakness and wasting, fasciculation of muscles, and diminished or absent reflexes. The upper motor neuron (UMN) signs are characterised by increased tone, spasticity, brisk reflexes, positive jaw jerk, Hoffman sign, extensor plantar reflexes (Babinski sign) and emotional lability (Rowland, 1993).

1.4.1.2 Progressive muscular atrophy (PMA)

As the name denotes, patients with PMA demonstrate signs of lower motor neuron degeneration such as progressive weakness and wasting of the muscles and visible muscle fasciculations. There is a lack of upper motor neuron signs. However in postmortem studies of patients with a clinical diagnosis of PMA, evidence of corticospinal tract involvement has been documented in a proportion of cases (Ince et al., 2003). Pure PMA is seen in childhood cases of MND, which are usually inherited (Krivickas, 2003, Wijesekera and Leigh, 2009).

1.4.1.3 Progressive bulbar palsy (PBP)

PBP is characterised by the presence of dysarthria and dysphagia secondary to spasticity and weakness of the pharyngeal and tongue muscles. Fasciculation of the tongue is normally seen and patients will usually have a brisk jaw jerk. Many patients will have UMN signs in the limbs but symptoms and signs may be confined to the bulbar regions at presentation (Hillel and Miller, 1989, Pouget et al., 1995, Krivickas, 2003).

1.4.1.4 Primary lateral sclerosis (PLS)

PLS, unlike ALS, is slowly progressive and predominantly a disorder of UMN signs and symptoms. Often patients gait is affected due to spasticity and weakness of the lower limbs (wading type gait). PLS cases are hyper reflexic and have increased tone in the limb muscles. International bodies interested in ALS have concluded that before the diagnosis of PLS could be made one needs to demonstrate a period of at least 4 years without any major LMN signs clinically or by electromyography

(Pouget et al., 1995, Zeitlhofer, 1996, Ince et al., 1998, Tan et al., 2003, van der Graaff et al., 2009).

1.4.2 Atypical MND

The MND phenotype is heterogeneous as explained above. Monomelic variation of MND (Hirayama Syndrome)(Rowland, 1998) is a rare but interesting sub type of ALS which affects usually one upper limb. Characteristically, the progression of weakness and wasting, in this variant, arrests after a period of several months. It tends to affect young males. There are a few other atypical MND phenotypes:

1.4.2.1 ALS with Parkinsonism

There are multiple case reports describing features of Parkinsonism associated with ALS. The Southern Marian island of Guam is not the only place with reports of MND with Parkinsonism. Features of Parkinsonism include, tremor, rigidity, bradykinesia and postural instability. Histopathological studies have shown that the characteristic feature of Parkinson's disease, ubiquitinated inclusions in the substantia nigra, can be found in patients with ALS (1966, Brody and Chen, 1968, Ahlskog et al., 1998, Hasegawa et al., 2007).

1.4.2.2 ALS with cognitive impairment and/ or dementia

There are several case series, which demonstrate ALS cases with overt dementia. It has been estimated that approximately 50% of ALS cases develop a form of cognitive impairment during the course of illness. Several studies have shown that as many as 40% of ALS cases had features of fronto-temporal lobe dysfunction (FTLD) on detailed neuropsychological testing, and neuroimaging studies suggested fronto-temporal lobe abnormalities in about 57% of ALS cases. In some studies as many as 36% of cases with FTLD, either have clinical or neurophysiological evidence of ALS (Evdokimidis et al., 2002, Lomen-Hoerth et al., 2002, Murphy et al., 2007a, Murphy et al., 2007b). Fronto temporal dementia (FTLD) accounts for about 20% of dementias with an age of onset under 65 years (Ratnavalli et al., 2002). *CHMP2B*, *TARDBP* and *C9ORF72* mutations have been associated ALS and ALS with FTLD (Dejesus-Hernandez et al., 2011, Murray et al., 2011) (Parkinson et al., 2006, Talbot and Ansorge, 2006). Association of ALS and FTLD with hexanucleotide expansion mutation in *C9ORF72* gene and the description of large pedigrees which have family members with ALS, FTLD or both

(Savica et al., 2012) has narrowed the gap between the two ends of the spectrum these conditions belonged to (Andersen, 2012).

1.5 Genetic causes of Amyotrophic Lateral Sclerosis

The clinical heterogeneity observed in ALS is partly underpinned by the observed genetic heterogeneity. Although Charcot in 1869 described ALS, it was Francois-Amilar Aran described a familial form of motor neuron disease in 1850. In 1880 Sir William Osler described the Farr family of Vermont with a ALS like disease with autosomal dominant pattern of inheritance. However, it was more than a century later that mutations in superoxide dismutase (*SOD1*) were identified in several families with autosomal dominantly inherited ALS, including the Farr family. Since then the genetic screening of familial ALS cases has led to the identification of several genetic loci (Table 1.1) associated with ALS. A direct link has been established so far for more than 23 loci and mutations in the responsible genes have been described (Table 1.1) (Ferraiuolo et al., 2011). The recent discovery of intronic hexanucleotide expansions of the *C9ORF72* gene is associated with about ~50% of fALS and about 10% of the sALS (Dejesus-Hernandez et al., 2011, Renton et al., 2011). The Recent advances in the investigation of genetic causes for fALS has contributed immensely to the understanding of the pathogenesis and the disease processes enhancing the susceptibility of motor neurons to degeneration. The different genes encoding different proteins are implicated in a variety of biological pathways, which could lead to a common pathway delivering a final blow to the motor neurons. Therefore targeting these pathways would form the first platform in discovery of therapeutic agents.

1.6 Disease mechanisms implicated in ALS

Altered RNA metabolism, excitotoxicity, oxidative stress, mitochondrial dysfunction, axonal transport defects, neuro muscular junction defects, glial cell induced neuronal toxicity, protein aggregation, endoplasmic reticulum (ER) stress, prion like aggregation and cell to cell spread of the 'prion' like aggregations subsequently leading to precipitation of essential cellular proteins have all been demonstrated to be involved in the pathogenesis of ALS (Fig 1.1) (reviewed by (Ferraiuolo et al., 2011).
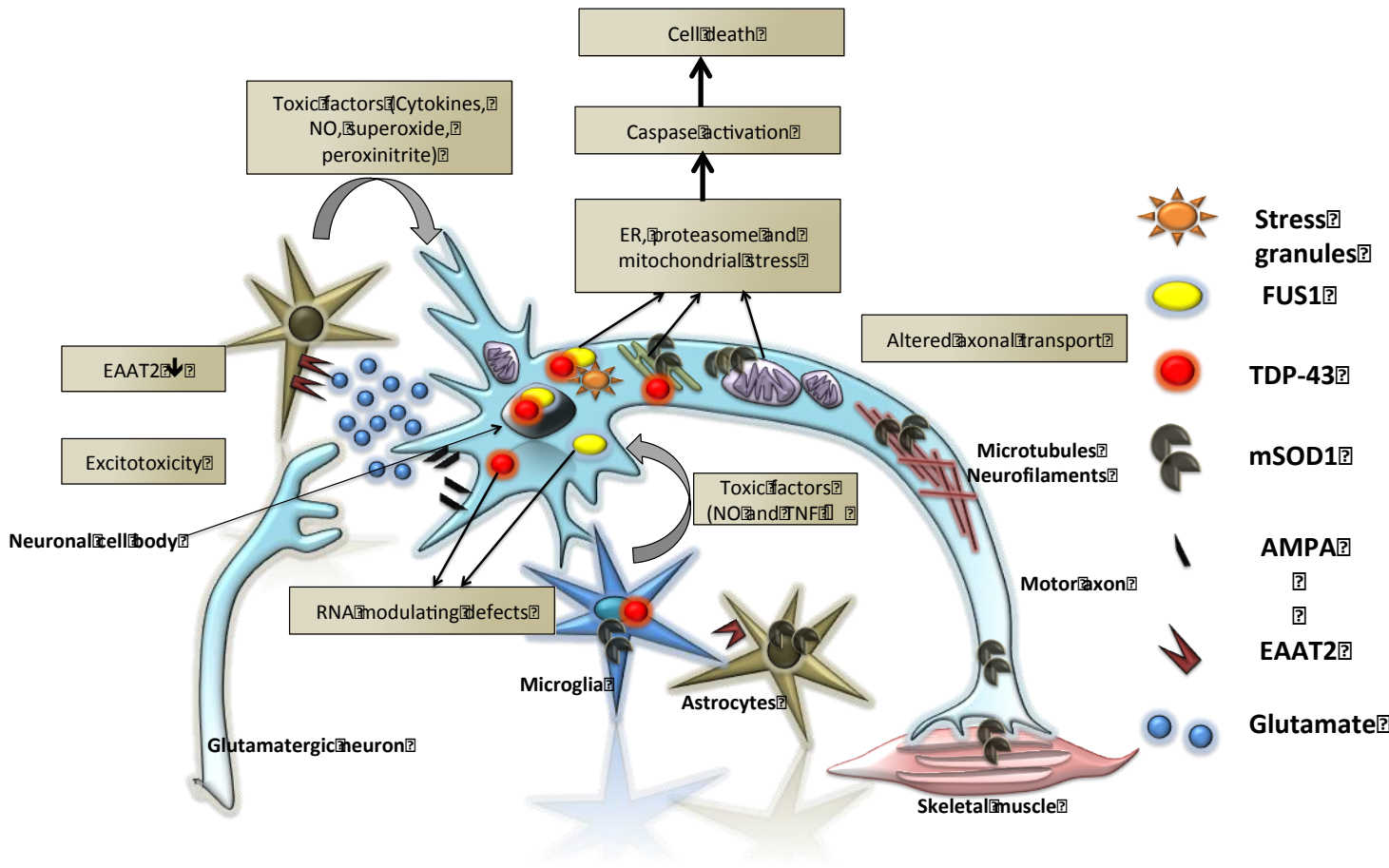
Figure 1.1 The pathophysiopalogical mechanisms underlying specific degeneration of motor neurons in amyotrophic lateral sclerosis (ALS). Mutant superoxide dismutase 1 (SOD1) directly affects motor neurons through diverse pathways, such as mitochondrial defects (reduced ATP production and increased free calcium release), dysfunction in the endoplasmic reticulum (ER) and the proteasome, and alterations in axonal transport, all of which lead to the activation of apoptotic cascades. However, SOD1-mediated toxicity in motor neurons is insufficient to mediate disease progression; non-neuronal neighbours, such as astrocytes and microglia, contribute to motor neuron damage in what is known as the non-cell-autonomous process. Astrocytes and microglia that express mutant SOD1 (mSOD1) secrete several potentially toxic factors into the cellular environment, which amplify the initial damage and drive the progression of the disease. In addition, the astroglial reuptake of synaptic glutamate (Glu) is reduced through the inactivation of excitatory amino acid transporter 2 (EAAT2), which leads to the excitotoxic death of motor neurons. The exact pathological mechanism by which mutant TAR DNA-binding protein (*TARDBP*, which encodes TDP43) and FUS are involved in amyotrophic lateral sclerosis is still unknown, but evidence points to RNA processing are involved in the selective death of motor neurons. Prion like aggregation and cell-cell spread of proteins is a novel and a viable concept. NO, nitric oxide; TNFα, tumour necrosis factor-α. Adapted from (Dion et al., 2009)

1.6.1   Altered RNA processing

1.6.1.1 Introduction

ALS is a clinically heterogeneous group of conditions, which as described earlier in the review, cause degeneration of motor neurons resulting in progressive motor weakness and eventual death (Shaw, 2001). It has been shown that motor neurons are not alone in sharing this fate, as whilst they are most susceptible to the disease process other cell groups in the central nervous system can also be affected (Blackburn et al., 2009, Henkel et al., 2009). In keeping with the above, pathological studies have described that the degenerative process not only involves the motor cortex, brain stem and the spinal cord, but also involves the frontal and temporal lobes to varying extents (Strong, 2008). This clinical heterogeneity is partly explained by the genetic heterogeneity observed especially in fALS cases (Table 1.1).

Studies in ALS associated genes and the encoding proteins, have brought insight into a multiplicity of biological processes which are implicated in ALS. The excitotoxicity, oxidative stress, mitochondrial dysfunction, axonal transport defects, neuro muscular junction defects, glial cell induced neuronal toxicity, protein aggregation, endoplasmic reticulum (ER) stress and inflammation have all been demonstrated to be involved in the pathogenesis of ALS etc (Fig 1.1) (Dion et al., 2009). Following the discovery of the association of genetic abnormalities in proteins like TDP-43 and senataxin (SETX), a firm link has been made between ALS and impaired RNA processing, as TDP-43 and SETX are molecules which are implicated in RNA metabolism (Ou et al., 1995, Buratti and Baralle, 2001, Kwiatkowski et al., 2009, Zhao et al., 2009). Further strengthening this association are the mutation screening studies which have shown that the mutations in another RNA processing molecule called, FUS/TLS1(Fused in Sarcoma/ Translocated in Lipo Sarcoma 1) are associated with ALS (Kwiatkowski et al., 2009).

Table 1.1 Genetic loci and genes associated with amyotrophic lateral sclerosis

	Locus	Gene	Gene name	Chromosome
1	ALS 1	**SOD1**	Cu/Zn superoxide dismutase 1, soluble (amyotrophic lateral sclerosis 1 (adult))	21q22.11
2	ALS 2	**ALS2**	amyotrophic lateral sclerosis 2 (juvenile) homolog (human). Alsin	2q33.2
3	ALS 3	**ALS3**	Unknown	18q21
4	ALS 4	**SETX**	Senataxin	9q34.13
5	ALS 5	**SPG11**	spastic paraplegia 11 (autosomal recessive)	15q14
6	ALS 6	**FUS**	fusion (involved in t(12;16) in malignant liposarcoma)	16p11.2
7	ALS 7	**ALS7**	Unknown	20p13
8	ALS 8	**VAPB**	Vesicle-associated membrane protein-associated protein B	20q13.33
9	ALS 9	**ANG**	Angiogenin	14q11.1
10	ALS 10	**TARDBP**	TAR DNA binding protein	1p36.22
11	ALS 11	**FIG4**	FIG4 homolog, SAC1 lipid phosphatase domain containing (S. cerevisiae)	6q21
12	ALS 12	**OPTN**	optineurin	10p13
13	ALS 13	**ATXN2**	ataxin 2	12q23-q24.1
14	ALS 14	**VCP**	valosin-containing protein	9p13
15	ALS 15	**UBQLN2**	ubiquilin 2	Xp11.21
16	ALS 16	**SIGMAR1**	sigma non-opioid intracellular receptor 1	9p13
17	ALS 17	**CHMP2B**	chromatin modifying protein 2B	3p12.1
18	ALS 18	**PFN1**	profilin 1	17p13.3

	Locus	Gene	Gene name	Chromosome
19	ALS 19	**ERBB4**	v-erb-b2 avian erythroblastic leukemia viral oncogene homolog 4	2q33.3-q34
20	ALS 20	**HNRNPA1**	heterogeneous nuclear ribonucleoprotein A1	12q13.1
21	ALS 21	**MATR3**	matrin 3	5q31.3
22	ALS-FTD 1	**ALS-FTD1**	Unknown	9q21-q22
23	ALS-FTD 2	**C9orf72**	chromosome 9 open reading frame 72	9p21.2
24	ALS	UNC13A	unc-13 homolog A (C. elegans)	19p13.12
25	ALS	DAO	D-amino-acid oxidase	12q24
26	ALS	DCTN1	Dynactin	2p13
27	ALS	NEFH	neurofilament, heavy polypeptide 200kDa, heavy chain	22q12.1-q13.1
28	ALS	PRPH	peripherin	12q12
29	ALS	SQSTM1	sequestosome 1	5q35
30	ALS	TAF15	TAF15 RNA polymerase II, TATA box binding protein (TBP)-associated factor, 68kDa	17q11.1-q11.2
31	ALS	SPAST	Spastin	2p24
32	ALS	ELP3	elongation protein 3 homolog (S. cerevisiae)	8p21.1
33	ALS	LMNB1	lamin B1	5q23.2

1.6.1.2 Outline of RNA metabolism under physiological conditions

Genes are transcribed into pre-mRNAs in the nucleus, which are then spliced in the spliceosome to form mRNAs. The nascent mRNAs are then bundled into functionally related entities along with other macromolecular structures called ribonucleoprotein (RNP) complexes to give rise to RNA granules. RNA granules contain ribosomal subunits, translational factors, scaffold proteins, helicases, RNPs, and RNA binding proteins (RBP) (Bolognani and Perrone-Bizzozero, 2008, Lin and Holt, 2008). RNA granules play an important role in regulating spatio-temporally co-expressed transcripts at translationally targeted sites (Bolognani and Perrone-Bizzozero, 2008). In neurons, three types of RNA granules are seen, which are stress granules (harbour translational factors, stalled mRNAs, RNPs until the period of stress is over); processing bodies called P bodies (where RNA decay occurs) and transport granules (which maintain mRNAs in silence until reaching translational target sites). Stress granules and P bodies are in dynamic equilibrium and share several molecules in common. Degradation of RNA occurs following deadenylation and/or decapping (3'-5' exonucleolytic activity), which occur in exosomes and P bodies (Hirokawa, 2006). mRNAs can also be degraded by micro RNAs (miRNA). These highly conserved, non coding RNAs, derived from endogenous genes are considered vital for the modulation of RNA processing, and for neuronal development and the development of dendritic spines, and are also implicated in neurodegeneration (Nelson et al., 2008).

Gene expression is finely regulated by a variety of mechanisms to give rise to the right complement of RNA and proteins in the correct position in the cell at the right time. In neurons, regulation of RNA processing can lead to asymmetrical protein translation (Lin and Holt, 2008). This process is recognised as an important pathway by which neuronal development, neuronal plasticity, neuroregeneration, and, when impaired neurodegeneration occur (Strong, 2009). There are many stages at which RNA processing could be impaired including gene transcription; RNA granule formation; stabilisation; transportation; translational control and degradation. In recent years several studies have examined the association of impaired RNA processing as a pathogenetic mechanism in ALS.

1.6.1.3 The evidence for impaired RNA processing in motor neuron degeneration related genes

Structurally diverse, neuronally expressed proteins mediate many different functions in neurons (Fig 1.1). Alternative pre-mRNA splicing is an important step in the generation of these structurally diverse proteins. In ALS and related motor neuron degenerative conditions, an alteration in mRNA splicing has been described as a key process responsible for the disease process. Specific gene changes associated with abnormal RNA processing in ALS are discussed below.

1.6.1.4 Peripherin

Peripherin is an intermediate neurofilament protein mainly expressed in neurons. Although rare, mutations of *PRPH* gene, which encodes peripherin, have been linked with ALS (Gros-Louis et al., 2004). Peripherin has also been found to associate with intraneuronal protein aggregates. A transgenic mouse model that over-expresses peripherin has also been shown to develop ALS (Robertson et al., 2003). The underlying genetic abnormality in ALS associated with defects in peripherin is alternative splicing. In the aberrant form of peripherin, a splice isoform retaining both exons 3 and 4 is expressed. However exon 3 contains a premature stop codon resulting in premature truncation of the peripherin protein. In the mutant SOD1 mouse model a toxic splice variant of peripherin is expressed, in which intron 4 is retained which gives rise to a toxic peripherin protein 32 amino acids larger than the predominant isoform (Xiao et al., 2008). In keeping with the toxic aggregation of aberrant peripherin due to impaired splicing, TDP-43, a protein implicated in transcription modulation has been shown to co-localise with peripherin inclusions in ALS (Sanelli et al., 2007).

1.6.1.5 SMN

Mutation in the survival of motor neuron *(SMN)* gene is implicated in spinal muscular atrophy (SMA), which is a progressive lower motor neuron degenerative condition. Both the SMN1 and SMN2 proteins are important in fulfilling the functioning in motor neurons. SMN contributes to the formation of spliceosome by assembling uridine rich small nuclear proteins, which are important constituents of the spliceosome, and SMN works in tandem with other SMN associated proteins, in doing so (Farrar et al., 2009). SMN associated with components of the RNP granules, such as hnRNP R and Q, takes part in RNP granule transport to the

dendritic processes and axonal growth cones (Zhang et al., 2006). In keeping with this, SMN antisense morpholino oligonucleotide knockdown of SMN in the zebrafish, leads to impaired motor axon architecture indicating defective motor axonal path finding (McWhorter et al., 2003).

1.6.1.6 Angiogenin (encoded by ANG)

Mutations in the *ANG* gene are associated with ALS type 9. Angiogenin is classified as a promoter of ribosomal RNA transcription (Wu et al., 2007). Angiogenin is also a tRNA specific ribonuclease, which, when stress activated, cleaves tRNA and inhibits translation. Angiogenin is functionally related to VEGF (vascular endothelial growth factor) in that it binds to an angiogenin binding element (CTCT repeats) and enhances ribosomal RNA transcription, which is important in the regulation of expression of VEGF (Gao and Xu, 2008). The relevance of this association is further enhanced by the findings that VEGF and angiogenin enhance the survival of G93A SOD1 mouse and that *ANG* deficient SOD1 G93A transgenic mice have a lower survival rate (Subramanian et al., 2008).

1.6.1.7 Senataxin (SETX)

A mutation in the *SETX* gene has been described to associate with ALS (Chen et al., 2004, Zhao et al., 2009) Classically *SETX* mutations are associated with cerebellar and motor neuron degeneration. The RNA helicase activity and RNA processing are thought to be the important functions of senataxin (Chen et al., 2004). RNA helicases are important in multiple nuclear activities such as unwinding of double stranded DNA, modification of RNA-RNA interactions, modification of chromatin structure and association with the spliceosome. A role for SETX as an RNA helicase is supported by its similarity to Immunoglobulin Mu binding Protein 2 *(IGHMBP2),* which is a DNA/RNA helicase. *IGHMBP2* mutations are also associated with a severe form of SMA associated with respiratory distress called SMARD1 (Grohmann et al., 2001).

1.6.1.8 TDP-43 and MATR3 (Matrin 3)

TAR DNA binding protein-43 is associated with modulating the transcription of several genes, for example HIV1 DNA, SP10, Apo II, HDAC and cdk6 (Ou et al., 1995, Abhyankar et al., 2007, Ayala et al., 2008a, Fiesel et al., 2009). These associations will be described in detail later in this chapter. There is an emerging body of information that dysfunctional TDP-43 results in impairment in RNA transcription,

translation, and protein-protein interactions, resulting in motor neuron degeneration. The importance of TDP-43 as an RNA processing protein associated with ALS is further confirmed by multiple mutations in *TARDBP* gene found in ALS cases (Table 1.2). Both TDP-43 and FUS are associated with the stress granule marker TIAR in cells subjected to exogenic stress (Andersson et al., 2008, Colombrita et al., 2009)(Anderson and Kedersha, 2008).

MATR3 is a protein that interacts with TDP-43 and is also known to have RNA and DNA binding properties. Mutations in *MATR3* gene associated with ALS cases have been recently described using exome sequencing (Johnson et al., 2014).

1.6.1.9 FUS/TLS 1

The recent discovery of the association of mutations in another RNA binding protein, Fused in Sarcoma/ Translocated in Liposarcoma 1 (FUS/TLS1) with ALS, further strengthens the claim that dysfunctional RNA processing is an important pathogenetic mechanism in ALS related neurodegeneration (Kwiatkowski et al., 2009). FUS/TLS1 is structurally similar to TDP-43 in that it contains an RNA recognising motif (RRM) and Glycine rich domain (GRD), which are considered important for interaction with DNA/RNA molecules (Corrado et al., 2009a, Lagier-Tourenne and Cleveland, 2009). Both TDP-43 and FUS/TLS1 are postulated to associate with the microprocessor complex and the Drosha complex, which are important in miRNA processing. miRNAs are important in regulating and in the degradation of mRNA (Nelson et al., 2008, Volkening et al., 2009).

In summary, impaired RNA processing appears to provide a common pathway for several disease mechanisms and biologically divergent processes associated with several abnormal neuronally expressed proteins to finally coalesce, so alteration in transcription, alternative splicing, translation, granule formation, RNA transport, SG assembly and miRNA related gene expression could be targeted in search for a therapeutic breakthrough.

Table 1.2 Mutations described in *TARDBP* gene encoding TDP-43

	Mutation	fALS	sALS	Onset	Cognitive impairment	Origin	References
1	D169G		1	Limb	No	France	(Kabashi et al., 2008)
2	N267S		1	Limb	Dementia	Italy	(Corrado et al., 2009c)
3	G287S		2	Bulbar	No	France, Italy	(Kabashi et al., 2008, Corrado et al., 2009b)
4	S292A	1		Bulbar, Limb	No	Chinese	(Xiong et al.)
5	G290A	1		Bulbar, Limb	No	Europe	(Van Deerlin et al., 2008)
6	G294A		1	Limb	No	Australia	(Sreedharan et al., 2008)
7	G294V	1	1	Limb	No. ?Yes	Italy	(Corrado et al., 2009b, Del Bo et al., 2009)
8	G295C			Bulbar	No	Netherland	(van Blitterswijk et al., 2014)
9	G295S	1	3	Bulbar, Limb	FTD features 3/4	Italy, France	(Benajiba et al., 2009, Corrado et al., 2009b, Del Bo et al., 2009)
10	G295R		2	Limb	No	Italy, North America	(Corrado et al., 2009b, Ticozzi et al., 2009)
11	G298S	1		Bulbar, Limb	No	China	(Van Deerlin et al., 2008)
12	Q303H		1	Spinal	N	Italy	(Da Costa et al., 2014)
13	M311V	1		Limb	No	Belgium	(Lemmens et al., 2009)
14	A315E	1		Spinal	Parkinsonism	Japan	(Fujita et al., 2011)
15	A315T	3		Limb	No	Europe, North America	(Gitcho et al., 2008, Kabashi et al., 2008, Ticozzi et al., 2009)
16	A321G		1	Spinal	No	UK	(Baumer et al., 2010)
17	A321V		2	Limb	No	UK	(Kirby et al., 2009)

	Mutation	fALS	sALS	Onset	Cognitive impairment	Origin	References
18	Q331K		1	Limb	No	England	(Sreedharan et al., 2008)
19	S332N	1		Limb	No	Italy	(Corrado et al., 2009b)
20	G335D		1	Limb	No	Italy	(Corrado et al., 2009b)
21	M337V	3		Limb	No	England, Italy	(Rutherford et al., 2008, Sreedharan et al., 2008, Corrado et al., 2009b)
22	Q343R	1		Limb	No	Japan	(Yokoseki et al., 2008)
23	N345K	2		Limb	No	North America	(Rutherford et al., 2008, Ticozzi et al., 2009)
24	G348C	4	4	Limb	No	Europe, North America	(Kabashi et al., 2008, Kuhnlein et al., 2008, Daoud et al., 2009, Del Bo et al., 2009, Ticozzi et al., 2009)
25	G348V	2		Limb	No	England	(Kirby et al., 2009)
26	N352S	3		Limb	No	Germany, US	(Kuhnlein et al., 2008)
27	N352T	1		Spinal	No	North America	(Ticozzi et al., 2009)
28	G357R	1		Bulbar	No	Denmark	(Chiang et al., 2012, Iida et al., 2012)
29	G357S		2	Spinal	No	Japan	(Iida et al., 2012)
30	R361S		1	Limb	No	France	(Kabashi et al., 2008)
31	R361T	1		Spinal	FTD	Norway	(Chiang et al., 2012, Iida et al., 2012)
32	P363A		1	Limb	No	France	(Daoud et al., 2009)
33	G368S		1	Bulbar	No	Italy	(De Marco et al., 2011)
34	Y374X		1	Limb	No	France	(Daoud et al., 2009)
35	G376D	2		Spinal	No	Australia, Italy	(Solski et al., 2012)
36	N378D	1		Bulbar, spinal	No	North America	(Ticozzi et al., 2009)

	Mutation	fALS	sALS	Onset	Cognitive impairment	Origin	References
37	N378S		1	Spinal	No	China	(Huang et al., 2012b)
38	S379C		1	Limb	No	Italy	(Corrado et al., 2009b)
39	S379P	2		Limb	No	Italy, North America	(Corrado et al., 2009b, Ticozzi et al., 2009)
40	A382T	5	6	Bulbar, Limb	No	Italy, France	(Kabashi et al., 2008, Corrado et al., 2009b, Del Bo et al., 2009)
41	A382P		1	Limb	No	France	(Daoud et al., 2009)
42	I383V	5		Limb, Semantic dementia	No, FTLD	North America	(Rutherford et al., 2008, Ticozzi et al., 2009, Gelpi et al., 2014)
43	G384R	1		Spinal	No	North America	(Ticozzi et al., 2009)
44	W385G	1		Spinal	No	France	(Millecamps et al., 2010)
45	p.T387del insN388P 389	1		Spinal	No	Italy	(Solski et al., 2012)
46	N390D	2	1	Limb	No	North America	(Kabashi et al., 2008, Ticozzi et al., 2009)
47	N390S		1	Limb	No	France	(Kabashi et al., 2008)
48	S393L		1	Limb	No	Italy	(Corrado et al., 2009b)

1.7 Pathology of ALS

1.7.1 Neuronal inclusions

The neurodegenerative process in MND and its subtypes involves degeneration of cortical, spinal and brain stem motor neurons as well as the motor axons. The presence of neuronal cytoplasmic inclusions is a pathological hallmark of neurodegenerative conditions. In ALS, three distinct types of inclusions are described. Ubiquitinated inclusions are seen in the perikaryon and the proximal axon of the spinal motor neurons and the cortical motor neurons of both fALS and sALS cases. The first type of inclusion described is Bunina body, which is a small eosinophilic inclusion found in cell body of the neurons. They are present in both fALS and sALS cases, they are positive for cystatin C immunoreactivity and are of lysosomal origin. They are present in the CNS up to 85% of ALS cases. The second group of inclusions, hyaline conglomerates, are found in the perikaryon and the proximal dendrites of spinal motor neurons. These inclusions are reactive for both medium and heavy chains, phosphorylated and unphosphorylated neurofilaments (SMI31 and SMI32 antibody staining) and are not specific to ALS. They are characteristically found in patients with specific SOD1 mutations (e.g. I113T, A4V). The most abundant inclusions are the loosely packed filament like 'skeins' and densely packed compact inclusions. These are the two different morphological patterns of staining with an ubiquitin antibody. Immunoreactivity of the inclusions to ubiquitin is in keeping with the pattern of selective vulnerability and it is characteristic in ALS. Until recently the major protein constituent of these inclusions identified by ubiquitin immunostaining was unknown. These ubiquitinated cytoplasmic inclusions are commonly seen in sALS cases but also seen in fALS cases with SOD1 mutations (Mackenzie et al., 2007, Tan et al., 2007). In MND cases with SOD1 mutations the inclusions have been shown to contain of alpha internexin, peripherin, neurofilament proteins, 14-3-3 proteins and SOD1 (Kawamoto et al., 2005, Volkening et al., 2009).

1.7.2 TDP-43: The major component of the neuronal inclusions

In 2006 mass spectroscopy and immunohistochemistry studies have identified TAR DNA binding protein 43 (TDP-43) as the major constituent of the ubiquitinated but tau and alpha synuclein negative inclusions in FTLD with Ubiquitinated inclusions (FTLD-U), the commonest form of FTLD, and in ALS with and without FTLD-U (Neumann et al., 2006) (Fig 1.2). These findings suggest that ALS and FTLD-U are conditions at different ends of a common clinico-pathological spectrum of neurodegenerative conditions, which are now collectively described as 'TDP-43 proteinopathies' (Liscic et al., 2008).
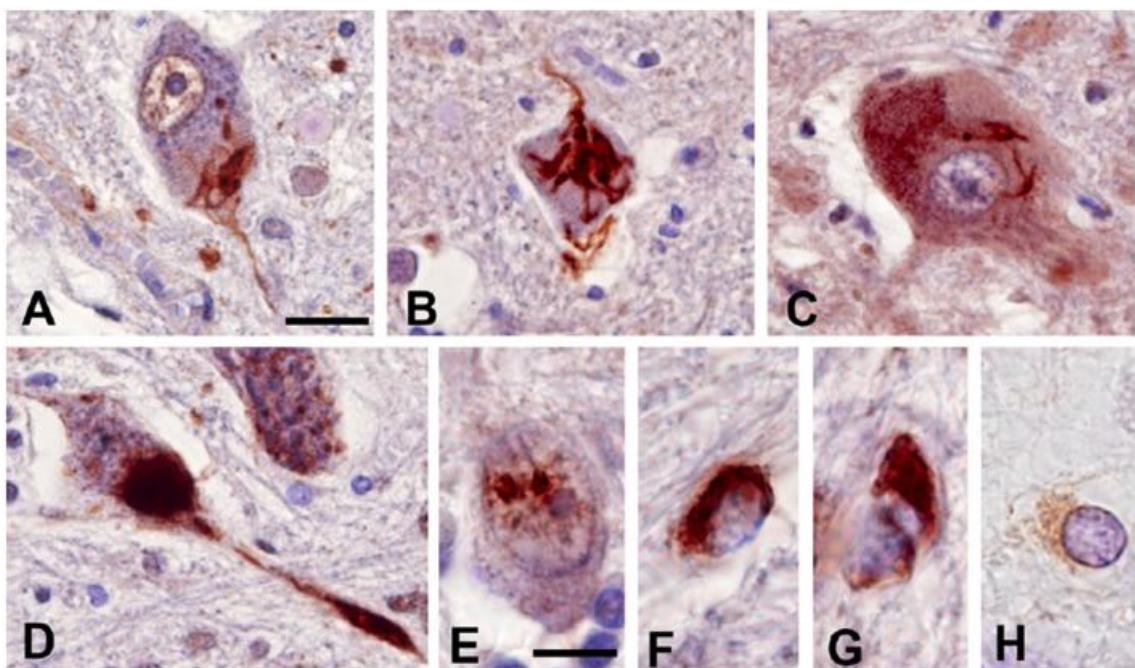
Figure 1.2. Immuno staining of the spinal cord in ALS. Skeins like lesions in the lumbar spinal cord are stained with anti ubiquitin and anti TDP-43. (A) and with both polyclonal **(B)** and monoclonal antibodies (C) to TDP-43. A compact rounded inclusion in a neuronal cytoplasm and dystrophic neurite-like structure in an apical dendrite are stained with a polyclonal antibody to TDP-43 in the anterior horn of the lumbar spinal cord (D). Two neuronal intra nuclear inclusions positive for TDp-43 are shown in the sacral spinal cord (E). TDP-43 positive glial inclusions curved (F) or bullet shaped is observed in the lumbar spinal cord. Similar glial inclusions positive for tau are also seen in the lumbar spinal cord (H). The sections are counter stained with haematoxilin. Courtesy of Arai et al (2006) (Permission to reuse obtained from Elseiver).

1.7.3 The concept of TDP-43 proteinopathy

The neuronal aggregation of proteins occurs in many neurodegenerative conditions as a result of protein mis-folding and the dysfunction of the ubiquitin proteasome system (UPS), which in some situations leads to amyloid formation.

However TDP-43 associated neurodegeneration with neuronal and glial inclusions, the inclusions lack the features of amyloid deposition (Neumann et al., 2007a). The key pathological features of TDP43 proteinopathies are TDP43 positive but alpha synuclein, tau, beta amyloid and neuronal intermediate filament protein negative, neuro-cytoplasmic inclusions (NCI), neuronal intra nuclear inclusions (NII) and dystrophic neurites (DN). Particularly in MND/ALS cases, glial cytoplasmic inclusions (GCI) have also been reported (Arai et al., 2006, Neumann et al., 2006, Neumann et al., 2007a, Neumann et al., 2007b, Nishihira et al., 2008). Some pathological studies have also described relative nuclear clearing and accumulation in the cytoplasm of TDP43 immunoreactivity from the surviving motor neurons with the above inclusions (Arai et al., 2006, Neumann et al., 2006, Cairns et al., 2007). Some reports have also mentioned the occurrence of nuclear inclusions (Arai et al., 2006, Neumann et al., 2006). The ubiquitinated TDP-43 in the inclusions also has a unique biochemical signature being: phosphorylated, C-terminally fragmented and relatively insoluble (Neumann et al., 2006, Hasegawa et al., 2008a, Hasegawa et al., 2008b). Since the first description of the association of TDP-43 with ALS and FTLD-U, numerous neuropathological studies have shown a link between TDP-43 and a variety of other neurodegenerative conditions such as the Guam ALS Parkinsonism Dementia group of conditions, FTLD, Alzheimer's dementia, hippocampal sclerosis, Parkinson's disease with Lewy bodies, Lewy body disease, Huntington's disease, inclusion body myopathy with Paget's disease of bone and fronto temporal dementia (IBMPFD) (Schwab et al., 2008) (Amador-Ortiz et al., 2007, Hasegawa et al., 2007, Nakashima-Yasuda et al., 2007, Maekawa et al., 2009), stressing the importance of protein aggregation and dysfunctional UPS as important mechanisms of neurodegeneration. Interestingly, the ubiquitinated neuronal inclusions in fALS cases due to SOD1 mutations were not thought to contain TDP-43 pathology suggesting that the underlying molecular pathomechanism in SOD1 related fALS is different from that of TDP-43 proteinopathies (Mackenzie et al., 2007, Tan et al., 2007). However several reports have described TDP-43 pathology in mutant SOD-1 cases ((Shan et al., 2009, Okamoto et al., 2011) and more recently in a G93A SOD-1 mutant mouse model (Marino et al., 2014).

Multiple reports of several *TARDBP* mutations associated with fALS and sALS cases have been well described (Kabashi et al., 2008, Kuhnlein et al., 2008,

Rutherford et al., 2008, Sreedharan et al., 2008, Van Deerlin et al., 2008, Yokoseki et al., 2008, Benajiba et al., 2009, Daoud et al., 2009, Del Bo et al., 2009, Kabashi et al., 2009, Kamada et al., 2009, Pamphlett et al., 2009, Pesiridis et al., 2009, Williams et al., 2009), which strongly reinforces the causal association of TDP-43 in ALS and refutes the possibility that TDP-43 is an innocent bystander (Rollinson et al., 2007, Gijselinck et al., 2009, Schumacher et al., 2009).

1.8 Trans active response (TAR) DNA binding protein (TARDBP) and its role in MND/ALS

1.8.1 Introduction

Major discoveries have been made in the last few years on the pathology, pathogenesis, biochemistry and genetics of ALS and FTLD. The experimental models of ALS have been largely dedicated to the study of the relatively rare fALS due to *SOD1* mutations. However there is no consensus, yet, as to how dysfunctional SOD1 results in selective motor neuronal loss except that SOD1 induced motor neuron damage is responsible for disease onset and glial cells containing mutant *SOD1* accelerate disease progression (Yamanaka et al., 2008). Therefore it is encouraging that the possibility has finally emerged, through identification of the TDP-43 association with ALS and FTLD-U, that a disease model relevant to sALS is now possible. TDP-43 was first cloned from a genomic screening attempt to identify factors that bind to the trans acting response domain (TAR) DNA of the human immune deficiency virus 1 (HIV-1) and repress transcription (Ou et al., 1995). The protein encoded by *TARDBP*, TDP-43 is considered the major pathological protein implicated in sALS, fALS due to non *SOD1* mutations and FTLD-U, which group of conditions, are now collectively considered as the 'TDP-proteinopathies' (Liscic et al., 2008). This pathological breakthrough, although a major leap in the understanding of ALS and FTLD-U, does not explain whether the presence of TDP-43 in the NCIs is a by-product, the primary event in motor neuron injury or indeed an event in a common pathway of the disease pathogenesis. Despite the multiple publications since the discovery of the role of TDP-43 in neurodegeneration, the function of TDP-43 still remains unclear. The following is a review of the literature to date describing the role of TDP-43 in ALS /MND.

1.8.2 TARDBP gene and basic structural features of TDP-43 protein

The TARDBP gene is located in the short arm of chromosome 1 at the position 36.22 (1p36.22) and contains 6 transcribed exons, with a cDNA length of 2748 nucleotides including the 5' and 3' UTR (Untranslated Regions). Exons 2-6 encode a 414 amino acid protein, TDP-43. There are 12 different transcripts reported, of which five are known to produce protein products (www.ensembl.org/Homo_sapiens/Transcript/Sequence_cDNA). TDP-43 is an evolutionary highly conserved protein not only amongst ortholgues of several different species, but also amongst its human paralogues i.e. hnRNP-A1 (heterogeneous nuclear Ribonuclear protein-A1). TDP-43 is a ubiquitously expressed protein, indicating that it is an essential gene required for the normal function of multiple different cell types (Neumann et al., 2006). TDP-43 belongs to a family of heterogeneous nuclear ribo nucleoproteins (hnRNP), which are well known for RNA binding and interaction with DNA via a nucleotide recognition motif called RNA recognition motif. Members of the hnRNP family of proteins are important in the generation, processing and modification of RNA and have functionally important roles in transcription, translation, stabilisation and transport of RNAs (Singh, 2001). This diversity of hnRNP functions is underpinned by the presence of modular domains through which they exert specific protein-protein interactions (Krecic and Swanson, 1999) (Fig 1.3). TDP-43 has a high degree of homology with the hnRNP proteins in the region of TDP-43 between amino acids 144-135 (Ou et al., 1995) a region called RNP binding domain, which is important for RNA binding. Similar to hnRNP core protein A1, this region of TDP-43 is included in the RNA binding motif 1(RRM1 -aa 106-176). RRM2 (aa 191-262) although not essential for $(UG)_m/(TG)_m$ dinucleotide repeat recognition which is important for RNA binding, is important for the correct formation of transcription factor complexes and CFTR exon 09 skipping (Buratti and Baralle, 2001, Bose et al., 2008). Studies have confirmed the presence of a nuclear localisation signal (aa 82-91) towards the N-terminus, which is important for nuclear shuttling, and a nuclear export signal within RRM2 (Ayala et al., 2008b, Winton et al., 2008b). The TDP-43 C-terminus itself is important in RNA processing and the modulation of splicing (Wang et al., 2004).
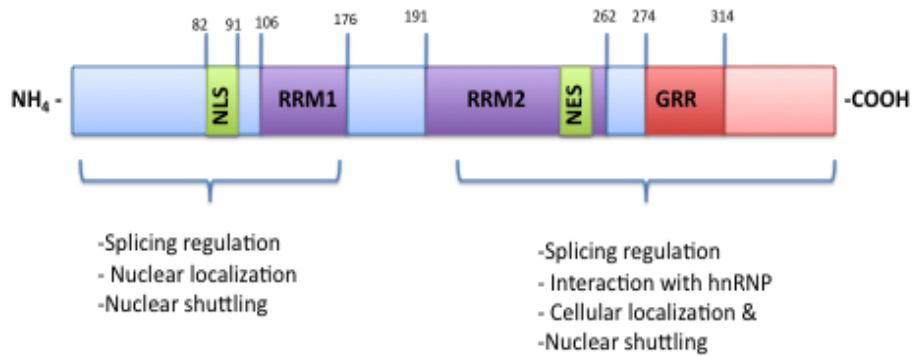
Schematic diagram of TDP-43 protein and its important domains

Figure 1.3 Schematic diagram of the ultrastructure of TDP-43 protein. At the N-terminus is the nuclear localisation signal (NLS), RNA recongnising motif 1 (RRM1) and RRM2. At the C-terminal end is a functionally vital Glycine rich region (GRR). GRR is also known as the glycine rich domain (GRD) in the text.

The C-terminus contains an area where ~ 40% of the amino acids are glycine residues, called the glycine rich domain (GRD) (Ou et al., 1995) (D'Ambrogio et al., 2009). TDP-43 GRD shares a 21% homology with the GRD of its human paralogue hnRNP A1, between the amino acids 274-314. The glycine residues in this region of TDP-43 are evolutionarily conserved and are regularly interspersed by aromatic amino acids as in hnRNP A1. We know from the study of other hnRNPs that the GRD is important for protein-protein interactions (Biamonti et al., 1994, Cobianchi et al., 1994, Pesiridis et al., 2009). This glycine rich region of TDP-43 is important for the RNA processing function of TDP-43 and, similar to hnRNPs, is required in the interaction with hnRNP A/B (Buratti et al., 2005) and has the amino acid sequence, Arg-Gly-Gly (RGG- box), which has been shown to bind to RNA in relation to other RNA binding proteins (RBP) (Kiledjian and Dreyfuss, 1992).

TDP-43 proteinopathy is characterised by aggregation of C-terminally fragmented (CTF), ubiquitinated and phosphorylated TDP-43 in NCI. There are 39 possible serine, threonine, tyrosine residues throughout TDP-43, which could potentially be phosphorylated, and more than 53% of these residues are positioned between amino acids 233-410 in the C-terminus (Hasegawa et al.,

2008a). Amino acid sequence analysis of TDP-43 reveals three potential caspase 3-recognition motifs, which could result in proteolytic cleavage. These are amino acids, DEND (aa 10-13), DETD (aa 86-89) and DVMD (aa 216-219) and caspase cleavage at the latter two sites results in 35 kDa and 25 kDa CTF TDP-43 proteins respectively (Zhang et al., 2009). Analysis of the TDP-43 structure helps us to understand the possible functions of TDP-43 and predicts the behaviour of wild type and mutated forms of the TDP-43 protein.

1.8.3 Mutations of *TARDBP* gene encoding TDP-43

Since the association of TDP-43 with the NCI of ALS and FTLD-U was discovered, many independent research groups around the world have carried out genetic screening studies in both sporadic and familial ALS cases and have described a number of mutations in the *TARDBP* gene confirming the pathological association of TDP-43 with the ALS/MND disease state. So far there have been 83 different genetic variations of the *TARDBP* gene reported. These consist of 47 missense mutations; one non-sense mutation and two benign missense mutations in the coding region and the seven mutations in the 5' UTR; five mutations in the 3' UTR and 21 intronic variations. To date, variations in the non-coding region of *TARDBP* are thought to be benign. The 48 different pathological *TARDBP* mutations are described in 86 apparently unrelated families (Table 1.2). A review of all mutations done in 2009 suggested that out of 71 index cases at the time 31 in 2846 sALS (1%) cases and 40 out of 1167 (3.4%) fALS cases screened had missense mutations whilst 8117 control cases were negative for the above mutations (Pesiridis et al., 2009) (Table 1.2). *TARDBP* mutations in fALS cases showed an autosomal dominant pattern of inheritance. Some of the mutations were described in ALS cases with pathological evidence of TDP-43 proteinopathy. Skein like NCI and relative depletion of TDP-43 from the nuclei of the surviving motor neurons were noted in the immunohistochemistry studies of postmortem material from ALS cases with G298S and Q343R mutations (Tan et al., 2007, Van Deerlin et al., 2008). Analysis of the clinical features of all the 48 reported mutations we noted that 37 out of reported 48 *TARBP* mutations were associated with pure spinal/limb onset ALS whilst 4 mutations were associated with pure bulbar onset symptoms. One ALS case with a G294V missense mutation had cognitive impairment whilst another report suggested an association of the G295S

mutation in two families with a history of cognitive impairment consistent with FTLD. *TARDBP* mutations, R361T from a Norwegian family (Chiang et al., 2012) and I383V of a North American family have been described to associate with FTLD whilst I383V associated with FTLD-U without ALS (Gelpi et al., 2014). Taken together these findings of mutations in ALS and FTLD with ALS suggest a commonality of TDP-43 proteinopathy in neurodegenerative disorders. Although mutation screening and copy number analysis of the *TARDBP* gene in both sporadic and familial FTLD cases have not discovered any mutations (Rollinson et al., 2007, Gallone et al., 2009, Gijselinck et al., 2009), the two cases with FTLD plus ALS/MND described above (Benajiba et al., 2009) and the R361T and I383V mutations associated with FTLD indicate that *TARDBP* mutations are not restricted to ALS (Gelpi et al., 2014) .

1.8.3.1 Mutation hot-spots and functional relevance of TARDBP mutations

Exon 6 of TDP-43 encodes for ~60% of the TDP-43 protein and approximately 70% of the TDP-43 mRNA. Exon 6 is also important for TDP-43 as it encodes an evolutionary highly conserved region of the TDP-43 C-terminus including the GRD. Except for one described mutation (D169G), all other pathogenic mutations so far described in the *TARDBP* gene occur in exon 6 (Kabashi et al., 2008). The most frequent *TARDBP* gene mutation is A382T (eleven reported cases) whilst G348C is the second most common (eight cases). Although the A382T position is not evolutionary conserved, G348C is. The alanine at position 382 could be a mutational 'hot spot' as another mutation has been reported at the same position (A382P, 1144 G>C) (Kabashi et al., 2008, Corrado et al., 2009b). Seven out of the total of nine reported glycine residues mutated in TDP-43 are within the evolutionary conserved elements of the GRD (Guerreiro et al., 2008, Kabashi et al., 2008, Rutherford et al., 2008, Yokoseki et al., 2008, Corrado et al., 2009b, Del Bo et al., 2009, Gijselinck et al., 2009, Ticozzi et al., 2009).

Hyperphosphorylation of C-terminally fragmented TDP-43 is an important finding in TDP-43 pathological aggregates. Therefore it is of interest to see if the missense mutations disrupted any potential phosphorylation sites or created new sites, which could result in abnormal hyperphosphorylation. Three mutations potentially abolish casein kinase 1 targeted phosphorylation sites S379 and S393 due to missense mutations: S379C, S379P and S393L (Corrado et al., 2009b,

Kametani et al., 2009). Interestingly nine other amino acids in the evolutionary conserved region of GRD are reported to be replaced by serine and threonine residues, which can be phosphorylated, which in turn could enhance aggregation (Kabashi et al., 2008, Kuhnlein et al., 2008, Corrado et al., 2009b). Missense mutations creating new sites for ubiquitination such as Q331K and N345K and two other missense mutations increasing the creation of disulphide bond formation (G348C and S379C) are predicted to increase the likelihood of aggregation formation.

1.8.3.2 Do TARDBP mutations cause loss of function or gain of function?

Whether TDP-43 related ALS is due to toxic gain of function or a loss of physiological function, needs to be investigated in both *in vitro* and *in vivo* models of both normal and dysfunctional TDP-43 cellular activity. Sreedharan and colleagues demonstrated that injection of Q331K or M337V TDP-43 mutants into the chick embryo resulted in developmental defects and enhanced apoptosis (Sreedharan et al., 2008) whilst the Q331K mutation has been shown to have a greater propensity to form aggregates (Johnson et al., 2009) suggesting a possible toxic gain of function. However, studies in a Drosophila model of ALS, where the impaired locomotive phenotype of drosophila generated by the drosophila TDP-43 orthologue TBPH gene suppression either by chromosomal deletion or the RNA interference method, was rescued by injection of human TDP-43 (Feiguin et al., 2009), suggesting a loss of function role for TDP-43. Supporting this theory are the findings from the TDP-43 transgenic mouse model, over-expressing the TDP-43 A315T mutation, where loss of nuclear TDP-43 is seen in the surviving motor neurons of the mice at late stages of disease indicated by limb weakness and difficulty in obtaining food and water (Turner et al., 2008). The loss of TDP-43 from the nucleus could potentially affect the normal RNA processing function of TDP-43. Aggregation of disease related proteins of neurodegenerative diseases are known to have a toxic gain of function. The analysis of the brain and cerebellar tissues obtained from TDP-43 A315T PrP (prion protein promoter) transgenic mice did not show TDP-43 positive cytoplasmic aggregation formation (Turner et al., 2008) as seen in the human cases, which further supports the loss of function mechanism of mutant TDP-43. It is still possible however, that the transgenic protein could precipitate the endogenous mouse TDP-43 or produce a soluble

TDP-43 fragment that drives the disease process, which might on the other hand, indicate a toxic gain of function.

1.8.4 Properties and functional roles of TDP-43

TDP-43 has structural homology with another RNA binding protein, hnRNP A1 as described earlier. The analysis of TDP-43 structure and the studies of hnRNP group of proteins, which are powerful splicing modulators and vital in diverse cellular functions (Biamonti et al., 1994, Cobianchi et al., 1994, Krecic and Swanson, 1999), inform us that TDP-43 also could possess several different functions important for the maintenance of the internal milieu of neurons and extra neuronal cells. The function of TDP-43 depends on its structural domains, localisation, and post-translational modifications and on interactions with other proteins. Knowledge of the function/s of TDP-43 is accumulating at a fast pace, and so far several different functions have been described in *in vitro* and *in vivo* models, including roles in: transcription repression/modulation (Ou et al., 1995, Abhyankar et al., 2007, Ayala et al., 2008a, Casafont et al., 2009); pre mRNA splicing modulation (Buratti and Baralle, 2001, Buratti et al., 2001, Mercado et al., 2005, Ayala et al., 2006, Ayala et al., 2008a, Bose et al., 2008); mRNA stability (Strong et al., 2007, Moisse et al., 2009a, Volkening et al., 2009); translational repression (Fiesel et al., 2009); biogenesis of micro RNA (miRNA) (Gregory et al., 2004); formation of RNA granules, trafficking, sequestering and degradation of RNA and possible functions in stress granule formation (Elvira et al., 2006, Colombrita et al., 2009, Moisse et al., 2009a, Moisse et al., 2009b, Volkening et al., 2009); cell cycle regulation (Ayala et al., 2008a) and several other processes depending on several protein-protein interactions of TDP-43 (Zhang et al., 2007, Gitcho et al., 2009, Kim et al., 2009). Overwhelming evidence point to a RNA modulating function for TDP-43 (Fig 1.4).

1.8.4.1 Transcriptional repression and translational modulation function of TDP-43

TDP-43 possesses two RNA recognising domains and a glycine rich domain, as do hnRNPs, which are known to bind to RNA and induce transcriptional repression. The discovery of the importance of TDP-43 in relation to human disease arose

from the study by Ou et al in 1999, investigating distinct regulatory functions of the Trans-Active Response (TAR) domain of the HIV-1 DNA. TDP-43 was identified as a 43 kDa, binding factor to the TAR DNA of HIV-1 virus using labeled TAR DNA in a UV cross-linking assay, in the presence of HeLa cell extract, hence the name TDP-43 (Ou et al., 1995). Both in-vitro and in in-vivo experiments indicated that TDP-43 mediated repression of HIV-1 pro virus expression resulted from either, dimerised TDP-43 or two TDP-43 molecules simultaneously binding to the polypyrimidine sequences of the HIV-1 promoter region in a *cis* acting fashion, whereby it interferes with the binding of TATA binding factors and transcription factors. The RNP motif 1 placed within RRM1 domain and the N-terminal amino acid sequence, but not the GRD, are important to execute the above function (Ou et al., 1995).

The execution of a spatio-temporally ordered programme of gene expression by tissue or the cell specific alteration in gene expression via promoter regions or silencing of gene expression via insulator regions is very important for the normal regulation of the tightly controlled internal milieu of neurons. Perturbation of this fine balance especially in neurons, could result in neuronal dysfunction and degeneration. Studies done on the round spermatid specific protein 10 (SP-10) gene by Acharya et al (2006) demonstrated that TDP-43 serves an insulator function whereby it represses the transcription of the SP-10 gene in somatic cells, in a tissue specific manner. TDP-43 binds, in a *trans* acting manner, to a canonical binding site, GTGTGT repeat sequence (GTm) opposite the *SP-10* promoter sequence, of the single stranded DNA using the N-terminus but not the C-terminus (Acharya et al., 2006). Confirming the above findings, Abhyankar et al (2007), in a reporter and effector construct assay, showed that TDP-43 could prevent the enhancer –promoter interaction *SP-10* gene, whereby TDP-43 acts as an insulator protein repressing transcription of the *SP-10* gene (Abhyankar et al., 2007). In contrast to the studies on HIV-1 transcription repression, the GRD of TDP-43 was found to be more important than the RRM1 domain for *SP-10* gene repression, indicating that interplay between the two domains is required for effective transcriptional repression (Abhyankar et al., 2007).
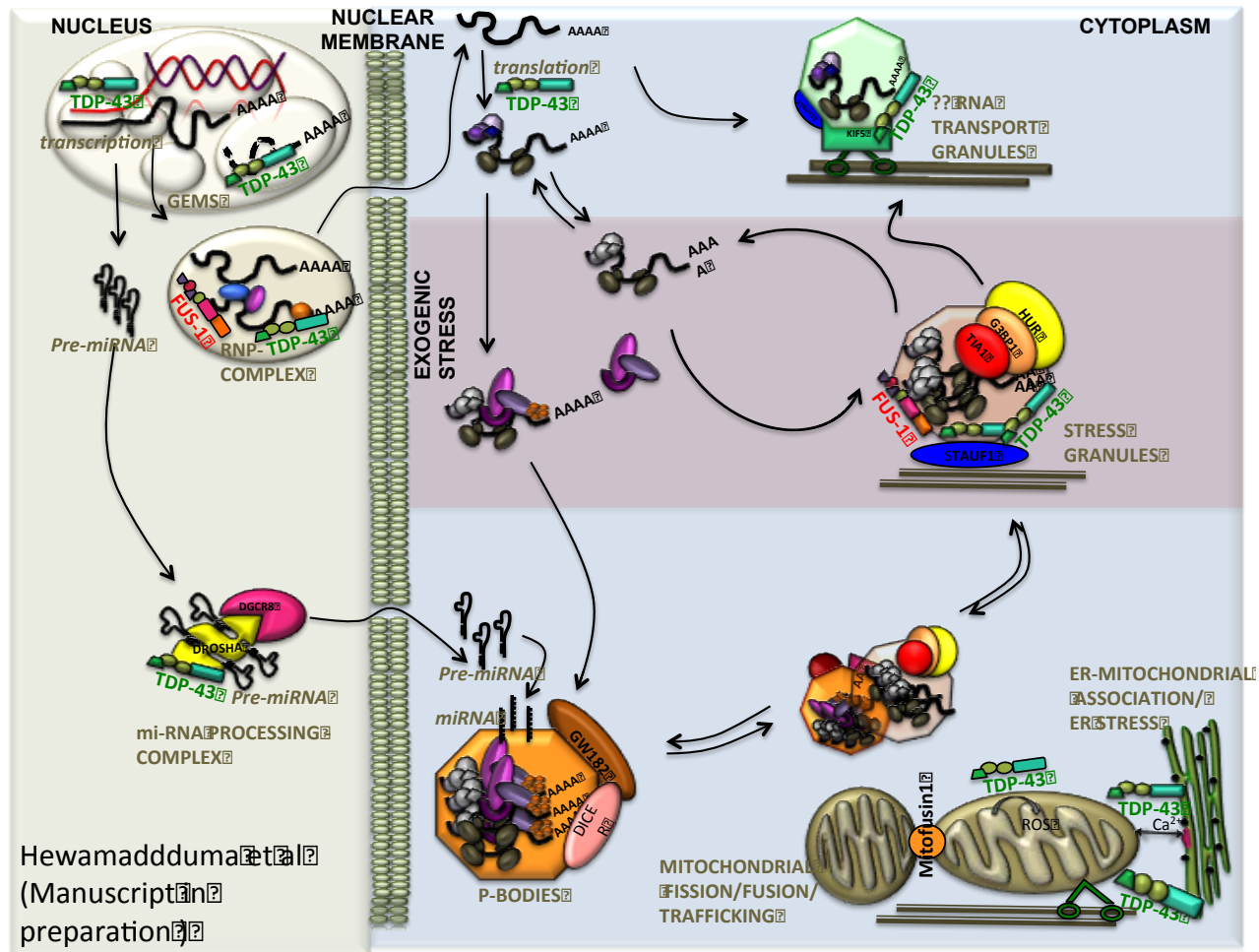
Figure 1.4 RNA modulating function of TDP-43: Possible mechanisms impaired when TDP-43/FUS1 are dysfunctional TDP-43. Transcription occurs in the nucleous and the pre-mRNA undergoes modifications by the splieosome into mature mRNA. Mature mRNA is assembled into to RNA granules along with several other molecules, i.e. RNPs, RBPs etc, to be targeted for spatio temporally determined localised translation. Therefore these RNA granules are actively transported out of the nucleous into the cytoplasm. These RNA granules then will be transported to predetermine sites of translation in different parts of the neuron. The fate of these RNA granules could vary i.e. in response to exogenic stress, RNA granules could form SG, which will consist of stalled translation complexes. When in association with P-bodies, RNA is degraded. P-body related RNA decay involves the participation of specific mRNA and miRNAs. The diagram also depicts the stages of miRNA development as well as involvement of RNA binding proteins implicated in ALS and their involvement in areas of RNA processing.

1.8.4.2 Pre mRNA splicing modulation function of TDP-43

Following transcription, pre mRNA undergoes splicing and post-transcriptional modification to become mature mRNA ready for the translational process to occur. The RRMs and the GRD of TDP-43 not only help it bind to DNA but also aid RNA binding using (UG)n repeats. The ability to bind to RNA gives TDP-43 scope to modulate pre mRNA splicing and mature mRNA regulation. The cystic fibrosis trans membrane conductance regulator (CFTR) gene exon 9 exclusion results in a dysfunctional protein. TDP-43 binds in a trans acting manner to the 3' splice site of CFTR pre mRNA in a (TG)m/(UG)n repeat sequence dependent fashion to enhance the exclusion of exon 09 whilst inhibition of the endogenous TDP-43 increased the exon 9 inclusion (Buratti et al., 2001). This could either be due to simple binding competition or TDP-43 interaction with proteins of the splicing complex, preventing the recognition of exon 9. A competitive RNA binding assay suggested that a minimum of 6 UG repeats are necessary for the efficient binding of TDP-43 to RNA. Deletion constructs of TDP-43 when assessed in a UV- cross linking assay to assess the essential RNA binding domains for the exon splicing revealed that the RRM1 domain, spanning residues 106-175, is crucial for this interaction. The RRM2, although not essential for RNA binding, helps form correct complexes needed for inhibition of splicing (Buratti and Baralle, 2001). In contrast, co-expression of TDP-43 deletion constructs with the CFTR exon 9 minigene by Bose et al (2008) showed that full length TDp-43 is required for exon 9 exclusion and the RRM motifs alone are insufficient (Bose et al., 2008). Taken together TDP-43 inhibition of splicing resulting in exon exclusion requires the interplay between RRM1 and RRM2 where RRM2 is necessary but not sufficient. Therefore, TDP-43 is similar to other RBP, for example, hnRNP A1, in utilising a double RRM motif-strategy to recognise and bind to RNA.

Confirming the exon exclusion function of TDP-43, Mercado et al reported that endogenous TDP-43 has a powerful negative effect on the splicing of the exon 3 of the *APOA2* gene. siRNA knock down of endogenous TDP-43 resulted in an increase in *APOA2* mRNA with Exon 3, despite the disruption of exon splicing enhancer sequence (ESE) regions, which are evolutionary, developed to balance the splicing activity of *APOA2*. This splicing modulatory function by TDP-43 is exerted via the typical TDP-43 binding substrate of a (UGn) repeat sequence in the second intronic region of *APOA2*. TDP-43 could be interacting with hnRNP H1 which is

another splicing inhibitor of *APOA2* whereby they prevent the recruitment of the U2AF65 exon splicing enhancer (Mercado et al., 2005). Altogether, TDP-43 when recruited to a (GU)n repeat sequence has a negative effect on splicing. TDP-43 not only influences exon exclusion but also enhances exon inclusion. A co expression study showed that TDP-43 enhances exon 7 inclusion in *SMN2* but did not change the exon-splicing pattern of *SMN1*, and required the RRM1 more than RRM2 (Bose et al., 2008). The TDP-43 mediated exon inclusion function does not require sequence specificity of the substrate pre mRNA . hnRNP proteins are implicated *trans* factors in both alternative and constitutive splicing of survival of motor neuron genes (*SMN1* and *SMN2*) exon 7. This splicing makes *SMN2* unable to compensate for any mutation in *SMN1*, resulting in a loss of functional SMN protein leading to spinal muscular atrophy (SMA) (Monani et al., 1999). An immunoprecipitation study using anti TDP-43 and anti Htra2-b1 antibody as the probe, demonstrated that TDP-43 exerted the exon inclusion effect via an interaction with Htra2-b1 in the presence of RNA. However RNAi knock down of endogenous TDP-43 did not affect the splicing pattern of *SMN2,* but altered CFTR exon 9 recognition indicating the TDP-43 effect is not an artifact. Therefore it is possible that TDP-43 binds to large multimeric splicing factors including hnRNP and Htra2 and inhibits the exon skipping effect of hnRNPs or forms new splicing complexes via protein-protein interactions to enhance inclusion of exon 7 (Bose et al., 2008).

Consistent with the role of TDP-43 in regulating pre mRNA is the microarray analysis of altered levels of transcripts, in cells depleted of TDP-43 by RNAi, which showed a 10-fold increase in the levels of *CDK6* transcript. CDK6 is essential in cell cycle regulation and in cell differentiation as Cdk6 enhances phosphorylation of pRb which is important for the regulation of factors controlling the cell cycle. Sequence analysis of the *CDK6* pre mRNA suggests a typical TDP-43 binding sequence, (GU)n repeats (n=25). Alteration of TDP-43 in chicken cells, which do not have *Cdk6* (GU)n repeats, does not alter the Cdk6 levels suggesting that human *CDK6* expression requires the binding of TDP-43 to the (GU)n repeats of the pre mRNA (Ayala et al., 2008a).

Confirming the findings in the *in vitro* and *in vivo* models that TDP-43 has a significant role in transcription regulation and pre mRNA modulation, is the evidence from Casafont et al (2009), wherein, in a primary cortical neuronal

culture system under physiological conditions, TDP-43 is co-localised within the nuclear compartments where pre mRNA splicing occurs (Buratti and Baralle, 2008, Casafont et al., 2009). For example, snRNP splicing factors in euchromatin areas and nuclear speckles where perichromatin fibrils are distributed. A recent study in HEK293T cells identified TDP-43 completely buried in Cajal bodies and also localised to Gemini of Cajal bodies (gems), which act as splicing factor storage sites or have a transcriptional regulation function (Fiesel et al., 2009) TDP-43 was found to be excluded from the nucleolus, peri chromatin granules and gene silencing centromeric and telomeric heterochromatin domains, which are free of transcriptional activity (Casafont et al., 2009).

TDP-43 role as a regulator of alternative splicing is demonstrated in a crosslinking and immunoprecipitation RNA clip assay coupled with RNA sequencing of brain tissues derived from mice treated with AMO to knockdown brain TDP-43. This study showed more than 39000 TDP-43 binding sites in the mouse transcriptome and lowering of TDP-43 resulted in reduced levels of more than 600 mRNAs and alteration of splicing pattern in more than 900 further mRNAs. Although acute lowering of TDP-43 is not reminiscent of the human disease model, it is appreciable the magnitude of RNA dysregulation associated with loss of TDP-43 from the nucleus where it plays its main roles of RNA modulation (Polymenidou et al., 2011). Furthermore, analysis of mice over-expressing WT and Q331K mutant TDP-43 demonstrated that ALS like phenotype develops independent of nuclear loss of over-expressed protein and cytoplasmic or nuclear accumulation, although loss of endogenous mouse Tdp-43 was associated with neurodegeneration. In addition these data further supports the notion that disturbance of the homeostasis of cellular levels of TDP-43 could cause wide spread alteration in splicing (Arnold et al., 2013).

1.8.4.3 mRNA stability and translational repression by TDP-43

TDP-43 also has structural similarities to two yeast proteins, a nuclear poly adenylated RBP involved in pre mRNA 3' UTR cleavage and polyadenylation, called HRP1 and a nucleolar protein, NSR1, implicated in 18S rRNA formation ((Lee et al., 1991, Wilson et al., 1994)), indicating a role in mature mRNA processing. Co-immunoprecipitation studies in both HEK293T cells over-expressing human neurofilament light chain (hNFL) and spinal cord lysates from ALS patients showed that hNFL mRNA 3'UTR interacts with endogenous TDP-43 and prevents

hNFL mRNA degradation when RNA synthesis is blocked by actinomycin treatment. (Strong et al., 2007, Glisovic et al., 2008). TDP-43 as previously well described uses UG elements in unique stem loop structures of the 3' UTR of the hNFL mRNA (Volkening et al., 2009). To understand the physiological functions of TDP-43, identification of TDP-43 responsive genes could be valuable. In a differential microarray analysis, Fiesel et al (2009) identified the histone deacetylase 6 (HDAC6) as a consistently suppressed gene in HEK293T cells depleted of TDP-43 by RNA interference (Fiesel et al., 2009). A biotin labeled HDAC6 mRNA pull-down assay coupled with a UV cross-linking immunoprecipitation study, identified that TDP-43 specifically interacts with HDAC6 mRNA. The RRM1 motif of TDP-43 is essential for this interaction. Depletion of the Drosophila TDP-43 orthologue TBPH also resulted in reduced HDAC6 expression levels (Fiesel et al., 2009).

In keeping with the biochemical data of the translational repression function of TDP-43 via mRNA repression is the finding of co-localisation of TDP-43 with a processing body (P-Body) marker GW182 in cultured neurons (Wang et al., 2008). TDP-43 behaviour in the neuronal dendrites has been paralleled with two other RNA granule markers, Staufen -1 and FMRP (Fragile X mental retardation protein), which also have a translational repression function and co-localise with P-Bodies. mRNA degradation, storage and miRNA mediated translational repression are some of the known functions of the P-body (Fillman and Lykke-Andersen, 2005). Taken together, TDP-43 and HDAC6 interaction both *in vitro* and *in vivo* models and TDP-43 co-localisation with P-body, provide evidence that TDP-43 has an important role in mRNA repression.

1.8.5 The role of TDP-43 in the formation of RNA granules, stress granules (SG), RNA sequestration, transport and decay.

Many RNA related processing mechanisms involve transcription and translation related functions. However RNA infrastructure involves a much wider group of functions, especially in eukaryotic cells. The RNA processes occurring within the nucleus are RNA mediated transcriptional regulation, transcription, the RNA processing cascade (mRNA, tRNA and rRNA processing) and RNP biogenesis and assembly. Within the cytoplasm, mRNA storage (RNA stress granules), translation (Ribosomes), RNA mediated translational regulation (P-bodies, miRNAs) and RNA degradation (P-bodies and exosomes) processes take place (Collins and Penny,

2009). TDP-43 has been described to play a role in some of these processes within the RNA-infrastructure network.

1.8.5.1 Recruitment of TDP-43 to the stress granules

Stress granules are cytoplasmic entities, which are formed following sublethal environmental stresses due to immediate block of the translational machinery with sequestration of actively translating mRNAs derived from disassembled polysomes, specific RNA binding proteins and stalled ribosomal subunits. Stress granules are in dynamic equilibrium with processing bodies (P-bodies) where constitutive ribonucleoprotein complexes, mRNA storage and decay and miRNA biogenesis occur, and polysomes where translation is initiated. Therefore SGs represent a protective mechanism to by-pass the stressful insult and to re-initiate translation after the stressful event has been overcome (Anderson and Kedersha, 2009).   Several environmental stressors have been reported to induce the formation of stress granules, for example, oxidative stress (arsenite), proteasome inhibition, osmotic stress and heat shock (Anderson and Kedersha, 2008). Studies done on transient transfection of TDP-43 in NSC-43 cells showed co-localisation of TDP-43 with stress granule markers, TIA-1 (T cell induced antigen 1) and HuR, when subjected to oxidative stress induced by arsenite treatment, ubiquitin proteasome system (UPS) inhibition by MG132 and by heat shock stress (Colombrita et al., 2009). The RRM1 domain of TDP-43, which is vital for its RNA associated functions, and the amino acid residues from 216 to 315 of the C-terminus are required for TDP-43 recruitment to the SG (Colombrita et al., 2009). Analysis of spinal cord samples of sALS cases reported TDP-43 positive inclusions but these were negative for the SG marker TIAR and HuR which is consistent with the fact that SG formation can be transient and in the cases studied SG could have formed earlier in the disease. Moreover, SG formation reported in the *in vitro* experiments are following acute stress, therefore SG formation in ALS motor neurons, which may have been subjected to chronic stress, may not be detectable in contrast to the *in vitro* studies. In disagreement with above findings is the work by Volkening et al (2009), who reported that the SG marker, TIA, and TDP-43 co-localised in neuronal cytoplasmic inclusions in sALS spinal cord material (Volkening et al., 2009).

TDP-43 also co-localised with staufen 1 and FMRP (Fragile X metal retardation protein) in a repetitive stimulation of a neural network model with

KCl (Wang et al., 2008). In an *in vivo* model of TDP-43 cytoplasmic localisation, Misse et al (2009) observed an enhancement of SG formation and TDP-43 recruitment to the SG, in a time dependent manner, in a neuronal injury paradigm of sciatic nerve axotomy, suggesting that TDP-43 localisation to SG is a response to neuronal injury (Moisse et al., 2009b).

TDP-43 has been shown to colocalise with staufen-1 and FMRP (Wang et al., 2008) which are well characterised RBPs, which in addition to taking part in SG formation, are also involved in mRNA transport and regulation of localised initiation of translation in neuronal dendrites (Hirokawa, 2006). Thus, TDP-43, although a nuclear protein, shuttles out to the cytoplasm to recruit itself to the mRNA triaging bodies, SG, where regulatory mechanisms of translational arrest take place, and regulates mRNA transport, in keeping with the other RBPs which shuttle efficiently in and out of the nucleus to participate in essential cytoplasmic functions.

1.8.6 Recruitment of TDP-43 to the processing body (P-body)

Processing bodies as explained above, are cytoplasmic aggregates, which unlike SG, occur in both physiological and stressful conditions. They mainly consist of 5' to 3' mRNA decay machinery, including decapping protein 1 (DCP1), and assemble on translationally stalled mRNA from disassembled polysomes. Some of the functions of P-bodies are mRNA decay, mRNA storage and miRNA biogenesis and miRNA mediated repression of translation (Kedersha and Anderson, 2007, Anderson and Kedersha, 2008). Neither, with oxidative stress in the NSC-34 cell model (Colombrita et al., 2009) nor in neuronal injury via mouse sciatic nerve axotomy, did TDP-43 localise to P-bodies. However, in a neuronal activity response analysing model, TDP-43 expression was increased following repetitive stimulation with KCl and co-localised with both staufen -1, an mRNA transport granule and SG marker, and with a P-body marker GW-182 (Glycine (G)-Tryptophan (W) protein 182). This suggests that TDP-43, in addition to mRNA triaging, sequestering and regulating the stability of mRNAs, is required for localised translation, which also probably could regulate the biogenesis of miRNA, and miRNA mediated translational repression.

1.8.7 Cell cycle regulation and association of TDP-43 with apoptosis and neuronal survival

Retinoblastoma protein (pRb) is a tumour suppressor protein essential for the regulation of cell cycle progression, cell differentiation and genomic integrity maintenance. Transition of the cell cycle from the G1 phase to the S phase depends on activation of certain gene transcription factors, which promote cell proliferation. Activation of these transcription factors occurs via inactivation of the pRb protein through its gradual phosphorylation. Phosphorylation of pRb is mediated by several Cdks. siRNA mediated knock down of TDP-43 in U2OS cells resulted in increased levels of Cdk6 which enhanced phosphorylation of pRb. As a result the cell cycle was disrupted by a decrease in cells in G0 phase and an increase in S, G2 and M phase cells. TDP-43 represses gene transcription (Ayala et al., 2008a), and SP-10 is important in terminal cell differentiation of round spermatid cells (Acharya et al., 2006). Taken together in the context of the central nervous system, TDP-43 could play a role in the development of the neural systems and terminal differentiation of the nervous system, but further studies are required to ascertain the relevance of cell cycle regulation in neurodegeneration.

Ayala et al (2008) also reported that loss of TDP-43 is associated with an increase in cell death. About 30% of TDP-43 depleted U2OS cells were TUNEL stain positive and about 15% of the cells contained YH2AX foci indicative of double stranded DNA breaks. These cells were also positive for PARP1 (Poly ADP ribose polymerase-1) cleavage in keeping with enhanced programmed cell death (Ayala et al., 2008a). Activation of pRb is reported to enhance apoptosis. Thus loss of TDP-43 could result in increased programmed cell death and apoptosis, and premature activation of programmed cell death in neuronal cells could result in premature neurodegeneration.

The Smad related TGF Beta signaling pathway is important in regulating levels of transcription factors, co-activators and co-repressors in a cell specific and ligand dose dependent manner. When TGF beta-receptors are activated, internalised TGF beta phosphorylated Smad 2 and 3 (pSmad2/3). pSmad2/3 translocates from the cytoplasm to the nucleus to control gene expression. TGF beta mRNA is up regulated following neuronal insult. Therefore the TGF-Beta –Smad signaling pathway is essential for maintaining neuronal survival (Flanders et al., 1998). Immunohistochemistry of lumbar spinal cord sections from sALS cases showed

disrupted translocation of pSmad2/3 to the nucleus. However in sALS spinal cord material pSmad 2/3 was found to co-localise with TDP-43 in the nucleus (Nakamura et al., 2008). Contrary to what these authors mention, this indicates that TDP-43 has a role in neuronal survival either as a positive role by sequestering pSmad 2/3 in the nucleus or as a negative effect, that pSmad2/3 attempts to counteract. The exact role of TDP-43 and pSmad2/3 interaction awaits further investigation.

1.8.8 TDP-43 as a neuronal plasticity and neuronal activity response factor

Neuronal plasticity is a process by which new learning and behavior occur by strengthening existing neural connections or by losing or gaining new, neuronal connections (Dubnau et al., 2003, Jin et al., 2004). In order to modulate neuronal plasticity, modulation of synaptic plasticity is vital. RNA binding proteins (RBP) FMRP, implicated in mental retardation and poor memory associated with fragile X syndrome (Jin et al., 2004), and staufen 1 considered important in long term memory of fruit flies (126), are vital for the regulation of synaptic plasticity of neurons. Similar to TDP-43, the above RBP also have RRM and a RGG box, shuttle in and out of the nucleus using NLS (nuclear localising signal) and NES (nuclear export signal) and co-localise with SG. Consistent with the above information are the results from the model of repetitive hippocampal neuronal stimulation with KCl, wherein TDP-43 co-localises with FMRP and staufen 1 in dendritic granules and behaved synergistically with FMRP and staufen 1 (Wang et al., 2008). Thus it appears that TDP-43, along with other RBPs plays the role of a neuronal activity response factor, which regulates transportation of mRNA, reassembly of the translational apparatus and modulation of localised translation in the dendrites, which are considered essential aspects of neuronal plasticity (Jin et al., 2004).

1.8.9 Scaffold for nuclear bodies and maintenance of nuclear membrane stability

The eukaryotic nucleus contains a number of substructures with several associated functions. These sub-structures relate to nuclear compartments with different biological functions related to transcription, splicing, transcription factor storage etc. The Cajal body or coil body contains snRNPs and contains the

signature protein coilin. The GEM body is another nuclear sub-structure containing several snRNPs, also including Cajal bodies, and SMN is a unique marker of the GEM bodies. SC35 nuclear speckles or inter-chromatin granules are classic sites of regulation and assembly of splicing. Wang et al (2009) described a nuclear body-containing mouse TDP-43 (mTDP) called TDP Bodies (TB) . Immuno-staining of HEK 293T cells transfected with mTDP showed co-localisation of TB with GEM bodies when SMN was used as the marker for GEM bodies. This co-localisation is mediated by an interaction between mTDP and SMN. TBs are also shown to associate with several other nuclear bodies, for example SC35, POD (Promyeloctic leukaemia body), but not with nucleoli and HDAC5 bodies (Wang et al., 2002). Taken together, TDP-43 containing bodies, TB, act as a nuclear scaffold for the other nuclear bodies which network through TB, trafficking various nuclear factors required for transcription (initiation, elongation, splicing, 3' cleavage) and splicing (assembly of spliceosomal factors), along with storage and recycling of snRNPs.

TDP-43 depletion in U2OS cells was associated with increased cell death nuclear membrane blebbing and aberrant nuclear morphology due to disruption of the distribution of the nuclear envelope protein emerin. The nuclear membrane defects, due to TDP-43 depletion, are mediated by changes in pRb levels (Ayala et al., 2008a).

1.8.10 TDP-43 protein-protein interactions: Clues to more functional roles (PGRN, VCP, pSmad 2/3, UBQLN)

TDP-43 like its other paralogues, interacts with other proteins and with each other, using its GRD. A GST pull down assay using GST-TDP-43 and subsequent mass spectroscopy identified several hnRNP proteins as potential interacting/binding partners. Amongst many functions of these hnRNPs, splicing regulation is prominent in hnRNPA1, hnRNPA2/B1 and hnRNP C1/C2 (Buratti et al., 2005), whilst hnRNP A3 is a recognised cytoplasmic RNA trafficking molecule (Ma et al., 2002). Confirming the above finding was the EMSA super-shift assay testing the binding efficiency of progressive deletion constructs of TDP-43 to hnRNP A2. This showed that TDP-43 C-terminal amino acids 321-366 were vital for this interaction. This was also confirmed in an *in vivo* assay with the Drosophila TDP-43 homologue TBPH (D'Ambrogio et al., 2009).

In a yeast two-hybrid screen using a human fetal brain cDNA library, Kim et al (2008) identified Ubiquilin (UBQLN) as a TDP-43 binding partner. Ubiquilin has an amino terminal ubiquitin like domain and a C-terminal Ubiquitin association domain (UBAD) (Kim et al., 2009). Ubiquilin is a protein of interest in the neurodegeneration in that it binds to Presenilin 1 and Presenilin 2 proteins, which are implicated in inherited form of Alzheimer's dementia due to presenilin mutations (Mah et al., 2000). Confirming the yeast-two-hybrid screening results, a GST pull down assay using GST TDP-43 showed interaction of UQBLN with TDP-43 using its UBAD. UBQLN over-expression resulted in sequestration of over-expressed and to a minor extent, the endogenous TDP-43 to cytoplasmic aggregates. Furthermore, treatment with Concanamycin A, an autophagosomal cargo proteolysis inhibitor, causes TDP-43 and UBQLN to co-localise in autophagosomes (Kim et al., 2009). Autophagy is a protective response, and TDP-43 interaction with UBQLN could be a cytoprotective response, and needs further investigation. Two further Yeast-two-hybrid screening studies on protein-protein interactions have identified, PM/Scl100 and XRN2 (indicated in mRNA decay), ZHX1 (implicated in transcriptional repression), NSFL1C and ARF6 (involved in membrane trafficking) and SETDB1 (important in chromatin remodeling regulation) as potential binding partners for TDP-43 (Buratti and Baralle, 2009). In an immunoprecipitation assay using protein extracts from the spinal cord specimens of a mutant SOD1 (A4T) case, TDP-43 pulled down SOD1 (A4T), WT SOD1 and 14-3-3 protein. However, the TDP-43 interaction with 14-3-3 appears to be dependent on RNA, as removal of RNA abolished the immunoprecipitation of the 14-3-3 with TDP-43 and there was no co-localisationof TDP-43 with 14-3-3 in immunohistochemistry studies of the same case. Nevertheless, TDP-43 interaction with SOD1 was confirmed by confocal imaging where both co-localised, to the cytoplasmic aggregates. Both TDP-43 and SOD1 have RNA binding capacity and interact with hNFL mRNA (Volkening et al., 2009). Thus, TDP-43 and SOD1 perhaps form a part of a large RNA binding protein complex. Using immunoprecipitation with a TDP-43 antibody and subsequent mass spectroscopy Volkening et al (2009) revealed several binding partners for TDP-43. A nuclear importation factor, Karyopherin; an RNA granule transportation factor in neurons, kinesin, and a molecular chaperone, chaperonin were amongst the hits (Volkening et al., 2009). This finding is consistent with the findings of Moisse et al (2009) who

showed in a mouse axotomy model that the presence of TDP-43 in the cytoplasm, is implicated in the neuronal injury response, where it assumes a role in active transportation of relevant mRNA's targeted for cytosolic localised assembly of the translational machinery (Moisse et al., 2009b).

In conclusion, TDP-43 has multiple cellular functions both in the nucleus and in the cytoplasm. These multiple functions of TDP-43 are exerted through its own structural characteristics and via other interacting proteins and molecules. The description of the association of mutations in another gene coding for a RNA/DNA interacting protein called fused in sarcoma / translocated in sarcoma (FUS/TLS) gene with ALS provides TDP-43 a partner in crime (Kwiatkowski et al., 2009, Vance et al., 2009). The findings that mutations in TDP-43 and FUS/TLS1 have established reasonably, that dysfunctional RNA processing is an important pathophysiological process in ALS and other neurodegenerative conditions, with potential therapeutic implications.

1.9 Localisation of TDP-43: Is cytoplasmic localisation a pathogenic or a protective response?

The discovery of the association of TDP-43 with neurodegenerative conditions like ALS and FTLD was made when TDP-43, which is largely a nuclear protein, was identified as the major component of the disease related inclusions in the cytoplasm of neurons and glia (Neumann et al., 2006). Since then it is considered that the cytoplasmic translocation of TDP-43 in motor neurons is a pathological characteristic of sALS and non-SOD1 fALS. The translocation of TDP-43 to the cytoplasm is also associated with relative clearing of TDP-43 from the nucleus (Neumann et al., 2006, Mackenzie et al., 2007). Several investigations have identified key features of TDP-43 localised to the NCI, for example, insoluble aggregation, ubiquitination, phosphorylation and C-terminal fragmentation of TDP-43. It still remains an enigma whether the cytoplasmic translocation of TDP-43 is solely reflecting a pathogenic process or a neuro-protective response to cellular injury.

1.9.1 Structural determinants of TDP-43 localisation

Under physiological conditions, *in vitro*, *in vivo*, and in postmortem investigations of material from neurologically normal cases, TDP-43 has been shown to largely

localise to the nucleus. Winton et al, 2008, estimated that in rat hippocampal neurons, about 15% of the total TDP-43 is detected in the cytoplasm (Winton et al., 2008a). Some investigators consider this cytoplasmic fraction of TDP-43, to have a functional role, whilst others argue for a pathological role. Ayala et al (2008) in an inter species heterokaryon assay described that WT TDP-43 shuttles in and out of the nucleus, rapidly and continuously (Ayala et al., 2008b). This finding is consistent with the function of the TDP-43 paralogues, hnRNP proteins, which are well described to travel between the two compartments (Krecic and Swanson, 1999). Structural analysis of the TDP-43 N-terminus revealed a bipartite nuclear localisation signal (NLS), which consists of a lysine-arginine-lysine sequence separated by 10 amino acids from the next Lysine-V-lysine-arginine sequence between amino acids 82-98. A deletion mutation construct over-expression study showed that the NLS is essential for targeting TDP-43 protein to the nucleus, and the deletion of the NLS resulted in cytoplasmic aggregation of not only the over-expressed, but also the endogenous TDP-43 (Winton et al., 2008a), in a manner, that recapitulates the nuclear clearing and cytoplasmic sequestration of TDP-43 seen in ALS and FTLD-U cases. These findings were confirmed by results from a study of mouse hippocampal neurons which also showed that cytoplasmic aggregation of TDP-43 was associated with sequestration of nuclear TDP-43, which contained ubiquitinated, insoluble and C-terminally fragmented TDP-43 (Winton et al., 2008a) as well as abnormal phosphorylation (Nonaka et al., 2009a). In keeping with above, the A90V mutation of TDP-43, located within the NLS but in between bipartite loci, was identified in association with fALS, and *in vitro* expression of A90V TDP-43 resulted in cytoplasmic aggregation of TDP-43 along with nuclear clearing, suggesting that perturbation of the NLS sequence could potentially be pathogenic (Winton et al., 2008b). Sequestration of endogenous TDP-43 by the over-expressed TDP-43 is predicted to be as a result of protein-protein interaction such as oligomerisation, which can affect the targeting of both (Ayala et al., 2005).

In keeping with the above finding are the observations made in a TDP-43 expression study in temperature sensitive BN2 cells containing a regulator of chromosome condensation 1 (RCC1) gene mutation. These BN2 cells, when subjected to a non permissive 39.5°C temperature, showed TDP-43 accumulation in the cytoplasm, along with the endogenous nuclear TDP-43 in a Ran GTP

dependent manner. BN2 cells with the *RCC1* gene mutation are non-permissive at 39.5 °C as the nuclear Ran GTP translocates to the cytoplasm, as a result the transportation of proteins to the nucleus is blocked (Winton et al., 2008a). The NLS is recognised by importin alpha/beta (also known as karyopherin), which is implicated in nuclear transportation of proteins (Otis et al 2006). Importin beta interacts with Ran-GTP. Interestingly, a recent immunoprecipitation assay identified karyopherin (importin) as a potential TDP-43 binding protein (Volkening et al., 2009). Confirming the above interactions are the observations by Sato et al (2009), wherein knock down of importin in SHSY-5Y cells by siRNA, excluded TDP-43 from the nucleus (Sato et al., 2009).

Winton et al, using bioinformatics, predicted that a leucine rich nuclear export signal (NES) is located within 239-250 amino acids, and in a mutagenesis study confirmed that disruption of the NES leads to accumulation of TDP-43 in distinct punctate inclusions within the nucleus, which were insoluble (Winton et al., 2008a). The observations in an interspecies heterokaryon model showed that TDP-43 shuttles in and out of the nucleus in a NLS/ NES dependent manner which was neither dependent on the transcriptional status of the cells nor the RRM1 domain (Ayala et al., 2008b). Deletional mutations of the C-terminus produced variable cytoplasmic translocation, but were noted to result in distinct nuclear inclusions, which were devoid of DAPI stain suggesting they were dense bodies. In contrast to the aforementioned observation are results from the yeast model where the C-terminal truncation of TDP-43 resulted in nuclear localisation but not cytoplasmic aggregation (Johnson et al., 2008). RRM1 deletion also resulted in the formation of nuclear inclusions and a redistribution of TDP-43 within the nuclear compartments (to the soluble nucleoplasm and the structure bound nuclear matrix and chromatin enriched in transcribed genes component) (Ayala et al., 2008b). Thus, TDP-43 is well structured to shuttle within the nucleus and in between the nucleus and the cytoplasmic compartments, and perturbation of this finely balanced transportation results in dramatic clearing of TDP-43 from the nucleus and aggregation in the cytoplasm and/ or nuclear inclusion formation, which recapitulates the abnormal compartmental localisation of TDP-43 seen in the ALS disease state.

The C-terminus is important in the alternative splicing function of TDP-43 and progressive deletion construct over-expression assays have shown that C-terminus

deletion results in cytoplasmic translocation of TDP-43 (Ayala et al., 2008b, Nonaka et al., 2009c). Ayala et al 2008 showed that progressive deletion of the C-terminus results in a progressive shift towards a cytoplasmic localisation of TDP-43 (Ayala et al., 2008b). In keeping with the above studies are the findings from the yeast TDP-43 proteinopathy model, where both the RRM motif and the C-terminus were shown to be important in TDP-43 localisation to the cytoplasm (Johnson et al., 2008).

1.9.2 Could the cytoplasmic localisation of TDP-43 be a cyto-protective response?

As described above, under physiological conditions 15% of TDP-43 is present in cytoplasm and perhaps also contributes to the component of TDP-43 which shuttles in and out the nucleus. In a tightly controlled cellular environment, it is impossible to believe that shuttling of TDP-43 to the cytoplasm did not have a beneficial role to the cell. A mouse sciatic nerve axotomy model presented by Moisse et al 2008, showed an enhanced expression of cytoplasmic TDP-43 immuno-reactivity following axotomy in the ipsilateral ventral horn motor neurons, along with lack of nuclear TDP-43 expression in some motor neurons (Moisse et al., 2009b). This is in keeping with observations made in the analysis of motor neurons in ALS spinal cords, where an up-regulation of TDP-43 was noted (Strong et al., 2007). Furthermore, TDP-43 was found to co-localise with the RNA transport granule marker staufen 1, but not with a P body marker (Moisse et al., 2009b), suggesting that TDP-43 is translocated to the cytoplasm following axonal injury and perhaps takes a role in transporting essential mRNAs required for axonal repair, indicating a physiological/biological response to neuronal injury. This response could be impaired in the presence of ALS related aberrant cellular resources such as deficient NFL mRNA (Moisse et al., 2009a).

In an axonal ligation model of the mouse hypoglossal nerve, Sato et al 2009, showed that the TDP-43 is transiently excluded from the nucleus and co-localised with cytoplasmic inclusions positive for staufen 1 and TIA 1, which are markers for RNA transport granules and stress granules, respectively, whilst the total TDP-43 mRNA level, assessed by laser capture micro-dissection of the hypoglossal motor neurons, was retained at a normal or increased level (Sato et al., 2009). The association of TDP-43 with RNA transport granules and stress granules of

hypoglossal nerve motor neurons whose axons are ligated further confirms that TDP-43 shuttles out the nucleus in response to axonal injury. TDP-43 was also isolated from mouse brain stem microsomal fractions of endoplasmic reticulum (ER) or autophagosome, suggesting the possibility that it is transported in vesicles (Sato et al., 2009). Furthermore, exclusion of nuclear TDP-43 was not lethal to the neurons and return of normal nuclear TDP-43 staining correlated with the return of ChAT (Choline acetyl transferase) staining, suggesting that redistribution of TDP-43 was dependent on the innervation status of the neurons (Sato et al., 2009). Translocation of TDP-43 to the cytoplasm is also seen upon ligation of the vagus nerve, suggesting that re-distribution of TDP-43 is not limited to motor neurons. However if the translocation of TDP-43 to the cytoplasm occurred over a long period of time, as perhaps it might occur in MND, due to continued bombardment of the neurons with cellular stressors, chronic sequestration of TDP-43 might cause neuronal toxicity. In support of this claim is the increased cell apoptosis consequent to the loss of TDP-43, following siRNA knock down of TDP-43 (Ayala et al., 2008a).

Although the axonal injury paradigm tested in the above studies demonstrated cytoplasmic translocation of TDP-43 following neuronal injury, immunohistochemistry analysis of brain tissues obtained from cases of anoxic and ischaemic brain injury and cerebral neoplastic lesions has not shown TDP-43 positive inclusions in the cytoplasm, raising the question of the specificity of TDP-43 inclusions in neuronal injury (Lee et al., 2008). The accumulation of the TDP-43 cytoplasmic inclusions represents a common pathway for a subset of heterogeneous group of neurodegenerative diseases as SOD1 ALS cases do not show TDP-43 pathology (Mackenzie et al., 2007).

TDP-43 co-localises with markers of stress granules such as staufen 1 and HUR (Colombrita et al., 2009). The formation of SG is a protective mechanism to by-pass the stressful cellular insult and to re-initiate translation after the stressful event has been overcome. Although TDP-43 is not essential for the assembly of the SG, it is reasonable to believe that association of TDP-43 with SG by translocating to cytoplasm represents a cyto-protective response.

1.9.3 Could the cytoplasmic localisation of TDP-43 represent a pathogenic process?

Since the trail blazing discovery of the association of TDP-43 with ALS and FTLDU by Neumann et al (2006) in a proteomic study, TDP-43 positive cytoplasmic inclusions have been described in several neurodegenerative conditions in addition to ALS and FTLDU, the so called TDP-43 proteinopathies. The hallmarks of TDP-43 proteinopathy are C-terminally fragmented, phosphorylated, ubiquitinated, insoluble cytoplasmic inclusions. It still remains an enigma as to whether these inclusions are the cause or the effect of ALS and if they are protective or harmful to the neurons. It is now well established from mutation screening analysis that mutant/aberrant TDP-43 causes ALS and that pathological studies on postmortem material from such cases have shown mis-localisation of TDP-43 to the cytoplasm, indicating that the mis-localisation could be harmful. This phenomenon is reminiscent of tau and alpha synuclein, the disease proteins, which form neuronal aggregations, and are implicated in neurodegenerative conditions which are collectively known as either tauopathies (Alzheimers dementia) or alpha synucleinopathies (Parkinson's and Lewy body dementia) (Goedert, 2001).

1.9.4 Phosphorylation of TDP-43

Although the pathological significance of phosphorylation is unclear, phosphorylation is important in regulating transcription and pre mRNA splicing. The other members of the hnRNP family are known to be phosphorylated *in vivo* which is an important post-translational modification, in protein-protein and protein-RNA interactions. In agreement with the above, phosphorylation of hnRNP K results in inhibition of mRNA translation and cytoplasmic accumulation (Habelhah et al., 2001) and stress induced MAP kinase 3/6-P38 mediated hyperphosphorylation of hnRNP A1 and cytoplasmic aggregation (van der Houven van Oordt et al., 2000). Structural analysis of TDP-43 suggests several potential phosphorylation sites and phosphorylation of TDP-43 may be responsible for aggregation. The phosphorylation of TDP-43 came into light in the pioneering study on TDP-43, when Neumann et al (2006) described a 45kDa band in addition to 43kDa band, and upon dephosphorylation the 45kDa band collapsed to 43kDa, indicating that TDP-43 undergoes phosphorylation. Furthermore, monoclonal anti

phosphorylated-TDP-43 antibodies detected C-terminal fragments of TDP-43, 24kDa and 26kDa bands in the urea fraction of the immunoblots of postmortem material from FTLDU cases and ALS cases .

However, interestingly, these monoclonal antibodies, specific to phosphorylated TDP-43, did not detect any immunoreactivity in control brains, suggesting that the monoclonal antibodies only detected specific post translational modifications or conformation/s unique to TDP-43 proteinopathy. In keeping with the above results, several pathology studies involving extensive analysis of normal cultured cells, rat, mouse and human brains, have failed to detect phosphorylated S409/410 TDP-43 (Inukai et al., 2008, Neumann et al., 2009). Hasegawa et al 2008, also did not detect immunoreactivity in normal brains with several different polyclonal antibodies specific to phosphorylated serine residue 91 and 92 (pS91 and pS92) residues of TDP-43 (Hasegawa et al., 2008a). Hasegawa et al 2008, described using several polyclonal antibodies, that five serine residues at the C-terminus of the TDP-43 were specifically phosphorylated and that Casein Kinase 1 or 2 is responsible for the phosphorylation (Hasegawa et al., 2008a).

The monoclonal antibodies engineered to detect aberrant phosphorylation of serine residues S409/410, detected NCI in familial and sporadic forms of FTLD-U due to mutations in progranulin, VCP and linkage to chromosome 9p and ALS cases. Taken together, these findings indicate that phosphorylation of TDP-43 is a disease specific phenomenon and hence likely to be pathogenic. *In vitro* studies have also shown that phosphorylation results in the formation of oligomers and filamentous structures. These abnormal filamentous structures can be neurotoxic and are reminiscent of taupathies and alpha-synucleinopathies (Goedert, 2001, Hasegawa et al., 2008a).

1.9.5 Ubiquitination of TDP-43

The formation of ubiquitin, a 76 amino acid protein, positive NCI in diseased brains is a pathological characteristic of many neurodegenerative conditions such as FTLDU, Parkinson's and Alzheimer's diseases. Whilst the residues of TDP-43 responsible for ubiquitination are yet to be demonstrated, residues corresponding to lysines are plausible candidates. The ubiquitin proteasomal pathway (UPP) and the autophagy-lysosomal pathway (ALP) are the two main protein degradation pathways. TDP-43 has been shown to interact with the proteasome targeting

factor, ubiquilin-1 (UBQLN) in a yeast two hybrid assay. Under physiological conditions UBQLN binds to ubiquitylated TDP-43 resulting in sequestration to autophagosomes, which could be a protective mechanism (Kim et al., 2009). However, aberrant TDP-43 (D169G TDP-43 mutant) could not bind to UBQLN, resulting in impaired sequestration, leading to aberrant cytoplasmic accumulation and in turn resulting in neuronal injury (Kim et al., 2009). Further strengthening the ubiquitination of TDP-43 as a pathogenic phenomenon are the TDP-43, 25kDa C-terminal fragment over-expression studies which showed increased aggregation formation in HEK293T cells upon treatment with the UPP inhibitor, MG132 and with ALP inhibitors. Both the ALP and UPP systems appear to be important in the clearance of aberrant TDP-43 and the accumulation of C-terminal fragments suggests derangement in the UPP and/ or the ALP pathway (Wang et al., 2009).

1.9.6 Cleavage

Neumann et al alluded to the fact that TDP-43 in the NCI of FTLDU and ALS cases are C-terminally fragmented in addition to the phosphorylation and ubiquitination changes described above. Since then Zhang et al 2007, reiterated that caspase-3 proteolytically cleaved TDP-43 to generate 25kDa and 35kDa fragments and described in detail the potential cleavage sites: DETD (aa 86-89) and DVMD (aa216-219). Zhang et al also described that, a candidate gene for FTLDU, progranulin, when down regulated, favours the above cleavage (Zhang et al., 2007). Furthermore, Igaz et al 2009, demonstrated the presence of 22kDa and 24kDa C-terminal TDP-43 fragments in the urea fraction of FTLDU brain extracts and recapitulated the pathological features of TDP-43 proteinopathy, by over-expressing the C-terminal fragments spanning amino acids 208-414 and slightly longer in a N2a cell culture system. They also demonstrated that the presence of CTFs is enough to initiate phosphorylation, ubiquitination and cytoplasmic aggregation (Igaz et al., 2009). These findings were in agreement with that of Nonaka et al 2009, who described several cleavage sites (at aa 208, 219 and 247) by protein sequencing (Nonaka et al., 2009c). Nishimoto et al described caspase 3 dependent (not detected in caspase-3 null mouse embryonic fibroblasts system) and independent CTF (detected in caspase-3 null mouse embryonic fibroblasts system and therefore thought to be translational isoforms produced by alternate translational start sites) that were of the same molecular weight: 25kDa and

35kDa. The 25 and 35kDa CTF were phosphorylated as in TDP-43 proteinopathy, but in a site-directed mutagenesis study where the phosphorylation sites were mutated the formation of the CTF was not altered and the pattern of localisation was not changed suggesting that phosphorylation is not essential for CTF generation and localisation to the cytoplasm (Nishimoto et al., 2009). Several studies have shown that 25 and 35kDa CTFs impair the nuclear functions of TDP-43 as indicated by the impaired splicing function of the CFTR exon splicing assay (Nishimoto et al., 2009, Nonaka et al., 2009c, Zhang et al., 2009). However, the CTF constructs used in most of the molecular biology studies of TDP-43 do not have the NLS, without which TDP-43 has been shown to have a defective localisation to the nucleus. To make matters more interesting, there is evidence to support that pathological aggregation of potentially toxic proteins i.e. polyglutamine and beta amyloid, might be neuroprotective and may not be involved in disease pathogenesis (Arrasate et al., 2004, Orr, 2004).

1.9.7 SUMOylation of TDP-43

Small ubiquitin like modifier (SUMO) proteins are a family of small proteins which are bound or removed from other proteins as a post translational modification, which is implicated in various cellular functions such as transcription, cell cycle regulation, nuclear cytoplasmic trafficking, apoptosis, stress response etc. The process of post translational modification where covalent bonding of SUMO proteins occurs is called SUMOylation (Vertegaal et al., 2004, Hay, 2005). In a complex quantitative proteomics approach involving SILAC (multiplex stable isoptope labeling with amino acids in culture) strategy, Seyfried et al 2010 identified significant co-localisation of SUMO 2/3 and ubiquitin within detergent insoluble aggregations of TDP-43 splice isoform called TDP-S6 (~28 kDa) in a cell culture system (Seyfried et al.). Confocal studies carried out on the same system showed co-localisation of TDP-S6 with SUMO 2/3 in nuclear inclusions. In keeping with above findings, TDP-43 has been shown to localise with nuclear bodies, PML bodies, which have been shown in independent studies, to co-localise with SUMO2/3 (Wang et al., 2002, Vertegaal et al., 2004). TDP-43 sequence analysis has suggested a canonical SUMO conjugation site spanning amino acids 135-138 amongst potential SUMO targeted lysines (Geiss-Friedlander and Melchior, 2007, Golebiowski et al., 2009). Confirming the TDP-43 SUMOylation theory, Golebiowski

et al 2009 identified a seven fold rise in TDP-43 and SUMO-2 conjugation in response to heat shock (Golebiowski et al., 2009).

If the proteins are ubiquitinated, phosphorylated and SUMOylated and translocated to the cytoplasm, leaving the nucleus devoid of TDP-43 for its transcription and translational functions, and targeted for proteasome mediated degradation, it can be hypothesised that TDP-43 translocation to the cytoplasm over a period of time is harmful to the neuron. The association of ARP1 (actin - related protein 1) and enrichment of SUMO 2/3 in the TDP-43 inclusions further strengthens the hypothesis that disruption of the TDP-43 equilibrium could result in an imbalance in the protein sorting pathways/ systems. ARP1 is a subunit of the macromolecular complex, dynactin, which interacts with microtubules and dynein. ARP1 is also implicated in protein transportation and vesicular trafficking (Schroer et al., 1996). Seyfried et al 2010 described the association of over-expressed TDP-S6 (Transcription isoform, 28kDa) with up regulation of poly-ubiquitinated linkages, which could facilitate the formation of inclusions and guide them for autophagy (Seyfried et al.). Another subunit of the dynactin complex, p150Glued, when mutated, causes ALS in mice and has also been associated with ALS in humans (Munch et al., 2004). The aggregation of TDP-43, following phosphorylation and SUMOylation, is likely to be the primary role of C-terminal fragments of TDP-43 which can also sequester the endogenous full length TDP-43 to the cytoplasmic inclusions, thus impairing the nuclear functions of TDP-43 resulting in neuronal dysfunction and degeneration.

1.9.8 Prion like behaviour of TDP-43

The concept of prion-like behaviour was applied to neurodegenerative conditions based on two observations. Firstly the Braak's proposal of propagation theory of Lewy related alpha synucleinopathy from the medulla oblongata rostral to the neo-cortex, which has some similarities to that of bovine spongiform encephalopathy (Braak et al., 2003). Secondly the notion of prion like spread similar to the infectious prions came about with observations relating to the molecular characteristics of seeded aggregation and spreading of neurodegenerative proteins, in particular the misfolded conformations of Abeta plaque aggregation shown in primate experiments when brain extracts obtained from human Alzheimer's disease patients were injected into primates (Baker et al., 1994). These findings

were also then confirmed in a mouse model where showed that presence of pre-formed Abeta aggregates hastens the Abeta aggregation (Kane et al., 2000). TDP-43 is considered to have prion like domain, where there is a Q/N rich region in the C-terminus. Proteins with Q/N rich domains, including TDP-43 have been shown to bind to polyglutamine inclusions. In deletion construct expression assays, residues 320-367 of TDP-43 have been demonstrated to be important for polyglutamine aggregate binding. Therefore it is possible that polyglutamine aggregates can propagate or seed aggregation of Q/N rich proteins like TDP-43. Interestingly polyglutamine aggregate interaction of TDP-43 results in sequestration of endogenous TDP-43 into the aggregations resulting in loss of nuclear TDP-43 (Fuentealba et al., 2010). This loss of nuclear TDP-43 is an important pathogenic step in the dysfunctional TDP-43 related neurodegeneration. In several mouse models, the loss of nuclear TDP-43 has been shown to precede neurodegenerative changes (Wegorzewska et al., 2009).

1.10 Animal models of TDP-43

Novel insights into the aetiopathogenesis and progression of ALS have been derived from rodent and various other animal models harboring fALS associated mutations, especially mutant SOD1 (mSOD1) (Gurney, 1997). Several key features of ALS have been replicated using these animal models, such as progressive loss of motor neurons, leading to weakness and premature death, neurofilament aggregation, ubiquitinated cytoplasmic inclusion formation etc (Julien and Kriz, 2006). For a considerable period of time, SOD1 mutant mouse models have dominated the quest for answers to explain the cause/s of ALS. ALS disease models also serve as a useful tool for testing potential therapeutic agents and options although there is no cure or a treatment found for ALS so far.

Since the discovery of the association of TDP-43 with ALS, several models of TDP-43 proteinopathy have been published (Table 1.3). The TDP-43 transgenic mice expressing human A315T TDP-43 mutation using the mouse prion protein.

Table 1.3 Animal models of TDP-43 (Adapted from (Vinsant et al., 2013))

Species	Line	Transgene	Promoter	TDP-43 proteinopathy						Phenotype		References
	TRANSGENIC			TDP-43 +ve inclusions	ubiquitin & TDP-43 TDP-43+ve inclusions	Cytoplasmic TDP-43	Nuclear loss TDP-43	Truncated (35 or 25 kDa)	Phospho	Cognitive dysfunction	Motor dysfun	
Mouse	Prp-TDP43A315T	Flag- A315T-hTDP-43	mPrP	NO	NO	YES	YES	YES	NA	NA	YES	(Wegorzewska et al 2009)
Mouse	WT TDP-43 line 21	WT-hTDP-43	mPrP	NO	NO	YES	NA	YES	NA	NA	YES	(Stallings et al 2010)
Mouse	A315 TDP-43 line 23	A315T-hTDP-43	mPrP	YES	YES (NCI, rare NII)	YES	NA	YES	YES	NA	YES	
Mouse	M337V TDP-43 line 39	M337V-hTDP-43	mPrP	NA	NA	YES	NA	YES	NA	NA	YES	
Mouse	TDP-43prp	WT-hTDP-43	mPrP	YES	YES (NCI and NII)	YES	NA	YES	YES	NA	YES	(Xu et al 2011)
Mouse	TDP-43WT TAR4/4	WT-hTDP-43	murThy1.2 promoter	YES	YES (NCI and NII)	YES	YES	YES	YES	NA	YES	(Wils et al 2010)
Mouse	TDP-43 Tg W3	WT-hTDP-43	murThy1.2 promoter	YES	YES (NII)	NA	NA	NA	NA	NA	YES	(Shan et al 2010)
Mouse	CaMKII-TDP-43 Tg	WT-mTDP-43	mCaMKII promoter	YES	YES (NCI)	YES	YES	YES	NA	YES	YES	(Tsai et al 2010)
Mouse	hTDP-43-WT W12	WT-hTDP-43	mCamKII- tTA x tet off	YES	YES (rare NCI and NII)	YES	NO	NO	YES	NA	YES	(Igaz et al 2011)
Mouse	hTDP-43-ΔNLS ΔNLS4	ΔNLS-hTDP-43	mCamKII- tTA x tet off	YES	YES (NCI)	YES	YES	NO	YES	NA	YES	
Mouse	CAG-TDP-43	WT-hTDP-43	CAG	NO	NO	NO	NA	NO	NA	NA	NO	(Tian et al 2011)
Mouse	TDP-43 WT	WT-hTDP-43	hum.end.prom	NO	NO	NO	NO	NO	NA	YES	YES	(Swarup et al 2011)
Mouse	TDP-43 A315T	A315T-hTDP-43	hum.end.prom	YES	YES (NCI)	YES	YES	YES	NA	YES	YES	
Mouse	TDP-43 G348C	G348C-hTDP-43	hum.end.prom	YES	YES (NCI)	YES	YES	YES	NA	YES	YES	
Mouse	hTDP-43M337V line 4 & 6	M337V-hTDP-43	mPrP	YES (NCI)	NO	YES	NA	YES	YES	NA	YES	(Xu et al 2011)
Mouse	TgTDP-25 (B) and (F)	hTDP-25	murThy1.2 promoter	NO	NO	YES	NA	YES	NO	YES	NA	(Caccamo et al 2011)
Mouse	iTDP-43WT 5a	WT-hTDP-43	mCamKII- tTA x tet off	YES	YES	YES	NA	YES	YES	NA	NA	(Cannon et al 2012)
Mouse	TDP-43WT	myc-WT-hTDP-43	mPrP	NO	NO	NO	NA	NA	NA	NA	NO	(Arnold et al 2013)
Mouse	TDP-43Q331K	myc-Q331K-hTDP-43	mPrP	NO	NO	NO	NA	NA	NA	NA	YES	
Mouse	TDP-43M337V	myc-M337V-hTDP-43	mPrP	NO	NO	NO	NA	NA	NA	NA	YES	
Mouse	p.M337V-hTDP-43 mt-TAR5/(	M337V-hTDP-43	Thy 1.2	YES	YES	NA	YES	YES	YES	NA	YES	(Janssens et al 2013)
Rat	miniTDP-43 wt	miniTDP-43WT	WT-hTDP-43 human promoter	NO	NO	YES	NA	YES (35 & 15 k	YES	NA		(Zhou et al 2010)
Rat	miniTDP43M337V	M337V-hTDP-43	hum.end.prom	NA	NA	YES	NA	NA	NA	NA	YES	
Rat	TRE-TDP43M337V	M337V-hTDP-43	CAG-tTA x tet off	YES	NA	YES	NA	YES (35 & 15 kD	YES	NA	YES	
Rat	NEF-tTA/TDP-43M337V	M337V-hTDP-43	human NEF-tTA x tet o	NO	NO	NA	NA	NA	NA	NA	YES	(Huang et al 2012)
Rat	ChAT–tTA-9/TDP-43M337V	M337V-hTDP-43	mouse ChAT-tTA x tet	YES	YES (NCI)	YES	NA	NA	NA	NA	YES	
monkey		Flag- WT- hTDP-43	AAV1 viral delivery									
C. elegans	TDP-1		ubiquitous (snb1)	NA	NA	NO	NO	NA	NA		YES	(Ash et al 2010)
C. elegans	WT-hTDP-43		ubiquitous (snb1)	NA	NO	NO	NO	NA	NA		YES	
C. elegans	WT-hTDP-43		ubiquitous (snb1)	YES	YES	NO	NO	YES	NO		YES	(Liachko et al 2010)
C. elegans	A315T-hTDP-43		ubiquitous (snb1)	YES	YES	NO	NO	YES	YES		YES	
C. elegans	G290A-hTDP-43		ubiquitous (snb1)	YES	NA	NO	NO	YES	YES		YES	
C. elegans	M337V-hTDP-43		ubiquitous (snb1)	YES	NA	NO	NO	YES	YES		YES	
C. elegans	WT-hTDP-43-YFP		ubiquitous (snb1)	YES	NA	NO	O	NA	NA		YES	(Zhang et al 2011)
C. elegans	Q331K-hTDP-43-YFP										YES	
C. elegans	M337V-hTDP-43-YFP		ubiquitous (snb1)	NA	NA	NA	NA	NA	NA		YES	
C. elegans	C25-hTDP-43-YFP		ubiquitous (snb1)	YES	NA	O	NA	NA	NA		YES	
Zebrafish	WT-hTDP-43		GABAergic neuron (un	NO	NA	NA	NA	NA	NA		NO	(Vaccaro et al 2012)
Zebrafish	A315T-hTDP-43		GABAergic neuron (un	YES	NA	NA	NA	NA	NA		YES	
Zebrafish	Zebrafish	WT-hTDP-43	ubiquitous (CMV)	NA	NA	NA	NA	NA	NA		NA	(Kabashi et al 2010)
Zebrafish	A315T-hTDP-43											
Zebrafish	G384C-hTDP-43											
Zebrafish	A382T-hTDP-43		ubiquitous (CMV)	NA	NA	NA	NA	NA	NA		YES	
Zebrafish	Y220X		ubiquitous	NA	NA	NA	NA	NA	NA		NA	(Hewamadduma et al 2013)

Species	Line (TRANSGENIC)	Transgene	Promoter	TDP-43 +ve inclusions	ubiquitin & TDP-43 TDP-43+ve inclusions	Cytoplasmic TDP-43	Nuclear loss	Truncated (35 or 25 kDa)	Phospho	Cognitive dysfunction	Motor dysfun	
Drosophila	Drosophila		dTDP-43									
Drosophila	WT-hTDP-43											
Drosophila	M337V-hTDP-43											
Drosophila	Q331K-hTDP-43											
Drosophila	209-414 a.a of hTDP-43		sensory neuron	NA	NA	NA	NA	NA	NA		NA	(Lu et al 2009)
Drosophila	WT-hTDP-43-RFP		eye (GMR)	YES	NO	YES	NA	NA	NA		NA	(Li et al 2010)
Drosophila	T202-hTDP-43-RFP		eye (GMR)	NA	NA	NA	NA	NA	NA		NA	
Drosophila	WT-hTDP-43-RFP		mushroom body (OK10	NA	NA	NA	NA	NA	NA		NA	
Drosophila	WT-hTDP-43-RFP		motor neuron (OK371)	O	NO	YES	NA	NA	NA		YES	
Drosophila	WT-hTDP-43		eye (GMR)	NA	NA	NA	NA	NA	NA		NA	(Hanson et al 2010)
Drosophila	WT-hTDP-43		motor neuron (D42)	YES (Rare)	NA	YES (Rare)	NA	NA	NA		NA	
Drosophila	WT-hTDP-43											
Drosophila	NES-mut-hTDP-43											
Drosophila	NLS-mut-hTDP-43M337V-hTDP-43		eye (GMR)	NA	NA	NA	NA	YES	NA		NA	(Ritson et al 2010)
Drosophila	WT-hTDP-43		eye (GMR)	NA	NA	NA	NA	NA	NA		NA	(Elden et al 2010)
Drosophila	WT-hTDP-43											
Drosophila	Q331K-hTDP-43		motor neuron (D42)	NA	NA	NA	NA	NA	NA		YES	
Drosophila	WT-hTDP-43											
Drosophila	A315T-hTDP-43		pan neuronal (elav) or	NA	NA	NO	NO	NA	NA		YES (D42)	(Voigt et al 2010)
Drosophila	G287S-hTDP-43											
Drosophila	G348C-hTDP-43											
Drosophila	A382T-hTDP-43											
Drosophila	N390D-hTDP-43		pan neuronal (elav) or	NA	NA	NO	NO	NA	NA		NA	
Drosophila	NLS-mut-hTDP-43		pan neuronal (elav) or	NA	NA	YES	YES	NA	NA		NA	
Drosophila	CTF-hTDP-43		NA	NA	YES	YES	NA	NA	YES (D42)			
Drosophila	FFLL-hTDP-43		NA	NA	YESa	NO	NA	NA	YES (D42)			
Drosophila	WT-hTDP-43		eye (GMR) or pan neur	NO	NA	YES	NO	YES	YES		NA	(Miguel et al 2011)
Drosophila	NES-mut-hTDP-43		YES	NA	NO	NO	YES	YES	NA			
Drosophila	NLS-mut-hTDP-43		NO	NA	YES	YES	YES	YES				
Drosophila	WT-hTDP-43											
Drosophila	A315T-hTDP-43		eye (GMR) or motor ne	aggregate in ax Y	NA	YES	NA	NA	NA		YES (D42)	(Estes et al 2011)
Drosophila	dTDP-43		mushroom body (OK10	YES	NA	YES	NA	NA	NA		YES (D42)	(Lin et al 2011)
Drosophila	CTF-hTDP-43		pan neuronal (elav)	YES	NA	YES	NA	NA	YES		NA	(Li et al 2011)
Drosophila	Mutant CTF of TDP-43 b		YES	NA	YES	NA	NA	NO	NA			
Drosophila	Mutant CTF of TDP-43C		NO	NA	YES	NA	NA	YES	NA			
Drosophila	WT-TBPH(dTDP-43)		motor neuron (D42)	NA	NA	YES	NA	NA	NA		YES	(Hazelett et al 2012)
Drosophila	UAS-dTDP-43-Flag		CCAP neuron (ccap)	YES	YES (NII)	YES	NO	NA	NA		NA	(Vanden Broeck et al 2013)
Drosophila	WT-TBPH(dTDP-43)		pan-neuronal (elav) or	NO (GMR)	NO (GMR)	NO (GMR)	NO (GMR)	NA	NA		YES (elav Y	(Diaper et al 2013)

	KNOCKOUT					Ubiquitin						References
	line	deletion		Embryonic leth	Loss of nuclear TDP-4							
Mouse	Tardbp-deficient	deleted exon 2 and 3	ubiquitous	YES	YES	NA				NA	NA	(Wu et al 2010)
Mouse	Tardbp−/−	gene trap insertion o	ubiquitous	YES	YES	NA				NA	NA	(Sephton et al 2010)
Mouse	Tardbp−/−	Gene trap and insert	ubiquitous	YES	YES	NA				NA	NA	(Kraemer et al 2010)
Mouse	Conditional Tardbp-KO	Er-Cre x TardbpF/F (f	ubiquitous	NO	YES	NA				NA	NA	(Chiang et al 2010)
Mouse	HB9:Cre-Tardbplx/−	HB9-Cre x Tardbplx (	spinal cord motor neur	NO	YES	YES				NA	YES	(Wu et al 2012)
Mouse	TDP CKO	VAChT-Cre x TDP-43f	motor neuron	NO	YES	NA				NA	YES	(Iguchi et al 2013)

80

promoter, become symptomatic around 90 days and showed an average age of survival of 153 days. Mice developed difficulties with gait and feeding as the disease progressed. This TDP-43 transgenic mouse model also demonstrated selective vulnerability of motor neurons, motor neuronal loss and axonal degeneration, ubiquitinated inclusions, C-terminal fragmentation and rarely, showed relative nuclear clearing when compared with non transgenic littermates (Wegorzewska et al., 2009). However this model failed to show the cytoplasmic mis-localisation of TDP-43 seen in the motor neurons of ALS cases. The other drawback of the model reported is the low number of backcrosses, and the fact that the data published are only from F1 and F2 generations. The variation in survival ranges between 100-240 days and it is possible that a drop in copy number could explain this variability. In the meantime it is also difficult to interpret the results due to the absence of data from a WT TDP-43 transgenic mouse as a control for comparison. Several reports have recently described severe gastrointestinal dysfunction and myenteric plexus degeneration as a cause of death in the PrP-hTDP-43 (A315T) transgenic mice. Some argue usefulness in this mouse model due to the lack of ALS like phenotype and features of TDP-43 proteinopathy in these mice (Hatzipetros et al., 2014, Herdewyn et al., 2014).

Wu et al (2010), generated a *tdp-43* null mouse using the BAC targeting system to knock out exon 2 and 3 of TDP-43. As a consequence TDP-43 loses its translational initiation codon (ATG in exon 02) leading to ablation of TDP-43 production. The homozygous *tdp-43* null mice only survived until the morula stage. Prior to this state homozygous *tdp-43* null mice were phenotypically indistinguishable from the WT mice. This phenomenon is most likely due to maternal transmission of TDP-43 mRNA to homozygous *tdp-43* null mice. Once the maternal mRNA is depleted, these mice die. A significant defect in the migration of inner cell mass has been noted. On the other hand in heterozygous *tdp-43 null* mice TDP-43 mRNA levels or the protein levels were unchanged when compared with WT control, indicating a possible feed back loop to maintain TDP-43 levels in the cell. Moreover, heterozygous *tdp-43 null* mice were more or less similar in behaviour, locomotor function and survival compared to WT mice (Wu et al.). Although it is difficult to interpret the findings of this study as supportive of loss of

function in ALS, certainly it confirms that TDP-43 is an essential protein in mouse embryonic development.

In keeping with the above findings is the knockout model of *Drosophila melanogaster* TDP-43 orthologue, TBPH by 'P element mobilisation'. The homozygous TBPH null flies died at the second instar larval stage. Interestingly TBPH heterozygous knockout flies showed *in vitro* evidence of impaired nuclear function due to reduced TBPH, as indicated by impaired HDAC6 mRNA levels. HDAC is implicated in autophagic degradation of accumulated protein and decides the fate of poly ubiquitinated proteins, supporting the hypothesis that TDP-43 is an RNA processing molecule (Fiesel et al., 2009). Somewhat in contrast to the above study is the TBPH deletion technique used to abolish TBPH resulting in TBPH null flies by Feiguin et al (2009). These flies were viable after embryogenesis and the majority underwent metamorphosis. Some had difficulty in eclosing and the ones that eclosed had gross locomotor deficiencies for example weak crawling, climbing and flying etc. Ultra-structure analysis in transgenic and TBPH suppressed with RNAi, flies showed abnormal presynaptiC-terminals of the neuromuscular junctions indicated by reduced axonal branching. Interestingly, behavioural, locomotive and ultra structural defects were rescued using a GAL4/UAS system to deliver human TDP-43 to TBPH-/- flies (Feiguin et al., 2009). Taken together the above models replicate the multiple functions of TDP-43 in a cell and confirm its importance in development and locomotion.

Zebrafish, through evolutionary duplication of its genome, has two *TARDBP* orthologues, one on chromosome 06 called *tardbp* and the other on chromosome 23 called *tardbpl*. Both of these orthologues have significant homology to the human *TARDBP*, in that chromosome 06 encoded *tardbp* has 72% homology and encodes all the structurally important components of TDP-43 whilst chromosome 23 encoded, *tardbpl,* which is only 54% homologous, does not contain the complete C-terminus (Figure 1.5). In an in situ hybridisation study of zebrafish, Shankaran et al (2008) showed ubiquitous expression of maternally expressed *tardbp* in the sphere stage and even by day three post fertilisation, *tardbp* expression was restricted but still seen uniformly in the head region (Shankaran et al., 2008). Kabashi et al (2010) replicated ALS like features in a zebrafish model by over-expressing human TDP-43 mutant constructs (A315T, G348C and A382T) in zebrafish embryos. The mutant construct injected zebrafish showed a motor

phenotype of abnormal coiling and escape response to touch stimulus compared to those injected with WT TDP-43. These fish also had shorter and disorganised branching of motor axons, identified by SV2 (marker of synaptic vesicles) and acetylated tubulin (marker of growing axons) antibodies. A similar motor phenotype was also observed by knocking down of the TDP-43 orthologue, *tardbp (chromosome 06 encoded),* using anti-sense morpholino oligo nucleotides (AMO) specific to *tardbp* which was confirmed by immunoblotting. However no motor neuronal or axonal loss was observed. The AMO related phenotype was rescued by injection of WT human *TARDBP* constructs but not by the mutant *TARDBP* (Kabashi, 2010). The problems in interpreting the above results are that AMO injection can result in non-specific cell death/ apoptosis. Therefore the effects of AMO need to be confirmed by another AMO targeting the same gene and or by co-injecting p53 AMO, which inhibits non-specific apoptosis especially in degeneration of the hindbrain (Roeben et al 2006). The above zebrafish model of TDP-43 proteinopathy supports both the toxic gain of function (by the mutant construction injections) as well as loss of function as plausible mechanisms of TDP-43 related neurodegeneration in ALS.

```
CLUSTAL 2.0.11 multiple sequence alignment

ZEBRAFISH_tardbp      MAEMYIRVAEEENEEPMEIPSEDDGTVLLSTVSAQFPGACGLRFRSPVSQCMRGVRLVDG 60
ZEBRAFISH_tardbpl     MTECYIRVAEDENEEPMEIPSEEDGTVLLSTVAAQFPGACGLRYRSPVSQCMRGVRLVEG 60
HUMAN_TDP43           -MSEYIRVTEDENDEPIEIPSEDDGTVLLSTVTAQFPGACGLRYRNPVSQCMRGVRLVEG 59
                       . ****:*:**:**:*****:*********:**********:*.*************:*

ZEBRAFISH_tardbp      ILHAPENGWGNLVYVVNYPKETVLPDNKRKMDEIDASSATKIKRGDQKTSDLIVLGLPWK 120
ZEBRAFISH_tardbpl     VLHAPEADWGNLVYVVNYPKD-----NKRKMDEMDAASAVKIKRGIQKTSDLIVLGLPWK 115
HUMAN_TDP43           ILHAPDAGWGNLVYVVNYPKD-----NKRKMDETDASSAVKVKRAVQKTSDLIVLGLPWK 114
                      :****: .************:      ****** **:**.*:**. *************

ZEBRAFISH_tardbp      TSEQDLKDYFGTFGEVIMVQVKRDVKTGNSKGFGFVRFGDWETQSKVMTQRHMIDGRWCD 180
ZEBRAFISH_tardbpl     TTEQDLKDYFGTFGEVIMVQVKRDAKSGNSKGFGFVRFTDYETQIKVMSQRHMIDGRWCD 175
HUMAN_TDP43           TTEQDLKEYFSTFGEVLMVQVKKDLKTGHSKGFGFVRFTEYETQVKVMSQRHMIDGRWCD 174
                      *:*****:**.*****:*****:*  *:*:********* ::*** ***:**********

ZEBRAFISH_tardbp      CKLPNSK-----QGIDEPMRSRKVFVGRCTEDMTADELRQFFMQYGEVTDVFIPKPFRAF 235
ZEBRAFISH_tardbpl     CKLPNSKYFLEQAGPDEPMRSRKVFVGRCTEDMTADELRQFFMQYGEVTDVFIPKPFRAF 235
HUMAN_TDP43           CKLPNSK-----QSQDEPLRSRKVFVGRCTEDMTEDELREFFSQYGDVMDVFIPKPFRAF 229
                      *******      . ***:************** ****:** ***:* **********

ZEBRAFISH_tardbp      AFVTFADDQASHVAAALCGEDLIIKGVSVHISNAEPKHNNTRQMMERA---GRFGNGFGG 292
ZEBRAFISH_tardbpl     AFVTFADDQ---VAQSLCGEDLIIKGTSVHISNAEPKHNNIHHLFS-------------- 278
HUMAN_TDP43           AFVTFADDQ---IAQSLCGEDLIIKGISVHISNAEPKHNSNRQLERSGRFGGNPGGFGNQ 286
                      *********   :* :********** ************,. ::;

ZEBRAFISH_tardbp      QGFAGSRSNMGGGGGGSSSSLGN---FGNFNLNPAMMAAAQAALQSSWGMMGMLA-QQNQ 348
ZEBRAFISH_tardbpl     -NFPGR-----------SPSLA-----------AMFERSQYQFPSSHV----------- 303
HUMAN_TDP43           GGFGNSRGGGAGLGNNQGSNMGGGMNFGAFSINPAMMAAAQAALQSSWGMMGMLASQQNQ 346
                       .* .           ...:.               **: :*  : **

ZEBRAFISH_tardbp      SGTSGTSTSGTSSSRDQAQTYSSANSNY--GSSSAALGWGTGSNSGAASAGFNSSFGSSM 406
ZEBRAFISH_tardbpl     ------------------------------------------------------------
HUMAN_TDP43           SGPSGNNQNQGNMQREPNQAFGSGNNSYSGSNSGAAIGWGSASNAGSGS-GFNGGFGSSM 405


ZEBRAFISH_tardbp      ESKSSGWGM 415
ZEBRAFISH_tardbpl     ---------
HUMAN_TDP43           DSKSSGWGM 414
```

Figure 1.5 Clustal W alignment of the amino acid sequence of the zebrafish orthologues of human TDP-43. There is significant identity towards the N-terminus. The Tardbp and Tardbpl are 72% and 54% idenitical to human TDP-43 protein respectively.

1.11 Zebrafish as a model of human diseases

Danio rerio, zebrafish, has been used for experimentation purposes since the 1930s. It was first developed as a model organism by Dr George Streisinger of the University of Oregon in 1970. Since then this model has been developed into a developmental biology platform on which many vertebrate developmental disorders have been studied. Increasingly, over recent years several neurodegenerative conditions have been investigated using the zebrafish model. The zebrafish nervous system arrangement has many similarities to that of the human. The representative anatomy includes fore-brain, mid-brain and hind-brains, diencephalon, telencephalon and cerebellum. The peripheral nervous

system includes motor and sensory components and an enteric and autonomic nervous system. Zebrafish also has specialised sensory organs such as the eye, olfactory system and shows functions of higher behaviours and neural integration such as memory, conditioned responses and social behaviours, although these are much simplified compared to those of humans. The main differences are that the zebrafish telencephalon only has a rudimentary cortex and the lateral line is one of the major fish sensory organs. The development of the zebrafish neuro-muscular system is well characterised and is stereotyped in that the establishment of 30 body muscle segments (fast twitch muscle medially and the slow twitch laterally), development of 3 primary motor neurons for each spinal cord hemi-segment which innervate non-overlapping muscle segments, fasciculation by secondary neuronal axonal projection to form 3 nerves on each side. The alteration of these nerves, axons and neuro-muscular junctions can be studied microscopically by using antibody staining (ZnP1) and/or using genetically engineered models, which express green fluorescent protein (GFP- islet 1 GFP fish, HB9) (Beattie et al., 2007). Zebrafish as a disease model has become attractive due to various advantages associated with it compared to other vertebrate models like mouse or rat. These advantages include the rapid development, accessibility, external embryonic development, high fecundity and optical transparency. The relatively small size makes it easier to store and maintain a large number of fish, requiring lesser resources. The applicability of invertebrate style genetic manipulations to generate answers for vertebrate specific disease related questions make it an ideal system to use for large scale genetic and therapeutic screening development and testing of new therapies (Grunwald and Eisen, 2002). One also needs to be aware of several major limitations in zebrafish as a model of neurodegenerative conditions such as its regenerative capacity, relative evolutionary distance to humans and differences in the organization of the nervous system are a few.

1.11.1 Targeting Induced Local Lesions in the Genome (TILLING)

In order to study the developmental biology of a human disorder in the zebrafish, ideally due to a genetic dysfunction, several approaches can be made. The reverse genetics approach is a method of studying the resultant phenotype following a genetic manipulation. Zebrafish mutants of human orthologues can be generated by a reverse genetics method called TILLING (targeting induced local

lesions in genomes) (McCallum et al., 2000) (Also see Fig 6.1). In mouse models, gene targeting by homologous recombination is a method used for the reverse genetics approach. The advantages of TILLING are the large size of the library screened, the ability to collect an allelic series of random mutations and better genotype-phenotype correlation with a large allelic series. In addition missense and gain of function mutations can be generated by the TILLING process (McCallum et al., 2000).

1.11.2 Transgenic zebrafish models

The optical transparency and the external development of the zebrafish embryos present researchers with the opportunity to microinject either mRNA or anti-sense morpholino oligonucleotides which results in transient alteration in gene expression. Retroviral mutagenesis, compartmentalisation and caging techniques allow tissue specific and temporally specified expression of a gene. The simple injection of constructs into fertilised oocytes can result in 50-80% efficient transgenesis using transposon-mediated transgenesis (Udvadia and Linney, 2003). It is also possible to use tissue specific promoters to over-express dominantly inherited genes related to human diseases to generate transgenic zebrafish lines. Thus, the zebrafish serves as an efficacious and practical disease model to study and understand the pathogenesis, improve diagnosis and discover therapeutic agents through drug and chemical screening related to neurodegenerative conditions and many other human disorders.

ALS aetiopathogenesis is a complex process involving, protein aggregation, axonal transport defects, mitochondrial dysfunction, impaired RNA processing etc (Figure 1.1), which is further complicated by heterogeneity in the associated genetic abnormalities indicating that a therapeutic option would most likely to materialise from a combination of therapeutic strategies acting in synergy. Therefore it is useful to identify new genes associated with ALS, understand the pathophysiology of the new genes/proteins by cellular and animal models in order to generate efficient biomarkers and therapies for ALS.

1.11.3 Zebrafish models of neurodegenerative conditions

Recently Ramesh et al, 2010, reported a stable transgenic model of mutant SOD1 zebrafish expressing G93R and G85R mutations. The fish survived until adulthood

but showed progressive muscle weakness, consequent swimming defects and early death. Neuromuscular junction defects were noted as early as 11dpf. These mutant fish also incorporate a heat shock promoter 70 driving DsRed (hsp70-DsRED) construct engineered into the human SOD1 gene, thus enabling the identification of the transgenic embryos by the heat shock method. However even prior to heat shocking, embryos with mutant SOD1 have been shown to activate the DsReD transcription signal in the neurons, indicating mutant SOD1 driven neuronal toxicity. This model is invaluable for high throughput drug screening to identify novel therapies to treat SOD1 related ALS (Ramesh et al., 2010).

Transient expression of human SOD1 mRNA in zebrafish embryos by Lindberg et al. 2005 showed dose dependent motor axon defects in the embryos. They also studied the protective role of VEGF (vascular endothelial growth factor) in the pathogenesis of ALS. Knockdown of VEGF in the embryos over-expressing human SOD1 showed severe axonal defects, whereas simultaneous over-expression of VEGF in SOD1 over-expressing zebrafish partially rescued the axonal phenotype indicating that VEGF confers neuroprotection in the presence of SOD1 mediated toxicity.

Als2 related mutations are associated with young onset ALS. Transient knockdown of *Als2* using AMO in the zebrafish demonstrated features of motor nerve defects and swimming abnormalities. Furthermore the zebrafish Als2 was also shown to be important for global embryonic development in contrast to the mouse als2 knockout model which was clinically unaffected due to another als2 species (Gros-Louis et al., 2008). Other neurodegenerative conditions studied using zebrafish as a model are spinal muscular atrophy related to mutations in *SMN* (McWhorter et al., 2003, Beattie et al., 2007), Parkinson's disease related to mutations in *PINK1* (Flinn et al., 2009), *Parkin* (Fett et al., 2010), *DJ1* (Baulac et al., 2009) and *LRRK2* (Sheng et al., 2010), Huntington's disease related to *Htt* ((Henshall et al., 2009) Alzheimer's dementia related to Tau (Bai et al., 2007), ((Paquet et al., 2009) and, hereditary spastic paraparesis associated with *spast* mutations (Wood et al., 2006).

1.12 Fibroblasts as a model of neurodegenerative disease

Modeling of neurodegenerative conditions in a cellular system derived from human tissues poses an intrinsic problem in that it is impossible to obtain cells or tissues from the disease affected CNS tissues from patients during life. Therefore the search for alternative tissues to develop cellular models has been underway for many years. The two favourite patient-tissues used to model neurodegenerative conditions are skin fibroblasts and lymphoblastoid cell lines. It is advantageous that many of the genes and proteins associated with neurodegenerative diseases are ubiquitously expressed in peripheral as well as CNS tissues. Both these tissues are easily obtainable from patients and control cases. The advantage of using patient derived tissues, particularly in studying a subset of inherited neurodegenerative conditions associated with mutations in a specific gene, is that the mutant protein levels are similar to the innate protein levels in the disease affected tissues in human cases with the relevant mutations. This is a distinct advantage compared to knockdown cellular models or over-expression models wherein the targeted protein is altered in a non-physiological manner which could result in off target effects. A proof of principle study by Mortiboys et al 2008, demonstrated that use of skin fibroblasts from a subset Parkinson's disease patients with a mutation in the *PARK2* gene, could help to understand the underlying pathological mechanisms which may cause neurodegeneration in the presence of mutant parkin (Mortiboys et al., 2008). Since the above study a recent study has also shown that fibroblasts are a useful model to study the underlying mechanisms, which might be implicated in neurodegenerative process in Parkinson's disease, associated mutations associated with mutations in both *PINK1* and *PARK2* genes. Using the fibroblasts from patients with mutations in *PINK1* and parkin, they demonstrated that the ubiquitin-proteasome system (UPS) is important in the maintenance of Mitofusin, which is important for mitochondrial function, morphology and recycling (Rakovic et al., 2011). Fibroblast models are important not only to study mechanisms involved in the neurodegenerative process, but can be used to identify readouts which subsequently can used for high throughput chemical screening to identify therapeutic targets (Mortiboys et al., 2008). Mitochondrial dysfunction is a well established pathophysiological disease mechanism in ALS (reviewed in (Shi et al., 2009)). Rodriguez et al, 2012 described mitochondrial morphological changes similar to those changes seen in central nervous system, in skin fibroblasts obtained from sALS cases (Rodriguez et al.,

2012). Increased susceptibility of motor neurons to oxidative stress is another pathophysiological mechanism indicated in the pathogenesis of ALS in both sporadic ALS and SOD1 related ALS (Barber et al., 2006). Supporting oxidative stress as a pathophysiological mechanism, skin fibroblasts obtained from sALS and SOD1 ALS cases have been shown to be at greater risk of oxidative damage from exogenous oxidative stressors such as H_2O_2 (Aguirre et al 1998). Furthermore impaired calcium handling in fibroblasts from ALS cases has also been demonstrated (Witt et al., 1994). Taken together, patient derived fibroblast cell culture systems can be regarded as a robust platform for investigating disease related mechanisms in ALS and other neurodegenerative disorders In addition to the significant precedence which exists in using cultured fibroblasts in the study of neurological and neurodegenerative disorders fibroblasts have an advantage over lymphoblasts in that transformation of lymphocytes to lymphoblasts to allow serial culture could alter cellular properties especially pathways involving calcium metabolism (Gibson and Peterson, 1987).

1.13 Hypothesis and aims of the PhD:

Since the discovery of TDP-43 as one of the major components of the neuro-cytoplasmic inclusions of the surviving motor neurons and glial cells in 2006 ((Neumann et al., 2006, Sreedharan et al., 2008) it still remains an enigma how dysfunctional TDP-43 dismantles the fine internal milieu of motor neurons over time. Over-expression of mutant and wild type TDP-43 has resulted in variable results as discussed earlier in the chapter 1. A variety of animal models have failed to unequivocally demonstrate the features of TDP-43 proteinopathy and associated clinical syndrome. We believe this is secondary to the tight control of TDP-43 levels at the cellular level. Therefore knocking down or over-expression of TDP-43 could be harmful to the cells and the animals. One might argue that results from models of such methodological approaches could be not interpretable. It has been described that mutant TDP-43 exerts its effect via toxic gain of function and/or by enhancing the effects of TDP-43 proteinopathy. Therefore we hypothesised that over expression of disease associated TDP-43 mutations (wtTDP-43) would results in distinct changes in cells compared to the wild type TDP-43 (wtTDP-43).

TDP-43 has been shown to take part in several RNA associated functions and interact with thousands of RNA targets. Therefore it is important to study the role of wtTDP-43 and disease associated mutations at a physiological level to avoid perturbation of a myriad of RNA-protein-TDP-43 interactions. Patient derived fibroblasts have been used as a platform to study various aspects of neurodegenerative conditions whilst providing a physiological level of disease related protein i.e. TDP-43. Patient derived fibroblasts have been utilised previously to study neurodegenerative disorders such as Parkinson's disease (Mortiboys et al., 2008) and ALS ((Mead et al., 2013). Fibroblasts obtained from ALS cases with mutations in *TARDBP* provide a valuable resource, which directly represents the genetic make of a patient and has physiological levels of the mutant TDP-43protein. TDP-43 is ubiquitously expressed. Therefore we hypothesised that patient derived fibroblasts would demonstrate some features of TDP-43 proteinopathy. Furthermore one of the RNA processing functions that TDP-43 implicated in is modulation of stress granule (SG) dynamics. Several studies have used changes in SG dynamics as a surrogate marker of RNA related function of TDP-43 (McDonald et al., 2011). However these studies have assessed the SG dynamics in cell models over-expressing TDP-43. Therefore we also hypothesised that physiological levels of mutant TDP-43 would have a distinct effect on RNA processing in fibroblasts compared to the controls.

It is yet unclear if dysfunctional TDP-43 is associated with neurodegeneration in a loss of function, toxic gain of function processes or indeed both. Loss of function models of TDP-43 in mice showed embryonic lethality. However zebrafish has several advantages wherein external development, optical translucency and accessibility to genetic manipulation, make zebrafish model an ideal model to study loss of function effects of TDP-43. A previous study did exploit these advantages of the zebrafish model in demonstrating a motor phenotype by transiently knocking down the zebrafish homologue, *tardbp* (Kabashi et al., 2010a). Furthermore it was not clear if the phenotype observed by this group was secondary to the off target effects of anti-sense morpholino oligonucleotides (AMO) used. Furthermore the conclusion that second zebrafish orthologue *tardbpl* has no functional use was drawn by inadequate interrogation. Therefore we hypothesised that zebrafish *tardbp* and *tardbpl* are both vital for the zebrafish

survival and a stable mutant would negate disadvantages of a transient knockdown model. In the light of this evidence and above hypothesis the following aims were formulated –

- To describe the effects of mutant and wild type TDP-43 overexpression in HEK293T cells and study mislocalisation of TDP-43.

- To establish the immunohistochemical differences between mutant TDP-43 associated ALS patients derived fibroblasts and those obtained from control cases.

- To study stress granule dynamics in fibroblasts associated with wild type and mutant TDP-43.

- To assess the phenotype of antisense morpholino oligo nucleotide (AMO) knockdown of zebrafish *tardbp* and *tardbl*, when the off target effects have been minimized.

- To establish the importance of zebrafish *tardbp* and *tardbpl* using a stable *tardbp* mutant zebrafish.

Chapter 02: Materials and Methods

2.1 Transient expression of TDP-43 in HEK cells

2.1.0 Cells used

- HEK cells- a kind gift from Dr Roy Milner. HEK cell passage at the time of use was 12..

2.1.1 Working solutions

All solutions were prepared in deionised water unless otherwise stated.

2.1.1.1 Bacterial Culture / Plasmid Propagation

- Luria-Bertani (LB) broth, Miller (Merck®).

- LB-Agar media, Miller (Merck®)

- Carbenicillin stock: 50 mg/ml in 50% ethanol solution. Filtered and stored at -20°C (for the selection of myc-tagged plasmid growth)

- Kanamycin stock: 50 mg/ml in water. Filtered and stored at 4°C. (for the selection of GFP-tagged plasmid growth)

- QiAGEN® mini prep kit- for DNA extraction from the bacterial cultures (QIAGEN.com)

- NucleoSpin® DNA extraction kit (Clontech labs) was used to extract DNA for transfecting rat cortical neurons.

2.1.1.2 Solutions used - Cell Culture and transfection

- Culture medium: DMEM (BioWhitaker®) with 2 mM L-Glutamine and Glucose, supplemented with 10% Fetal Calf Serum and Penicillin-Streptomycin cocktail.

- Penicillin-Streptomycin cocktail: Contains 10,000 units/ml of penicillin (penicillin G sodium base) and 10,000 μg/ml of streptomycin (streptomycin sulphate) in 0.85% saline.

- PBS (pH 7.2): 135 mM NaCl, 3.2 mM Na_2HPO4, 0.5 mM KH_2PO4, 1.3 mM KCl.

- EDTA-Trypsin solution: 0.5 mM EDTA (pH 8.0) with 0.05% trypsin (Sigma-Aldrich®).

- Exgen 500 cell transfection medium (cosmobio.co.jp)

2.1.1.3 Immunocytochemistry

- Permeabilising solution: 0.01% Triton X-100 (w/v) in PBS.

- Quenching solution: 1 M glycine.

- Blocking solution: PBST containing 1% Goat Serum (w/v).

- Hoechst stain: Hoechst made up in PBS in the ratio 1:1000 (v/v).

2.1.1.4 Immunoblotting

2.1.1.4.1   Cell Harvesting

1X Laemmli Sample Buffer (LSB): 62.5 mM Tris-HCl (pH 6.8), 2% (w/v) SDS, 10% Glycerol, Beta mercaptoethanol (2-ME) 5% (v/v), Bromophenol blue 0.001% (w/v) (Laemmli 1970).

2.1.1.4.2   Western Blotting (SDS-Polyacrylamide Gel Electrophoresis)

- 30% Acrylamine-bis acrylamide (37:5:1) solution (Protogel™)

- 10% (w/v) Sodium Dodecyl Sulphate (SDS)

- 4X Resolving gel buffer (pH 8.8): 1.5 M Tris base and 0.4 % (w/v) SDS

- 4X Stacking gel buffer (pH 6.8): 0.5 M Tris base and 0.4 % (w/v) SDS

- 10% (w/v) Ammonium Persulphate (APS)

- Resolving gel (~15ml; for 2 gels): 4.5 ml water with 6 ml of 30 % Acrylamine-bis acrylamide solution, 3.8 ml of upper Tris (pH 6.8), 150 µl of 10% SDS and 10% APS and 16 µl of TEMED.

- Stacking gel (~10ml; for 2 gels): 4.9 ml water with 1.3 ml of 30 % Acrylamine-bis acrylamide solution, 2 ml of upper Tris (pH 5.0), 80 µl each of 10% SDS and 10% APS and 16 µl of TEMED

- 1X Electrophoresis running buffer: 25 mM Tris, 250 mM glycine and 0.1% (w/v) SDS.

- 1X Electro-blotting transfer buffer: 25 mM Tris, 250 mM glycine and 10% (w/v) methanol.

- Washing solution (PBS-Tween-20 (PBST)): PBS with 0.2 % (w/v) Tween-20 (Polyoxyethylene-Sorbitan Monolaurate).

- Blocking solution: PBST containing 5% w/v dried skimmed milk (Casein block).

2.1.2 Transient expression of myc- tagged wild type TDP-43 (wTDP-43) and the disease associated mutations of TARDBP

2.1.2.1 Isolation of plasmid DNA

Myc-tagged TDP-43 constructs of wtTDP-43 and the three mutant constructs were a kind gift from Dr Sundarajan (Sandy). 4ml bacterial cultures were made from the bacterial glycerol stocks of the above constructs, which were grown in LB broth containing 8µl of Carbenicillin solution (50µg/ml) overnight at 37^0 C on a shaker at 400 rpm. Plasmids were isolated using the QiAGEN mini prep kit using the product protocol. Plasmid DNA thus extracted was analysed using the Nanodrop1000 spectrophotmeter machine to obtain a quantitative and a qualitative assessment.

2.1.2.2 Transient transfection

HEK cells were cultured in T75 flasks in Dulbecco's modified Eagles medium (DMEM) at 37^0C. When the cells reach 90% confluency they were harvested by incubating the cells with 1X Tripsin for 4-5min at 37^0C . Trypsin was neutralised using the culture medium removed from the cell flask. Cells were counted using a haemocytometer and centrifuged at 400 rpm for 4 min to obtain the cell pellet, which was later re-suspended in a pre-calculated amount of fresh DMEM. The cells then were seeded as appropriately onto 13X13mm coverslips (Menzel Glaser) and cultured for 24 hours in (~40,000 cells per well in a 12 well plate for cell culture). When the cells reached a degree of confluency (usually around 24hrs of culture) they were transfected with 1µg *TARDBP* DNA (WT, M337V, Q331K or A315T) using ExGen 500 transfection medium as per product protocol.

2.1.2.3 Optimising the transfection efficiency

To optimise the transfection efficiency several modifications were made to the above protocol.

2.1.2.3.1 Four hour wash step

Four hours following transfection, cell culture media was removed under sterile conditions and cells were gently washed twice with pre-warmed media and left to incubate at 37^0C in the third wash for the remaining 20 hours.

2.1.2.3.2 Titration of the DNA concentration

The transfection protocol suggested the use of 1µg of DNA along with the ExGen500 medium. Serial dilutions of wtTDP-43 DNA were transfected to assess the transfection efficiency. Dilutions used were 1, 0.5, 0.25, 0.125 and 0.0625µg.

Every transfection was followed by a wash step as described in section 3.1.2.2.1. After 24hrs post transfection, the proportion of transfected to total cells (total nuclei as indicated by Hoescht stain) was calculated to identify the best condition for transfection.

2.1.2.4 Analysis of cytoplasmic and nuclear staining pattern resulting from transient expression of WT and mutant TDP-43

2.1.2.4.1 Immunostaining with Anti-myc antibody

24 hours after transfection when the cells were about 80% confluent, cells were either subjected to exogenous stress as outlined below or fixed for staining. In the case of the latter, DMEM medium was removed, coverslips were gently washed with PBS and fixed using 3.7% paraformaldehyde (Sigma) for 30 minutes. Coverslips plated with transfected HEK cells thus fixed were then washed for 5 minutes X 3 with 1XPBS and either stored at 4°C overnight in PBS/0.001% Azide (Sigma) or subjected to immunostaining with anti-myc antibody at a dilution of 1:2000 and to develop fluorescence Alexafluor 488 anti- mouse secondary antibody was used at a dilution of 1:1000 (Abcam).

2.1.2.4.2   Cellular Immunostaining protocol

Media was removed from the coverslips and the cells were washed twice with PBS. 3.7% formaldehyde (Sigma UK) in 1XPBS was added for 20 minutes to fix the cells. Formaldehyde was removed and the cells washed three times with PBS. When the cells were left overnight or longer 0.001% Azide in 1XPBS was added. If not the remaining formaldehyde was quenched with 100µl of 1M Glycine (Sterile filtered) (Sigma UK) per cover slip for 10 minutes followed by three 1XPBS washes. Cells were permeabilised with 0.1% TX100 (Triton X 100, Sigma UK) in 1XPBS for 10 minutes at room temperature followed by three 1XPBS washes. Thereafter the cells were blocked for background non-specific antibody binding by blocking with 5% normal goat serum (NGS) in PBST (1XPBS and 0.1% Tween20 (BioRad.com)). Primary and secondary antibodies were diluted separately in PBST and added on to coverslips accordingly. Coverslips were incubated in primary antibody for an hour prior to three x 5 minute washes with PBST following which the secondary antibody was added for a further hour and followed by three PBST wash steps as for the primary antibody. All antibody incubations were done at room

temperature. After the third wash 2-3 drops of 1:1000 Hoescht was added for 30-40 seconds. Coverslips were subjected to a further three washes with PBST. Then coverslips were mounted onto glass slides in 60µl of 50% sterile filtered glycerol (Sigma UK) and sealed using transparent nail varnish (Boots UK). Slides were stored at 4°C prior to imaging. All working solutions of antibodies and NGS were stored at 4°C.

2.1.2.4.3   Imunostaining for endogenous TDP-43

HEK cells were cultured and fixed as described above without transfection. Polyclonal rabbit anti TDP-43 antibody (Proteintech group) at 1:500 dilution was used as the primary and goat anti-rabbit Alexa Fluor 488 antibody (Abcam) was used as the fluorescent secondary along with Hoescht at 1:1000 dilution to stain the nuclei.

2.1.2.4.4   Immunostaining for stress granules

We used anti HUR, TIA and TIAR antibodies (Abcam.com) to stain for stress granules. For HEK cells TIAR was the best. Other antibodies (HUR (Abcam.com) were also used to assess for TDP-43 co-localisation with stress granules.

2.1.3   HEK cell response to exogenous stress: Formation of stress granules as an indicator of the stress response

As described in 2.1.2.4.1 section when cells reached 80% confluency they were subjected to exogenous stress as described by previous groups (See Table 2.1)

Table 2.1 Agents used to obtain a stress response from the HEK cells

Agent	Mechanism of stress	Concentration	Duration (minutes)	Source
Arsenite	Allosteric regulator	0.5mM	30, variable	Sigma UK
H_2O_2	Oxidative	0.6mM	60	Sigma UK
Menadione	Reactive oxygen species	10mM in 1:1000 dilution	120 -480	Kind gift from Dr Mortiboys
FCCP	Uncouples complex V	10μM	90	Kind gift from Dr Mortiboys
Sorbitol	Osmotic	0.4M	30-120	Sigma UK
Heat Shock	Heat stress	42°C	30	
Thapsigargin	ER stress	4μM	90	Sigma UK

2.1.4   Microscopy and image analysis

2.1.4.1 TDP-43 localisation upon transient over-expression of TARDBP

An upright light microscope with viewing channels for fluorescence was used with a X63 magnification oil immersion lens. More than 100 consecutive cells were counted for each slide. When analysing subcellular TDP-43 localisation the following categories of staining were observed.

- Nuclear only (N) (Figure 2.1 panel A and B)
- Nuclear and cytoplasmic (N+Cy) (Figure 2.1 panel C and D)

❖   The cells were also assessed for the following features:

- Nuclear inclusions (Figure 2.1 panel E and F)
- Cytoplasmic inclusion (Figure 2.1 panel D arrow)
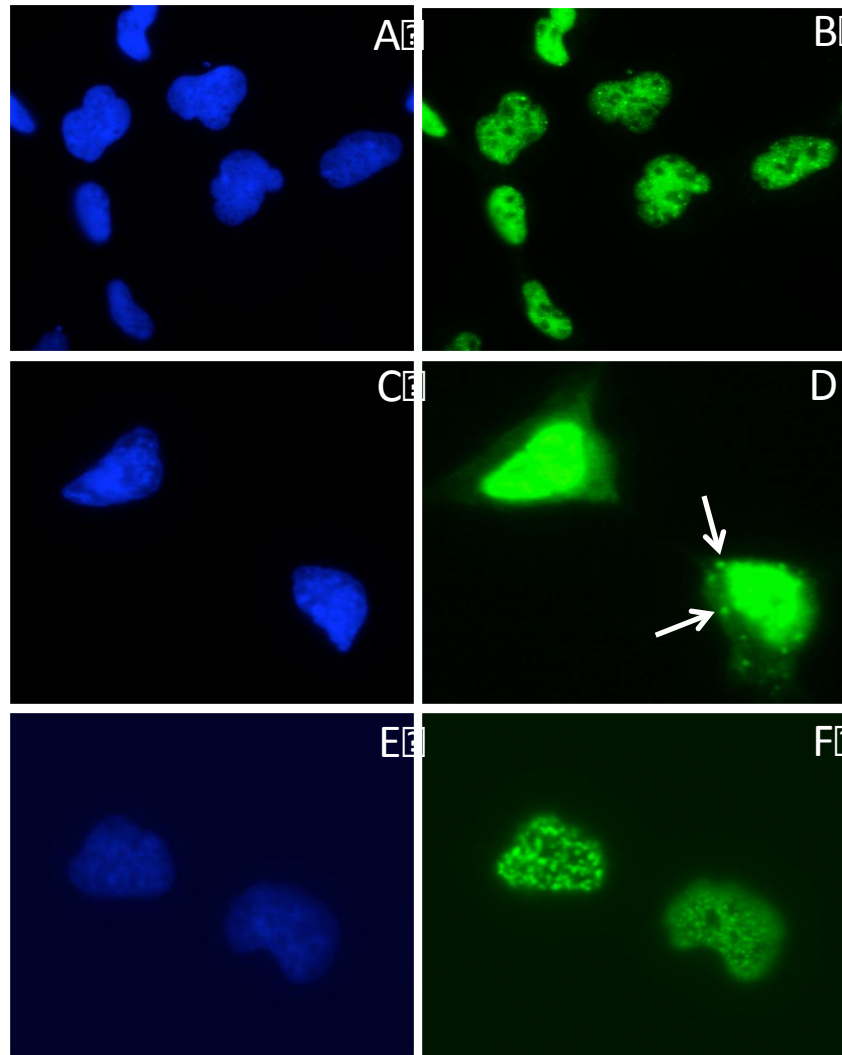
Figure 2.1 Characterisation of cellular distribution pattern of myc-tagged TDP-43. A-B) TDP-43 staining (green) predominantly nuclear (following optimised transfection with a 4hr wash and reduced DNA concentration. **C-D)** Cytoplasmic mis-localisation of TDP-43 and cytoplasmic puncta formation (arrow) **E-F)** Nuclear inclusions in keeping with sNBs.

2.1.4.2Assessment of stress granule response and localisation of endogenous TDP-43 in HEK cells to exogenous stress

The proportion of cells demonstrating stress granule formation was analyzed. Compared to unstressed cells (Fig 2.2 A-B), cells stressed with arsenite (Fig 2.2 C-D) formed distinct cytoplasmic entities called stress granules marked by anti TIAR antibody. Although McDonald et al., 2009 used ≥2 as a threshold we increased the threshold to 3 stress granules per cell in order to increase the specificity ((McDonald et al., 2011). A cell was considered to have formed stress granules if it formed ≥3 punctate lesions (Figure 2.2 panel C arrow) positive for a stress granule marker (anti TIAR, HUR or TIA antibodies). If the number of punctate lesions for a

cell was ≤2, then it was considered negative for stress granule formation (Figure 2.2 panel C and D empty arrow). TDP-43 antibody as described in section 2.1.2.4.3 was used to stain for endogenous TDP-43 whilst anti TIAR antibody was used to detect stress granules. Images were merged using ImageJ software to assess for co-localisation of SG markers with TDP-43.
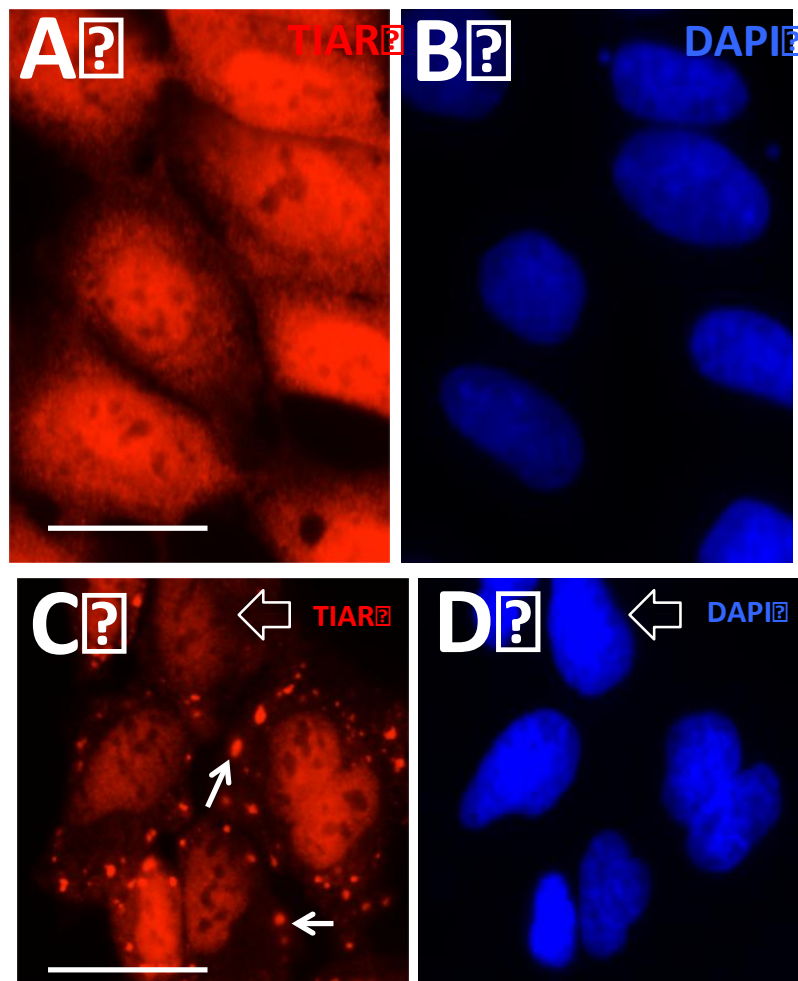
Figure 2.2 Induction of stress granules by exposure to 0.5mM arsenite. A-B) Unstressed HEK293T cells, TIAR staining is both nuclear and smooth cytoplasmic in nature. **C-D**) upon exposure to arsenite, cells form distinct cytoplasmic puncta in keeping with previous descriptions of SG formation. Arrows point towards the punctate cytoplasmic lesions. The empty arrow points towards a cell with less than 3 SG. In this panel the TIAR antibody was used to detect SGs. Scale bar 100μm.

2.2 TDP-43 expression and stress response analysis in human fibroblasts from controls and cases with disease associated mutations in *TARDBP* gene

2.2.0 Ethical aspects

Fibroblasts were cultured from skin biopsies obtained from healthy controls and ALS cases carrying mutations in the *TARDBP* gene. Skin biopsies were obtained following receipt of written informed consent according to local ethics committee guidelines and regulations. Studies involving retrieval of human fibroblasts have (STH14653 REC: 07/Q2305/9) NRES Committee Yorkshire & The Humber approval.

2.2.1 Human fibroblast cell culture medium and chemicals

Fibroblast cell cultures were grown in Ham's F-10 medium (Gibco) supplemented with 10% fetal calf serum (Biosera), 1% penicillin-streptomycin antibiotic solution, 0.25% holo-transferrin (Sigma) and 2.5ng epidermal growth factor (Sigma). Unless stated otherwise all chemicals were obtained from Sigma Aldrich (UK). Phosphate buffered saline (PBS) was Ca^{2+}, Mg^{2+}, free PBS from Sigma Aldrich (U.K) (Mortiboys et al., 2008).

2.2.2 Establishing primary human fibroblast cell cultures

Fibroblast cell cultures were established at the Metabolic Biochemistry and Tissue Culture unit of the Sheffield Children's NHS Foundation Trust. Skin biopsies were collected from the forearm of the subject under sterile conditions and placed in 5 ml of DMEM media (Gibco). The biopsy was dissected under sterile conditions and explants were trapped under a coverslip placed on the flat base of a Nunc tube (Thermo scientific) using a sterilised glass tube. The samples were incubated with 3mls of fibroblast culture medium (see section 2.2.1) in an incubator maintained at 37°C with 20% O_2 and 5% CO_2. When the fibroblasts grew out from the explanted tissue and covered either side of the coverslip, the cells were trypsinised (see section 2.2.3) and transferred to T25 flasks for further expansion.

2.2.3 Maintenance of primary human fibroblast cell cultures

Monolayers of primary fibroblast cell cultures were routinely maintained in T75 flasks with 20 ml of fibroblast cell culture medium (see Section 2.2.1) at 37°C in incubators supplemented with 20% O_2 and 5% CO_2 unless stated otherwise. Cultures when confluent at 70-80% were serially passaged by washing with Ca^{2+}

and Mg^{2+} free PBS (Gibco) and treatment with Trypsin (0.5µg/L)-EDTA(0.2µg/L) (Lonza) for 2 min at 37°C to detach cells from the flask surface. Trypsin was inactivated with serum containing media and the cell suspension was centrifuged at 400 rpm for 4 minutes. The cell pellet was re-suspended in media and plated in fresh T75 flasks at a dilution of 1:3. Fibroblast cell lines were maintained and used for experiments up to passage 10 to ensure that they were in the proliferative phase of their growth curve and to prevent reaching the stage of senescence (Hayflick and Moorhead, 1961).

2.2.4 Cryo-preservation of primary human fibroblast cell cultures

Cultures at a confluency of 70-80% were cryo-preserved using a freezing solution of fetal calf serum (FCS) (final concentration 90%) and dimethyl sulfoxide (DMSO) (final concentration 10%, Sigma). The cell pellet and cryo-preservation suspension was aliquoted into cryovials and placed at -80°C in a Nalgene freezing container (Thermo scientific) containing isopropanol, which lowers the temperature by 10°C per minute. After overnight incubation, the cells were transferred to liquid nitrogen for long-term storage.

2.2.5 Plating, immunostaining and mounting of fibroblasts

When cells were 80% confluent, they were trypsinised and centrifuged as per the protocol outlined in 2.2.3. Cells were plated in a 24 well plate (Griener Bio-One), onto 13X13mm coverslips (Menzel Glaser) pre-coated with 20µg/ml Poly-L-Lysine (Sigma) (post Poly-L-lysine coated coverslips were washed with 1XPBS X 3 washes), and cultured for 24 hours in fully supplemented F10 medium. After 24 hours, when the cells were 80% confluent, cells were either subjected to exogenous stress as outlined below or fixed for staining. In the case of the latter, F10 medium was removed, coverslips were gently washed with PBS and fixed using 3.7% paraformaldehyde (Sigma) for 30 minutes. Coverslips plated with fibroblasts thus fixed were then washed for 5 minutes X 3 times with 1XPBS and either stored at 4°C over night in PBS/0.001% Azide (Sigma) or subjected to immunostaining.

2.2.5.1 Immunostaining of human fibroblasts: TDP-43

Fibroblasts were stained as described in section 2.1.2.4.2. Coverslips were incubated with polyclonal rabbit anti-human N-terminal TDP-43 antibody (Proteintech group) at 1:500 dilution (with 0.1% PBST) for 1 hour followed by 3X5 minute PBST washes. Anti-rabbit 488 Alexa Fluor antibody (green) (Abcam) was added at 1:1000 dilution (with 1%PBST) and incubated at room temperature for 1 hour whilst protected from light. The rest of the staining protocol was completed as described before. The coverslips were then sealed using non-toxic grease composed of equal parts lanolin, Vaseline and paraffin wax, forming an airtight chamber or with nail varnish.

2.2.5.2 Immunostaining of human fibroblasts: p62

TDP-43 is considered to form a major component of the ubiquitinated cytoplasmic inclusions. P62 is used as a surrogate marker of ubiquitinated proteins. Therefore we used p62 as a marker of ubiquitinated aggregates. Mouse anti-p62 antibody (Sigma UK) was kindly provided from Prof P. Ince's lab at SITraN. A dilution of 1:1000 was used as the primary and anti-mouse Alexa Fluor 488 (Sigma, UK) was used as the secondary antibody. The rest of the protocol for antibody staining is as 2.1.2.4.2.

2.2.5.3 Immunostaining of human fibroblasts: phospho-TDP-43

Mouse anti p409/410 TDP-43 antibodies were a kind gift from Dr Robin Highley of SITraN (www.ptglab.com). A dilution of 1:2000 was used as the primary and anti-mouse Alexa Fluor 488 (Sigma, UK) was used as the secondary antibody. The rest of the protocol for antibody staining is as described in section 2.1.2.4.2.

2.2.5.4 Immunostaining for stress granules

We used mouse anti-HUR and TIAR (ABCAM, Cambridge UK) and mouse anti eGF1∞ (Scbt.com) as markers for stress granules. TIAR and HUR were later preferred as studies of stress granules showed co-localisation of TDP-43, with stress granules identified by using anti HUR antibody.

2.2.5.5 Immunostaining for GEM bodies

Mouse anti SMN antibody (ABCAM, Cambridge UK) (A generous gift from Dr K Ning) was used to immunostain GEM bodies and counter stained with DAPI to detect nuclei. Cells were viewed using an oil immersion lens with X63 magnification. Cells in four random sections were counted per coverslip (approximately 100 nuclei), in at least three replicates for each control and mutant cell line.

2.2.6   Assessment of fibroblast response to exogenous stressors

Fibroblasts were plated as described in section 2.2.5 and when the cells reached about 80% confluency the fibroblasts were subjected to an external stressor for a variable period of time (Table 2.1). Sodium arsenite was diluted with F10 medium down to a concentration of 0.5mM and incubated with cells for a period of 30 minutes as described previously (Anderson and Kedersha, 2002). Sorbitol was used as an osmotic agent to cause cellular stress at a concentration of 0.5M for durations of 30, 60 and 120 minutes to assess for optimal stress (indicated by maximum number of stress granule appearance) (Kedersha et al., 2005). Cells were heat shocked using a temperature of 42°C for 30min with the cell-culture plate in place to prevent evaporation. Thapsigargin was diluted in 0.5% ethanol and further diluted with F10 media to minimise the alcohol in the cell culture medium and to obtain a final concentration of 4μM and then the cells were stressed for 45 minutes (Bosco et al., 2010a). Unstressed controls were incubated with the same media without the stressors. Fibroblasts from three different age and gender matched normal healthy controls and three different cases carrying mutations in the *TARDBP* gene (M337V, A321V, G287S) were used in the experiments (Table 2.2). The stress response was defined as the ability of the cells to form stress granules. If a cell were to form more than three stress granules it was considered as a positive response as previously described in section 2.1.4.2.

Table 2.2 ALS patient and control fibroblast details

Age at Biopsy (Years)	Fibroblast I.D	Control/ Mutation	Gender	Onset of Symptoms	Disease Duration (Months)
Controls					
43	FIBCON02	Control	Female	-	-
50	FIBCON04	Control	Male		
38	FIBCON09	Control	Male		
54	FIBCON11	Control	Male	-	-
77	FIBCON19	Control	Female	-	-
Patients					
56	*TARDBP* G287S	FIBPAT55 sALS	Male	51	76.5
62	*TARDBP* M337V	FIBPAT51 fALS	Male	58	94
40	*TARDBP* A321V + C9ORF72 hexanucleotide repeat	FIBPAT48 fALS	Female	37	58
54	FIBPAT18	sALS	Male	53	47
67	FIBPAT21	sALS	Female	66	16
39	FIBPAT26	sALS	Male	38	32.5
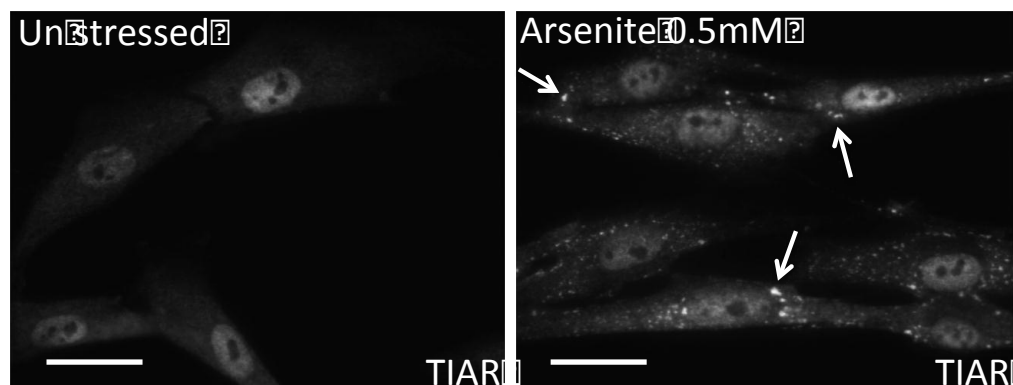
Figure 2.3. Stress granule formation in fibroblasts stressed with sodium arsenite compared with unstressed fibroblasts. All of the stressed cells have formed stress granules, which are immunostained using antibodies to TIAR. White arrows point towards the stress granules. Cells are from the same case.

2.2.7 Assessment of stress recovery response in the fibroblasts

Both control and patient fibroblasts were subjected to stress with sodium arsenite at 0.5mM over a time course of 0 minutes (unstressed), 15, 30 and 45 minutes to assess the difference in response to exogenous stress between control and mutant fibroblasts. Furthermore we also assessed the recovery response over 150 minutes after having stressed for 45 minutes as above. The media was removed and the cells were washed with fresh media (three washes) and allowed to recover over 15, 30, 45, 90, 120 and 150 minutes post stress. Cells were then fixed and immunostained as described above for TDP-43 and stress granules.

2.2.8 Confirmation of punctate lesions formed in response to exogenous stress as stress granules

The punctate lesions, which form in the cells upon exposure to exogenous stressors, particularly agents such as Arsenite and Sorbitol, are considered stress granules. However to confirm this phenomenon an inhibitor of translation elongation, such as cycloheximide, that traps mRNA within polysomes and prevents the formation of stress granules was used to demonstrate that the punctate lesions are indeed stress granules (Mollet et al., 2008). Both control and patient (G287S) fibroblasts were cultured in media with and without 10µg of cycloheximide for an hour prior to stressing with 0.5mM Arsenite for 30 minutes. The cells were fixed and stained as described before.

2.2.9 Image Analysis

Images were saved in a 16-bit Gray scale format and transferred as a TIFF file onto a computer processing ImageJ software before being opened as a stack of images. More than one hundred cells analyzed per cover slip. Slides were anonymised during the labeling process and analysed in a blinded fashion.

2.2.7.1 Assessment of cytoplasmic mis-localisation of the TDP-43 in mutant fibroblasts

Fibroblasts stained for TDP-43 (N-terminal antibody, Proteintech group) and Hoescht for nuclei were analyzed using an upright light microscope (Nikon Eclipse 80i microscope). Exposure was set at 230ms to obtain sub-saturated images of the nucleus of the mutant fibroblasts stained with the anti-TDP-43 antibody. Exposure, gain, and offset were stored to the computer to unify the settings across all image acquisition processes including normal controls (n=3, three replicates for each control) and mutant fibroblasts (n=3, three replicates for each mutant). A colour palette (red) was used to identify the saturated nuclei (most control fibroblasts Figure 2.4 A&B). The presence of nuclei was confirmed by Hoechst staining. Thus nuclear staining was objectively categorised into three groups: Normal (Saturated nuclear stain Figure 2.4 panel A), Sub-saturated (Reduced nuclear stain Figure 2.4 panels C&E, solid arrows), Empty (Nuclear stain less than that of the cytoplasm Figure 2.4 panels C & E, empty arrows). The number of cells with
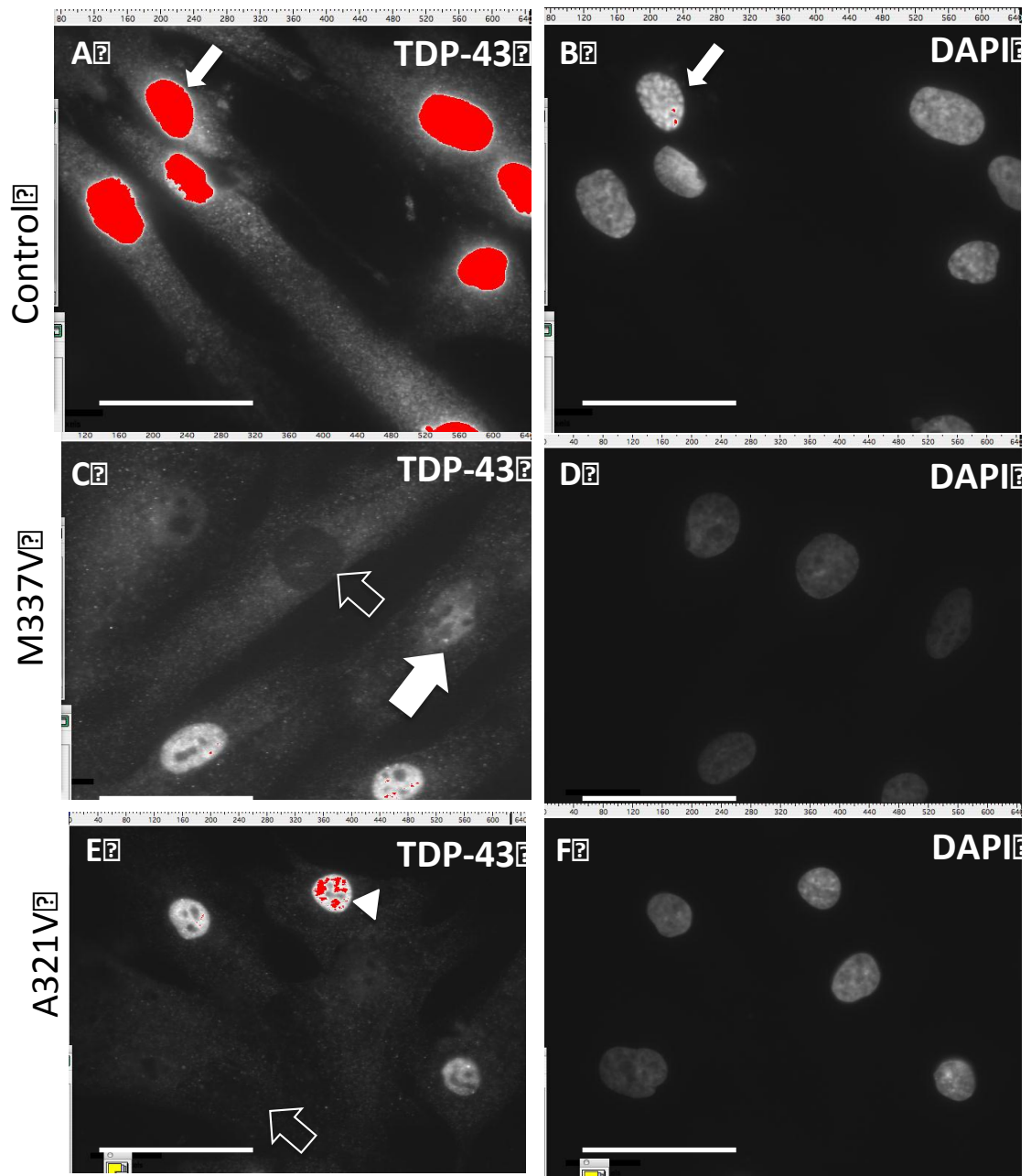
Figure 2.4 Categorisation of TDP-43 localisation in fibroblasts derived from control and mutant cases. This figure depicts different levels of TDP-43 expression within the nucleus. (A) Fibroblasts from control cases saturated with TDP-43 in the nucleus (indicated by the solid white arrow) (B) DAPI stain confirming the position of the nuclei. (C &D) Empty arrow marks a nucleus empty for TDP-43 staining in a mutant TDP-43 (M337V) fibroblast. The solid arrow shows a nucleus with reduced expression of TDP-43 as does the arrow in panel E.

empty, sub-saturated and saturated nuclear staining was counted in 10 different consecutive fields starting from the top left hand side of a coverslip. Coverslips were analysed blinded as mentioned above.

2.3 Zebrafish: Transient knockdown of *tardbp* and *tardbpl* and stable *tardbp* mutant characterisation

2.3.1   Chemicals

Antisense morpholino oligonucleotide (AMO) were designed and obtained from www.genetools.com, USA. RT PCR primers specific for *tardbp, tardbpl* and *tardbpl-FL* were designed and obtained from Sigma-Aldrich (Poole, Dorset ,UK). The znp-1 mouse monoclonal antibody was used to label motor axons, and mouse anti islet-1 to identify neuronal cell bodies were obtained from DSHB, University of Iowa, USA). Rest of the chemicals used were obtained from Sigma-Aldrich (Poole , Dorset, UK) unless stated otherwise.

2.3.2   Zebrafish husbandry

Adult zebrafish and embryos were raised at 28.5^oC. Wild-type (WT) animals were from the AB strain. Embryo collections, AMO (antisense morpholino oligonucleotide) microinjection and maintenance of the mutant and WT zebrafish lines were conducted according to standard protocols and in accordance with United Kingdom Animals (Scientific Procedures) Act 1986. The *tardbp*Y220X, mutant (*tardbp^{fh301}*) line was generated using the TILLING process undertaken in the Fred Hutchinson Cancer Research Centre, Seattle, USA, under Animal Care protocol 1342, which is reviewed and approved annually by the FHCRC Institutional Animal Care and Use Committee and is in accord with the recommendations of the American Veterinary Association.

2.3.3   Identification of zebrafish orthologues of TDP-43

The full-length human *TARDBP* cDNA sequence (**ENSG00000120948)** was BLAST searched against the zebrafish genome using both the ensembl and Genescan genome browsers. Two putative transcripts *tardbp* (ENSG0000040031) and *tardbpl* (ENSG00000004452) were identified. The predicted amino acid sequences were aligned against the human amino acid sequence using Clustal W2 software (www.clustalW.org). Genescan predicted the possibility of a longer version of *tardbpl* (*tardbpl-FL*). Therefore to ascertain *in silico* predictions, overlapping primers specific for *tardp*l and *tardbpl-FL* were designed to amplify the coding sequences of the reverse transcribed zebrafish RNA and obtained from Sigma UK.

2.3.4   Generation of a *tardbp* nonsense allele (*tardbp^fh301*)

The *tardbp^fh301* mutant was generated in the AB background and identified in a TILLING screen. The mutant was recovered by *in vitro* fertilisation of AB eggs using a cryo-preserved sperm sample from a single heterozygous F1 male. Heterozygous F1 adults were outcrossed into the AB background and heterozygous F2 adult fish identified by fin clipping and genotyping. The F2 heterozygous (*tardbp^fh301/+*) animals were bred with AB fish for three further generations to obtain F5 mutant heterozygotes. All experiments were carried out on F6 progeny homozygous for the c.660 C>A (*tardbp^fh301/fh301*) and their wild type (*tardbp^+/+*) siblings. TILLING screen was carried out in Fred Hutchinson's laboratory in Seattle, Washington, USA as part of collaboration.

2.3.5   Generation of homozygous *tardbp* mutant zebrafish (*tardbp^fh301/fh301*) and identification of genotype

F6 heterozygous adult mutant zebrafish, which were 3 months old, were set up in a heterozygous-heterozygous in cross to generate the homozygous fry. These fry were brought up in the same tank. At 3 months of age the fish were anaesthetised using tricane and the caudal fin was clipped as previously described (Kawakami et al., 2000). Clipped piece of fin was placed in a 96 well plate with 50μl of DNA easy reagent from DNAeasy kit (Qiagen) and stored at 4°C. Following fin clipping the fish were housed individually. DNA was extracted using DNAeasy kit (Qiagen). A pair of primers was designed (*tardbp*_genFWD 5'CAAGGTATAGATGAACCAATGAGGA_3' and *tardbp*_genREV 5 GTCATCTGCAAAGGTGACAAAAG 3') for PCR amplification of the extracted DNA. 10μl of the PCR reaction was digested over night with *CViQI* at 25°C according to *New England BioLabs* standard protocol for *CViQI* enzyme and analyzed by electrophoresis. In initial experiments, DNA extracted during the genotyping was also sequenced to verify the mutation. PCR reaction was as follows-

95°C for 5minutes

95°C	for 45 seconds	
50-65°C	for 45 seconds	30 cycles
72°C	for 45 seconds	
72°C	for 10min	

4°C   Hold

2.3.6 Measurement of weight and length of adult zebrafish

At the same time of fin clipping the anaesthetised fish were weighed using a digital scale to three decimal points of a gram. The fish were also placed on a measuring tape and the standard length was measured from the tip of the lower jaw to the end of the hippural plate as shown in figure 2.3.1 in millimeters. Once the genotype data was available the weight and length of the three genotype categories were pooled.
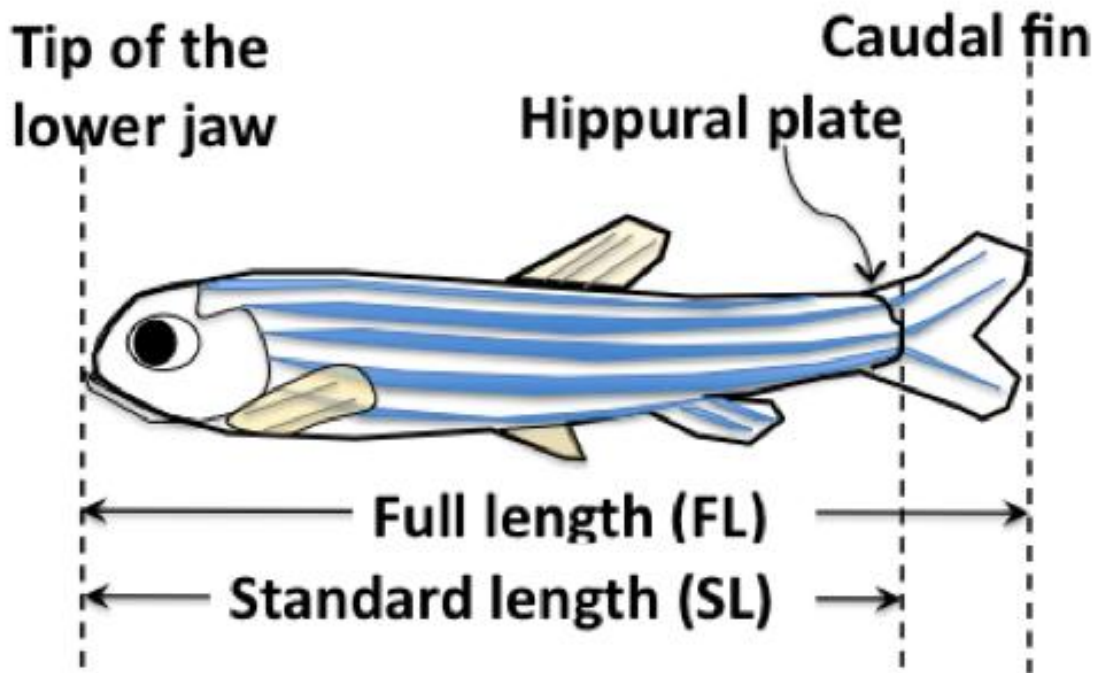
Figure 2.5 Schematic diagram of important surface anatomy and measurements. Anaesthetised zebrafish were placed on a tape measure and standard length was measured from tip of the lower jaw to the hippural plate to the closest milimitre (mm) to obtain the standard length (SL). Full length was not measured as the zebrafish were first subjected to fin clipping for genotyping.

2.3.7 Antisense morpholino oligonucleotide (AMO) mediated gene knock down

2.3.7.1 *tardbp* knockdown

An AMO was designed to block the translation initiation site (ATG) of *tardbp* (*AMO-tardbp^{ATG} sequence :* 5' TACATCTCGGCCATCTTTCCTCAGT 3'). The standard control AMO (*AMO-Control- designed against human ß globin*) (www.genetools.com) was also used to distinguish the specificity of the effects seen from the knockdown of *tardbp*. Furthermore an AMO against zebrafish p53 (*AMO^{p53}*) was also used along

with the *AMO-tardbp^{ATG} (Genetools, LLC, Philomath, OR, US)*. The AMO was dissolved in nuclease-free sterile water to obtain a stock solution of 4nmol/µl. The optimal dose was established by injecting a range of *AMO-tardbp^{ATG}* doses (1.8, 2.5, 5, 7.2 and 16ng) along with 8ng of p53 AMO). To monitor the accuracy of injections, phenol red (Sigma, Poole, UK) was added at a final concentration of 1% prior to injecting the zebrafish embryos.

Once the light cycle starts at 8am fish embryos were collected every 15 minutes till about 11:30am. The embryos were injected with each category of AMO using an air pressure injector (Narashige IM-300 gas line injector). Glass capillary needles were prepared using a Model P-97 Flaming/Brown micropipette pulling machine (Sutter Instruments Co., USA)- programme 90 to obtain ultra fine needles. 1nl of AMO mixture (gene specific AMO+p53 AMO) was injected into the yolk sac of 1-2 cell stage embryos. The injection volume was calibrated using a Graticule. The injected embryos were re suspended in E3 (http://cshprotocols.cshlp.org/content/2011/10/pdb.rec66449.full) medium with methylene blue and incubated at 28 °C. A range of concentrations of AMO was injected to identify the optimal concentration. At the optimal concentration there was minimal death of embryos at 36hpf but the amount of AMO was sufficient to produce a macroscopic phenotype.

At 24hpf post optimal AMO injection, 0.003% 1-phenyl 2-thiourea (PTU) was added to the embryos to suppress the pigmentation, if the embryos were used for microscopic evaluation. Embryos were counted and checked for abnormalities and documented at 4, 8, 24, 32-36, 48 and 72hpf for any obvious morphological changes. Survival of the embryos injected with *AMO-tardbp^{ATG}*, AMO controls and uninjected controls was monitored for 72hpf.The number of dead, curly tailed and 'monster' looking embryos were counted at each time point for all injection categories. Control AMO and uninjected embryos from the same batch of embryos were used as controls. At least four independent experiments were carried out per injection category and each experimental repeat included at least 100 embryos per category. Embryos were then processed as required for immunohistochemistry and immunoblotting.

One nanolitre of the optimal AMO dilution was injected into the yolk sac of the embryos at the 1-2 cell stage. Survival of the embryos injected with *AMO-tardbp^{ATG}*, AMO controls and uninjected controls was monitored for 72hpf. At least

four independent experiments were carried out per injection category and each experimental repeat included at least 100 embryos per category. Embryos were observed at 4, 8, 24, 32-36, 48 and 72hpf for any obvious macroscopic phenotype changes. Embryos injected with 16ng of *AMO-tardbp^{ATG}* did not survive whilst 7.2ng of *AMO-tardbp^{ATG}* resulted in a severe curly tail phenotype with death as early as 24hpf. Therefore 2.5ng of *AMO-tardbp^{ATG}* was selected as the optimal dose for injection. The curly tail phenotype and any changes in the hindbrain clarity were recorded and observed until 48hpf. The optimal dose of *AMO-tardbp^{ATG}* was injected in triplicate into at least 100 embryos per experiment. Embryos were then processed as required for immunohistochemistry and immunoblotting.

2.3.7.2 Antisense morpholino oligonucleotide (AMO) mediated knock down of *tardbpl*

A translation-blocking AMO was designed to knockdown *tardbpl* (*AMO-tardbpl^{ATG}*) (5' CCACACGAATATAGCACTCCGTCAT 3'). The standard control AMO (*AMO-Control*) (www.genetools.com) was also used to distinguish the specificity of the effects seen from the knockdown of *tardbpl*. Furthermore an AMO against zebrafish p53 (*AMO^{p53}*) was also used along with the *AMO-tardbpl^{ATG}(Genetools, LLC, Philomath, OR, US)*. The AMO was dissolved in nuclease-free sterile water to obtain a stock solution of 4nmol/μl. The optimal dose was established by injecting a range of *AMO-tardbpl^{ATG}* concentrations along with 8ng of p53 AMO (5' GCGCCATTGCTTTGCAAGAATTG 3'). To monitor the accuracy of injections, phenol red (Sigma, Poole, UK) was added at a final concentration of 1% prior to injecting the zebrafish embryos. The same *tardbpl* ATG site AMO was also injected into the *tardbp^{fh301/ fh301}* stable mutant. We chose two concentrations, high dose (16ng) and low dose (5ng) to knockdown *tardbpl-FL* transcript.

2.3.7.3 Splice site targeted antisense morpholino oligonucleotide (AMO) mediated knock down of *tardbp*

Two splice site targeting AMOs were designed against the *tardbp* transcript. The first splice AMO was called *tardbp^{SpI}* AMO (TDPS1) which targets exon 3 splice acceptor site (exon 3-intron 3-4 junction) (5' TATATCAGTATATTTT==ACCT==GCACC 3'). The second splice AMO, *tardbp^{SpII}* AMO (TDPS2) targets exon two which harbours the ATG site (5' TAATTGTACCACAT==ACCT==TTTGGGT 3'). As described above varying concentrations of both TDPS1 and TDPS2 AMOs were injected into

WT embryos to establish a concentration which provided an obvious macroscopic phenotype .

2.3.8   Biochemistry and Immunoblotting

2.3.8.1 Protein extraction

Six month old HOM (*tardbp$^{fh301/fh301}$*) and WT (*tardbp$^{+/+}$*) adult zebrafish (four zebrafish per group) were sacrificed using 2% Tricaine (Sigma, UK) to obtain brain, spinal cord, eyes, muscle, heart, gills and liver for protein and RNA extraction. Protein extraction from embryos was carried out at 36hpf or 48hpf. At least 100 embryos were collected for each category studied and deeply anaesthetised as for adult zebrafish with Tricaine. The embryos were initially processed without deyolking. Later a deyolking step was added due to the relative insufficiency of the target protein (Tardbp/Tardbpl) in relation to the abundant yolk proteins such as vitellogelin. Embryos were washed in PBS and placed in a 1.5ml tube tube. 10µl of the deyolking buffer (Stock solution was: 10ml of Ringer's solution + 30 µl of 100 mM   PMSF + 1 ml of 10 mM EDTA) was added per embryo, to the embryos and shaken at level 3 of a shaker/vortex machine (Gennie) for 5 minutes at 4 °C or on ice. The tubes were then centrifuged at 4 °C at 300Xg for 40 seconds. The supernatant was carefully removed and lysis buffer (RIPA (25mM Tris•HCl pH 7.6, 150mM NaCl, 1% NP-40, 1% sodium deoxycholate, 0.1% SDS) buffer with 1% SDS and protease cocktail inhibitor and phophatase inhibitor (phosphostop- Roche) (1µl per embryo) was added to the pellet and the samples were immediately snap frozen in liquid nitrogen and stored at -80°C. The samples were thawed on ice and sonicated using a probe sonicator at 50% amplitude for 5 pulses   until the sample was clear. The sample was then boiled at 98°C for 5 minutes with vigorous vortexing every 1-2 minutes before centrifuging at 14000 rpm for 15 minutes. The supernatant was retrieved and stored at -80 °C or used for analysis.

2.3.8.2 Protein estimation using BCA assay

A BCA assay was performed to estimate the amount of protein in the sample. The BCA assay was preferred to the Bradford assay as the SDS in the lysis buffer does not interfere with the BCA assay (Gates, 1991). A serial dilution of 2mg/ml BSA in RIPA buffer was prepared and 25µl of each standard concentration was aliquoted

in flat bottom 96 well plates in triplicates. Unknown protein samples were diluted by 15 fold and were aliquoted in volumes of 25μl in triplicates. The working reagent was prepared by adding 240μl BCA reagent A to 12mls of reagent B. The total volume to be used was calculated for the number of standard and sample wells. 200μl of the working reagent was added to each well and the plate was mixed gently on a shaker for 30 seconds. The plate was placed in 37°C for approximately thirty minutes. Following the incubation the plate was allowed to equilibrate with the normal room temperature. The plate readings were taken using a plate reader (Fluostat Omega v1.01, Bmg Labtech) at 562nm wavelength. The standard curve was tabulated by using a quadratic curve-fitting algorithm (Mars Data Analysis software 2.10.R2, Build 13, Bmg Labtech). Final concentrations of proteins extracted were calculated using the above algorithm.

2.3.8.3 Preparation of SDS page gel, resolving of proteins, transferring to PVDF membrane and detection of proteins of interest

Twenty milliliters of 12% resolving gel was first made (8ml of 30% Polyacrylamide, 5ml of 1.5M Tris (pH 8.0), 200μl of 10% SDS, 6.6ml of dH2O was mixed first and just before pouring, 200μl of 10% Ammonium persulphate and 8μl of TEMED was added to catalyze the reaction. Water saturated Butanol was used to layer on the top of the resolving gel and once the resolving gel was set 8ml of stacking gel was prepared (1.3ml of Polyacrylamide, 2ml of 1M Tris (pH 6.8), 80μl of 10% SDS and 4.5ml of dH2O was mixed before adding 80μl of 10% Ammonium persulphate and 8μl of TEMED just before pouring. An appropriate comb was placed to create the wells. The gels were then placed in a tank and equilibrated in the running buffer. Samples were mixed in amounts equivalent to 40μg of total protein and mixed with 4X Laemili sample buffer before loading on to the gel with gel loading tips. 5μl of the All blue protein ladder (Biorad) was loaded for identification of proteins by size.

The gel was initially run at 60V to help stacking and resolved at 90V. Thereafter the proteins were transferred to a PVDF membrane at 250mA over 1 hour. Prior to this step the membrane was equilibrated in 100% methanol for 5 minutes and 5 minutes in the transfer buffer. The protein transferred membrane was then blocked in 5% milk in 0.25% PBS/Tween20 for one hour before probing with polyclonal rabbit anti human TDP-43 proteintech antibodies (Catalogue number 12942-1-AP) or (cat number 10782-2-AP) to detect Tardbp or Tardbpl.

The mouse monoclonal α tubulin antibody (1:10,000) (Sigma UK) was used for a loading control. The membrane was incubated in 1:1000 hTDP-43 antibody over night at 4 ºC and washed with PBS + 0.25% Tween 20 three 5 minute washes. Membranes were then incubated in the α tubulin antibody (1:10,000) in PBS + 0.25% Tween 20 and 0.001% Sodium azide (to inactivate the HRP) for 1 hour on a rolling machine. The washed membranes were incubated in rabbit anti mouse HRP (1:10,000) antibody for 1 hour. The membrane was incubated in goat anti rabbit HRP antibody (1:2000) as the secondary antibody. The membranes were washed with 3, 5 minutes PBS/Tween20 washes. The membranes were developed using the EZ-ECL chemiluminescence HRP kit according to product protocol. (Geneflow.co.uk). Membranes were exposed to hyperfilm (Kodak) and developed using the Kodak photo developer solution and fixed using a fixer solution (Kodak) in a dark room or viewed directly using the GBox-HR Gel Doc system with a 4 megapixel, 16 bit, peltier cooled CCD camera and Genesnap software (Syngene, US). Densitometry was carried out using the G box hardware and software, Genetools software (Syngene, US) (www.integratedscientificsolutions.com).

2.3.9   Immunohistochemistry on whole mount embryos

Immunohistochemistry was carried out on whole-mount 36hpf embryos as previously described (Beattie et al., 2000). The znp-1 mouse monoclonal antibody (1:400) was used to label motor axons, and mouse anti islet-1 to identify neuronal cell bodies (both from DSHB, University of Iowa, USA).

Motor axonal projection defects were assessed by counting the number of axons that were either prematurely truncated or abnormally branched at or just below the horizontal myoseptum. A total of 10 axons immediately caudal to the yolk bulge in both hemi- segments of each zebrafish, were counted to standardize the counting across all groups. Each hemi- segment was scored out of 10 for the number of axons with premature truncating or branching or both defects. At least 30 embryos per category for each of 4 experimental repeats were counted. The number of motor neurons and Rohon Beard neurons stained with anti islet-1 were counted across eight myo-segments from immediately caudal to the yolk bulge to the end of the yolk extension. Images were obtained using a Zeiss light microscope with bright field settings. Images were analyzed using Image J (rsbweb.nih.gov/ij/) software.

2.3.9.1 Obtaining and preparing of WT zebrafish embryos for immuno staining

Embryos from different AMO injected categories were incubated at 28 °C for 36 hours in E3 medium in petri dishes. At 24hours post fertilisation (hpf) 300ul of 0.3% stock PTU solution (1-Phenyl 2-Thiourea, Sigma Aldrich, Sweden) warmed at 28°C was added to each Petri dish to suppress the development of pigmentation. Prior to fixation dead embryos were removed and the live embryos were dechorinated manually and anaesthetised with Tricaine as explained above. A total of 50 embryos were transferred to a 1.5ml micro-centrifuge tube and as much E3 medium as possible was aspirated before adding 4% paraformaldehyde (PFA from Sigma Aldrich, Sweden AB, 2g of PFA powder weighed and mixed under a fume hood in 50ml of phosphate buffered saline (PBS, 1 tablet dissolved in 200ml of distilled water) and warmed in a water bath at 65 °C until PFA dissolved, PFA was cooled to room temperature before adding to fish) and fixed overnight at 4°C. On the following day fixed embryos were washed with 1XPBS solution in two 5 minute washes. Embryos were then transferred to 25%, 50%, 75% and 100% methanol in PBS solution to dehydrate and stored at -20 °C.

2.3.9.2 Immunostaining of fixed dehydrated embryos

Embryos which were stored at -20 °C were rehydrated in Methanol/PBS solutions :75%, 50% and 25% for 15 minutes in each dilution, prior to suspending them in PBS alone. The embryos (30-50 per 1.5ml tube) were permeabilised using ice cold acetone (Acetone crack for 7minutes on ice and then 0.25% Tryspsin (Invitrogen) in PBT (1% Triton X-100 (from Sigma Aldrich, Sweden AB) in PBS) for 8 minutes on ice. Trypsin was inactivated using an equal volume of 1% normal goat serum (NGS) in PBT (Sigma, Aldrich, Sweden AB). Embryos were then washed with 3, 5 minute washes in PBT. Embryos were then blocked in blocking buffer (10% NGS v/v, 1% Bovine serum albumin w/v (BSA, Sigma Aldrich, Sweden AB), 1% Dimethyl sulphoxide (DMSO) in PBT (PBDT)) for 1-3 hours whilst being shaken on a horizontal shaker at minimal shaking level to prevent dismembering the embryos. Afterwards primary antibodies were added. Polyclonal rabbit anti human TDP-43 (Protein Tech ltd) antibody was used at 1:100, mouse anti islet 1 monoclonal antibody (ZIRC) at 1:400 in antibody dilution buffer. Embryos in the

antibody dilution buffer with primary antibodies were shaken on a horizontal plate shaker at 4°C overnight. The embryos were washed in 5 PBT washes over 3-5 hours at room temperature. Anti rabbit Alexa 488 anti rabbit fluorescent secondary antibody at 1:1000 dilution and anti mouse Alexa 568 red fluorescent antibody at 1:1000 dilution were prepared and embryos were incubated in the secondary antibodies over night at 4 °C on a horizontal shaker at slowest speed. The embryos were washed on the following day as described above in 5 PBT washes over 3-5 hours. Hoechst solution used in 1:1000 dilution of 1ug/ml stock solution was added to the embryos for 5 minutes and washed with PBT in 3, 5 minute washes. Topro 3 was used later as the Hoechst penetration into the deeper zebrafish tissues was weak and Topro 3 was added to the embryos along with the secondary antibodies. Tubes with the embryos were covered in tin foil during and after the secondary antibody steps to prevent loss of fluorescence following exposure to light.

2.3.9.3 Znp-1 staining to identify the axonal architecture with DAB stain development of AMO injected zebrafish

Embryos were fixed and permeabilised as mentioned in section 2.3.9.2. Mouse monoclonal znp-1 antibody was used at 1:500 dilution in the antibody dilution buffer (5% NGS, 1%DMSO, 1%Albumin in PBS), as a marker for axonal architecture. After 4-5 30 minute washes over 3-5 hours anti mouse immunoglobulins from thermo scientific AB conjugate kit were used as the secondary at 1:400 dilution over night. On the following day after 4-5 30 minute washes with PBT (1% TritonX-100 in PBS) over 3-5 hours embryos were treated with A and B conjugate mix made as per kit protocol for 1 hour. The AB conjugate mixture was incubated for 30min at room temperature prior to adding to the embryos. The embryos were then washed in two 30minute PBDT washes and two 30minute PBT washes over 2 hours. A DAB (Sigma, UK) tablet was dissolved in 15ml of Tris HCL pH 7.5 (made with double distilled water) and covered with tin foil prior to use, to avoid light inactivation. DAB solution was added to the embryos whilst checking for the brown DAB stain development under a dissecting microscope. When sufficient colour had developed, excess stain was washed with PBS in 3-4 washes over 5-10minutes. Embryos were then transferred to a series of glycerol concentrations prior to storing at -20°C in 80% Glycerol/PBS.

2.3.9.4 The assessment of axonal architecture

Ten pairs of axons were identified in the trunk portion of the embryo as illustrated in figure 2.6A. The axons were counted on both hemi sides of the fish for abnormalities in length (truncations) and branching (figure 2.6B). The same set of axons was counted on every embryo. 30-50 embryos were randomly selected and counted for the above abnormalities in all injection categories and also for the un injected controls. The abnormalities were scored out of 10 per hemi side. 0 out of 10 being a completely normal to 10 out of 10 abnormalities being the worst. Abnormal branching, truncation and the total axonal abnormalities were calculated separately similar to the technique used by McWhorter et al 2003 (McWhorter et al., 2003).
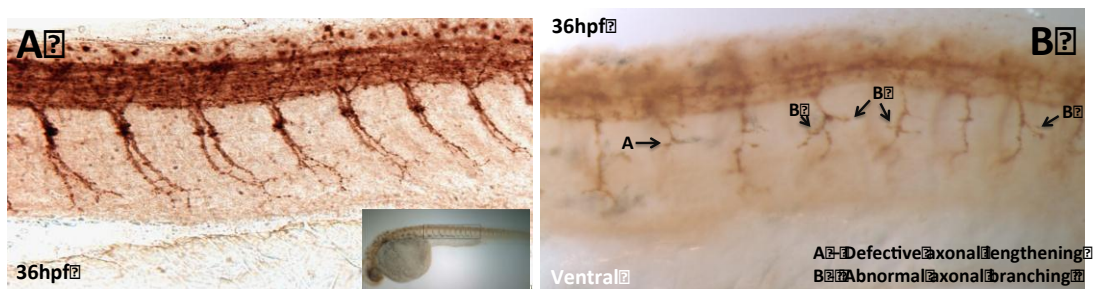
Figure 2.6 Counting of axonal defect in zebrafish embryos. A) (Inset) Laterally mounted 36 hours post fertilised (hpf) zebrafish embryo stained with znp1 and developed with DAB. Rectangular mark indicated the position of the 10 pairs of axons counted for defects. Panel A shows a normal axons of a 36hpf embryo. **B)** Different types of axonal defects observed. **Arrow A** indicates premature truncation, **Arrow B** indicates aberrant branching

2.3.9.5 Mounting of immunostained zebrafish embryos

Immuno stained embryos were transferred into a series of glycerol/PBS solutions from 25%, 50% to 75%, 20 minutes in each concentration to allow the embryos to equilibrate (at which point they sink to the bottom of the tube). Once the embryos have equilibrated in 75% Glycerol/PBS solution they were stored at -20ºC prior to mounting. Embryos were deyolked manually under the dissecting microscope and mounted on glass slides with wells made from electric insulation tape to hold the embryos (head and tail mounted separately) with a drop of glycerol or Vectashield mounting medium (for immunofluroescence staining).

2.3.9.6 Confocal microscopy

Confocal microscopy was used to obtain high clarity magnified images and to ascertain the localisation and the distribution of the endogenous TDP-43 orthologues. Vecatshield mounting medium was used to prevent bleaching due to intense laser light. To prevent 'bleed through' the sequential scanning method was used. Section thickness was set at 1μm to reduce background and to maintain sensitivity. Argon laser was selected to obtain the nuclear staining of Hoechst and far-red sensor for the Topro 3. Embryos were dissected into two, to obtain head and the trunk parts, which were mounted separately (head mounted dorsally-ventrally and the trunk mounted laterally). The same exposure settings were used for all samples. We used Leica TCS SP5 Confocal Microscope and images were captured using x63 objective.

2.3.10 RNA extraction and generation of first strand c.DNA synthesis

For RNA extraction samples were collected as described in section 2.7. Tissues from adult zebrafish or embryos were obtained as described earlier and total RNA was extracted using the Trizol reagent (Invitrogen, UK).

2.3.10.1 RT-PCR to illustrate abnormal splicing

Thirty six hours post fertilisation WT and TDPS1 (*tardbp* splice morpholino 1- *tardbp^{Sp1}* AMO) injected embryos were collected. About 50 embryos were put into a 1.5ml tube and washed with DEPC H_2O. 500μl of Trizol was added to the embryos and aspirated with progressively smaller gauge needles to homogenize and stored at -80°C. If stored at -80°C, samples were incubated at room temperature for 5 minutes prior to processing. The samples subjected to Trizole treatment were incubated at room temperature for 15 minutes to allow for complete dissociation of the nucleoprotein complexes. Then 125μl of $CHCl_3$ was added and inverted 8-10 times over 15 seconds by hand. Tubes were incubated at room temperature for 3 minutes before centrifuging at 13,000 rpm for 15 minutes at 4°C. The tubes were carefully removed. About 200μl of the upper aqueous phase was of the supernatant removed to a fresh 1.5ml tube without disturbing the precipitate and 150μl of isopropanol was added and incubated at room temperature for 10 minutes. The tubes were centrifuged at 13,000 rpm for 15 minutes at 4°C. If a pellet was not seen 1μl of pellet paint and 5μl of Sodium acetate was added to the

solution and centrifuged again at 13,000 rpm for 15minutes. Finally 300µl of 75% ethanol in DEPC H_2O was added to re-suspend the pellet. The tubes were centrifuged at 7000 rpm for 5 minutes at 4°C. The supernatant was discarded and the pellet was air dried (not completely but sufficiently so that no excess fluid was on the inside of the tubes. The pellet was re-suspended in 15-20µl of nuclease and RNAse free DEPC H_2O. The RNA yield was quantified using the Nano-drop machine using nucleic acid (RNA) estimation programme choosing the 260nm wavelength.

2.3.10.2 RT-PCR to illustrate abnormal splicing: c.DNA generation

1µg of RNA from 2.3.10.1 section was used for the synthesis of first strand c.DNA synthesis and subjected to DNAse treatment. One microlitre of 10X DNAse buffer was added to 1µl of DNAse enzyme and adding nuclease and RNAse free DEPC H_2O made a total reaction volume of 10µl. Samples were incubated at room temperature for 15 minutes. 1µl of 25mM EDTA was added to each tube before incubating at 65°C for 10 minutes. To the tube from the DNAse step 1µl of pdN6 and 1µl of dNTPs were added and incubated for further 5 minutes at 65°C. The samples were chilled and pulse centrifuged to collect. To each tube 4µl of 5X buffer and 2µl of 0.1M DTT and 1µl of nuclease and RNAse free DEPC H_2O were added. The samples were then transferred to a PCR machine and a programme was set up at 25°C for 10 minutes followed by 42°C for 2 minutes at which point the programme was paused to add the superscript II enzyme and the programme was then un-paused to run for further 50 minutes at 42°C followed by 15 minutes at 72°C. Thereafter the samples were held at 15°C until collection and stored at -20°C.

2.3.10.3 Amplification of c.DNA to detect effects of impaired splicing

c.DNA made from samples (0.8, 1.6, 2.4, 4.8, 9.6 and 16ng) of TDPS1 (*tardbp[SpI]* AMO) and Un-injected (Dechorinated) and Uninjected (Non Dechorinated) were subjected to three PCR reactions with the three sets of primers (Table 2.4) and figure 2.7. Master mixes for 10 reactions made with 40µl Reddy mix, 4µl of forward primer, 4µl of reverse primer and 132µl of DEPC H_2O were made. 1µl of sample c.DNA was added to 9µl of master mix onto a 96 well non skirted plastic plate. Actin primers were used as a positive control whilst 10µl of each master mix was used as a negative control without adding any c.DNA. Samples were then run on a PCR machine and amplified using a touch-down PCR programme.
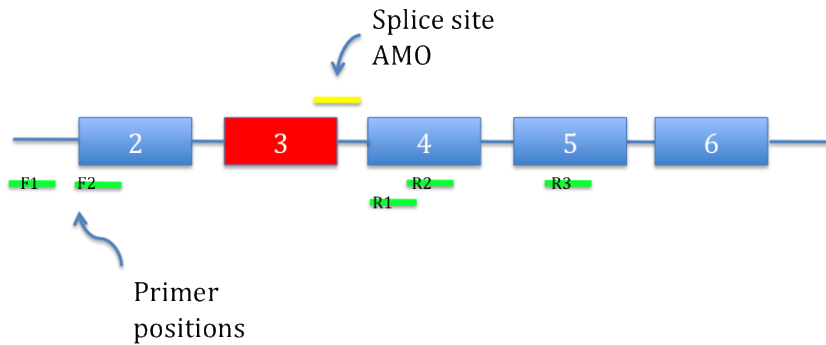
Figure 2.7 Placement of splice AMO (yellow bar) and the positioning of the primers (green bars).
Primer set 01 (F1+R1), set 02(F2+R2) and set 03 (F1+R3) were used to amplify the *tardbp* c.DNA to
detect any aberrant splicing. If the exon three were to be spliced out all three primer sets should pick up
the shortened c.DNA fragment as well as un spliced variants. It is also possible that the exon 04 (exons
are blue boxes with white numbers indicating the number of the exon) could also be spliced out. Therefore
a third set of primers was designed, which would take the above possibility into consideration. It is also
possible that the intron in which the splice site is on could be included in the c.DNA resulting in a higher
product size than the expected

**Table 2.3 Primers used for the analysis of the novel splice alteration of
TDPS1 and TDPS2 AMO injections (based on Fig 5.12)**

	Primer sequence
Set 1F	5' GCT TTT GAG GGT CGT TCT TG 3'
Set 3F	5' GCT CGA CTG AGG AAA GAT GG 3'
Set 1R	5' CGC TCC ATC ATC TGC CTA GT 3'
Set 2F	5' GAG AAT GAG GAG CCA ATG GA 3'
Set 2R	5' ATC AAT CAT GTG CCG CTG T 3'
Set 3R	5' ACA CTG ACG CCC TTG ATG AT 3'

***2.3.10.4   Real time quantitative PCR (RT-qPCR) to assess the expression of
the zebrafish TDP-43 orthologues – tardbp, tardbpl and tardbpl-FL in the WT
and tardbp*** *fh301/fh301* ***mutant***

Gene   specific   primers   were   designed   for   *tardbp*   (forward   5'
CGTCACCTTCGCAGACGATCAGGTT   3'   and   reverse
5'GCCTAAGCACAATAATATTCATCACCTCTTTTCCAATT 3', *tardbpl-FL* (forward 5'

121

CGTCACCTTCGCAGACGATCAGGTT 3' and reverse 5'GCCCACGATCCATC ATTTGCCTACTATT 3'). A set of primers, which amplifies a common sequence within both *tardbpl* and *tardbpl-FL,* was used as an internal control for RT-qPCR (forward 5' TCTGGTGTACGTGGTTAATTATCCAAAAGATAACA3' and the reverse 5' AGA GGT GAT CAT GGT GCA GGT GAA AAG). Two housekeeping genes, which have been well characterised for use in zebrafish (EF1alpha, forward [5' CTGGAGGCCAGCTCAAACAT 3'], reverse [5' ATCAAGAAGAGTAGTACCGCTAGCATTAC 3'] and RP113 alpha, forward [5' TCTGGAGGACTGTAAGAGGTATGC 3'] , reverse [5' AGACGCACAATCTTGAGAGCAG3']) were used for standardising the RT-qPCR results as previously described (Tang et al., 2007). Primers were optimised and efficiency assessed by analysing the standard curves. Real time PCR was performed using an ABI Prism 7900 HT sequence detection system (Applied Biosystems) using an Evergreen fluorescent label . RT-qPCR products were subsequently run on an agarose gel to assess the size of the amplified products.

2.3.11 Neuro muscular junction (NMJ) staining

11dpf and 14dpf larvae were anaesthetised with 1% Tricaine and were fixed in 4% paraformaldehyde (PFA) over night at 4°C. At least 25 embryos were fixed per group. Embryos were then washed in two distilled water washes for 5 minutes in each wash prior to a final wash in phosphate buffered saline (PBS) for 5 minutes. Embryos were then subjected to acetone crack for 10 minutes on ice followed by three further washes using distilled water over 15 minutes. Thereafter embryos were trypsinised with 0.25% Trypsin on ice for 4 minutes. Trypsin effect was aborted using 1% normal goat serum in PBS for 5 minutes. Embryos were washed in PBS for a further 15 minutes. Larvae were incubated in PBDT buffer for blocking (1% BSA, 1% DMSO, 0.5% TritonX 100, 1X PBS) plus 5% normal goat serum for 2 hours and incubated with Alexa 488 conjugated to alpha bungaratoxin (1:100, Molecular probes, Invitrogen, Eugene, USA) for 30 minutes. This molecular probe was then washed three times with PBDT 3X 15 minute washes. Following washes larvae were incubated with mouse monoclonal antibody against SV2 presynaptic marker (1:50, Developmental Studies Hybridoma Bank, Iowa, IA, USA) overnight at 4°C. All incubations with antibodies or markers have been done on a rotatory shaker. Secondary antibody, goat anti mouse antibody conjugated with Alexa-594

antibody was used at 1:1000 dilution. Larvae were finally eventually washed in 4X PBST washes before clearing through a Glycerol series. Glycerol cleared embryos were then mounted for confocal microscopy (Leica confocal microscope and Zeiss confocal microscope). NMJ staining was analysed using image J.

2.3.12 Assessment of the swimming of the larvae

Swimming behavior of the larvae at 5dpf was assessed by probing each embryo externally. 30 embryos were tested per group. Their escape response was analyzed; the best response out of three probing attempts was recorded. The escape response was categorised into four categories: normal swimming (3), reduced speed (2), corkscrew movement or minimal movement (1) and no movement (0).

2.3.13 Statistical analysis

When three or more groups were compared, one-way ANOVA, with Bonferroni's post-test comparison method was used. When only two groups were compared a unpaired t-test was used. Results of three independent experiments were used in every analysis.

Chapter 03:

Transient overexpression of TDP-43 in HEK293T cells

3.0   Introduction

TDP-43 is regarded as a highly conserved RNA binding protein, which has multiple functions in the nucleus as well as in the cytoplasm. Examination of pathological samples from patients with ALS has shown that TDP-43 forms a major component of the neuro-cytoplasmic ubiquitinated inclusions in motor neurons (Neumann et al., 2006, Neumann et al., 2007a, Borroni et al., 2010). C-terminal fragmentation and relative nuclear clearing have been suggested as additional features of the TDP-43 proteinopathy. In several other neurodegenerative conditions studies investigating the major proteins associated with neurocytoplasmic inclusions, have broadened the understanding of the pathophysiological mechanisms of the disease and have lead to significant interest and focus of therapeutic targeting in some conditions, e.g. APP in Alzheimers dementia and alpha synuclein in Parkinson's disease (Haass and Selkoe, 2007). Therefore the discovery of TDP-43 as the major component of the neurocytoplasmic inclusions in non-SOD1 related ALS is potentially a paradigm changing discovery. Mutations in the *TARDBP* gene, which encodes TDP-43, have been linked to both ALS (Kabashi et al., 2008, Sreedharan et al., 2008, Benajiba et al., 2009, Corrado et al., 2009b, Del Bo et al., 2009, Barmada and Finkbeiner, 2010), as well as FTLD (Borroni et al., 2009, Barmada et al., 2010). Therefore we set out to investigate if expression of disease associated mutations in *TARDBP* would recapitulate the observed pathological phenomena of relative nuclear clearing and cytoplasmic mis-localisation (Arai et al., 2006, Neumann et al., 2006) compared to expression of wild type TDP-43 (wtTDP-43). Furthermore it is unclear how mutations in the *TARDBP* gene contribute to the process of neurodegeneration at the molecular level. It has been hypothesised that mutant TDP-43 perhaps contributes to the disease process by a toxic gain of function by enhancing the features of TDP-43 proteinopathy as described above i.e nuclear clearing and aggregation in the cytoplasm (Yamashita et al., 2014). Therefore we set out to over-express wtTDP-43 and mutant protein

to investigate whether we could recapitulate any features of TDP-43 proteinopathy.

3.1 Transient expression of wtTDP-43 and a disease causing mutation A315T (mutTDP-43) is toxic to HEK293T cells

As described in the methods section, N-terminally *myc*-tagged full length TDP-43 WT, Q331K, A315T and M337V constructs were transiently expressed in HEK293T cells using Exgen. Analysis of subcellular localisation of TDP-43 revealed that, although TDP-43 was mainly nuclear in distribution, ~40% of the cells transfected with wtTDP-43 (Fig 3.1, panel A and B) and 25-30% of mutant TDP-43 transfected cells showed TDP-43 translocation to the cytoplasm (Figure 3.1 D). Previous studies in primary cortical neurons from rats reported only about 10-15% of the transfected cells were noted to have an early cytoplasmic mis-localisation (Barmada et al., 2010). Therefore we speculated at this stage that the transfection reagent could cause additional cellular stress to result in a greater cytoplasmic translocation of TDP-43. Therefore a wash step was introduced after 4 hours following transfection to negate any additional stress caused by the Exgen transfection medium. This additional wash step lowered the cytoplasmic mis-localisation of wtTDP-43 (by ~15%) (Fig 3.1 A and C) but did not alter mis-localisation of mutant TDP-43 (Fig 3.1 D-F). In addition, the wash step also lowered the transfection efficiency (Figure 3.2 panel E, second bar). However during TDP-43 DNA dose titration we discovered that the DNA dose used for transfection is inversely proportional to the transfection efficiency (Fig 3.2 E). 0.125µg of wtTDP-43 DNA provided the best transfection efficiency of ~80% ($p<0.05$) (Fig 3.2 D-E). A similar dose titration experiment using A315T mutant DNA constructs showed a modest improvement of transfection efficiency with 0.25µg of mutTDP-43 DNA but the transfection efficiency failed to improve further with 0.125µg of DNA (Fig 3.2, F). These findings suggest that higher doses of TDP-43 both WT and mutant TDP-43 DNA are toxic to the HEK293T cells. TDP-43 expression is finely balanced in the cells. Therefore over-expression of 1µg of TDP-43 DNA appears to lower the transfection efficiency.
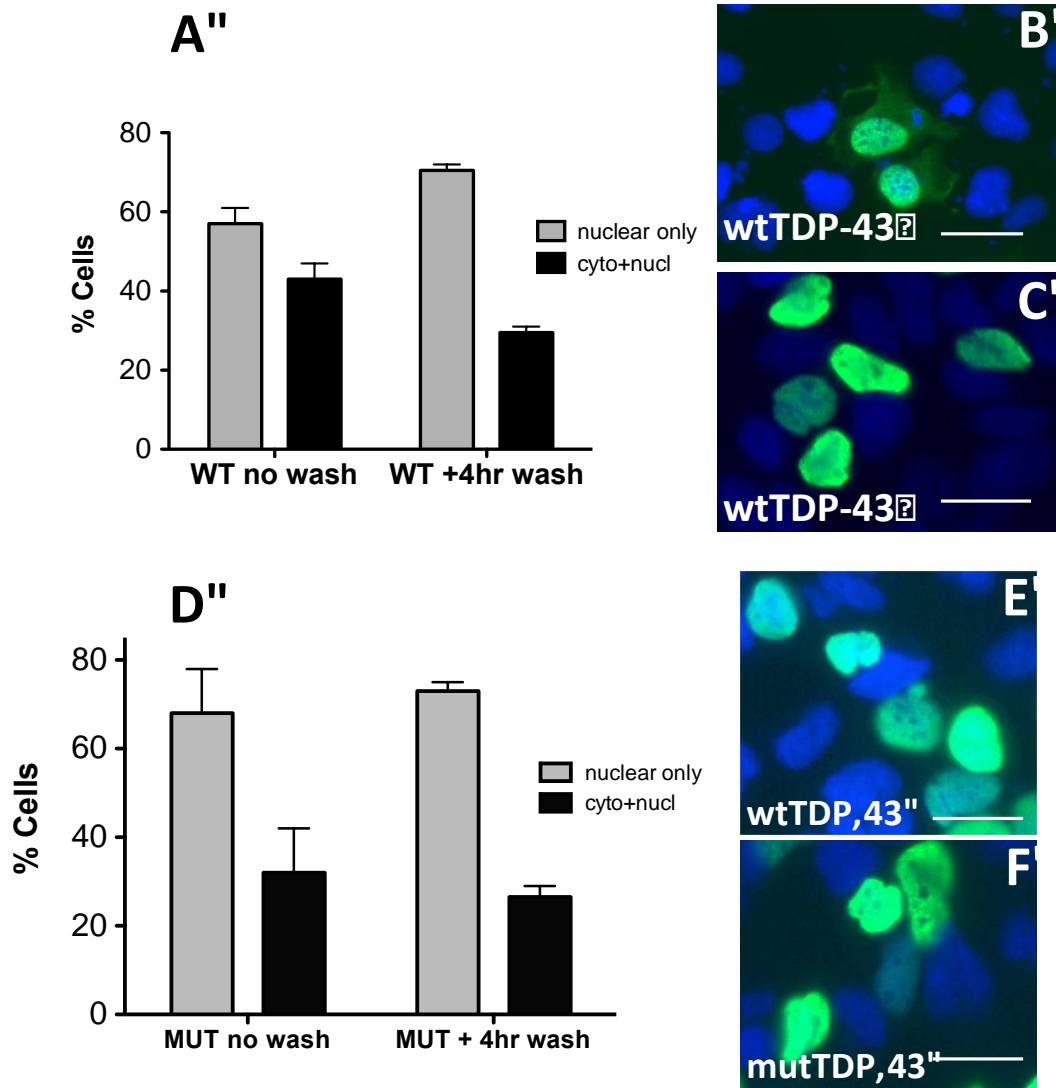
Figure 3.1 HEK293T cells transfected with wtTDP-43 and mTDP-43 (A315T) with and without a 4h wash step. All pictures of cells are on wtTDP-43 expressing cells. A) wtTDP-43 expressing cells pre- and post- 4h wash step. ~60% of the transfected cells showed a prominent nuclear expression of TDP-43 (grey bars) whereas ~40% of the cells also showed a significant cytoplasmic localislisation (black bars) **(B)** in addition to nuclear staining. **C)** Following the wash step nuclear localislisation of wtTDP-43 improved to ~70% of the transfected cells. **D)** mutTDP-43 expressing cells showed ~30% cytoplasmic expression which did not alter much after the wash step **(E-F).** Immunocytochemistry anti *myc* (TDP-43) green, DAPI- Blue. Scale bar 100µm

We postulated that cells expressing a higher dose of TDP-43 DNA perhaps underwent apoptosis in keeping with studies, which now show that expression of full length wtTDP-43 and mutant TDP-43 DNA are toxic to the cells (Wegorzewska et al., 2009, Tsai et al., 2010, Wils et al., 2010, Xu et al., 2010, Zhou et al., 2010, Arnold et al., 2013).

Over-expression of human A315T mutant using thy-1 promoter in mice led to a motor neuron disease like phenotype and ubiquitinated inclusions in the cortical motor neurons without TDP-43 positive inclusions (Wegorzewska et al., 2009). It is not clear whether or not the authors used a phosphorylation dependent TDP-43 antibody. Nevertheless these findings suggested that over-expression of A315T mutTDP-43 is toxic to the neurons and the formation of TDP-43 positive cytoplasmic aggregates is not necessary to cause neuronal toxicity. Therefore it is possible that the lower transfection efficiency noted with A315T mutant transfections indicates A315T mutation related toxicity when compared to wtTDP-43 (Fig 3.2 F). We also observed that the percentage of the cells expressing cytoplasmic wtTDP-43 was directly proportional to the dose of transfected wtTDP-43 (Fig 3.3). wtTDP-43 DNA at 0.125µg resulted in significantly lower cytoplasmic mis-localisation (<10% of the cells transfected) when compared to 1µg of wtTDP-43 transfected cells(>40%) (paired t-test with Mann Whitney U test, $p < 0.05$,) as did 0.25µg of DNA with <15% of the cells mis-localising to the cytoplasm (unpaired t test $p < 0.05$).

These data suggest that wtTDP-43 is toxic to the HEK293T cells when expressed at higher concentrations. In support of our findings is the study of over-expression of wtTDP-43 and A315T mutTDP-43 in rat cortical neurons, which suggested that the presence of cytoplasmic TDP-43 is significantly associated with neuronal toxicity and death in both WT and A315T mutant TDP-43 (Barmada et al., 2010, Wu et al., 2013). Although we have not assessed the expression levels either by immunoblotting for TDP-43 levels in the DNA titration study or quantitating the fluorescence level in the immunocytochemistry samples, we noted that the cytoplasmic mis-localisation is associated with a higher dose of DNA used for transfection. We have not conducted a similar DNA dose response analysis of cytoplasmic mis-localisation of mutTDP-43 in HEK293T cells.
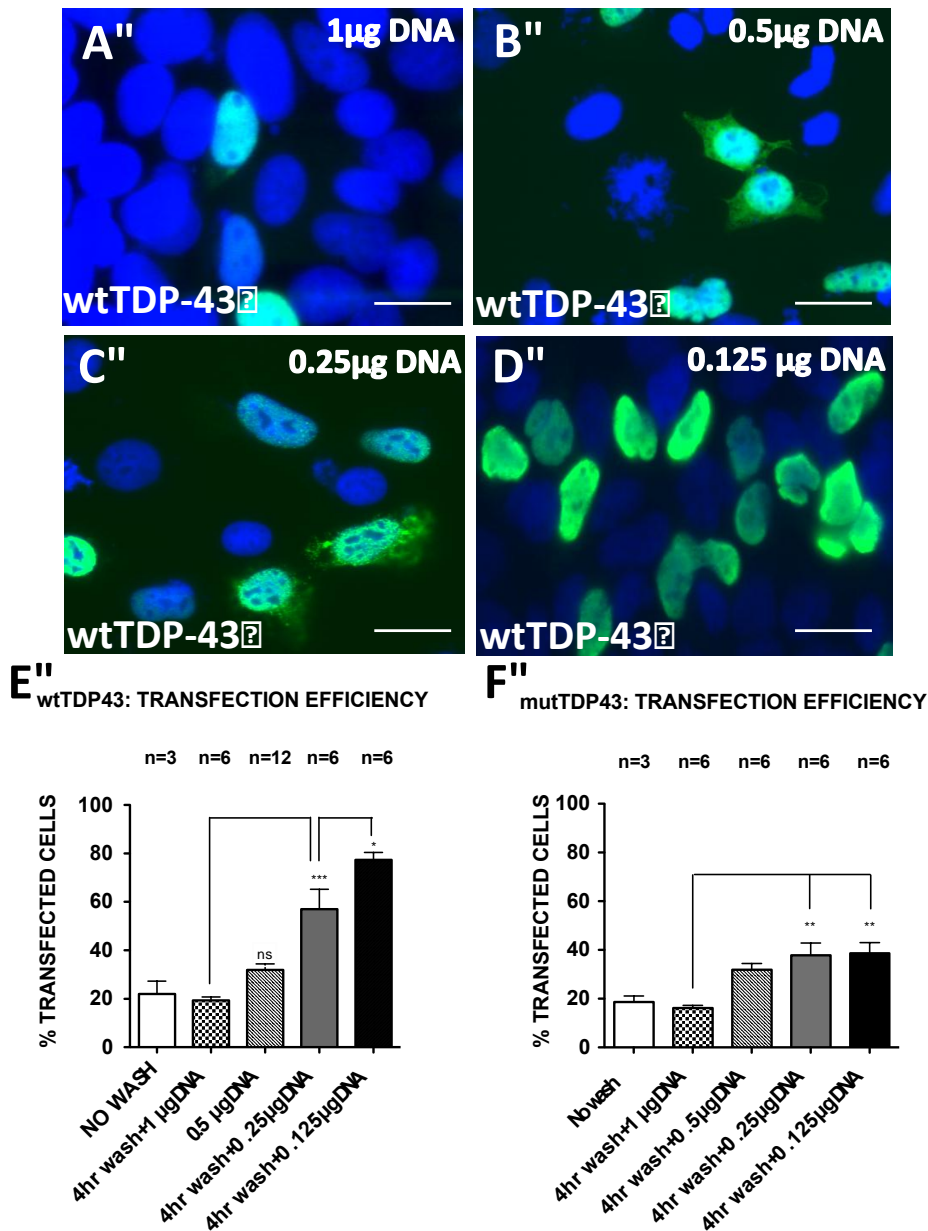
Figure 3.2 Titration of DNA dose in unstressed HEK293T cells transfected with wtTDP-43 and mTDP-43 followed by a 4h wash step. A) 1µg of wtTDP-43 DNA expressing cells. Transfection efficiency was ≤20%. **B)** Transfection efficiency improved to ~35% by reducing the DNA dose by 50% (0.5µg). **C)** A significant improvement in transfection efficiency when the DNA dose was reduced to 0.25µg (1/4th of the dose) (p<0.001). **D)** 0.125µg of DNA provided the best transfection efficiency at ~80% of the cells (p<0.05). **E)** Graphical representation of the transfection efficiency data for wtTDP-43. NO WASH category had 1µg of DNA transfected. **F)** Graphical representation of the effects of DNA titration for A315T mutant TDP-43, NO WASH category had 1µg of DNA transfected. Transfection efficiency improves with 0.25 and 0.125µg vs 1µg (p<0.012) but at best, the transfection efficiency of muttdp-43 remained below 40%. One way ANOVA with Bonferroni's post test comparison method used. **p<0.001, *p<0.05). Immunocytochemistry: anti *myc* (TDP-43) green, DAPI- Blue. Oil immersion lens magnification: x63. Scale bar 100µm).
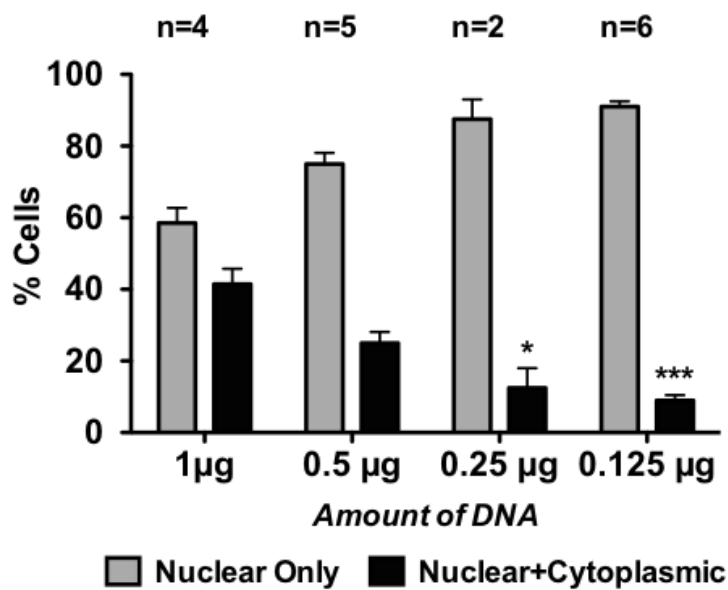
Figure 3.3 Mis-localisation of wtTDP-43 DNA is directly proportional to the transfected dose of DNA. A progressively lower proportion of cells showed cytoplasmic mis-localisation of TDP-43 when the dose of transfected DNA was reduced. DNA concentrations of 0.25μg and 0.125μg were associated with a significantly lower proportion of cells expressing cytoplasmic TDP-43 (p<0.05* and p<0.0001 ***) compared to 1μg of DNA. Unpaired Student t –test was used to analyse the data). Average and the standard error of the mean (SEM) used.

However, over-expression models of wtTDP-43 and mutTDP-43 in yeast, neuronal cell lines such as NSC34 and primary motor neurons have shown that disease associated mutations such as Q331K and M337V (yeast cells) (Johnson et al., 2009) and A315T, G348C and A382T (Primary motor neurons, NSC34) (Barmada et al., 2010, Kabashi et al., 2010b, Wu et al., 2013) and N390D (NSC34)(Wu et al., 2013) are toxic to the aforementioned cells. Therefore we attempted to over-express A315T, M337V and Q331K disease associated mutations of *TARDBP* gene in the HEK293T cells to assess the cytoplasmic mis-localisation and possible TDP-43 positive inclusion formation.

129

3.3 Over-expression of myc-tagged TDP-43 resulted in lower levels of the endogenous TDP-43 protein levels

The wtTDP-43 and the mutTDP-43 constructs were *myc*-tagged. Therefore during our experiments we used mouse anti *myc* antibodies to detect TDP-43 over-expression resulting from transfection of the constructs. As seen in Fig 3.4A wtTDP-43, A315T and Q331K construct expression is similar when controlled for loading (M337V –due to a technical failure was omitted from this immunoblot). We later acquired a rabbit anti TDP-43 antibody (targeting an epitope on the N-terminus of TDP-43, Proteintech group, UK). When the protein extracts used in the above immunoblot were probed with the anti TDP-43 antibody we noticed that the *myc* tagged TDP-43 (Fig 3.4 B) ran 3-4kDa higher than the endogenous TDP-43 (Fig 3.4 B). Furthermore it appears that when controlled for loading (alpha tubulin) (Fig 3.4 C), suppression of expression is detected from finding less endogenous TDP-43 protein. This finding from a preliminary study is in keeping with increasing evidence of autoregulation of TDP-43 and similar RNA binding proteins (Buratti & Baralle 2011). We demonstrated in a loss of function *tardbp* zebrafish model that knock down of *tardbp* resulted in an over-expression of the orthologue *tardbpl-FL*, which coded for an almost identical protein called Tardbpl-FL (Buratti and Baralle, 2011a, Hewamadduma et al., 2013). A mutant TDP-43 transgenic mouse expressing human wtTDP-43 under the Thy-1 promoter showed that endogenous mouse TDP-43 was down regulated in response to the over-expression of human wtTDP-43 (Xu et al., 2010) suggesting that there are cellular mechanisms to maintain tight control of TDP-43 levels.
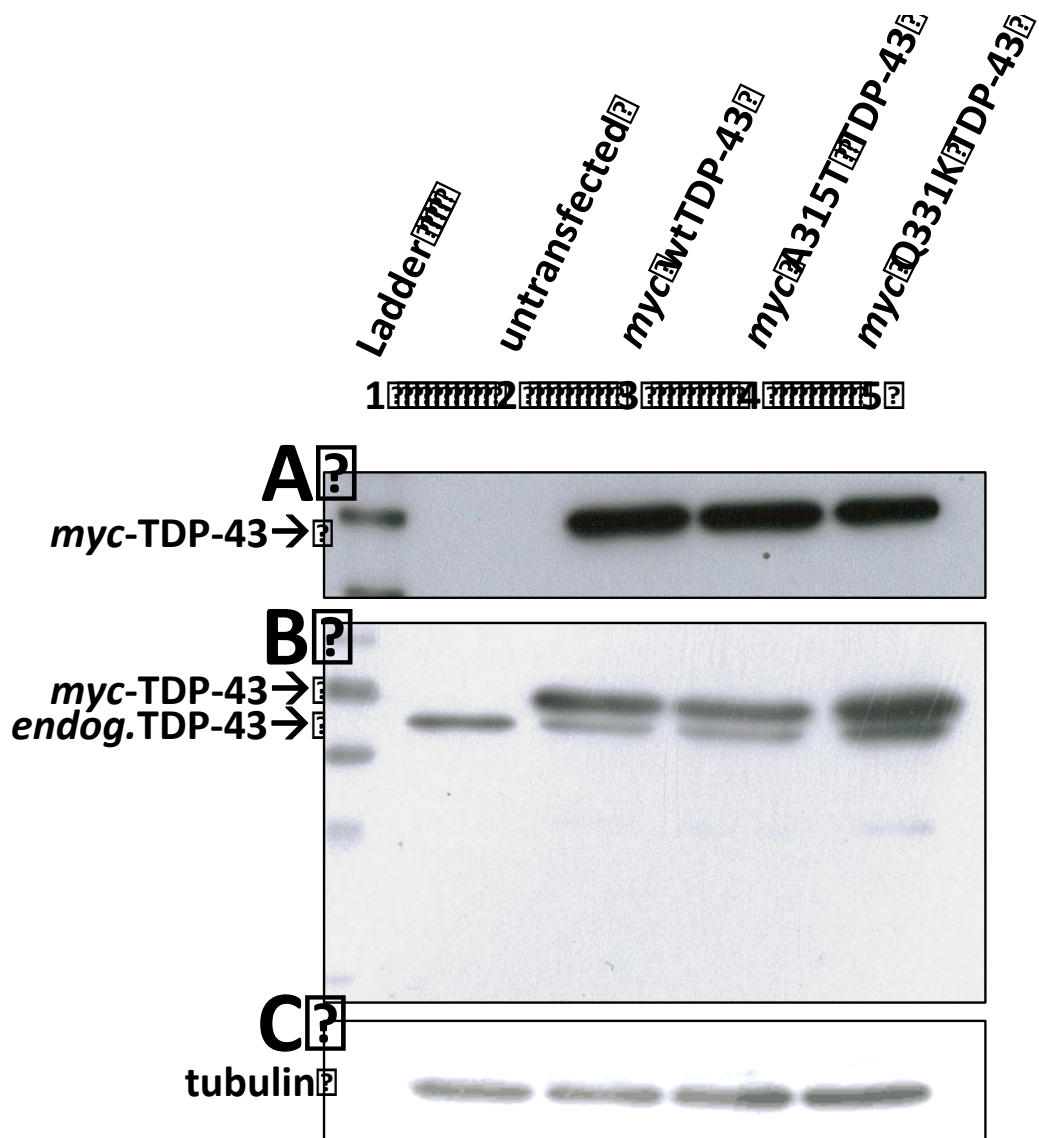
Figure 3.4 Over-expression of *myc* tagged TDP-43 is associated with lower levels of endogenous TDP-43 protein. A) Protein extracts from untransfected and three transfected HEK293T cells were probed with mouse anti *myc* antibody. The untransfected cell extracts show no *myc*TDP-43. **B)** Protein extracts probed with rabbit anti human TDP-43 antibody (1:500). Lane 1: biotynlated ladder. Lane 2: un-transfected cells depicting the endogenous level of TDP-43. Lane 3&4: *myc* wtTDP-43 and A315T. Endogenous TDP-43 level is suppressed compared to endogenous TDP-43 in lane 2 in both wt and mutTDP-43. Lane 5: over loading of Q331K sample. Therefore correction with densitometric analysis is necessary prior to interpretation. Secondary antibody- horse anti rabbit HRP. **C)** Alpha tubulin used at 1:10,000 dilution. Exposure is one minute for both anti human TDP-43 and alpha tubulin western blots.

3.4   Expression of lower levels of wtTDP-43 and mutTDP-43 does not cause significant cytoplasmic mis-localisation

As described in section 3.2 we observed that transfection of 1μg of *TARDBP* DNA into HEK293T cells using Exgen and its standard protocol resulted in an increase in cytoplasmic mis-localisation and reduced transfection efficiency. These findings, along with previous studies on over-expression of TDP-43 in cellular and animal models, suggest that tight control of TDP-43 expression is required and mis-localisation of TDP-43 to the cytoplasm could be a surrogate marker of TDP-43 induced toxicity (Gendron et al., 2010). We hypothesised that over-expression of mutTDP-43 would be more toxic than wtTDP-43 and as such we would observe a significantly higher cytoplasmic TDP-43 mis-localisation. Therefore we counted the HEK293T cells expressing purely nuclear myc tagged TDP-43 (Fig 3.5 panels A and B), cells with cytoplasmic and nuclear TDP-43 (Fig 3.5 panels C and D) and cells with punctate lesions (≥1) in the cytoplasm (Fig 3.5 panel D, arrows). Interestingly we noted that the TDP-43 expression was nuclear in more than 80-85% of the transfected cells in both wtTDP-43 and mutTDP-43 expressing cells (Fig 3.6 A). We also noted that occasionally TDP-43 was redistributed to the cytoplasm. There was no significant difference in cytoplasmic distribution of TDP-43 between the wtTDP-43 and the mutTDP-43 categories and amongst the three mutTDP-43 constructs, although there appeared a weak correlation between the Q331K and M337V mutants to have greater propensity to aggregate in the cytoplasm (Fig 3.6 B). Although in postmortem samples of brain and spinal cord from ALS cases with TDP-43 proteinopathy, aggregation of cytoplasmic TDP-43 inclusions was noted (Arai et al., 2006, Neumann et al., 2006), mouse models over-expressing wtTDP-43 and A315T mutTDP-43 using a Thy-1 promoter did not show aggregation of TDP-43 positive cytoplasmic inclusions when probed with an anti TDP-43 polyclonal antibody (Wegorzewska et al., 2009, Xu et al., 2010) suggesting that cytoplasmic inclusions are not a prerequisite for the pathogenesis of dysfunctional TDP-43 related neurodegeneration. Others argue that a phosphorylation dependent TDP-43 antibody to detect TDP-43 positive cytoplasmic lesions before ruling out the possibility of TDP-43 inclusion bodies. It is possible that a different antibody detecting a C-terminal epitope of TDP-43 could have detected TDP-43 inclusions containing C-terminal fragments of TDP-43 (Igaz et al., 2008, Yang et al., 2010).

3.5 Over-expression of full length wild type and mutant TDP-43 constructs mainly localise to the nucleus.

We over-expressed the wtTDP-43 and the three mutTDP-43 constructs at the lowest DNA concentration, which provided the maximum transfection efficiency, 0.125ug per transfection. Analysis of localisation of TDP-43 by the anti-*myc* antibody revealed mainly nuclear distribution of TDP-43 with wtTDP-43 as well as all three, A315T, Q331K and M337V mutant constructs and the average proportions of cells with nuclear only TDP-43 staining were 92, 92, 91 and 86 % respectively (Fig 3.6A) in keeping with wtTDP-43 and A315T mutTDP-43 expression studies in the NSC34 cells (Wu et al., 2013). Occasionally we observed that TDP-43 did mis-localise to the cytoplasm. However the proportion of the cells seen with cytoplasmic TDP-43 was less than 10% for wtTDP-43 and mutTDP-43 except for M337V (14% of cells, $p>0.05$, not significant, paired t-test) (Fig 3.6 B). We did not observe neurocytoplasmic TDP-43 inclusion formation with the anti-*myc* antibody. This is in keeping with a mouse model of wtTDP-43 over-expression, which showed no significant TDP-43 positive cytoplasmic inclusion body formation, when tested using a phosphorylation independent antibody to detect TDP-43. In addition, two mouse models expressing the disease associated TDP-43 mutation A315T, also did not show colocalisation of phosphorylation independent TDP-43 with ubiquitinated inclusions (Wegorzewska et al., 2009, Stallings et al., 2010) suggesting that cytoplasmic inclusion formation is not essential for the pathogenesis of TDP-43 related motor neuronal dysfunction. However upon using a phosphorylation dependent anti-TDP-43 antibody, TDP-43 positive cytoplasmic inclusions were detected (Xu et al., 2010). We also occasionally noted TDP-43 localising to inclusions in the nucleus as depicted in Fig 3.5 E-F panels. Statistical analysis did not show a significant difference between wtTDP-43 and mutTDP-43 constructs, although there was trend indicating that Q331K and M337V mutTDP-43 were more likely to form nuclear inclusion (Fig 3.6 A)(Q331K and M337V: X=2.5±4.3, n=7 and 2.06±3.35, n=6 vs wtTDP-43: X =0.64±1.1, n=8, p=0.32). Nuclear inclusion formation has been reported with familial forms of ALS with FTLD but not in sporadic ALS (Seilhean et al., 2004)(sALS) suggesting that wtTDP-43 might not mis-localise to nuclear inclusions whilst mutTDP-43 potentially could (Mackenzie and Feldman, 2004).
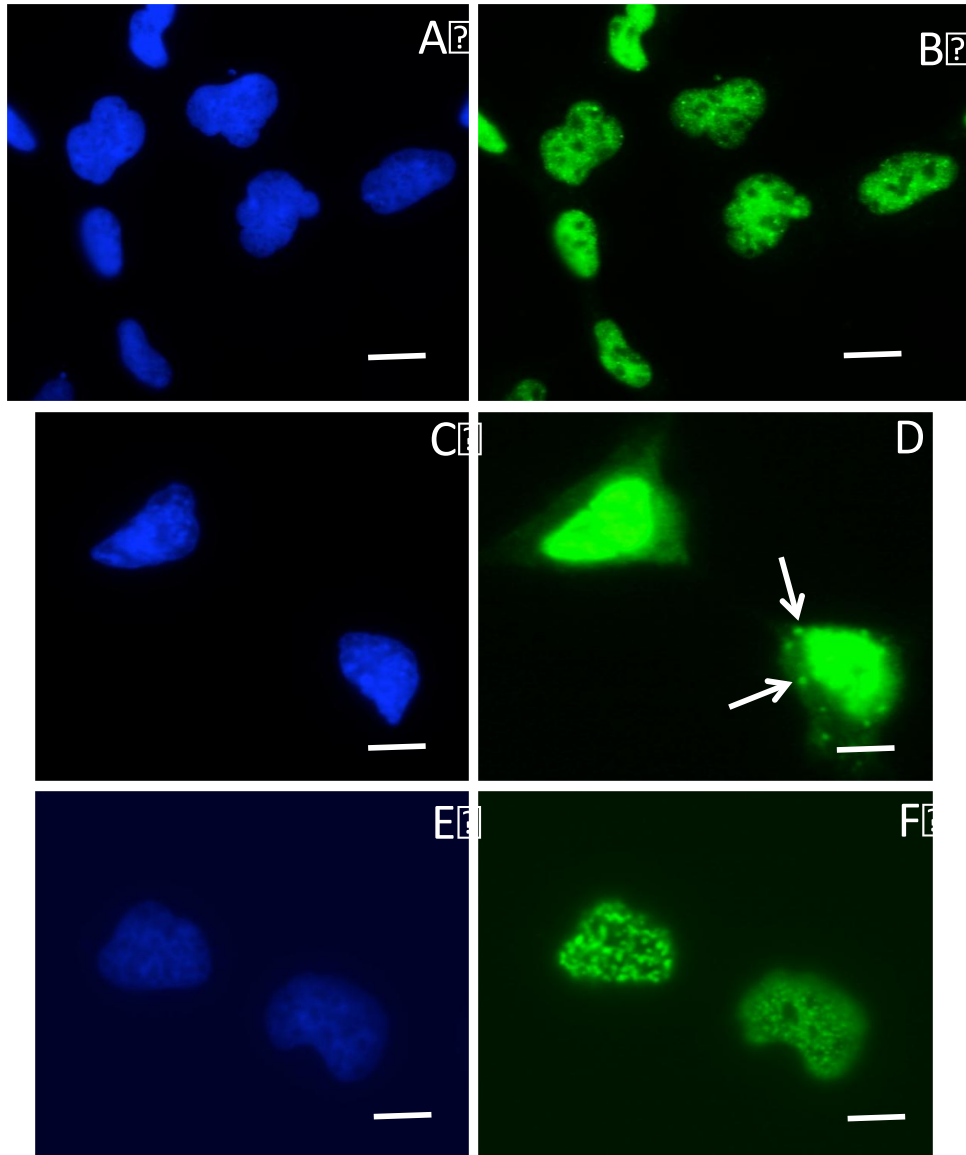
Figure 3.5 Patterns of *myc* tagged wild type and mutant TDP-43 cellular distribution. A-B) Nuclear only distribution of TDP-43 in unstressed HEK293T cells. **C-D)** Nuclear and cytoplasmic distribution of TDP-43 and TDP-43 positive cytoplasmic inclusion formation. White arrowheads point towards the TDP-43 positive inclusions. **E-F)** Nuclear only staining of TDP-43 which form punctate appearances in the nuclei Q331K and M337V vs wtTDP-43: X=2.5±4.3, n=7 and 2.06±3.35, n=6 vs X =0.64±1.1, n=8, p=0.32. Blue stain is DAPI for nuclear staining, Green- anti *myc* antibody detecting TDP-43. Sale bar 50μm.
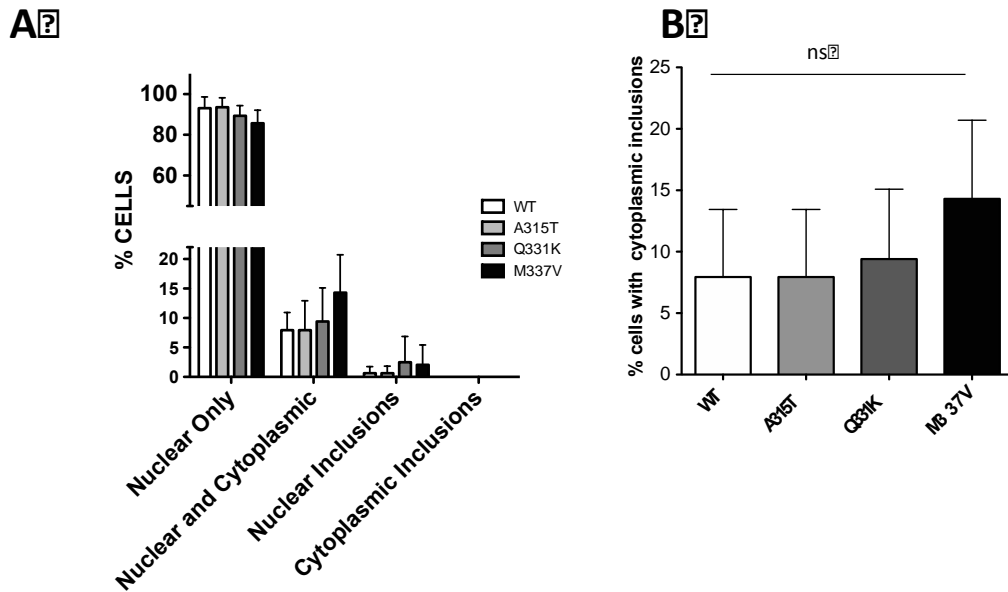
Figure 3.6 Patterns of *myc* tagged TDP-43 cellular distribution.
A) Full length WT, A315T, Q331K and M337V mutant constructs were over-expressed in HEK293T cells. Expression patterns of the respective constructs were qualitatively analyzed. 85-90% of the WT and mutant constructs localised to the nuclei. About 7% of the WT TDP-43 over-expressing cells demonstrated cytoplasmic localisation and inclusion formation. The mutant TDP-43 protein formed cytoplasmic inclusions variably but not frequently. Rarely some cells showed nuclear inclusion formation. This was observed mainly in Q331K and M337expressing cell. **B)** Cytolplasmic inclusion formation and mis-localisation when analyzed showed a trend in the mutant TDP-43, particularly M337V to form cytoplasmic inclusions. But statistically there was no significant difference. Standard deviation and the average proportion of cells demonstrated in the graphs. One way ANOVA with Bonferoni multiple column comparison, p>0.05)

3.6 Use of exogenous stress to induce mis-localisation of TDP-43

In patients with ALS and FTLD associated with TDP-43 proteinopathy a recognised feature in the pathological samples is the TDP-43 positive ubiquitinated neuro-cytoplasmic inclusion formation (Neumann et al., 2006). However under basal conditions we did not observe any significant mis-localisation of wtTDP-43 or mutTDP-43 to cytoplasmic inclusions. The exact nature of the mechanisms involved in the pathogenesis of ALS is complex. It is widely accepted that an interplay between genetic and environmental factors could play a key role in manifestation of the motor neuronal death in ALS. Amongst many environmental stressors oxidative stress has been shown by many studies as a key modulator of neuronal fate and there is an extensive body of evidence for oxidative damage to

proteins in postmortem tissues from ALS patients (Barber and Shaw, 2010). In addition to oxidative stress, mitochondrial dysfunction has been implicated in the pathogenesis of ALS due to observations such as morphologically abnormal mitochondria in motor neurons of ALS patients, decreased electron transport chain activity and mitochondrial membrane potentials and calcium homeostasis and reduction in mitochondrial antioxidant defense mechanisms (Beal, 2000). Endoplasmic reticulum associated stress and related unfolded protein response have been found to play a role in selective motor neuronal death or dysfunction in ALS. An enhanced ER stress response has been reported in ALS animal models (Kieran et al., 2007). Therefore we hypothesised that a double hit phenomenon of an underlying genetic predisposition to motor neuron dysfunction i.e. mutant TDP-43, when exposed to an environmental or an exogenous stress could precipitate features of TDP-43 dysfunction such as cytoplasmic mislocalisation, and inclusion formation more prominently in mutTDP-43 compared to wtTDP-43 overexpressing cells.

3.6.1 Treatment with hydrogen peroxide (H_2O_2) mis-localises full length wtTDP-43 and mutTDP-43 to the cytoplasm and into cytoplasmic inclusions.

H_2O_2 has been used in previous models of ALS to induce oxidative stress to demonstrate SOD1 associated ALS motorneuron vulnerability to oxidative stress. Previous studies have used 0.6mM H_2O_2 for 6h to induce oxidative stress in NSC34 cells (Cookson et al., 1998) and we used similar conditions in HEK293T cells. Although the distribution of wtTDP-43 and mutTDP-43 was largely nuclear (Fig 3.6 A) following treatment with H_2O_2 a proportion of the transiently expressed TDP-43, regardless of whether mutant or wld type, translocated to the cytoplasm and formed cytoplasmic inclusions. This observation is important as redistribution of TDP-43 from the nucleus to the cytoplasm and formation of cytoplasmic aggregates are prominent characteristics of TDP-43 associated diseases (Mackenzie and Rademakers, 2007).

Although it has been suggested that the mutations targeting the C-terminal fragment of TDP-43 increases its propensity to aggregate, misfold or /and mislocalise and thereby underpin toxicity (Johnson et al., 2009, Nonaka et al., 2009c), we did not see a difference between mutant and the wtTDP-43 in the propensity to mis-localise TDP-43 to the cytoplasm upon H_2O_2 treatment. 100% of the wtTDP-43 and A315T mutant transfected cells, showed TDP-43 mis-localisation to the cytoplasm, whilst Q331K and M337V cells showed 98% and 86% respectively. Cytoplasmic inclusion formation was observed in more than 20% of wtTDP-43 and A315T mutants whilst more than 25% of the M337V transfected cells showed TDP-43 positive aggregation formation. It is possible that under oxidative stress heat shock proteins as well as the ubiquitin-proteasome system (UPS) are activated to clear TDP-43 from the nucleus, as a result of which TDP-43 is translocated to the cytoplasm for clearing by the UPS. To be certain we need to double lable for myc tagged TDP-43 and ubiquitin. On the other hand it is also likely that an aggregation prone protein like TDP-43 when over-expressed induces cellular stress and this balance is tipped by a second hit from H_2O_2 induced stress resulting in conformational changes in TDP-43 i.e. due to phosphorylation, which in return impairs nuclear export or shuttling into the nucleus. As a result TDP-43 accumulates in the cytoplasm.

A

% CELLS

Nuclear Only   Nuclear and cytoplasmic

E

ns

% cells with cytoplasmic inclusions

WT   A315T   Q331K   M337V

TDP'43"   **DAPI"**   **TDP'43/DAPI"**

B"   C"   D"
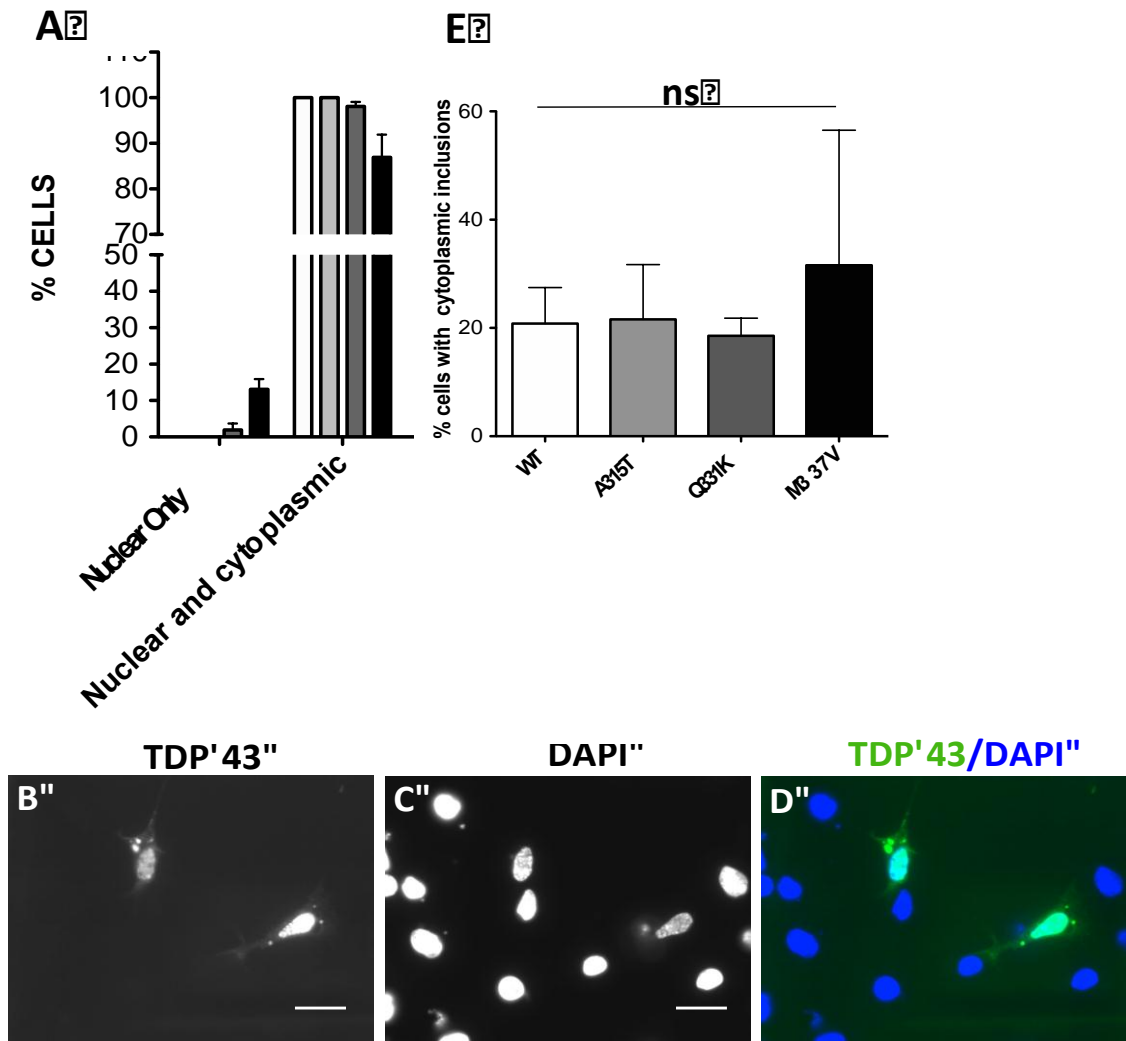
Figure 3.7 Cellular localisation of TDP-43 following treatment with 0.6mM H$_2$O$_2$ for 6h. A) More than 90% of the cells stressed with H$_2$O$_2$ show nuclear and cytoplasmic localisation of *myc* tagged TDP-43. wtTDP-43, A315T and Q331K followed almost identical pattern, whilst M337V responded with a similar trend but more than 10% of the cells showed a nuclear only staining. **B-D)** Cytoplasmic TDP-43 positive inclusions were seen in all mutTDP-43 and wtTDP-43 cells following treatment with H$_2$O$_2$. **E)** More than 20% of the cells demonstrated this phenomenon.. Blue stain is DAPI for nuclear staining, Green- anti *myc* antibody detecting *myc* tagged TDP-43. Scale bar 50μm. Compare with *myc*-TDP-43 in unstressed cells (Fig 3.5 A-B)

138

There appears to be no significant difference between wtTDP-43 and mutTDP-43 in their response to H_2O_2 mediated oxidative stress. This may also be explained by the fact H_2O_2 treatment is more an acute stress, and the response to this acute stress overwhelms the stress of over-expression of full length TDP-43 constructs regardless of presence of abscence of a mutation (Gendron et al., 2013).

3.6.2 Treatment with 0.5mM sodium arsenite causes aggregation of *myc* tagged TDP-43 in the nucleus.

Treatment with sodium arsenite causes oxidative stress directly by a reaction similar to Fenton's reaction (Pang et al., 2009). Arsenite treatment also results in depletion of glutathione, induction of heat shock proteins (hsp), stimulation of NFkB (nuclear factor kappa B) and induction of glucose transporters resulting in nutrient deprivation, and each of these mechanisms can result in inhibition of protein translation and as a result promote the formation of stress granules (SG)(Anderson and Kedersha, 2002). Stress granules are dynamic cytoplasmic aggregates formed temporarily as a result of external cellular stress, by dismantling the translational machinery to allow only the translation of the most vital proteins for the cells to survive the stress (Anderson and Kedersha, 2008). Sodium arsenite is widely used in the study of stress granule formation and related RNA biology (Anderson and Kedersha, 2009). TDP-43 has been shown to co-localise with SG (Colombrita et al., 2009). Major protein components of SGs have been recognised in TDP-43 positive inclusions from postmortem brain and spinal cord samples of ALS cases (Liu-Yesucevitz et al., 2010). Therefore we hypothesised that cells transfected with wtTDP-43 and mutTDP-43 would form stress granules upon treatment with sodium arsenite. More than 95% of the cells demonstrated a nuclear only TDP-43 distribution (Fig 3.8 A-C). We did not observe any cytoplasmic anti myc positive puncta formation (Fig 3.8 C). Although we did not use an antibody to assess SG formation, we now know that HEK293T cells do form SG when treated with sodium arsenite under similar
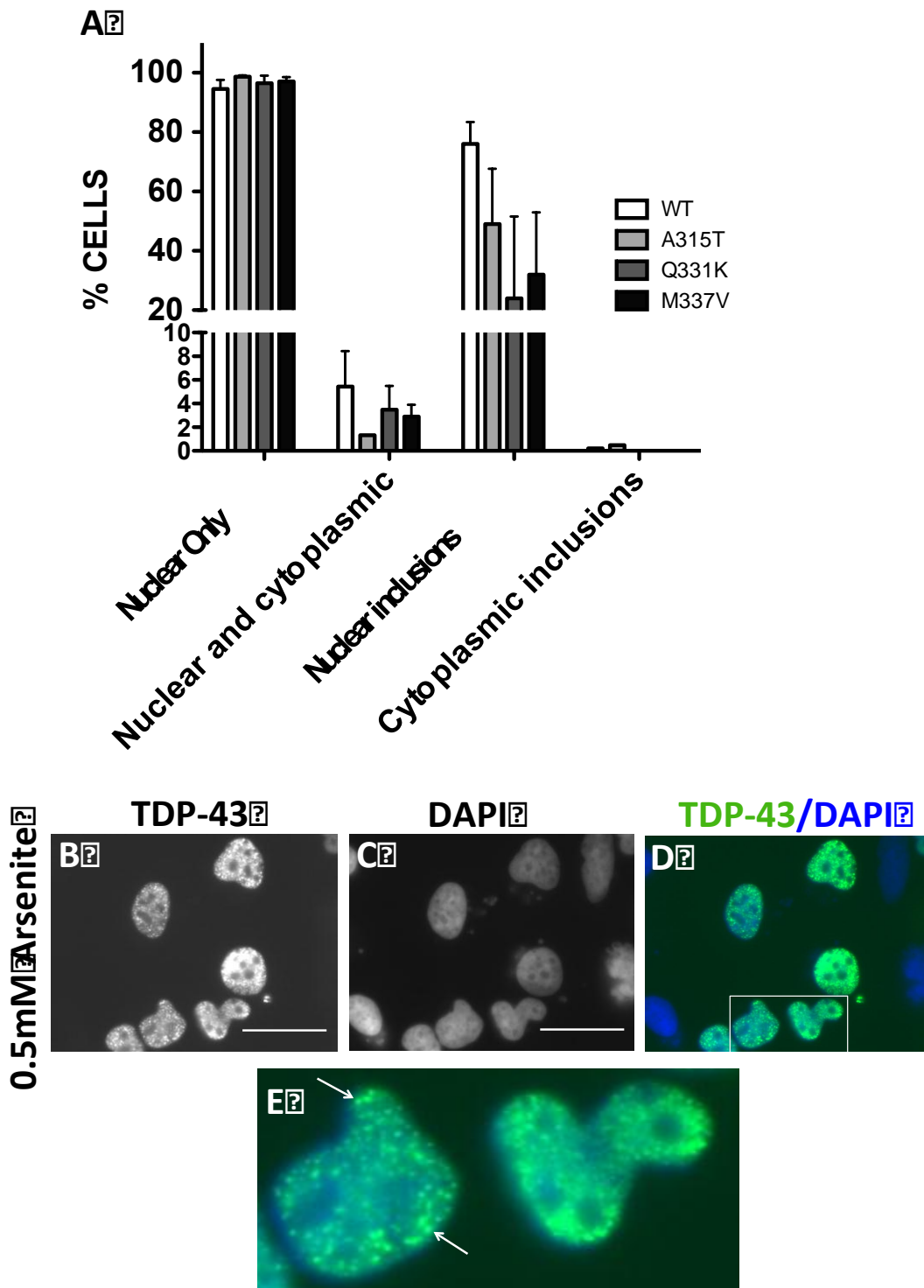
Figure 3.8 *myc*-TDP-43 positive nuclear inclusion body formation in response to treatment with 0.5mM arsenite for 30 minutes. A) TDP-43 localisation was mainly nuclear in distribution in more than 90% of the cells stressed with sodium arsenite. **B-D)** Nuclear distribution was not uniform as TDP-43 formed granular and punctate nuclear staining when stressed with arsenite. **E)** Enlarged section marked in panel D depicting the formation of numerous nuclear inclusion formation positive for TDP-43 when tested for *myc* tagged TDP-43 (arrows). Blue stain is DAPI for nuclear staining, Green- anti *myc* antibody detecting *myc* tagged TDP-43. Scale bar 100µm. Compare with *myc*-TDP-43 in unstressed cells (Fig 3.5 A-B)

conditions (Fig 3.13). These findings suggest that wild type or mutant myc tagged full length TDP-43 did not translocate to cytoplasmic inclusions upon treatment with arsenite. However we noted that the transfected HEK293T cells, wt and mutTDP-43, showed multiple nuclear inclusion formation (Fig 3.8 E, arrows). Although there was no statistically significant difference amongst the groups (due to large standard deviations) wtTDP-43 appeared to form more nuclear inclusions than the mutants (Fig 3.8 A). This association of TDP-43 positive nuclear inclusion formation, in response to arsenite stress has not been published in the public domain (Pubmed). Ubiquitin positive nuclear inclusions have been described in postmortem pathological samples obtained from familial FTLD and ALS cases but not in sporadic FTLD or ALS cases (Mackenzie and Feldman, 2004). Further studies are needed to understand the exact mechanism responsible for the formation of these nuclear inclusions.

3.6.3 Other oxidative stress inducers: Menadione and FCCP (Trifluorcarbonylcyanide Phenylhydrazone) did not alter TDP-43 localisation in wtTDP-43 or mutTDP-43 transfected HEK293T cells

Menadione induces cellular stress by inducing Ca2+ dependent apoptosis via opening of the mitochondrial permeability transition pore (Criddle et al., 2006). FCCP induces oxidative stress by disrupting mitochondrial function by uncoupling the respiratory chain complex IV from V (Caputo and Bolanos, 2008). Both menadione and FCCP have has used to induce stress by disrupting mitochondrial function in cellular models of neurodegenerative diseases such as Parkinson's disease (Gandhi et al., 2009). As we observed different patterns of TDP-43 localisation with arsenite and H_2O_2 two agents which are known to cause oxidative stress, we hypothesised that by using two agents which induce oxidative stress via disrupting mitochondrial function we could reproduce either pattern of TDP-43 distribution. Upon menadione treatment (Fig 3.9 A-D) and FCCP treatment (Fig 3.10 A-D) TDP-43 distribution was mainly nuclear (more than 85% of the cells). Although less than 15% of the cells in both wtTDP-43 and mutTDP-43 mis-localised to the cytoplasm these proportions were neither significant amongst wtTDP-43 and mutTDP-43 categories nor between stressed (menadione and FCCP) and unstressed (Fig 3. 6 A) experiments. We also did not see nuclear inclusion formation. Although TDP-43 has been linked to mitochondria in a mouse

model of TDP-43 (Xu et al., 2010) we did not see a difference in myc tagged TDP-43 localisation between the wtTDP-43 and mutTDP-43 cells in response to mitochondrial stressors. However this observation by no means excludes an association of TDP-43 and mitochondrial dysfunction as we have not used any mitochondrial assays to assess effects of TDP-43 on mitochondrial function with and without mitochondrial stressors.
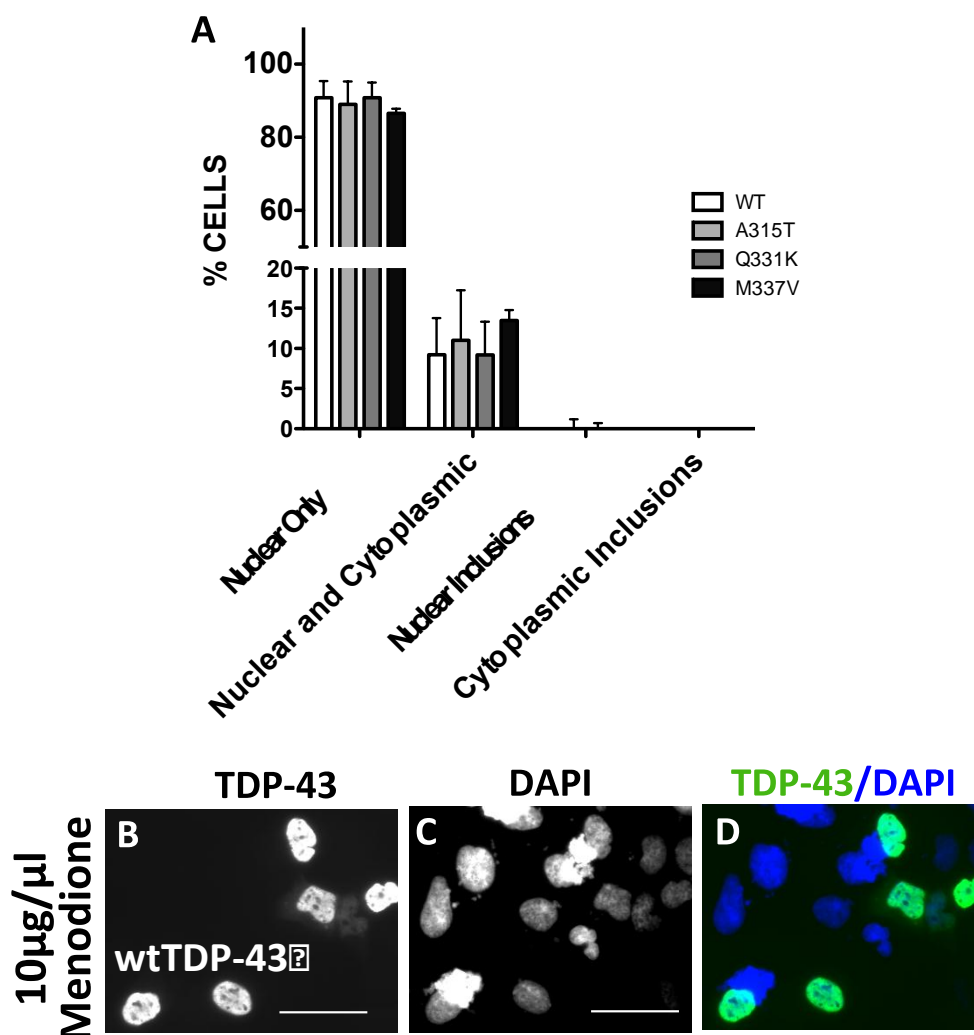
Figure 3.9 *myc*TDP-43 localisation after treatment with menadione for 2h A) TDP-43 localisation was mainly nuclear in distribution in more than 90% of the cells stressed with menadione. **B-D)** Nuclear distribution was uniform and no difference was noted between wtTDP-43 and mutTDP-43 transfected cells Blue stain is DAPI for nuclear staining, Green-anti *myc* antibody detecting *myc* tagged TDP-43. Scale bar 100µm. Compare with *myc*-TDP-43 in unstressed cells (Fig 3.5 A-B)

A"
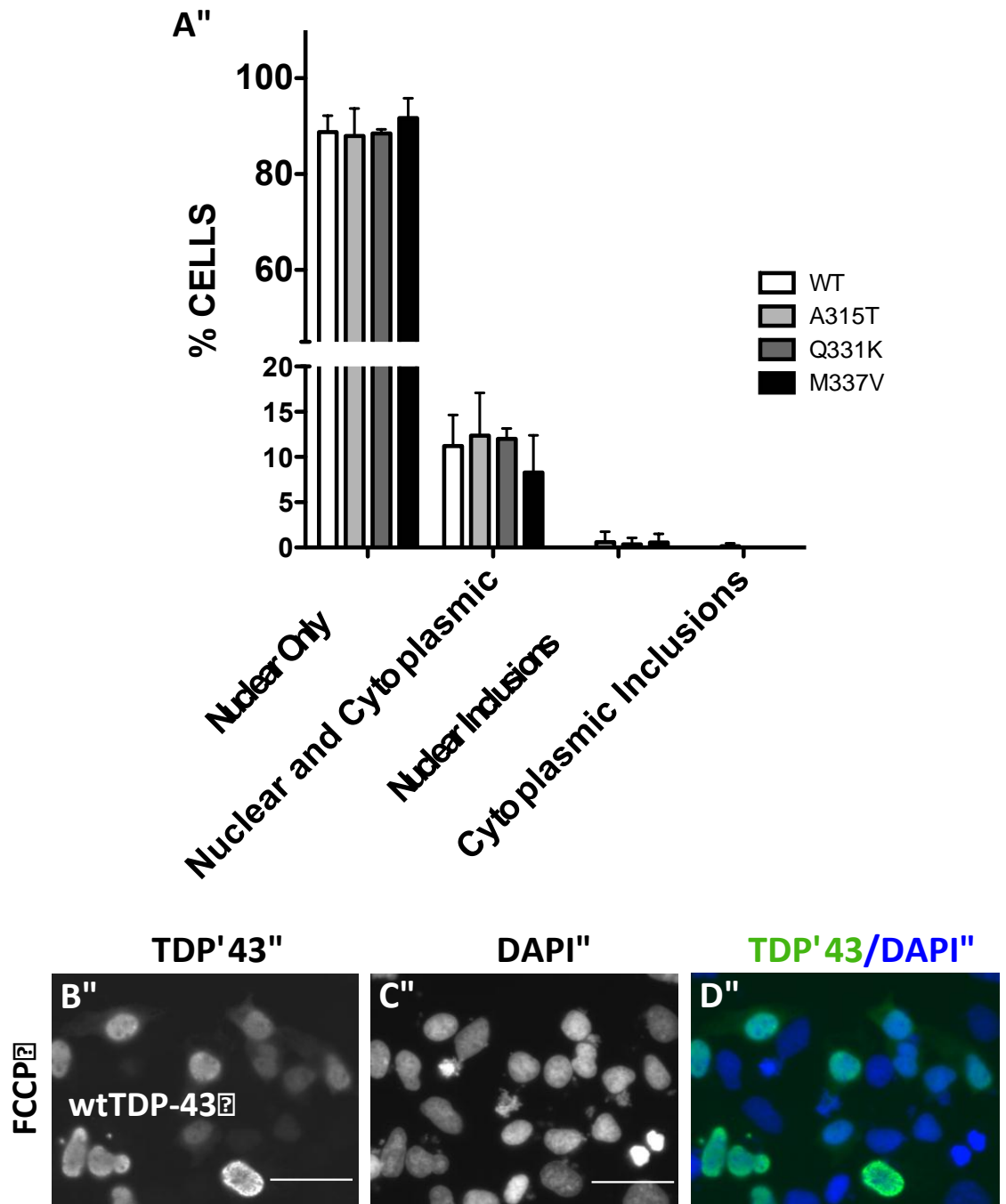
Figure 3.10 *myc*TDP-43 **localisation after treatment with FCCP for 120 minutes. A)** TDP-43 localisation was mainly nuclear in distribution in more than 90% of the cells stressed with FCCP. **B-D)** Nuclear distribution was uniform and no difference was noted between wtTDP-43 and mutTDP-43 transfected cells Blue stain is DAPI for nuclear staining, Green- anti *myc* antibody detecting *myc* tagged TDP-43. Scale bar 100μm. Compare with *myc*-TDP-43 in unstressed cells (Fig 3.5 A-B)

3.6.4 Treatment with 0.4M sorbitol causes aggregation of *myc* tagged TDP-43 in the nucleus

Sorbitol induces cellular stress by osmotic stress pathways. Sugar sorbitol is an intermediate of an ATP independent metabolic route that generates fructose from glucose (Forbes et al., 2008). Since elevated levels of sorbitol have been shown to induce cellular stress in previous studies (Dewey et al., 2011), we performed an experiment to detect whether the osmotic stress would have detected effects on the wtTDP-43 and mutTDP-43 localisation. Upon treatment of TDP-43 transfected HEK293T cells, we noted a prominent nuclear localisation of the myc tagged TDP-43 proteins (Fig 3.11 A-D). In addition we also noted granular nuclear staining with nuclear inclusion formation upon stressing the cells for 2h. We noticed very occasional cytoplasmic inclusion formation only in wtTDP-43 (Fig 3.11) but there was no increase in gross cytoplasmic mis-localisation of TDP-43. There was no difference in the cytoplasmic distribution of *myc* tagged TDP-43 between wtTDP-43 and mutTDP-43.

However nuclear inclusion formation was observed in up to 40% of . wtTDP-43, A315T and Q331K cells (Fig 3.11A) but only up to 8% of the M337V transfected cells. We could not see a statistical difference when compared to wtTDP-43 with paired t test (p>0.05) due to the variability within the groups. The differences between M337V and the other TDP-43 mutants could be secondary to the nature of the mutation affecting the TDP-43 protein folding and thereby exposure of the residues to different kinases activated by the induced stress process (Meyerowitz et al., 2011, Shodai et al., 2013).

3.6.5 Heat shock resulted in localisation of TDP-43 to nuclear stress bodies (nSBs)

Heat shock leads to immediate and complete blockage of DNA replication and transcription, pre-mRNA splicing, nucleo-cytoplasmic transport and translation (Mahl et al., 1989, Morimoto and Santoro, 1998). Induction of heat shock at 42 ^{0}C for 30 minutes resulted in complete nuclear only distribution of TDP-43 in both wtTDP-43 and mutTDP-43 transfected HEK293T cells (In all transfected cells). No cytoplasmic distribution of TDP-43 was noted (Fig 3.12 A-C). The most interesting observation was that both wtTDP-43 and mutTDP-43 formed punctate lesions in the nuclei.
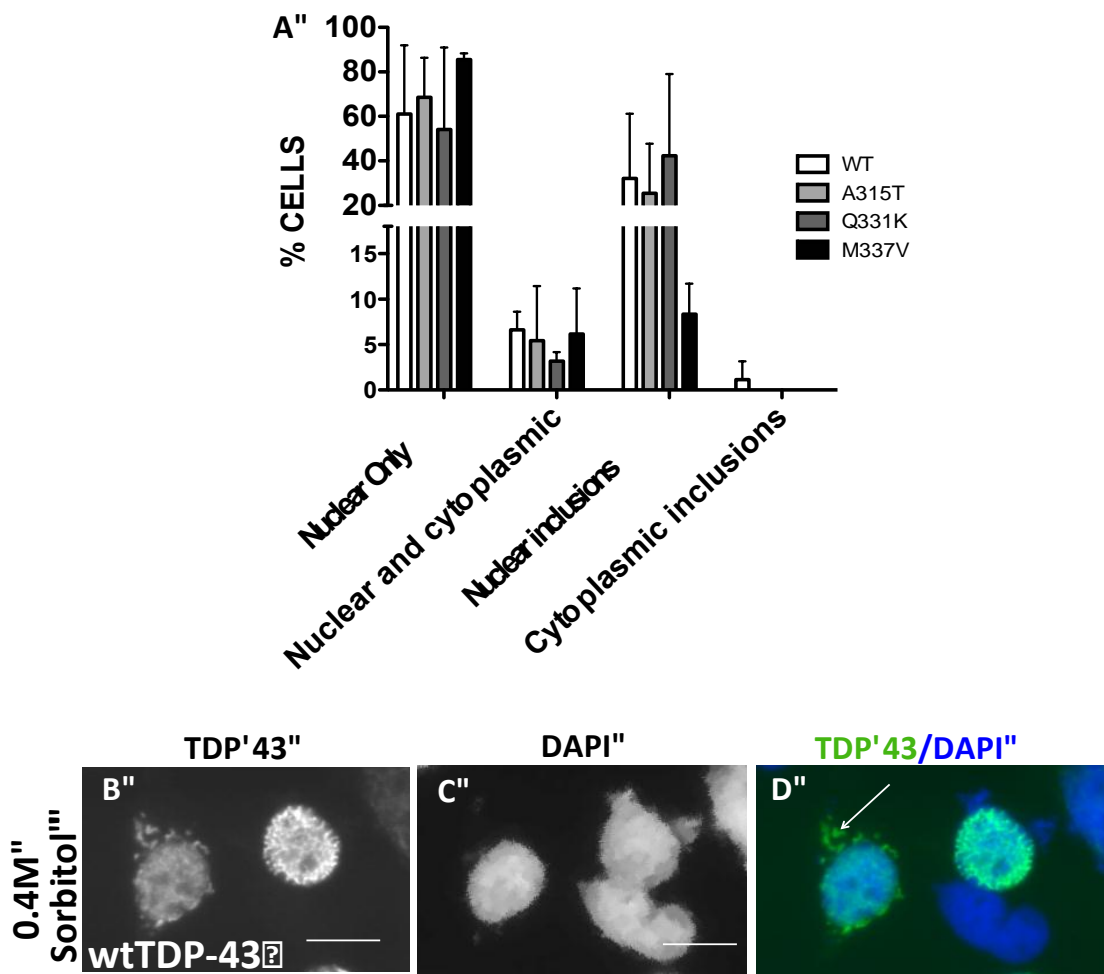
Figure 3.11 *myc*TDP-43 localisation after treatment with 0.4M sorbitol for 60 minutes. A) TDP-43 localisation was mainly nuclear in distribution in more than 90% of the cells stressed with sorbitol 0.4M. **B-D)** Nuclear distribution was granular and myc tagged TDP-43 positive inclusion formation was noted in the nuclei. Cytoplasmic inclusion formation was also observed as indicated by the arrow. Only 8% of the M337V transfected cells showed nuclear inclusion formation but no statistical difference was noted between wtTDP-43 and M337V transfected cells. (Paired t test p> 0.05). Blue stain is DAPI for nuclear staining, Green- anti *myc* antibody detecting *myc* tagged TDP-43. Scale bar 50µm. Compare with *myc*-TDP-43 in unstressed cells (Fig 3.5 A-B)

There was minimal nuclear matrix staining noted between the punctate staining (Fig 3.12 E). Heat shock has previously been shown to recruit several hnRNPs to nuclear complexes called nuclear stress bodies (nSBs) (Mahl et al., 1989). Heat shock factor 1 (HSF1) has been shown to form nuclear granules after heat shock. hnRNP-A1 which is similar in structure to TDP-43, has been shown to form complexes with a protein called HAP (hnRNP A1 interacting protein) or Saf-B (scaffold attachment factor B) (Renz and Fackelmayer, 1996). HAP/Saf-B and HSF1 are recruited to nSBs upon heat shock (Weighardt et al., 1999). Therefore our findings are consistent with the scenario where, in response to heat shock TDP-43 interacts with the HSF1 protein, which is an important regulator of the transcriptional process associated with heat shock, and directs TDP-43 to nSBs regardless of whether the TDP-43 is WT or mutant. The distinct nature of these punctate lesions we observed after heat shock will require co-labeling with markers for known nuclear proteins recognised in demonstrating a similar anatomical distribution or localisation such as HSF1.
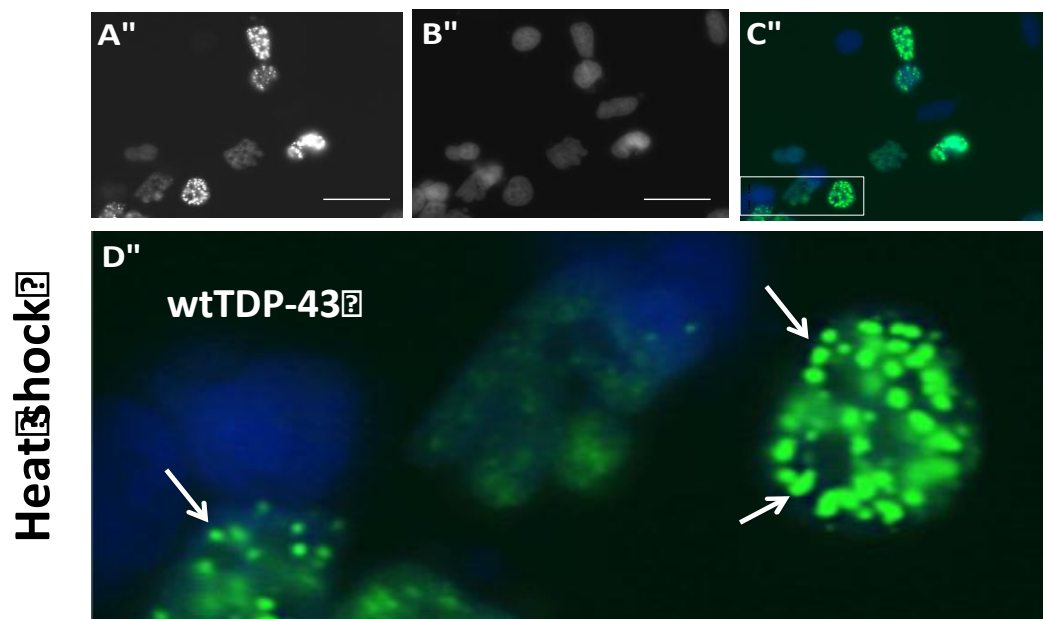
Figure 3.12 *myc*TDP-43 localisation after heat shock at 42 ^{0}C for 30 minutes.
A-C) TDP-43 localisation was mainly nuclear in distribution. Minimal nuclear matrix staining was noted. **D)** Enlarged section boxed in panel C. Distinct nuclear punctate staining pattern similar to that seen with nuclear stress bodies. No difference was noted between wtTDP-43 and M337V transfected cells. Blue stain is DAPI for nuclear staining, Green- anti *myc* antibody detecting *myc* tagged TDP-43. Scale bar 100µm. Compare with *myc*-TDP-43 in unstressed cells (Fig 3.5 A-B)

3.7 Endogenous wtTDP-43 co-localises to stress granules in response to treatment with sorbitol and heat shock.

3.7.1 Introduction

It has been reported that RNA binding proteins like hnRNPA1 and hnRNP Q localise to the cytoplasm and cytoplasmic inclusions called stress granules in response to activation of certain stress signaling pathways when certain cell lines are exposed to specific stressors (Anderson and Kedersha, 2009).

When a sub-lethal exogenous stress is induced, regulation of gene expression especially by RNA binding proteins (RBP) is translocated to cytoplasmic foci and halted at the post transcriptional level. Translational machinery is immediately halted and disassembled with sequestration of the actively translating mRNAs and the RBP to distinct cytoplasmic entities which are called stress granules (SG) (Anderson and Kedersha, 2008). The majority of the mRNAs silenced in SG are 48S ribosomal complexes, whilst essential transcripts like heat shock proteins are selectively translated to support cellular pathways to manage the extrinsic stress. Therefore it is considered that the phenomenon of SG formation represents a protective mechanism to enable the cell to cope with the imposed stress (Anderson and Kedersha, 2002). Major components of the SG include the T cell induced antigen -1 (TIA-1), TIA-1 related protein (TIAR) and Hu R antigen (HuR), survival of motor neuron (SMN) protein, Ras-GAP SH3 domain binding protein (G3BP), staufen, fragile X mental retardation protein (FMRP), the 48S pre-initiation complex, early translation initiation factors and micro RNA associated argonaute proteins (Anderson and Kedersha, 2008).

TDP-43 belongs to a superfamily of of RNA binding proteins called hnRNPs (D'Ambrogio et al., 2009). Transfected full length TDP-43 and endogenous TDP-43 have been shown to co-localise with TIA-1 labeled SG in a neuroblastoma cell line (Liu-Yesucevitz et al., 2010). However, we did not see TDP-43 mis-localising to the cytoplasmic inclusions when we examined transiently transfected HEK293T cells. We probed for epitope tagged exogenous TDP-43 using an anti *myc* antibody. The expression levels of TDP-43 protein are tightly regulated therefore we believe that over- expression of TDP-43 can be detrimental to its normal function and increase stress levels in cells. Therefore we examined the response of endogenous TDP-43 to external stressors. We assessed the localisation of endogenous TDP-43 by performing immunocytochemistry using a polyclonal rabbit anti human TDP-43

antibody raised against an N-terminal epitope of the human TDP-43 protein (Proteintech group UK). We hypothesised that endogenous TDP-43 will co-localise with one or more of the recognised major components of stress granules.

3.7.2   Endogenous TDP-43 does not co-localise with SG in response to treatment with sodium arsenite 0.5mM for 30min.

We observed, as expected, stress granule formation in HEK293T cells in response to treatment with sodium arsenite at 0.5mM for 30 minutes (Fig 3.13 panel F and H) using an antibody to label TIAR. However, we did not notice endogenous TDP-43 localising to cytoplasmic or nuclear inclusions (Fig 3.13 panel E) upon arsenite treatment. The co-labeling for endogenous TDP-43 and TIAR confirms that TDP-43 in HEK293T cells does not co-localise with the stress granule marker TIAR in response to arsenite treatment. We also did not see nuclear inclusion body formation, which we observed following arsenite treatment of wtTDP-43 and mutTDP-43 transfected HEK293T cells (Section 3.6.2). It is possible that the amount of cytoplasmic endogenous TDP-43 is too small (Fig 3.13 panel A and E) so that any translocation to the inclusions is undetectable by the immunofluorescence method used. Our findings are not in keeping with experiments done on neuroblastoma cells (Liu-Yesucevitz et al., 2010) and human lymphoblasts (McDonald et al., 2011) where endogenous TDP-43 was shown to co-localise with SGs. This difference could be partly explained by the inherent differences in cell lines and also by the duration of arsenite treatment (1 hour by (Liu-Yesucevitz et al., 2010)).
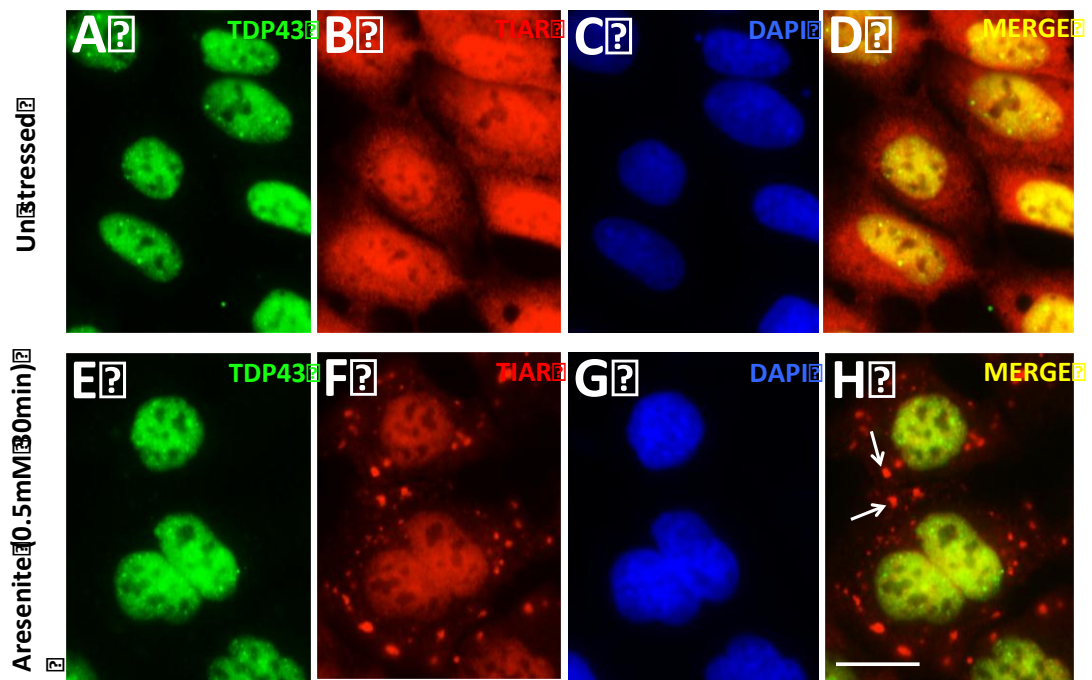
Figure 3.13 Endogenous TDP-43 does not localise to cytoplasmic or nuclear inclusions and does not co-localise with stress granules following treatment of HEK293T cells with 0.5mM arsenite for 30 minutes.
A) Endogenous TDP-43 is largely in the nucleus under basal conditions **B)** Endogenous TIAR is nuclear as well as cytoplasmic in distribution. **C)** DAPI stain of the nuclei **D)** TDP-43 and TIAR co-localise in the nucleus but not in the cytoplasm**.** **E)** Treatment with arsenite does not alter endogenous TDP-43 distribution nor does it promote the formation of TDP-43 cytoplasmic or nuclear inclusions. **F)** Arsenite treatment induces stress granule formation as labeled by TIAR. **G)** DAPI-normal appearing nuclei. **H)** Double labeling of the arsenite treated HEK293T cells does not show co-localisation of endogenous TDP-43 with the cytoplasmic inclusions (Arrows). Scale bar 50µm. Endogenous TDP-43 detected by rabbit anti human TDP-43 antibody targeting a N-terminal epitope of TDP-43.

3.7.3 Induction of cellular stress with menadione, FCCP or H_2O_2 did not induce TDP-43 cytoplasmic or nuclear inclusions, nor the production of TIAR positive stress granules.

Although menadione, FCCP or H_2O_2 are not classical stress granule inducers, we attempted to recapitulate the responses of transiently transfected HEK293T cells to assess if the endogenous TDP-43 localisation response would be different when compared to the transfected TDP-43. Treatment of HEK293T cells with menadione for 4 hours or FCCP for 120 minutes did not alter the distribution of endogenous TDP-43 from the nucleus. No stress granule formation was noted with either stress (Fig 3.14 A-H). Treatment with H_2O_2 produced significant cytoplasmic

translocation of endogenous TDP-43 (Fig 3.14 panel I, empty arrow). However cytoplasmic TDP-43 positive inclusion formation was not observed. There was also no stress granule formation noted with TIAR (Fig. 3.14 J). TDP-43 co-localisation with ubiquitin or phospho-TDP-43 positive inclusion formation cannot be ruled out, as we have not tested for the expression of these proteins in our experiments.

3.7.4 Treatment of HEK293T cells with 0.4M sorbitol for 2 hours induces stress granules and endogenous TDP-43 co-localises with the stress granule protein TIAR

Sorbitol is used as an osmotic stress inducer. Treatment of the HEK293T cells with 0.4M sorbitol for 30 minutes resulted in increased TDP-43 mis-localisation to the cytoplasm (Fig 3.15 A). However nuclear inclusion formation was not observed. No HEK293T cells showed SG formation (Fig 3.15 B), upon treatment with sorbitol for 30 minutes. SG formation was observed when stressed for 2 hours. Endogenous TDP-43 was observed to translocate to cytoplasm and form cytoplasmic inclusions (Fig 3.15 E and I). These TDP-43 positive cytoplasmic inclusions co-localised with the stress granule marker TIAR suggesting that endogenous TDP-43 translocates to the stress granules in response to the treatment with sorbitol (Fig 3.15 H and J: arrows). However, not all cells with TIAR positive SGs incorporated endogenous TDP-43 (Fig 3.15 I, Empty arrows and panel J- black star).

What mechanisms dictate whether cells form TDP-43 positive SGs, remains to be investigated. Dewey et al reported similar findings in an HEK293T cell model, confirming that endogenous TDP-43 co-localises with TIAR positive SG in response to sorbitol but not with 0.5mM arsenite for 30 minutes (Dewey et al., 2011). Endogenous TDP-43 is also directed to SG in primary cultured glia in response to sorbitol. TDP-43 knockdown resulted in poor recovery of the cells stressed with sorbitol suggesting that TDP-43 helps recovery from osmotic and oxidative stress caused by sorbitol (Dewey et al., 2011).
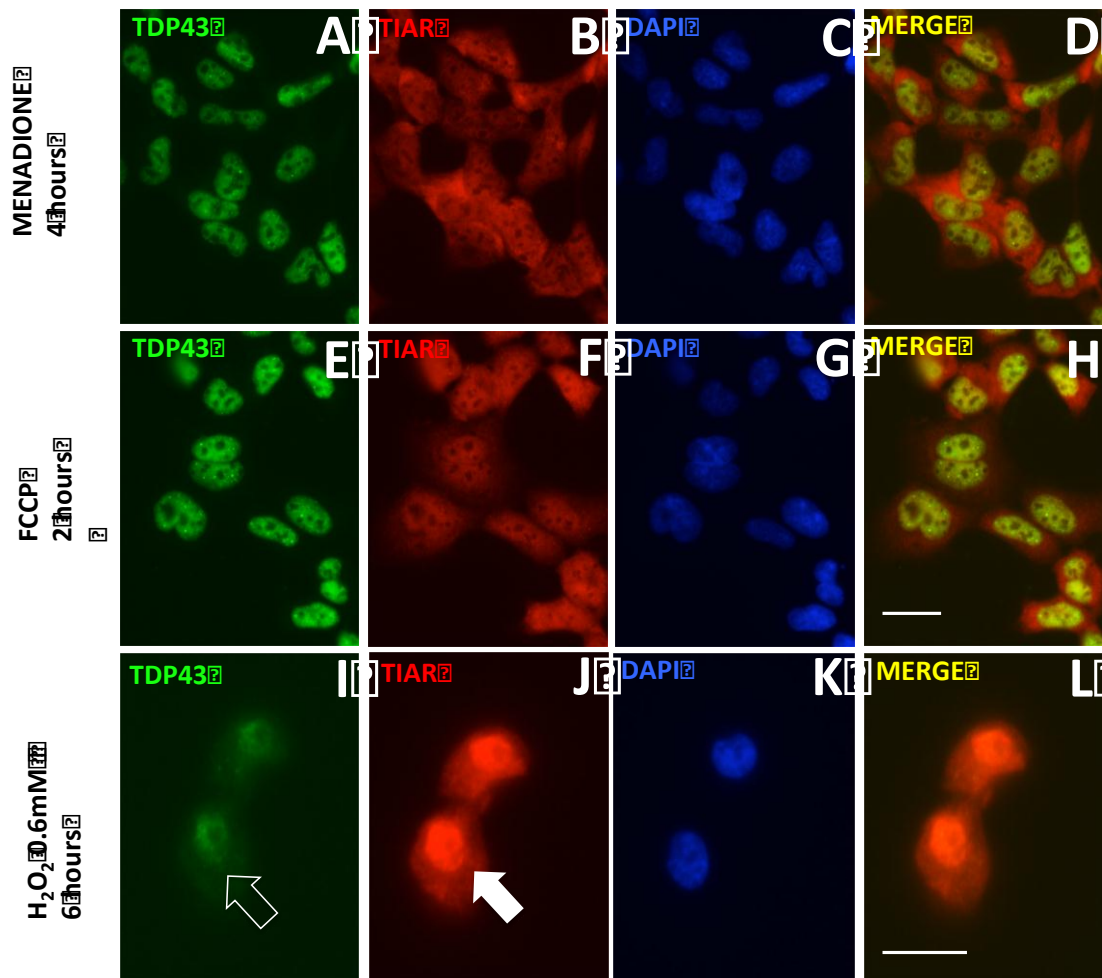
Figure 3.14 Endogenous TDP-43 in HEK293T cells following treatment with menadione, FCCP and H$_2$O$_2$.

A) 10µg/µl Menadione treated HEK293T cells (we increased the treatment duration to 4h to increase the chance of inducing SGs). Endogenous TDP-43 is largely nuclear and no cytoplasmic inclusions and no stress granule formation **B-D)**. **E-H)** 10µM FCCP treatment for 2h did not produce nuclear or cytoplasmic inclusions or stress granules. **I-L)** Exposure to 0.6mM H$_2$O$_2$. for 6h resulted in misclocalisation of endogenous TDP-43 to cytoplasm (Empty arrow). Again no stress granule formation or cytoplasmic inclusion formation was seen (Arrow). Scale bar 50µm. Endogenous TDP-43 detected by rabbit anti human TDP-43 antibody targeting a N-terminal epitope of TDP-43 (Proteintech group.UK 1:500), (TIAR 1:500).
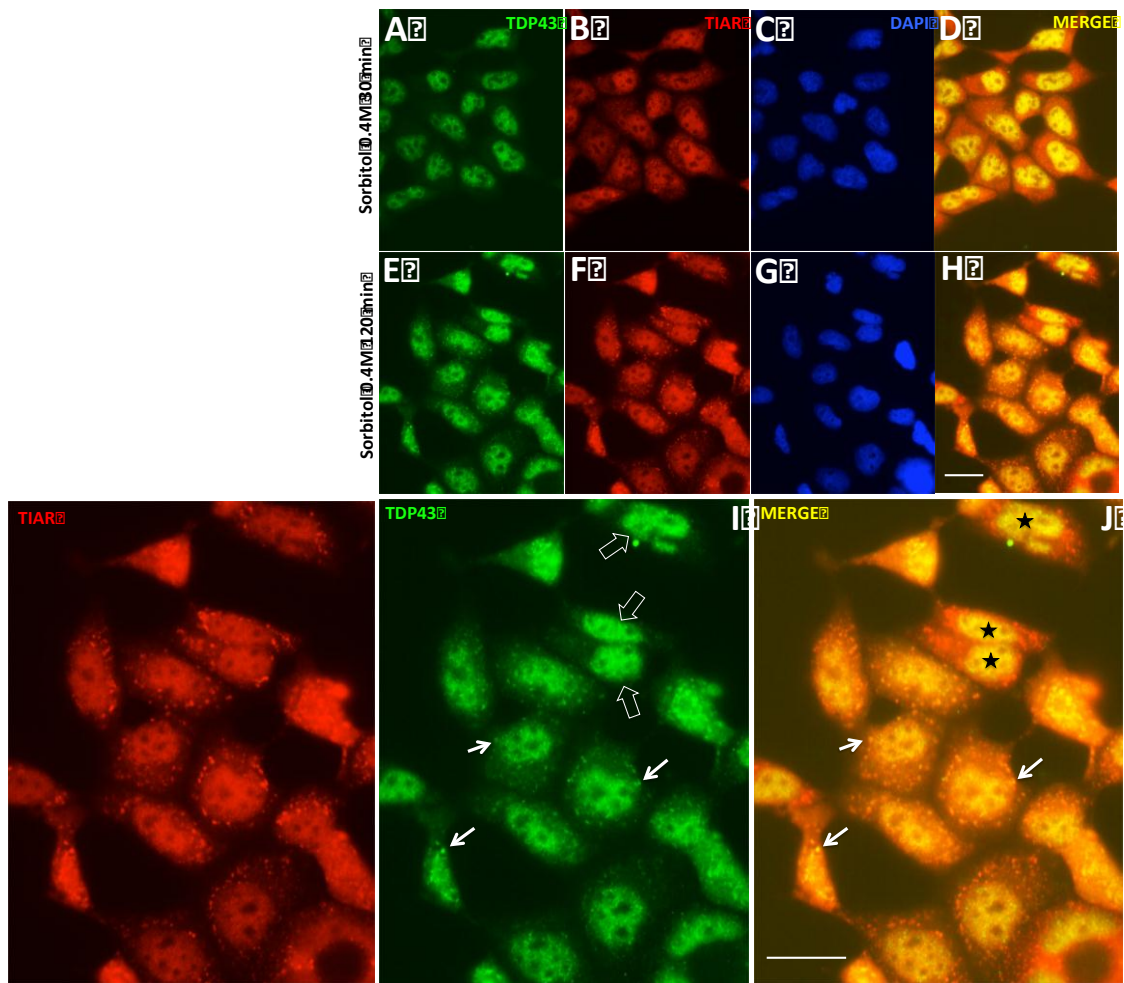
Figure 3.15 Endogenous TDP-43 in HEK293T co-localises with TIAR positive stress granules in response to 0.4M sorbitol for 2h.
A-D) Treatment with sorbitol 0.4M for 30 minutes, (A) resulted in cytoplasmic mis-localisation of endogenous TDP-43. (B) A few cells formed TIAR positive SGs. (D) No co-localisation of TDP-43 and TIAR seen. **E-H)** 0.4M Sorbitol for 2h. (E) Endogenous TDP-43 formed cytoplasmic inclusions in response to prolonged exposure to sorbitol. (F) Distinct TIAR positive SGs formed. (H) Co-localisation of endogenous TDP-43 and TIAR stress granule marker suggesting sorbitol drives endogenous TDP-43 to SGs. **I)** Enlarged picture of panel (E) demonstrating that TDP-43 positive inclusions (arrows) are present in most cells but not all. Empty arrows mark cells lacking TDP-43 positive inclusions. **J)** Enlarged picture of panel (H) indicating co-localisation of endogenous TDP-43 with TIAR positive SGs (arrows). Black stars mark cells with TIAR positive SGs with no endogenous TDP-43 co-localisation. Scale bar 50µm. Endogenous TDP-43 detected by rabbit anti human TDP-43 antibody targeting a n-terminal epitope of TDP-43 (Proteintech group.UK 1:500), (TIAR 1:500).

3.8   Discussion

A key step in understanding the mechanisms of dysfunctional TDP-43 as an important player in ALS related neurodegeneration is to understand, if ALS associated mutations cause cellular toxicity and if so how the autosomal dominant point mutations alter the normal function of TDP-43. Since the discovery of the link between ALS and TDP-43 in 2006 by Neumann et al (2006) evidence has shaped a hypothesis that mis-localisation of nuclear TDP-43 to the cytoplasm/cytoplasmic inclusions contributes to disease process (Nonaka et al., 2009b). In order to confirm toxicity we need to assess the toxicity of TDP-43 overexpression by a direct method such as propdidium iodide staining for dead cells at the 4h wash step. However the exact nature of this process remains an enigma. When we over-expressed the full-length wtTDP-43 and mutTDP-43 we observed that even wtTDP-43 is toxic to the cells when over-expressed. Although we have not demonstrated toxicity directly by an assay two observations support this claim: *(i)* we noted that cytoplasmic TDP-43 staining was directly proportional to the transfected TDP-43 DNA concentration. In keeping with these findings Barmada et al 2010 reported that presence of cytoplasmic TDP-43 after transfection is associated with increased risk of cell death (Barmada et al., 2010), *(ii)* Secondly transfection efficiency was inversely proportional to the concentration of transfected TDP-43 DNA which suggests that high expressing cells did not survive which indicates perturbation of physiological levels of TDP-43 is toxic to the cells (Xu et al., 2010). This is an important observation as the vast majority of ALS cases are sporadic in nature and most of the sporadic ALS cases that manifest TDP-43 pathology do not have a mutation in the *TARDBP* gene. Several mouse models over-expressing wtTDP-43 have developed a motor neuron disease like phenotype along with some features of TDP-43 proteinopathy (Stallings et al., 2010, Wils et al., 2010). However, our observation that a drop in the proportion of transfected cells expressing full length wtTDP-43 or mutTDP-43 is consistent with the scenario that alteration of the level of full length TDP-43 is associated with cellular toxicity and cytoplasmic mis-localisation. TDP-43 expression at 24h post-transfection did not show significant cytoplasmic inclusion formation. In support of this observation a previous study on transient expression of TDP-43 in rat cortical neurons has suggested that inclusion body formation was not required for the mutTDP-43, A315T to cause toxicity and suggested that

diffuse expression of a soluble form of TDP-43 underpins the neurotoxic effects (Barmada et al., 2010). Several studies on transgenic animal models of TDP-43 expressing A315T mutation (Flag tagged mutant (Wegorzewska et al., 2009) and untagged (Stallings et al., 2010)) and M337V mutation (Stallings et al., 2010) did not show TDP-43 co-localising with ubiquitinated inclusions when tested with phosphorylation independent anti- TDP-43 antibodies raised against different epitopes of the TDP-43 protein. Igaz et al could only demonstrate TDP-43 positive neurocytoplasmic inclusions in less than 0.1% of the motor neurons in a transgenic mouse model over-expressing NLS-deleted human TDP-43 constructs even when a phosphorylation dependent antibody was used, confirming that TDP-43 positive aggregation formation is not essential for neurodegeneration (Igaz et al., 2011). However transgenic drosophila flies carrying the A315T mutation showed neurocytoplasmic aggregation of TDP-43 (Gregory et al., 2012).

It is still unknown if and how cytoplasmic TDP-43 mis-localisation causes cytotoxicity. A possible mechanism has been suggested following a study where in a lentiviral delivered over-expression model of TDP-43 in mice showed that TDP-43 modulates processing of APP via enhanced BACE activity. TDP-43 may alter BACE levels via increasing the cytosolic membrane stability and thereby increasing APP cleavage. Increasing the cytoplasmic presence of TDP-43, which is largely a nuclear protein, could result in an additional cytoplasmic function of modulating processing of APP via regulating BACE, which then leads to production of Aß, which is associated with FTLDU (Herman et al., 2012). Arnold et al (2013) described widespread effects on TDP-43 sensitive splicing in both wtTDP-43 and mutTDP-43 over-expressing transgenic mouse models suggesting that maintenance of homeostatic levels of TDP-43 is vital for normal splicing functions in the central nervous system (Arnold et al., 2013). Co-expression of a subunit of the 20S proteasome complex together with TDP-43 in a drosophila model showed that over-expression of TDP-43 is handled by the proteasome. When impaired by a further insult there is enhanced toxicity in a HSP70 chaperone protein dependent manner, where HSP70 over-expression rescued the toxicity (Estes et al., 2011).

Loss of nuclear TDP-43 is one of the pathological signatures of TDP-43 proteinopathy (Neumann et al., 2007a). However we did not see any cells over-expressing TDP-43, with relative nuclear clearing. In keeping with our studies, several mouse models over-expressing wtTDP-43 and mutTDP-43 (A315T) also

did not show significant nuclear clearing of TDP-43 nor did they show TDP-43 positive cytoplasmic inclusions even though these mice developed a motor neuron disease equivalent phenotype (Wegorzewska et al., 2009, Xu et al., 2010). However, we noted that TDP43 over-expression resulted in suppression or down-regulation of the endogenous TDP-43 (Fig 3.4 B). In keeping with this observation is a study of an inducible transgenic mouse model of human TDP-43 lacking the nuclear localisation signal, which resulted in neurotoxicity independent of neurocytoplasmic aggregation formation and was associated with a significant loss of endogenous TDP-43 from the nucleus and in this model the loss of endogenous TDP-43 was the only correlate to neurodegeneration (Igaz et al., 2011). In addition transfected TDP-43 down regulating the endogenous TDP-43 is consistent with a known feature of TDP-43 wherein TDP-43 auto-regulates itself and its homologues (Budini and Buratti, 2011, Hewamadduma et al., 2013)

We noted reduced transfection efficiency following over-expression of wtTDP-43 and mutTDP-43. However, we did not analyze cell death directly following transfection with wtTDP-43 and mutTDP-43, although it has been shown that wtTDP-43 and mutTDP-43 are likely to be more toxic to motor neuronal cells such as NSC34 than non-motor neuronal cells like HEK293T or Neuro2a cells (Wu et al., 2013). Co-staining with an antibody to ubiquitin or phosphorylation dependent TDP-43 antibody is also important to evaluate TDP-43 positive inclusion formation. It is also possible that we did not see a difference in cytoplasmic mis-localisation or response to exogenous stress between the wtTDP-43 and mutTDP-43 expressing cells due to unequal expression levels of TDP-43. Therefore measuring the expression levels either by immunoblotting or analysis of immunofluorescence level is important as   studies have shown that the expression level of an aggregation prone protein is an important predictor of inclusion body formation (Arrasate et al., 2004).

The transient over-expression model of wtTDP-43 and three disease associated mutant forms of TDP-43 (A315T, G287S and Q331K) did not show significant differences amongst the groups in response to external cellular stress, although the three mutant lines reacted slightly differently to each stress. We observed that in response to H_2O_2 induced oxidative stress TDP-43 translocated to the cytoplasm in nearly all cells and formed cytoplasmic inclusions. It is unclear if the TDP-43, trapped in these inclusions, is ubiquitinated or directed to UPS

mediated decay. Treatment with sodium arsenite, sorbitol and heat shock have directed TDP-43 into cytoplasmic entities called SGs in previous studies (Colombrita et al., 2009, Biamonti and Vourc'h, 2010, Liu-Yesucevitz et al., 2010, Dewey et al., 2011, McDonald et al., 2011, Aulas et al., 2012, Parker et al., 2012). However, we did not notice any cytoplasmic mis-localisation of TDP-43 upon arsenite, sorbitol and heat shock treatment of HEK293T cells, in keeping with the concept that TDP-43 aggregates and translocates to different RNA binding proteins, RNA complexes and subcellular locations/compartments depending on the type and nature (transfected or not) of the cell and the nature of the stress. Therefore it was not a surprise when we noted intranuclear aggregation of TDP-43 into distinct puncta in response to arsenite, sorbitol and heat shock. These intranuclear aggregates, particularly those seen with heat shock, are in keeping with nuclear stress bodies as described in section 3.6.5 (Fig 3.12). Nuclear stress bodies (nSBs) are unique sub-nuclear entities which are formed rapidly and transiently in response to a variety of stressors, particularly heat shock, by initiating direct interaction between heat shock protein 1 (HSF1) and active transcription sites for non- coding satellite III sequences (Biamonti and Vourc'h, 2010). nSBs are rarely seen in unstressed cells and the number increases with stress. nSBs are known to play a role in global reprogramming of gene expression through mechanisms such as chromatin remodeling, trapping of transcription and splicing factors etc in stressed cells (Eymery et al., 2009). In keeping with our findings Udan-Jones et al published a report on reversible nuclear aggregation of TDP-43 to nSBs in response to heat shock and demonstrated that this reaction is regulated by an interaction between HSP40/HSP70 co-chaperone system and the C-terminal prion-like domain of TDP-43 (Udan-Johns et al., 2013). The prion-like domain is considered to be the amino acids 286 to 331 (Guo et al., 2011) which encompasses the two TDP-43 mutations we studied, suggesting that inter mutation variations although not significant (our data) could be explained by variations in the ultrastructure and misfolding of the resultant mutTDP-43 protein.

HSF1 has been shown to form nuclear aggregates in response to heat shock treatment and also with several other different cellular stressors such as exposure to heavy metals, oxidative stress, anti-inflammatory drugs, amino acid analogues, arachnoid acid etc (Christians et al., 2002). Therefore, we hypothesise that the translocation of full length TDP-43 to nuclear aggregates in response to arsenite

and sorbitol treatment is consistent with the formation of nSBs. However treatment of cells with a metabolite such as leptomycin B which specifically inhibits nuclear export signal dependent transportation of nuclear proteins has shown to rearrange nuclear TDP-43 distribution to nuclear inclusions similar to what we observed following treatment of cells over-expressing TDP-43 with sorbitol and arsenite (Winton et al., 2008a). Furthermore disruption of the nuclear export signal by mutagenising the same did not produce punctate nuclear lesions but produced fine nuclear granular staining of TDP-43 (Winton et al., 2008a).

TDP-43 is described to have prion-like properties mainly at the C-terminal Q/N rich domain. Proteins with prion-like domains are well known to aggregate (Udan and Baloh, 2011). Moreover, expression of full-length wtTDP-43 has been associated with toxicity. Therefore, to study the effects of TDP-43 on cellular response to stress in an over-expression model is error prone as TDP-43 is an aggregation prone protein, which is toxic when its equilibrium is altered. Therefore, we extended the above stress studies to untransfected HEK293T cells and studied the response of endogenous TDP-43 to cellular stress, in particular, the co-localisation of endogenous TDP-43 with stress granules. The rationale for this is based on the recent studies which show stress granule marker proteins were found as additional components of TDP-43 or FUS positive cytoplasmic inclusions in pathological samples of ALS and FTLD patients (Volkening et al., 2009, Liu-Yesucevitz et al., 2010, Bentmann et al., 2012). Furthermore, several proteins implicated in other neurodegenerative conditions have been shown to either recruit to SGs or modulate the stress granule response to cellular stress e.g. tau, ataxin-2, SMN, angiogenin (Wolozin, 2012) suggesting that SG dynamics are implicated in ALS and FTLD, but also play an important role in other neurodegenerative diseases. We did not observe TDP-43 co-localisation with the SG marker TIAR in response to exposure to arsenite, in keeping with a similar study on HEK293T cells (Dewey et al., 2011) although several previous studies (Colombrita et al., 2009, McDonald et al., 2011) demonstrated that endogenous TDP-43 co-localised with SGs in response to treatment with arsenite. This could be due to differences in the specific cell type used and other technical reasons. It is well known that the composition of SGs can wary depending on the cell type and the conditions of the stress (Anderson and Kedersha, 2008). In addition, we also noted that endogenous TDP-43 did not form nuclear aggregates, which appeared

as nSBs when transfected HEK293T cells were exposed to arsenite treatment. These data suggest that in a state of over-expressed mutant or wild type TDP-43, the cell shares some features similar to diseases where misfolded prion-like proteins accumulate (Udan and Baloh, 2011). As TDP-43 also has a prion-like C-terminal domain, it is possible that it senses the altered protein homeostatic state in the cell and promotes self-aggregation. Therefore in the non over-expressed state endogenous TDP-43 functions differently by not engaging in the process of nSB formation. In other cell models, following arsenite treatment, TDP-43 takes a role in cytoplasmic SG formation. McDonald et al demonstrated that SG formation is impaired when TDP-43 is knocked down. However, in a different cell line, Colombrita showed that TDP-43 is neither essential for nor influences SG formation and is not vital for surviving acute stress (Colombrita et al., 2009, McDonald et al., 2011). Although the contrasting observations can be due to differences in the models used, overall the findings to date suggest that acute knock-down or over-expression of TDP-43 is perhaps not the best method to study the physiology and pathophysiology of a protein which has multiple nuclear and cytoplasmic functions, but need to be investigated at an endogenous level which is physiologically similar to the processes occurring during the disease state in human patients.

Treatment with sorbitol was associated with endogenous TDP-43 co-localising with the stress granule marker TIAR in keeping with a previous study on a similar HEK293T cell model (Dewey et al., 2011). Endogenous TDP-43 translocated to SGs in approximately 75% of the cells upon exposure to sorbitol but none with stress induced by arsenite (Fig 3.16). Interestingly, we also observed a difference in the pattern and the size of the SGs formed when HEK293T cells are exposed to arsenite and sorbitol. Arsenite exposed cells formed more defined larger SGs (Fig 3.13) whilst exposure to sorbitol resulted in numerous smaller granular SGs (Fig 3.15). These findings need to be verified by quantitating the SG size, but these observations are consistent the notion with that specific cell types handle different stressors in different ways (Anderson and Kedersha, 2009).

Cytoplasmic inclusions positive for TDP-43 are commonly pointed out in human pathological samples as are nuclear inclusions in familial ALS and FTLD cases, whilst VCP related FTLD cases are commonly found to have nuclear inclusions (Neumann et al., 2006, Neumann et al., 2007b, Parker et al., 2012). The

concept of pre-inclusions has been suggested to precede cytoplasmic inclusion formation and these pre-inclusions have morphological similarity to SGs (Dewey et al., 2012, Parker et al., 2012). Therefore it is also possible that the nSBs observed in response to heat shock, arsenite and sorbitol in the over-expressed TDP-43 HEK293T cells could represent pre-nuclear inclusion formation which is reversible initially before becoming more permanent over a period of time. Furthermore, elevated levels of TDP-43 have been described in pathological samples of ALS/FTLD cases (Mishra et al., 2007, Strong et al., 2007). These observations therefore are consistent with the theory that dysfunctional TDP-43 could elevate its levels in the brain and prion-like nature of TDP-43 enhances its aggregation. We have noted from the cell stress studies that TDP-43 in different cells responds to stress in a 'cell type' dependent or specific manner, suggesting that aggregation of TDP-43 under stressful disease conditions may pose a greater toxicity to motor neurons than the non motor neurons, resulting in an increase motor neuron vulnerability to dysfunctional TDP-43.
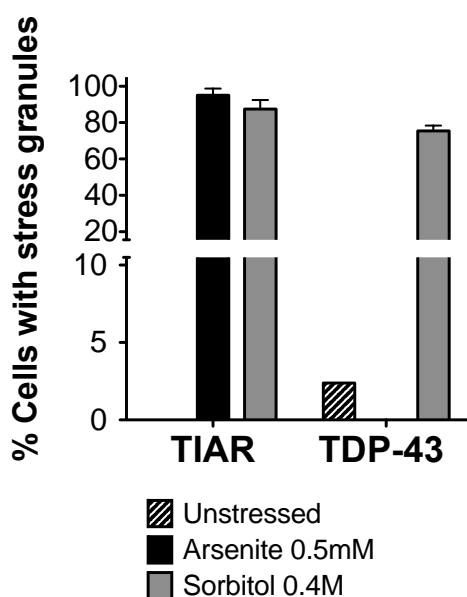
Figure 3.16 Endogenous TDP-43 localisation to stress granules.
TIAR positive SGs formed in response to both 0.5mM arsenite and 0.4M sorbitol in more than 80% of the cells. However endogenous TDP-43 only localised to SGs upon treatment with sorbitol but not with arsenite (75%).

159

Chapter 04:

Patient derived cells, fibroblasts, can be used as a platform to study TDP-43 related functions

4.0   Introduction

Our previous observations when wild type TDP-43 (wtTDP-43) and mutant TDP-43 (mutTDP-43) over expression in HEK293T cells suggested the possibility of toxicity. However we did not observe a significant difference in TDP-43 distribution between the two groups. This result is consistent with several other cellular and animal models where over-expression of both mutant and wild type TDP-43 full-length protein has been shown to be toxic, although mutant TDP-43 in some animal models caused greater toxicity (Janssens et al., 2013). Furthermore aggregation prone proteins such as hnRNPs and the C-terminal end of TDP-43 can give rise to misleading results when over-expressed and may not accurately represent the pathophysiological process underlying the neurodegeneration of ALS. TDP-43 levels are maintained stringently and the fact that perturbation of this delicate balance is harmful to the cells is now well established. Traditionally over-expression models of disease associated mutations are used to accelerate the phenotype associated with mutations or variations in proteins, to study the effects of such mutations on cells or animal models. However with regards to a tightly controlled protein, TDP-43, non-physiological elevation of TDP-43 expression appears to be harmful and this perhaps overshadows the effects of the expressed mutation. Therefore an ideal model to study the effects of dysfunctional TDP-43, we propose, is a model wherein wtTDP-43 and mutTDP-43 levels are unaltered and maintained at physiological levels. Such a model could only be established from patient derived cells or tissues. However, to establish a model with the disease associated tissues, particularly in motor neuron disease is nearly impossible. In a live motor neuron disease patient, to obtain a spinal cord or brain sample is unethical and would be potentially harmful to the patient. Obtaining such tissues immediately after death has the disadvantage of artifacts caused by post-mortem delay. Furthermore, to assess dynamic cellular functions such as RNA

metabolism or cell signaling is nearly impossible to achieve using postmortem tissues.

Skin and neuronal tissues have similar embryological origin, the ectoderm. Skin fibroblasts can be cultured from skin biopsies obtained from both ALS cases and age and gender matched controls. Fibroblasts have an advantage over lymphoblasts in that transformation of lymphocytes to lymphoblasts to allow serial culture could alter cellular properties especially pathways involving calcium metabolism (Gibson and Peterson, 1987). A considerable precedent exists in using cultured fibroblasts in the study of neurological and neurodegenerative disorders. Fibroblasts from patients with Alzheimer's dementia associated with mutations in presenilin-1 mutations have been used to study stress signaling pathways involved in disease related mutations and control cases (Mendonsa et al., 2009), to understand disease related pathophysiology and aging (Huang et al., 1994). Fibroblasts from cases with Parkinson's disease related to mutant Parkin have been used to elegantly demonstrate impaired mitochondrial morphology and function (Grunewald et al., 2010) and studies on PINK1 mutant fibroblasts from Parkinson's disease cases have shown impaired ubiquitination of relevant proteins (Rakovic et al., 2011). Advantages outweigh the potential disadvantages in the use of fibroblasts. Some of the disadvantages are that neuronal proteins of interest associated with neurodegeneration might not be expressed in the fibroblasts; variations in culture methods could potentially make comparison of studies amongst different labs difficult to interpret. This fact is illustrated in studies in AD related fibroblasts where robust differences in calcium metabolism between non-AD and AD fibroblasts could not be replicated (Peterson et al., 1988, Borden et al., 1992).

However, fibroblasts from ALS cases have not been directly used as frequently as in Alzheimer's dementia or Parkinson's disease. The development of induced pluripotent stem cells (iPSCs) using ALS patient derived fibroblasts, although a promising technology (Dimos et al., 2008), has been shown to have significant variations in the expression levels of the disease associated target proteins amongst clones of iPSCs derived from a single cell line, which limits its utility as a robust model (Egawa et al., 2012). In this chapter we demonstrate that fibroblasts derived from ALS cases can be used to demonstrate some features of TDP-43 proteinopathy and show some promise as a model to interrogate

mechanisms of dysfunctional TDP-43 for example, dysregulation of RNA metabolism associated with mutations in the *TARDBP* gene, by using stress granule dynamics as a surrogate marker of RNA metabolism.

4.1 Fibroblasts from cases with mutant TDP-43 demonstrate loss of nuclear TDP-43 compared to control cases.

One of the prominent features of TDP-43 proteinopathy is mis-localisation of TDP-43 to the cytoplasm and/or relative loss of nuclear TDP-43. To ascertain this feature of TDP-43 we stained three different control fibroblasts lines age matched to three mutant lines carrying single copies of the mutant *TARDBP* gene (M337V, A321V and G287S) expressing physiological levels of TDP-43. As explained in the material and methods section, we assessed the relative immunofluorescence to score the TDP-43 localisation. We noted that in all three control fibroblasts cell lines endogenous wild type TDP-43 (wtTDP-43) was localised to the nucleus (Fig 4.1 panels A-C, representative pictures of all control three cells lines) in more than 85% of the cells (Fig 4.2 A), whilst only a very subtle amount of TDP-43 staining was observed in the cytoplasm. In contrast, the mutant fibroblasts carrying the M337V TDP-43 mutation resulted in significant cytoplasmic TDP-43 mis-localisation compared to the controls cells associated with relative nuclear clearing of TDP-43 (Fig 4.1, panels D-F, empty arrow) in more than 50% of the cells (p<0.0001)(Fig 4.2 B). More than 30% of M337V mutant fibroblasts showed almost complete loss of nuclear TDP-43 compared to the control cells (p<0.0001)(Fig 4.2 B). Furthermore about 10% of the G287S mutant fibroblasts also showed complete loss of nuclear TDP-43 (Fig 4.1, panels G-I, Empty arrow) whilst more than 65% of cells showed relative loss of (sub-saturated in mutant TDP-43 cases compared to controls) nuclear TDP-43 compared to controls (Fig 4.2B, p<0.0001). A321V mutant fibroblasts did not show as many nuclei fully depleted of TDP-43 compared to M337V cells (<10%), but had the highest number of cells (>70%) (Figure 4.2B) with a reduction in nuclear TDP-43 (Fig 4.1, panels J-L). A321V fibroblasts also showed less cytoplasmic TDP-43 compared to the other two mutant fibroblasts (Fig 4.1 J).
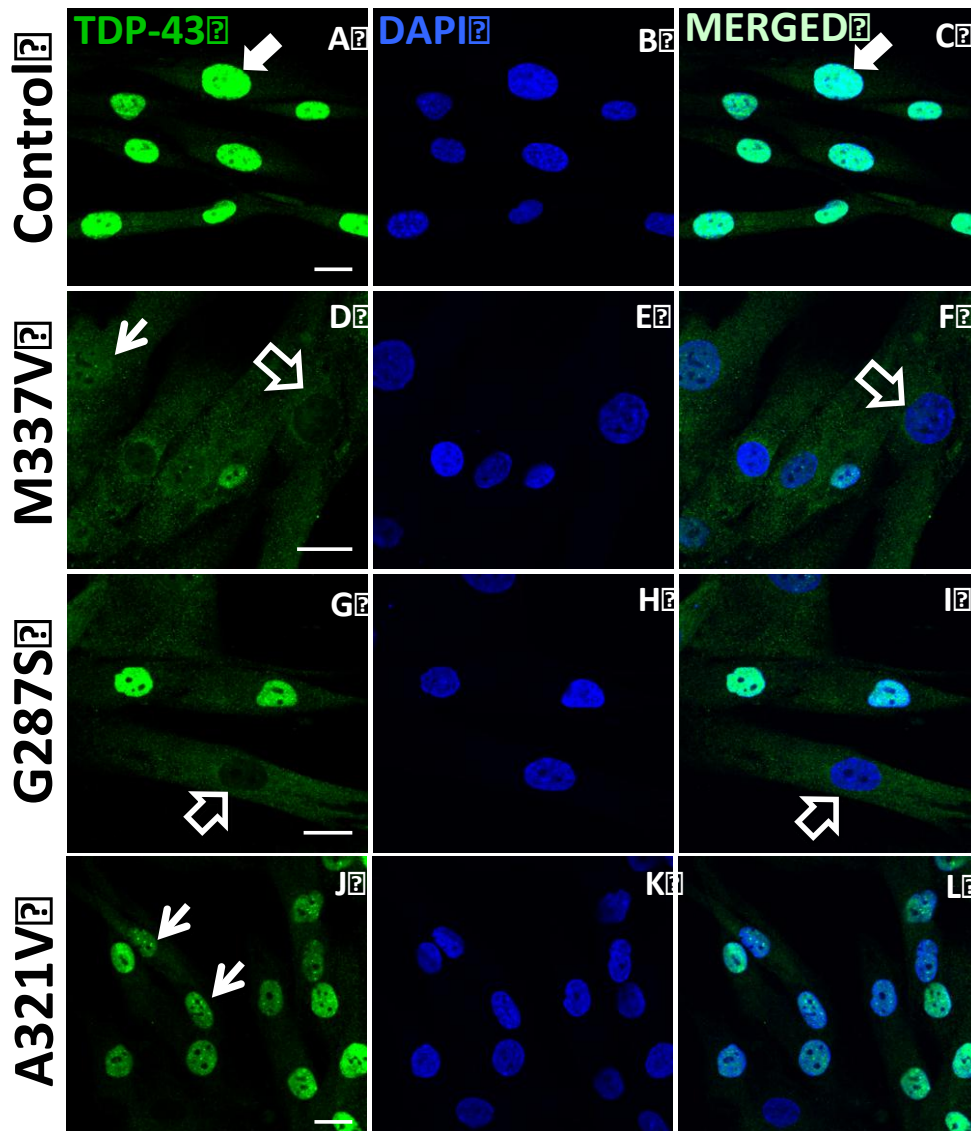
Figure 4.1 Endogenous TDP-43 localisation in control and disease associated mutant TDP-43 fibroblasts: M337V, A321V, G287S. A-C) Representative pictures of control fibroblasts demonstrating predominantly nuclear distribution of TDP-43, under basal conditions. Solid arrow pointing towards a nucleus packed with TDP-43. The same cell has slight cytoplasmic staining for TDP-43. **D-F)** M337V mutant fibroblasts show dramatic reduction of nuclear TDP-43. Empty arrow pointing at a nucleus where TDP-43 is completely mis-localised to the cytoplasm. Arrow points to a nucleus sub-saturated in TDP-43 and increased cytoplasmic TDP-43 **G-I)** G287S mutant also shows empty nuclei (empty arrow) and increased cytoplasmic TDP-43 **J-L)** A321V mutant did not show many empty nuclei, but the nuclear TDP-43 was reduced compared to the control fibroblasts. Green- TDP-43 antibody: Polyclonal rabbit anti human TDP-43, epitope in the C-terminus (1:500). DAPI- used as a nuclear stain (1:1000). Scale bar 20μm.
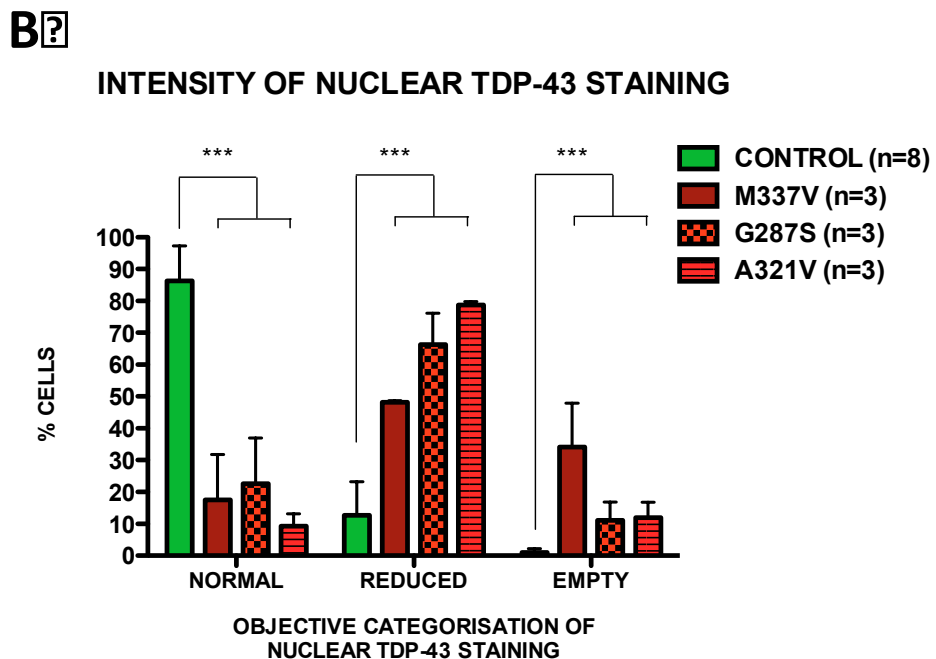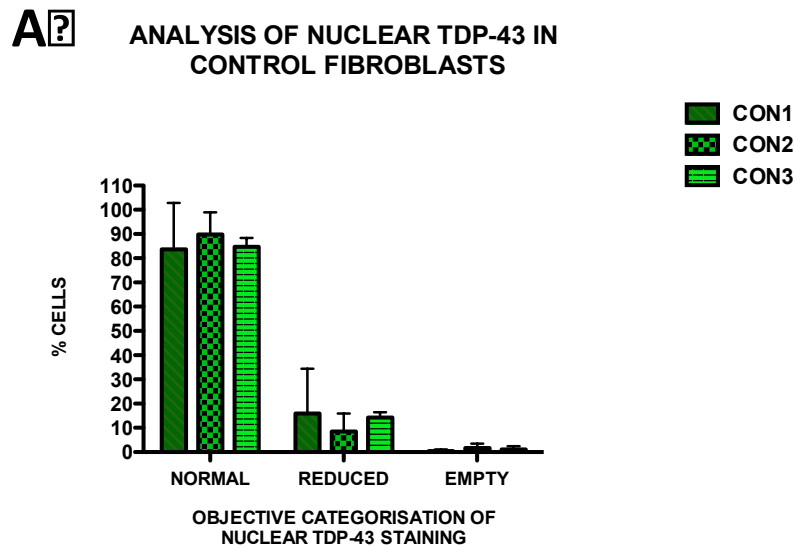
Figure 4.2 Patterns of endogenous TDP-43 localisation in control and disease associated mutant TDP-43 fibroblasts: M337V, A321V, G287S. A) Fibroblasts from three different healthy age-gender matched control cases showed that more than 80% of the cells had predominantly nuclear TDP-43 staining. Less than 15% of the cells showed reduced nuclear staining when assessed using failure to saturate model. Very occasionally cells with no nuclear TDP-43 staining were observed. **B)** In contrast to fibroblasts from control cases, fibroblasts from MND patients with TARDBP mutations showed a marked reduction in nuclear TDP-43 staining. More than 30% of M337V mutant fibroblasts showed no nuclear TDP-43. A321V and G287S mutant fibroblasts also showed a significantly higher number of nuclei with reduced TDP-43 compared to the controls. One way ANOVA with multiple column comparison with Bonferoni post test correction was used, ***$p < 0.0001$

Our finding that in the control cells the majority of the TDP-43 is localised to the nucleus and a small proportion of TDP-43 is in the cytoplasm is consistent with previous reports on postmortem analysis of brain and spinal cords wherein TDP-43 in non ALS/FTLD controls was largely nuclear (Neumann et al., 2006)ref. Postmortem studies on ALS and FTLD cases describe nuclear loss and associated cytoplasmic mis-localisation of TDP-43 as one of the hallmarks of TDP-43 proteinopathy. Varying degrees of loss of TDP-43 from the nuclei have been described in ALS and FTLDU pathological samples (Neumann et al., 2007a). It was interesting that we observed a similar phenomenon of loss of or lack of nuclear TDP-43 in the TDP-43 mutant fibroblasts compared to the controls (Fig 4.2 B).

4.2 Abundant accumulation of cytoplasmic phosphorylated TDP-43 (pTDP-43) in fibroblasts from mutant TDP-43 cases but not in control cases.

Abnormal protein accumulation is a well recognised characteristic of neurodegenerative diseases. Post-translational modifications such as phosphorylation increases the aggregation propensity of proteins (Kumar et al., 2011). Aggregated TDP-43 observed in neurodegenerative diseases is often ubiquitinated and phosphorylated (Neumann, 2009). Phosphorylation sites of TDP-43 are now well characterised (Inukai et al., 2008, Neumann et al., 2009). Cytoplasmic accumulation of phosphorylated TDP-43 is also considered an important facet of TDP-43 proteinopathy (Neumann et al., 2009). We have already observed relative nuclear loss of TDP-43 and increased cytoplasmic accumulation, which is one of the main features of TDP-43 proteinopathy, in the mutant fibroblasts. Over-expression of C-terminally fragmented TDP-43 increases cytoplasmic accumulation and phosphorylation at serine residues 409/410 (Brady et al., 2011). Phosphorylation has been shown to play an important part in the regulation and accumulation of TDP-43 and is considered to drive the toxicity associated with mutant TDP-43 (Liachko et al., 2010). Furthermore postmortem studies have also shown that TDP-43 proteinopathy extends to the extra-motor neuronal cells such as glia and cerebellar tissues (Brettschneider et al., 2012). Therefore we hypothesised that TDP-43 mis-localised to cytoplasm is phosphorylated in TDP-43 mutant fibroblasts compared to the controls. We used a monoclonal mouse anti-human phosphorylated TDP-43 antibody to residues

S409/S410, which was a kind gift from Dr Robin Highley and Professor Paul Ince. A similar antibody has been used in the study of phosphorylated TDP-43 in FTLD and ALS cases (Neumann et al., 2009). We counted and quantified the cells, which harboured distinct lesions such as rounded, elongated lesions, increased diffuse or granular cytoplasmic phosphorylated TDP-43 staining above the background compared to control cells. Imaging of all cells captured was assessed using a confocal microscope using standard setting for image capture.

The three age matched control fibroblast cell lines did not show any cytoplasmic phosphorylated TDP-43 (Figure 4.3). However, we observed a distinct pattern of phosphorylated TDP-43 distributed in fine nuclear punctate lesions, which appeared similar to appearances described for nuclear speckles, which are classically defined as positive for SC35 staining (Vos et al., 2009). This pattern we now refer to as 'speckle pattern'. This speckle pattern of pTDP-43 staining was observed in the nuclei of control fibroblasts (Figure 4.3 A circled nucleus, solid arrow, enlarged in panels G-I, arrow). It is unclear whether this 'speckle pattern' conforms to an anatomical entity such as nuclear stress bodies that we observed when over-expressing TDP-43 in HEK293T cells. However, the above pattern of phosphorylated TDP-43 was observed under basal conditions, which makes the speckles less likely to be nSBs, as nSBs are almost exclusively formed under conditions of external stress (Biamonti and Vourc'h, 2010). We have not co-stained with markers of nuclear speckle proteins or para-speckle proteins to ascertain the nature of the above pattern of distribution of phosphorylated TDP-43 in the control cells.

In contrast to the control cells, significant accumulation of cytoplasmic phosphorylated TDP-43 was noted in the mutant fibroblasts. This was especially prominent in the M337V fibroblasts (Figure 4.4, panels A-C). We noted both diffuse granular pattern of cytoplasmic staining and at times cytoplasmic inclusions, which takes an elongated shape (Fig 4.4 panel A arrow), or circular shaped (Fig 4.4 panel A arrowhead), and granulated cytoplasmic patterns (Fig 4.4 panel G arrow), of distribution of phosphorylated TDP-43 in M337V fibroblasts. We also noted some phosphorylated TDP-43 in the nuclei of the M337V case but this was not prominent (Figure 4.4, panel A and C). Similarly in
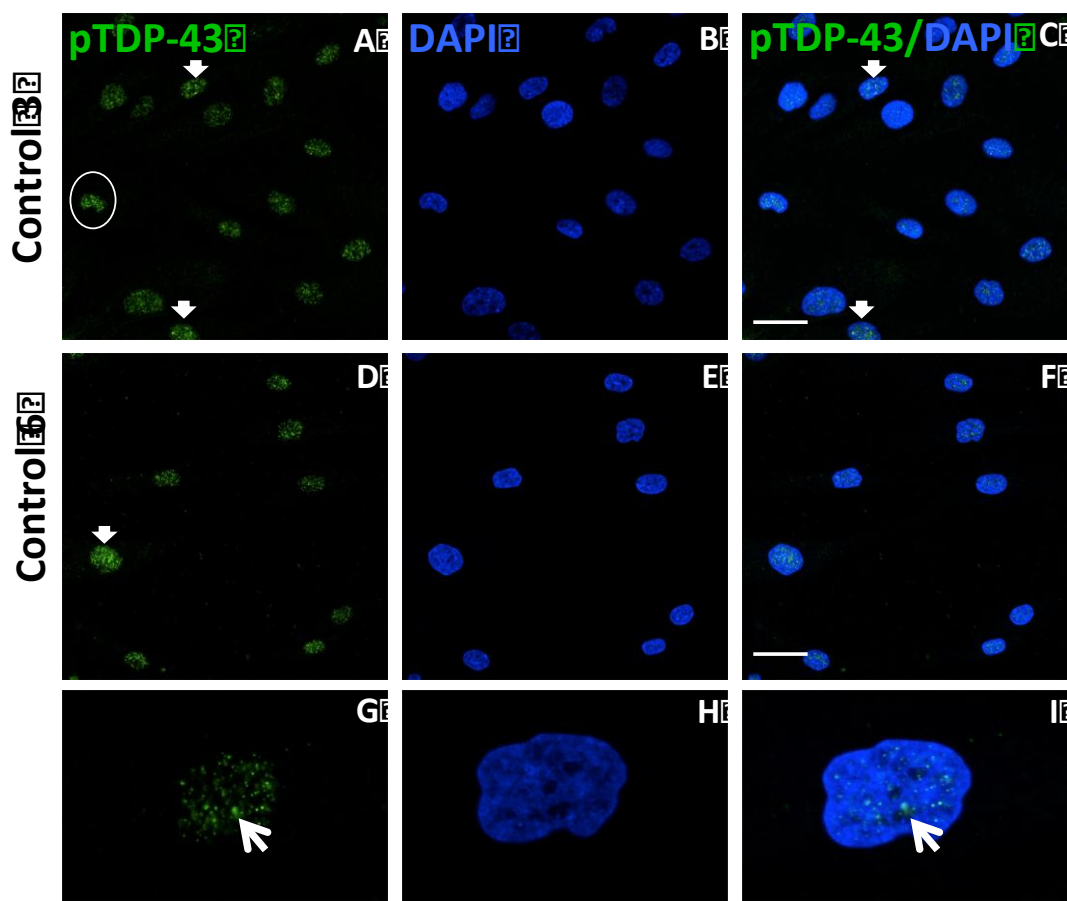
Figure 4.3 Minimal phosphorylated TDP-43 (pTDP-43) staining in control fibroblasts. A-C) Control 1- Representative pictures of control fibroblasts demonstrating no cytoplasmic accumulation of phosphorylated TDP-43 under basal conditions. A nuclear localisation of pTDP-43 noted in a punctate pattern (Solid arrow). **D-F) Control 6-** Fibroblasts also show no cytoplasmic pTDP-43. Circled area is magnified in **G-I)** Representative nucleus demonstrating that nuclear localisation of pTDP-43 in the controls is distributed in a punctate pattern in the sub- nuclear compartment. Arrow pointing towards a nucleus with pTDP-43 puncta. Mouse monoclonal anti phosphorylated TDP-43 antibody (1:1500). DAPI-nuclear stain (1:1000). Scale bar 40μm.

G287S fibroblasts we noted large phosphorylated TDP-43 cytoplasmic inclusions (Figure 4.4, panel D-F) and diffuse granular staining. However compared to the M337V (60% of the cells) and A321V (40%) mutant lines, the G287S mutant fibroblast line showed less cytoplasmic phosphorylated TDP-43 staining (20% of the cells). All three mutant fibroblast lines M337V, G287S and A321V, showed significantly higher proportion of cells with cytoplasmic pTDP-43 staining compared to all control fibroblast lines (Figure 4.4 J, p>0.01). All three mutant fibroblast lines also showed fine-punctate pattern of phosphorylated TDP-43 staining distribution in the nuclei, which was pronounced in mutant TDP-43
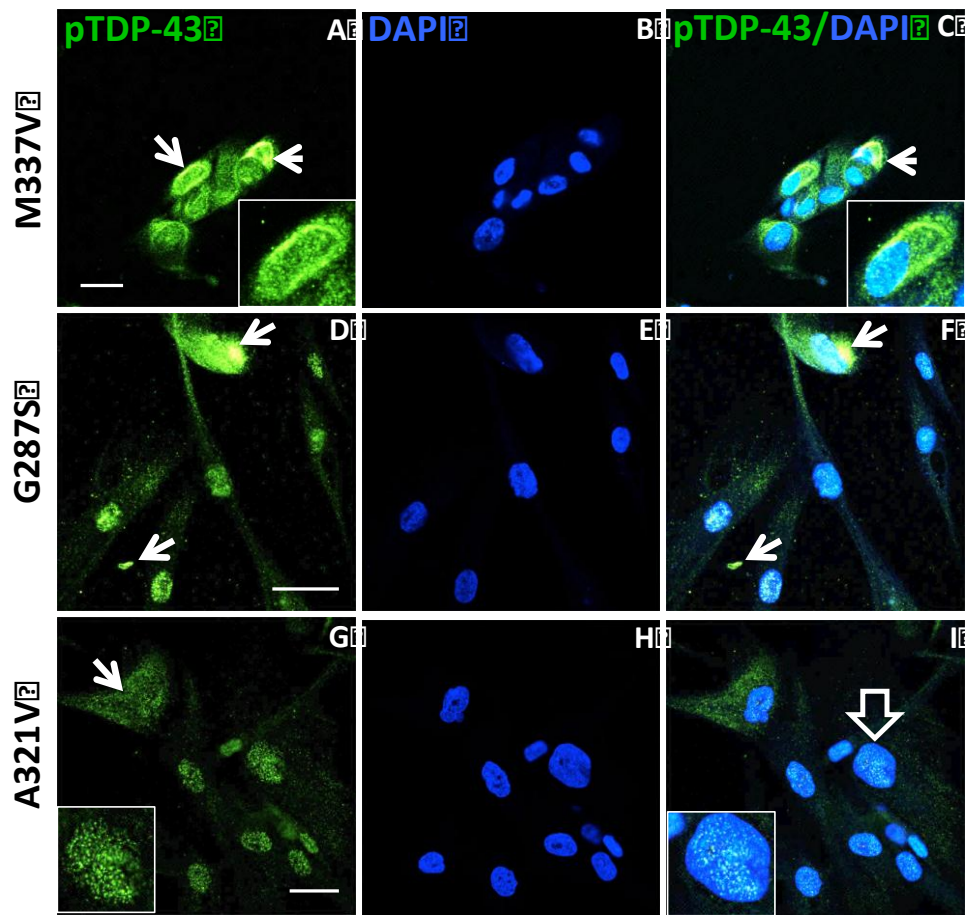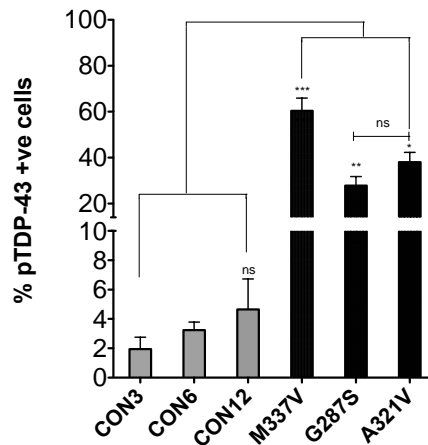
Figure 4.4 Significantly increased distribution of cytoplasmic phosphorylated TDP-43 (pTDP-43) in three different TDP-43 mutant fibroblasts. A-C) M337V- Representative pictures of fibroblasts demonstrating significant cytoplasmic accumulation of phosphorylated TDP-43 under basal conditions, in both inclusions and in a diffuse pattern. Nuclear pTDP-43 is observed in a fine punctate pattern. **D-F) G287S-** Fibroblasts also show large cytoplasmic inclusion formation (arrow) and some cytoplasmic diffuse staining at a less frequent pattern compared to M337V **G-I) A321V-** Demonstrated cytoplasmic pTDP-43 staining. More frequently nuclear pTDP-43 staining was punctate in pattern. **J)** ONE WAY ANOVA, Multiple column comparison with Bonferoni post test correction showed proportion of cells with pTDP-43 cytoplasmic staining was significantly higher in all mutTDP-43 fibroblasts lines (M337V, p<0.001; A321V and G287S, p<0.01) compared to all control cases. Scale bar 40µm.

fibroblasts compared to the control fibroblasts but we have not formally analysed the differences in nuclear pTDP-43 staining pattern. In future an immunoblot could be performed to compare the levels of pTDP-43 between controls and mutant fibroblast cell lines in nuclear and cytoplasmic fractions.

4.3   p62 positive inclusions and cytoplasmic accumulations are common in mutant TDP-43 and rare in control cases.

We counted and analysed the fibroblasts, which showed at least two or more p62 positive cytoplasmic or nuclear punctate lesions, in control and mutant fibroblasts. None of the three control fibroblasts (age and gender matched to mutant fibroblasts) showed significant p62 staining. Only about 5-12% of the control fibroblasts showed p62 positive cytoplasmic inclusions (Fig 4.5, panels A-C, arrow). We did not observe any nuclear p62 positive inclusions in the controls. In contrast we observed a significant amount of cytoplasmic and nuclear p62 positive inclusions and diffuse cytoplasmic staining in the mutant fibroblasts (Fig 4.6). Furthermore there was also a noticeable difference in the intensity of p62 positive lesions amongst the three mutant fibroblast lines. p62 distribution in M337V fibroblasts was observed in approximately 40% of the fibroblasts and compared to control fibroblasts the M337V cell line harboured significantly more p62 positive inclusions (Fig 4.6, A-C)(Fig 4.6 J, $p<0.05$). However G287S cells demonstrated a greater presence of p62 staining in almost 85% of the cells (Fig 4.6, panels D-F) compared to the controls (Fig 4.6, J, $p<0.001$). There were distinct puncta and cytoplasmic granular staining of p62 noted in G287S and A321V mutant fibroblasts (Fig 4.6 panels D-I). A321V mutant fibroblasts also showed significantly increased endogenous p62 positive inclusions in 70% of the cells (Fig 4.6, G-I) compared to controls (Fig 4.6 J)($p<0.001$). Although A321V mutant fibroblasts harboured significantly more p62 positive lesions, compared to M337V mutant fibroblasts ($p>0.05$), there was no significant difference compared to those carrying the G287S mutation ($p>0.05$) (Fig 4.6 J). Whilst it was an interesting finding to note that the TDP-43 mutant fibroblasts have a greater p62 inclusion load compared to the controls it is also noteworthy that there were variations in p62 staining amongst the three dominantly inherited disease associated mutations.
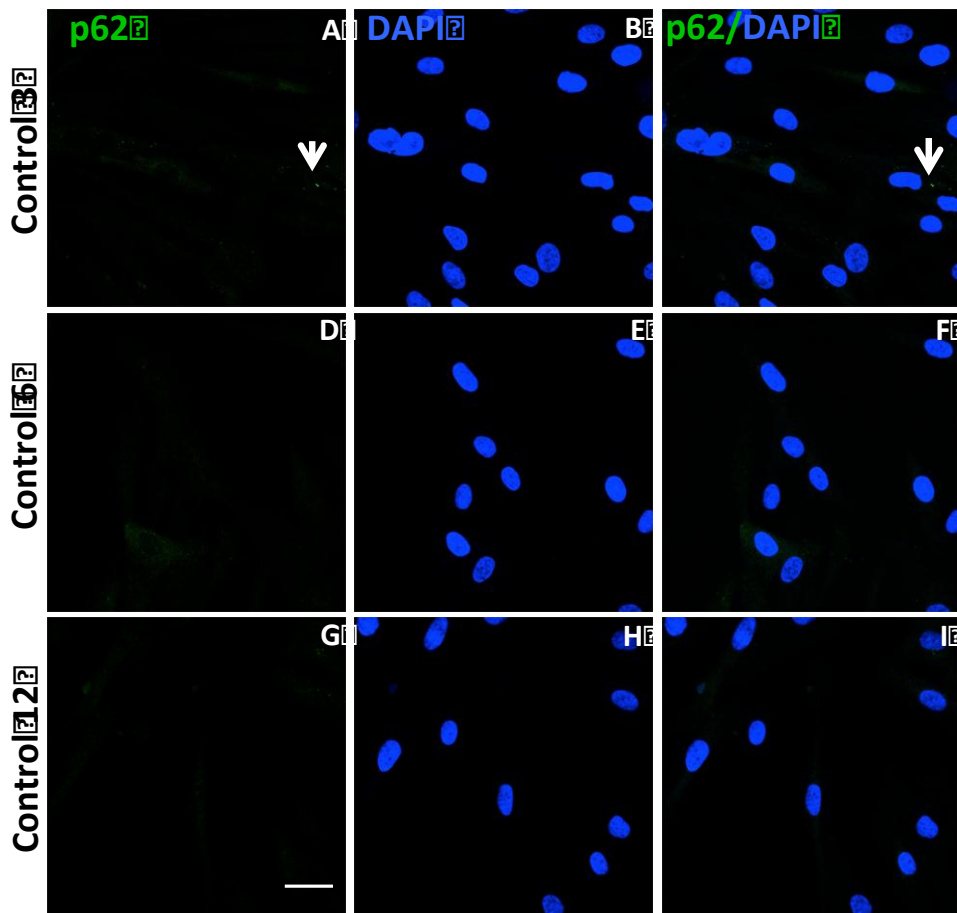
Figure 4.5 Minimal p62 staining in control fibroblasts. A-C) control 3 **-**Occasional p62 positive lesion in the cytoplasm noted (arrow). **D-F)** Control 6 and **G-I)** Control 12- representative pictures show no cytoplasmic p62 staining. Scale bar 10µm. Mouse monoclonal anti human p62 antibody used at 1:2000 dilution. DAPI used for nuclear stain. Scale bar 50µm.

Figure 4.6 Significant p62 staining in all three mutant TDP-43 fibroblasts, M337V, A321V and G287S. A-C) M337V- Distinct punctate lesions positive for p62 in the cytoplasm noted (arrow). In addition there is also a diffuse staining in cytoplasm in most cells. **D-F) G287S –** Shows significant cytoplasmic inclusions, diffuse staining and nuclear p62 positive inclusions. Boxed area is enlarged and arrow points to an intra nuclear p62 positive lesion which is also present in **A321V** mutant fibroblasts **(G-I). J)** ONE WAY ANOVA, Multiple column comparison with Bonferoni post test correction showed p62 cytoplasmic inclusions are present in a significantly higher number of cells in mutTDP-43 (M337V, $p < 0.05$; A321V, $p < 0.001$ and G287S, $p < 0.001$) compared to the controls. G287S and A321V fibroblasts had significantly more p62 staining compared to M337V cells ($p < 0.001$ and $p < 0.05$ respectively..(Mouse monoclonal anti human p62 antibody used at 1:2000 dilution. DAPI used for nuclear stain. Scale bar 50µm.
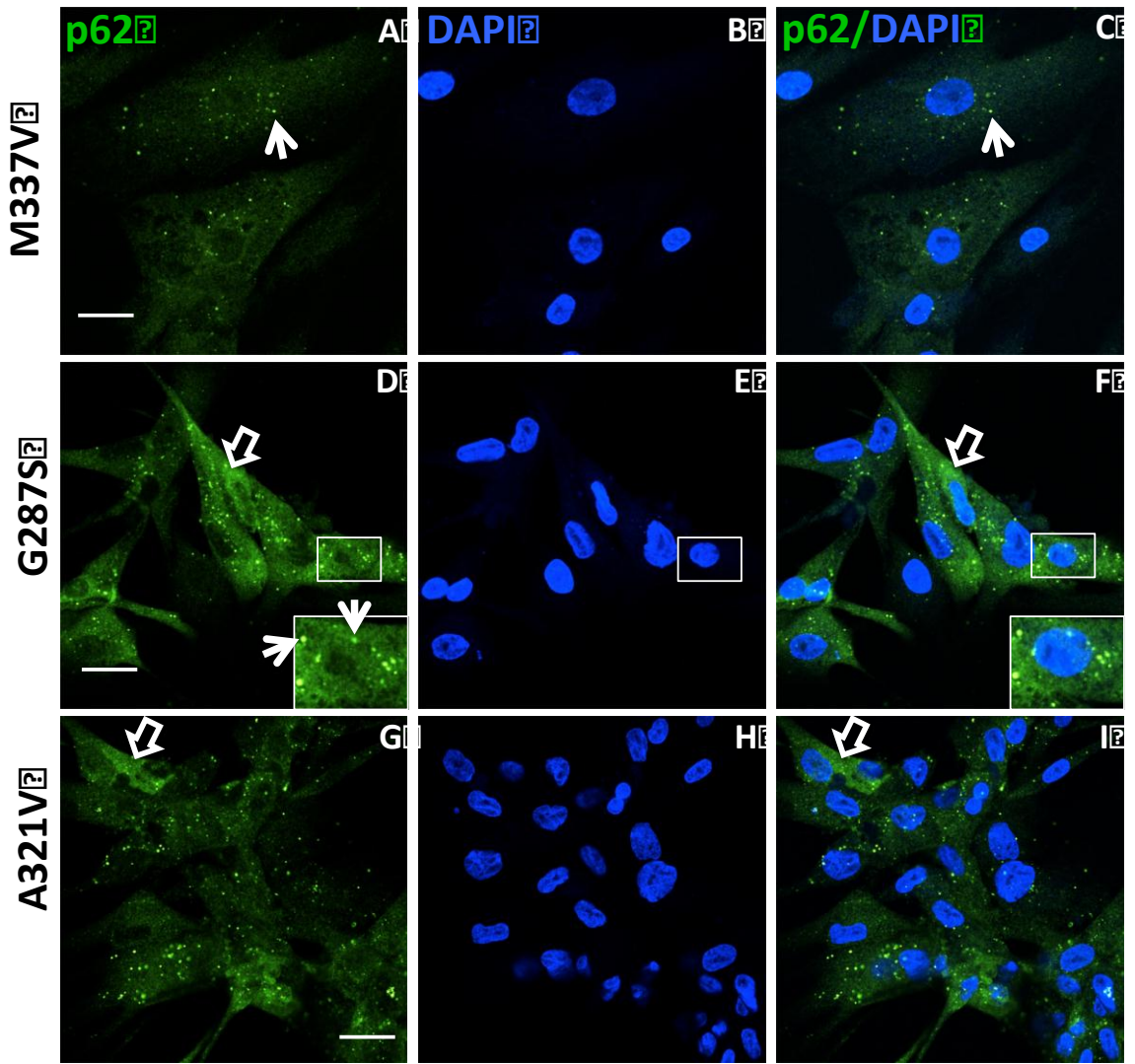
J   **p62 staining of control and mutant TDP-43 fibroblasts**
experimental repeats n= 3
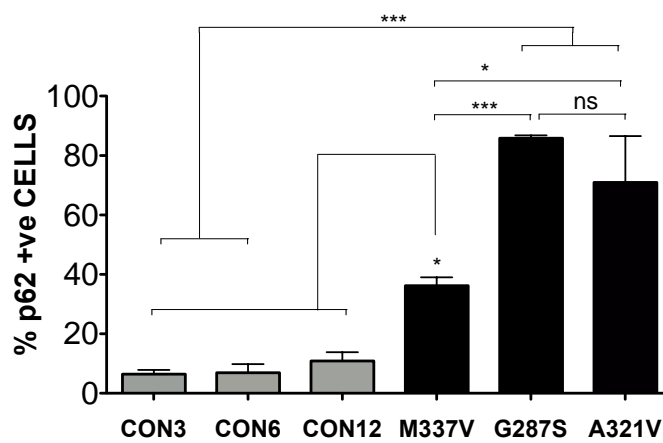
4.4 Endogenous wild type TDP-43 in control fibroblasts does not localise to stress granules upon treatment with H₂O₂, Arsenite and Sorbitol.

In chapter 3, we did not observe endogenous or over-expressed TDP-43 recruitment to stress granules in HEK293T upon treatment with various cellular stressors except with sorbitol (0.4M). In contrast several neuronal and non neuronal cell models have demonstrated endogenous and over-expressed TDP-43 recruitment to stress granules (Colombrita et al., 2009, McDonald et al., 2011, Meyerowitz et al., 2011). Previous studies relating to mutant TDP-43 have been conducted in over- expression cell models. We have highlighted in the previous chapter the limitation of mutant and wild type TDP-43 over-expression models (Chapter 3). Recruitment of endogenous mutant TDP-43 to stress granules has not been reported before in patient derived fibroblasts to the best of our knowledge at the time of our study. We used 0.5mM arsenite, 0.4M sorbitol, and 0.6mM H₂O₂ to induce stress granules as indicated in the materials and methods section (Chapter 2, section 2.2.6). Representative figures from at least three experiments from three controls are depicted in figure 4.7. Both 0.5mM arsenite and 0.4M sorbitol treatments induced stress granules in the control fibroblasts as observed in HEK293T cells (Chapter 3, section 3.7.4, Fig 3.13 and Fig 3.15) when we used TIAR as a marker for SG (Fig 4.7 E-H and I-L). However we did not observe a robust endogenous TDP-43 recruitment to SG either with arsenite or sorbitol treatment. In HEK293T cells we did observe a significant number of cells recruiting endogenous TDP-43 to SGs upon sorbitol treatment (Chapter 3.7.4, Fig 3.15). We assumed that the differences we observed between HEK293T cells and fibroblasts were secondary to differences in the properties of the cellular models studied. When we assessed the number of fibroblasts which generated a stress response by counting the fibroblasts with three or more stress granules, we noted that in the control fibroblasts about 20-30% of the cells staged a stress response within 30 minutes of treatment with arsenite in comparison to ~80% of the HEK293T cells at 30 minutes post arsenite treatment (p=0.0014) (Fig 4.8). HEK293T cells and control fibroblasts did not show any SG formation at basal conditions (unstressed). Therefore not depicted in the graph (Fig 4.8). These data suggest that control fibroblasts are more tolerant of
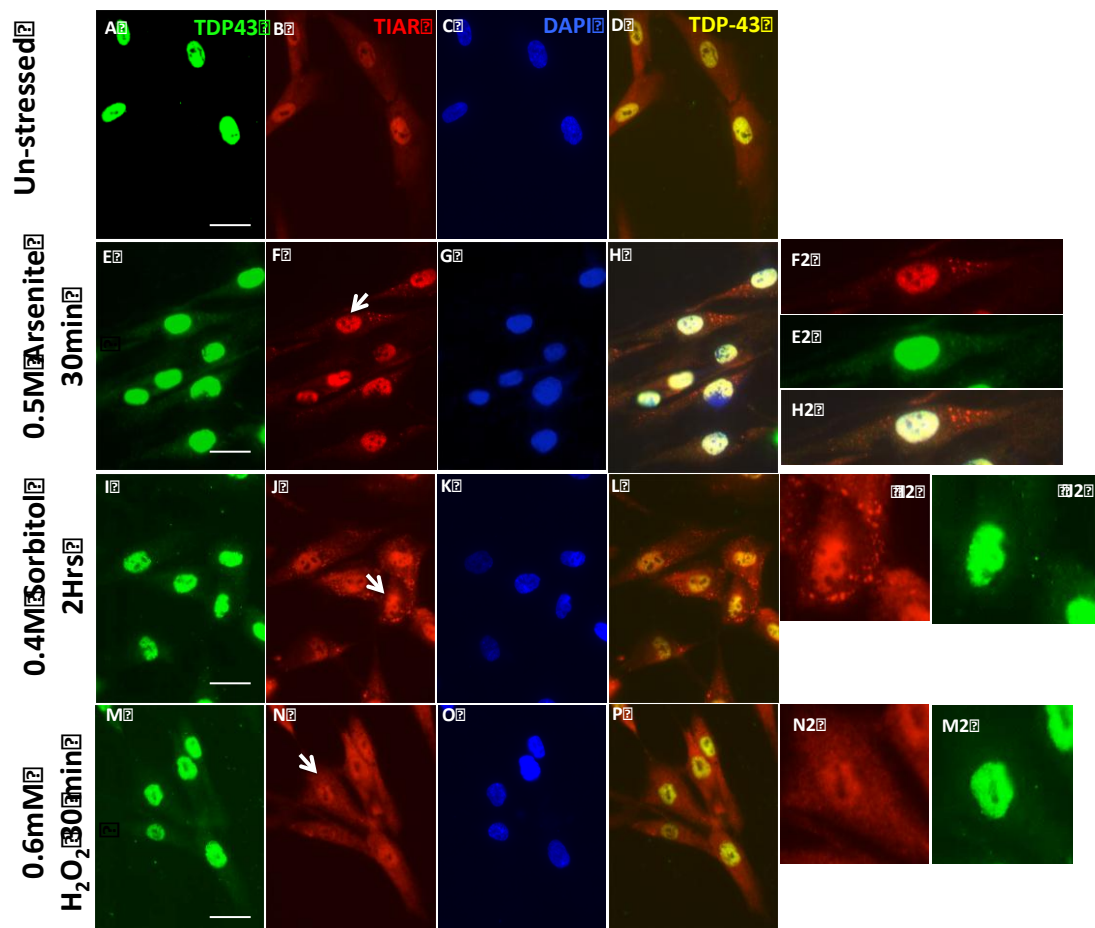
Figure 4.7 Endogenous TDP-43 does not localise to SG in control fibroblasts though these cells form SG in response to Arsenite and Sorbitol treatment. A-D) Unstressed control fibroblasts show nuclear TDP-43 and predominantly nuclear TIAR staining. **E-H)** Treatment with 0.5mM Arsenite for 30min- produced stress granules positive for TIAR staining, with no endogenous TDP-43 recruitment to the SG. Cell pointed with an arrow in panel F has been digitally enlarged to demonstrate stress granules **(E2, F2, H2) I-L)** Treatment with 0.4M Sorbitol- also produced TIAR positive SGs with no endogenous TDP-43 recruitment. Cell pointed with an arrow in panel J has been digitally enlarged to demonstrate stress granules **(I2, J2). M-P)** H_2O_2 treatment produced no SG (Cell in panel N is digitally enlarged in **N2-M2).** 10µm scale bar. Rabbit polyclonal antibody against human TDP-43, 1:500, mouse monoclonal antibody against TIAR, 1:1000, DAPI nuclear stain 1:1000. Scale bar 50µm.
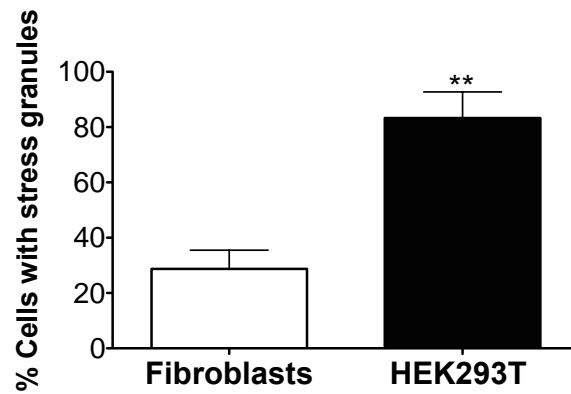
Figure 4.8 HEK293T cells form stress granules more robustly than control fibroblasts in response to 0.5mM arsenite treatment. At 30 minutes post treatment with arsenite, more than 80% of HEK293T cells produced 3 or more stress granules (n=8). In contrast only about 25% control fibroblasts (data from two controls pooled together) (n=7) showed 3 or more SGs within 30 minutes of arsenite treatment. Unstressed HEK293T and fibroblasts had no SGs at unstressed state (Not plotted in the graph). Unpaired *t* test, with Mann-Whitney test, two tailed p value = 0.0014.

arsenite induced stress or tend to stage a delayed response compared to other (HEK293T) cell models. McDonald et al noted almost 100% of HeLa cells generating a SG response when treated with arsenite for 30 minutes. However the same group studying patient derived lymphoblastoid cells showed that less than 20% of the cells formed stress granules in response to arsenite treatment for 30 minutes (McDonald et al., 2011).

4.5   M337V, A321V and G287S mutant TDP-43 fibroblasts form SG and direct mutTDP-43 to SG upon treatment with Sorbitol, but not arsenite or H₂O₂.

A previous study on lymphoblastoid cells derived from patients carrying D169G and R361S *TARDBP* mutations showed a variable response between the two mutant cell lines, in that the proportion of D169G mutant lymphoblastoid cells that formed stress granules was similar to that of control cells, whereas a smaller proportion of R361S mutant lymphoblastoid cells formed SGs (McDonald et al., 2011) suggesting that stress granule dynamics can be affected by the specific *TARDBP* mutation and SG dynamics therefore could be used to study the mechanisms or differences amongst different *TARDBP* mutations. Therefore we

studied stress granule formation response to arsenite, sorbitol and H_2O_2 in M337V, A321V and G287S mutant fibroblasts.

We did not see any stress granule formation or endogenous TDP-43 localisation to distinct cytoplasmic lesions in any of the TDP-43 mutant fibroblasts, when treated with H_2O_2. These results are in keeping with observations from the HEK293T cells where we did not observe distinct cytoplasmic lesion formation with endogenous TDP-43 or the stress granule marker TIAR when treated with H_2O_2 (Chapter 3, section 3.7.3). However we noted that there was increase of cytoplasmic TDP-43 in the cells treated with H_2O_2. This could happen if H_2O_2 interferes with nuclear export or import signaling of nuclear bound proteins and requires further study to clarify the significance of this observation.

In response to arsenite all the three mutants did form stress granules (SG) and these SGs were distinct (**M337V**, Fig 4.9, E-H; **A321V**, Fig 4.10, E-H and **G287S** Fig 4.11, E-H). We did not observe a noticeable recruitment of TDP-43 to the TIAR positive SGs. We did not quantify the number of cells with TDP-43 and TIAR co-localised SGs as they were so rare. This finding is in contrast to the findings of several studies which have shown the co-localisation of stress granule markers and endogenous TDP-43 in response to treatment with arsenite in different cell lines such as Lymphoblastoid cells (McDonald et al., 2011), BEM17 cells (Liu-Yesucevitz et al., 2010) and in response to paraquat in SY5Y cells (Meyerowitz et al., 2011). However when the TDP-43 mutant fibroblasts were subjected to 0.4M sorbitol treatment endogenous TDP-43 was observed to co-localise with TIAR positive SGs (Fig 4.9, 4.10 and 4.11 panels I-L). Interestingly we noted that the SG response is not as robust with sorbitol treatment, as it is with 0.5mM arsenite treatment in that fewer SGs were formed when treated with sorbitol. We also observed that M337V mutant fibroblasts (Fig 4.9 I-L) formed comparatively more SGs than the A321V (Fig 4.10 I-L) and G287S fibroblasts (Fig 4.11 I-L). This observation suggests that different TDP-43 mutations potentially have a varied effect on the cellular stress handling functions.
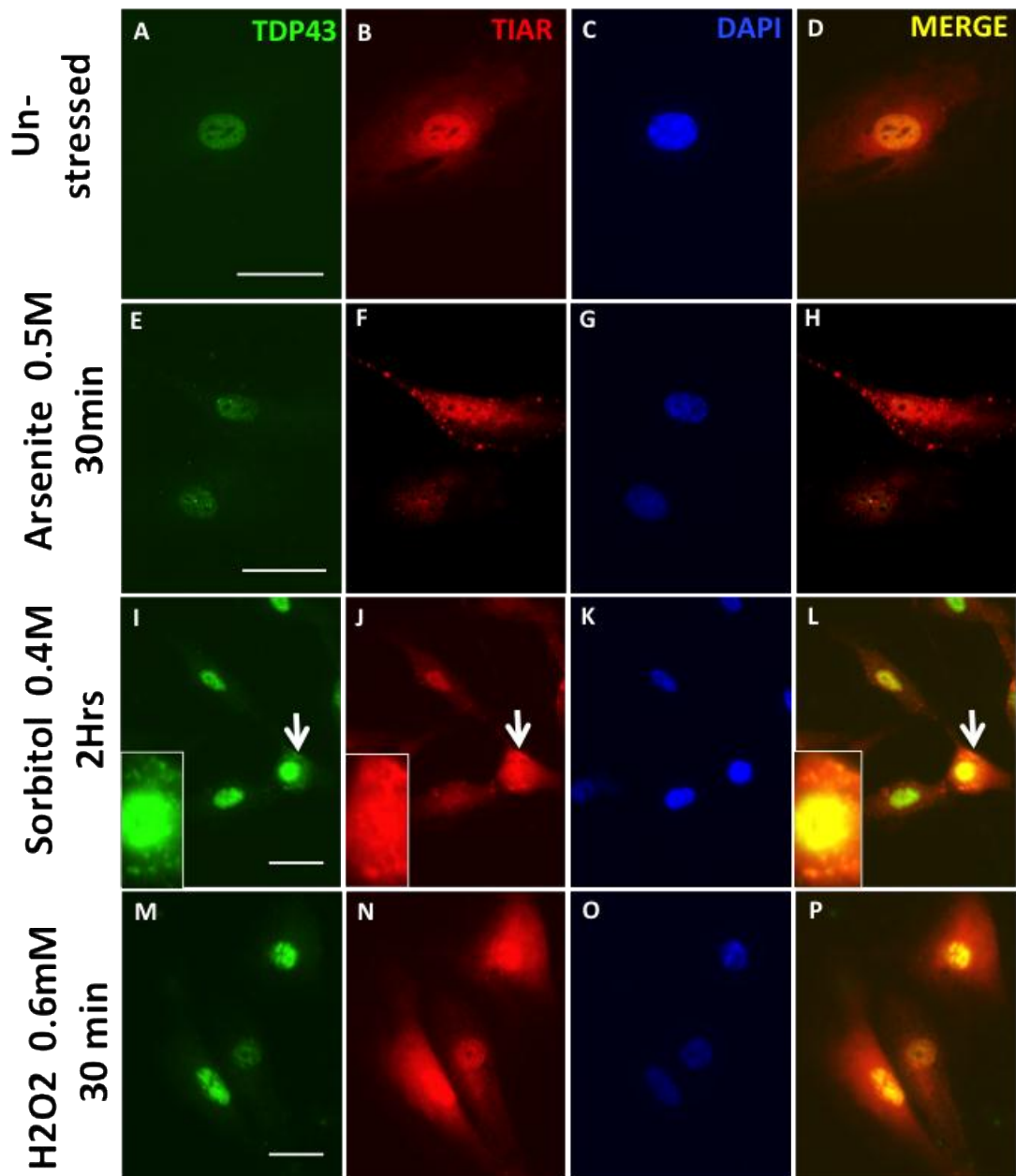
Figure 4.9 M337V mutant fibroblasts show endogenous TDP-43 localise to SGs in response to treatment with sorbitol but not with arsenite or H_2O_2 . A-D) Unstressed M337V mutant fibroblasts show reduced nuclear TDP-43 and predominantly nuclear TIAR staining. **E-H)** Treatment with Arsenite- produced stress granules positive for TIAR staining, with no endogenous TDP-43 recruitment to the SG. **I-L)** Treatment with 0.4M Sorbitol also produced TIAR positive SGs some of which co-localised with endogenous TDP-43, arrow points to the cell digitally enlarged to demonstrate co-localisation of TDP-43 and TIAR. **M-P)** H_2O_2 treatment produced no SG but there was cytoplasmic mis-localisation of TDP-43. 10µm scale bar. Rabbit polyclonal antibody against human TDP-43, 1:500, mouse monoclonal antibody against TIAR, 1:1000, DAPI nuclear stain 1:1000. Scale bar 50µm.
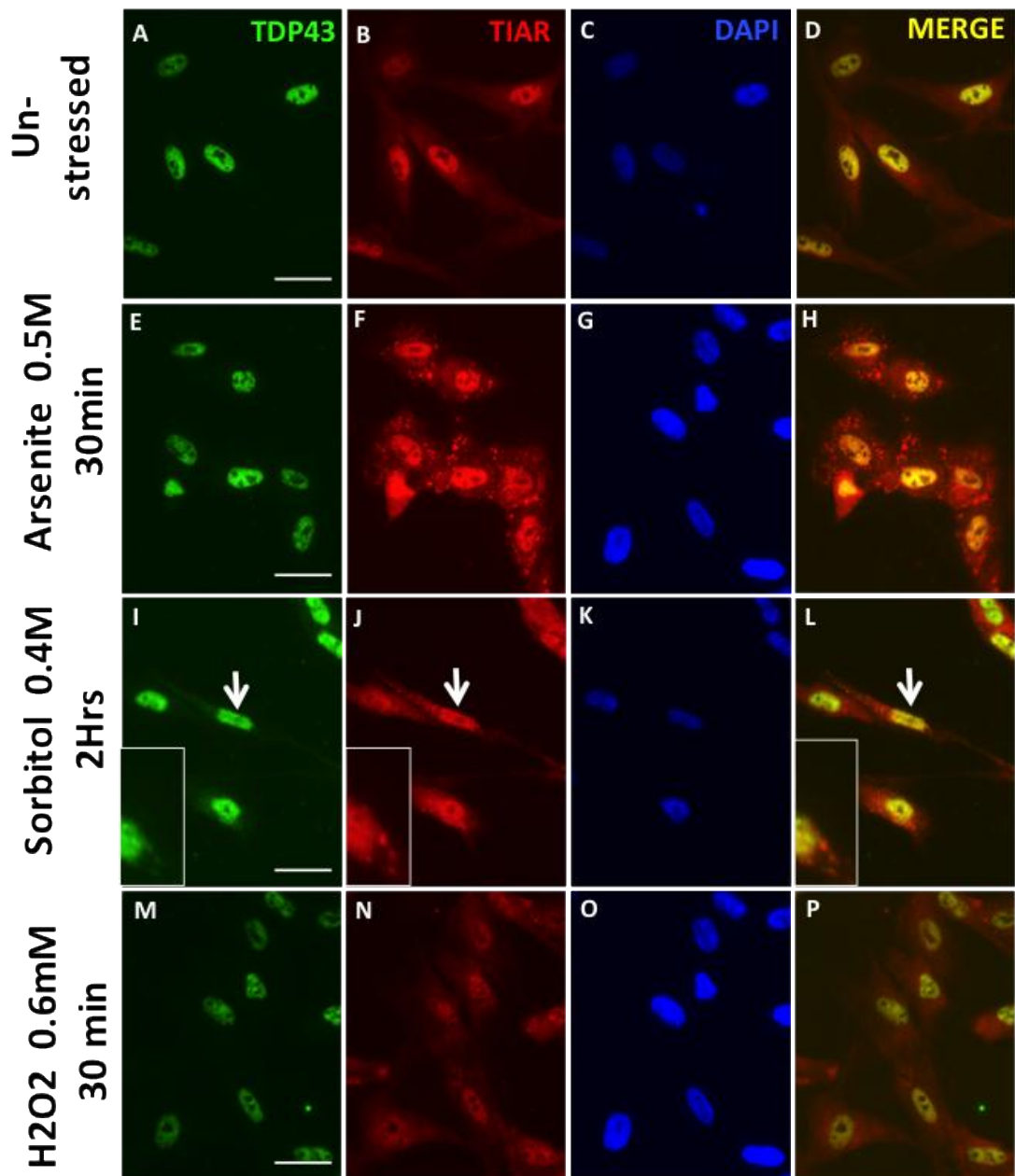
Figure 4.10 A321V mutant fibroblasts recruit endogenous TDP-43 to SG in response to treatment with sorbitol but not with arsenite or H₂O₂.
A-D) Unstressed A321V mutant fibroblasts show reduced nuclear TDP-43 and predominantly nuclear TIAR staining. **E-H)** Treatment with Arsenite- produced stress granules positive for TIAR staining, with no endogenous TDP-43 recruitment to the SG. **I-L)** Treatment with 0.4M Sorbitol also produced TIAR positive SGs some of which col-localised with endogenous TDP-43, arrow points to a cell digitally enlarged to demonstrate co-localisation of TDP-43 and TIAR. Note the increased cytoplasmic TDP-43 staining **M-P)** H₂O₂ treatment produced no SG and no cytoplasmic mis-localisation of TDP-43 noted. 10µm scale bar. Rabbit polyclonal antibody against human TDP-43, 1:500, mouse monoclonal antibody against TIAR, 1:1000, DAPI nuclear stain 1:1000. Scale bar 50µm.

ENDOGENOUS TDP43 LOCALIZATION IN ... STRESS (G287S)
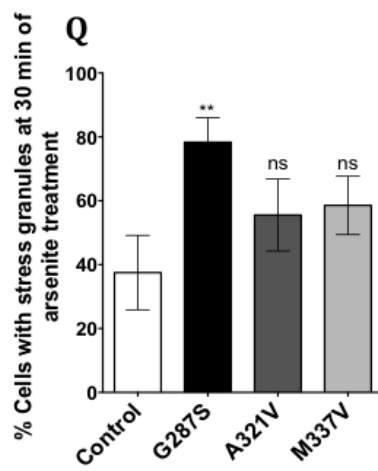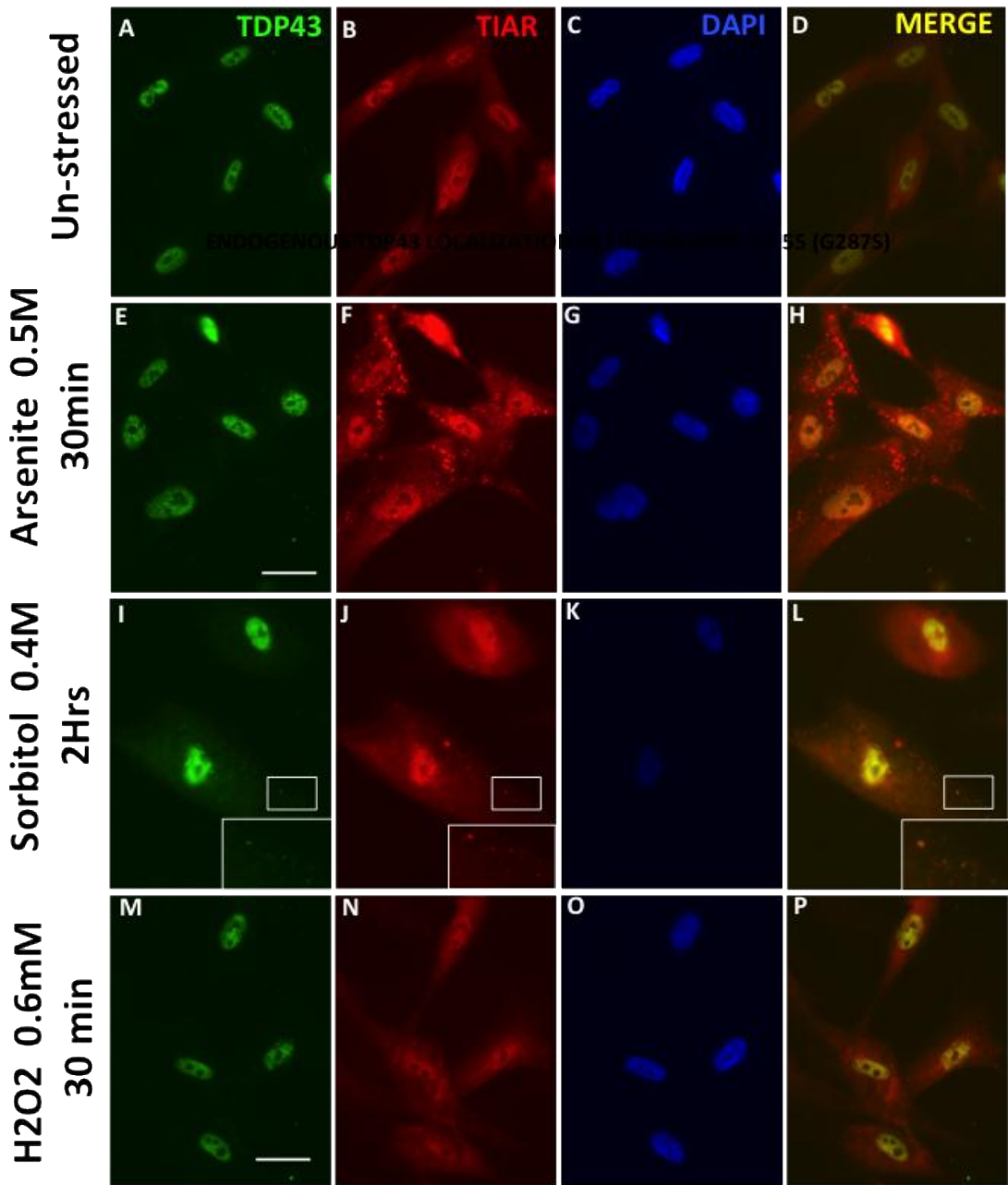
Figure 4.11 G287S mutant fibroblasts recruit endogenous TDP-43 to SGs in response to treatment with sorbitol. A-D) Unstressed G287S mutant fibroblasts. **E-H)** Treatment with arsenite-produced stress granules positive for TIAR staining, with no endogenous TDP-43 recruitment to the SG. **I-L)** Treatment with 0.4M sorbitol- also produced TIAR positive SGs some of which col-localised with endogenous TDP-43 (Boxed area). Note the increased cytoplasmic TDP-43 staining **M-P)** H_2O_2 treatment produced no SGs. **Q)** A significantly higher proportion of G287S fibroblasts assembled SGs at 30min following arsenite treatment compared to the control and other TDP-43 mutants. Rabbit polyclonal antibody against human TDP-43, 1:500, mouse monoclonal antibody against TIAR, 1:1000, DAPI nuclear stain 1:1000. Scale bar 50µm.

4.6 Thapsigargin treatment recruits TDP-43 to TIAR positive stress granules

Thapsigargin treatment has been shown to produced stress granules, which are positive for TIAR and HUR SG markers. Furthermore these SGs also co-localise with human hnRNP Q (Quaresma et al., 2009). Thapsigargin induces cellular stress via pathways involving the endoplasmic reticulum (ER) and Thapsigargin enhances caspase dependent TDP-43 cleavage in NSC34 cells (Suzuki et al., 2011). As TDP-43 is a member of the hnRNP family and thapsigargin is known to induce stress granules and modifies TDP-43, we hypothesised that TDP-43 would be recruited to SGs induced by Thapsigargin. We tested this hypothesis by treating control fibroblasts with Thapsigargin (100µM) for 90 minutes. We indeed noted TIAR positive SG formation in the human fibroblasts and these stress granules also recruited TDP-43 (Fig 4.12). Upon closer investigation we noted that TIAR positive SGs only recruited TDP-43 to part of the SGs (Fig 4.12E-H) suggesting that TDP-43 might associate with some of the TIAR positive components in the SGs. It is possible however, that if the cells were stressed for longer than 90 minutes, TDP-43 would have sufficient time to be completely recruited to TIAR positive SGs. Both of these possibilities need to be studied in future studies as the purpose of this experiment was to see if Thapsigargin stress induced SGs, which recruited endogenous TDP-43. This observation that TDP-43 localises to SGs induced by thapsigargin in control fibroblasts, extends the list of stressors that could stimulate formation of SGs, which also recruits TDP-43. A future study needs to be designed and completed on all three mutant TDP-43 cell lines to ascertain if a difference would be observed in rate and number of SGs formed in response to thapsigargin treatment.
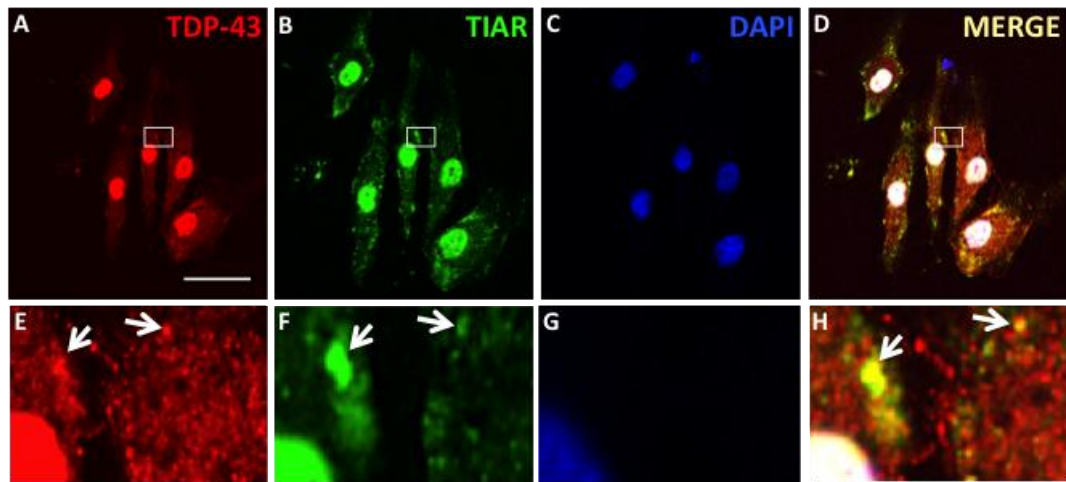
Figure 4.12. Control fibroblasts treated with thapsigargin recruit endogenous TDP-43 to stress granules A) TDP-43 localisation to cytoplasmic granules and larger inclusions **B)** TIAR SG marker representing SG C) DAPI nuclear marker **D)** Merging of channels confirm co-localisation of TDP-43 with TIAR positive SG **E-H)** Boxed area digitally enlarged demonstrates that TDP-43 localises to part of the SG but not to the whole SG (E-H). Arrows indicate the SGs focused upon. Note the increased cytoplasmic TDP-43 staining. 10μm scale bar. Rabbit polyclonal antibody against human TDP-43, 1:500, mouse monoclonal antibody against TIAR, 1:1000, DAPI nuclear stain 1:1000. Scale bar 100μm.

4.7 The proportional increase in the number of cells with stress granules in response to arsenite is different between mutant TDP-43 and the control fibroblasts

We did not observe a noticeable TDP-43 co-localisation to stress granules in fibroblasts, when treated with arsenite, in contrast to observations made in previous published reports. However, we noted a difference between the mutant TDP-43 and control fibroblasts, in the proportion of cells, which formed TIAR positive stress granules following 30 minutes of arsenite treatment. Therefore we hypothesised that the proportional increase in the number of cells with stress granules following arsentie treatment would be different between mutant and control fibroblasts. Furthermore we used HUR as a marker of stress granules instead of TIAR as a previous report indicated that TDP-43 can modify the mRNA levels of TIAR (McDonald et al., 2011). The control fibroblasts mounted a maximum stress response at 45 minutes of arsenite stress and this time point was similar in the TDP-43 mutant fibroblasts as well. However, the proportion of cells with HUR positive SGs was significantly higher in the mutants compared to the controls in response to post arsenite stress: at 15, 30 and 45 minutes (Fig 4.13, Fig 4.15B-D)). The representative pictures of the A321V fibroblasts and control fibroblasts are depicted in Fig 4.13 for

illustration purposes. The response to arsenite stress amongst the age and gender matched control fibroblasts was similar, therefore we pooled the data together to compare with the mutant fibroblasts. The G287S mutant fibroblasts assembled SGs in a robust fashion and showed a significantly heightened stress, as judged by the increase in the cells with response at all time points of stress induction (at 15min $p<0.05$, 30min and 45min $p<0.01$)(Fig 4.15B). A321V mutant fibroblasts also mounted a stress response curve in similar shape to the G287S fibroblasts and the proportion of fibroblasts with SGs was significantly more at 15 and 45 minutes of stress compared to the controls ($p<0.05$) (Fig 4.15C). M337V mutants followed a similar SG assembly profile to that of controls. We were only able to perform two experiments with M337V fibroblast line and therefore statistics have not been performed (Fig 4.15D). Although G287S and A321V mutants formed a robust SG assembling response, it was interesting to note that the two mutants (G287S and A321V) differed with each other in the severity of the SG response in that G287S' SG response was elevated at 30 minutes (~80% vs 58%) and 45 minutes (82% vs 74%) highlighting differences between TDP-43 mutations in the SG assembly response (Fig 4.15 B-C).
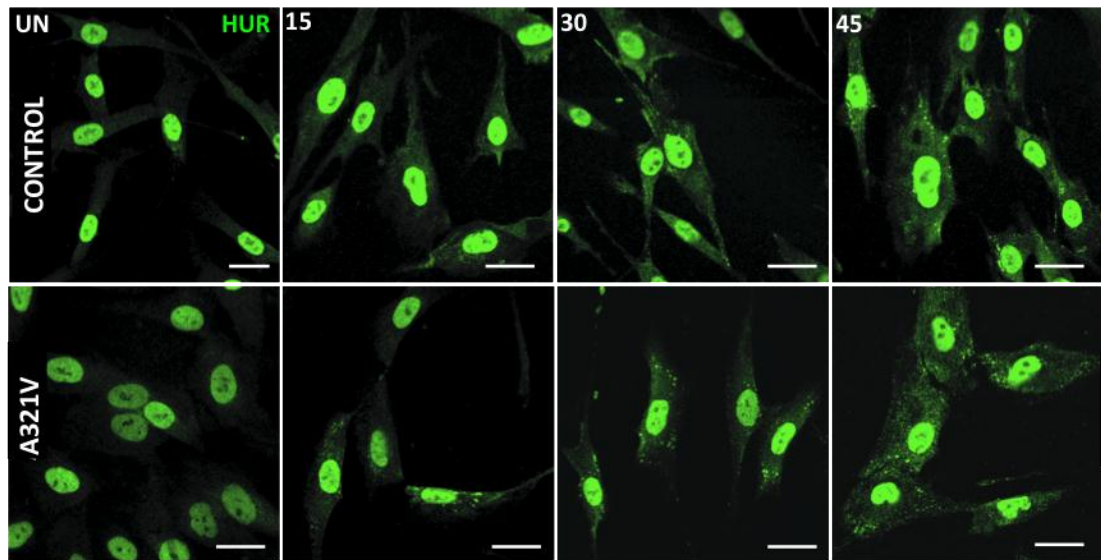
Figure 4.13. mTDP-43 fibroblasts (A321V) produce SGs earlier in response to arsenite than control fibroblasts carrying endogenous wtTDP-43. UN- Un stressed cells. 15, 30, 45 minutes of arsenite stress, demonstrating progressive increase in SGs in the A321V mutant cells compared to the controls. Control fibroblasts demonstrating the SG response to arsenite treatment. SGs can be readily identified at 30 min post treatment with arsenite. A321V mutant fibroblasts demonstrate more robust SG formation with 15 minutes of exposure to arsenite**).** Proportionately more mutant fibroblasts formed SGs**.** Mouse monoclonal antibody against HUR, 1:1000, Scale bar 50µm.
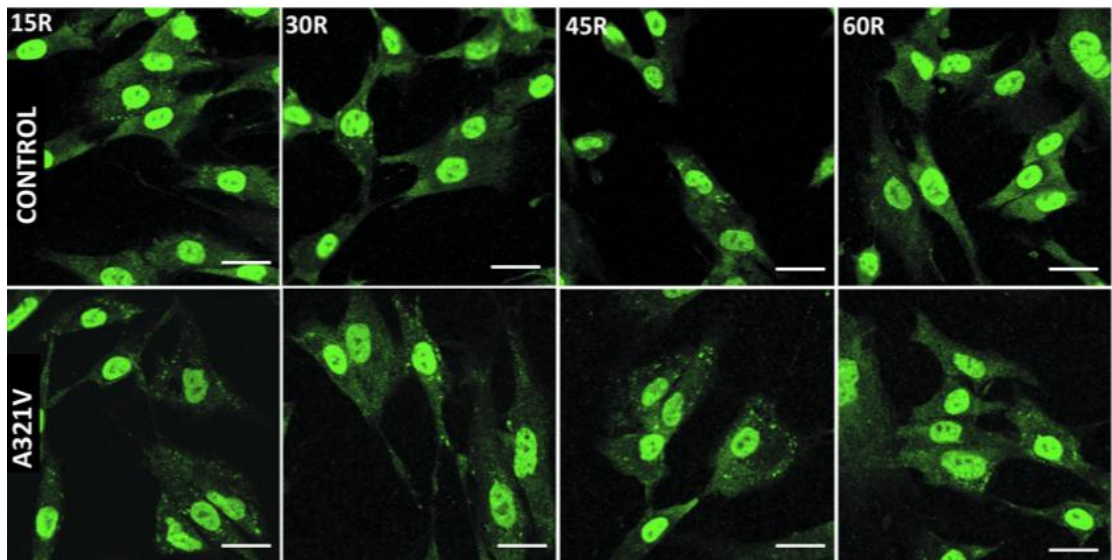
Figure 4.14. mTDP-43 fibroblasts (A321V) take longer to disassemble SGs following stress recovery compared to control fibroblasts 15R, 30R 45R, 60R are number of minutes post stress release. Control fibroblasts steadily disassemble SGs upon stress recovery and no SGs observed within 60 minutes of recovery from stress. A321V mutant fibroblasts prolonged delay in disassembling the SGs after exposure to arsenite stress for 45 minutes **(H).** Mouse monoclonal antibody against HUR, 1:1000, Scale bar 50µm.

182

4.8 Rate of stress granule disassembly is slower in mutant TDP-43 compared to the control fibroblasts

McDonald et al 2011 reported that following cessation of stress control and TDP-43 knockdown HeLa cells continued to assemble SGs until about 60 minutes post stress release and afterwards TDP-43 knockdown cells disassembled SGs faster than the controls (McDonald et al., 2011). There are abundant data on the severity of dysregulation of TDP-43 related functions upon complete knockdown of TDP-43 (Fiesel et al., 2011). Therefore we hypothesised that under physiological levels of mutant TDP-43, stress granule assembly and disassembly might be different to when TDP-43 is knocked down. Interestingly we noted that the control fibroblasts disassembled SGs almost immediately after arsenite stress was released (Fig 4.14, representative pictures demonstrating progressive disassembly of SGs upon stress release up to 60 minutes) and continued disassembly of SGs almost completely by 150 minutes following post-stress release (Fig 4.15A). In contrast G287S mutant fibroblasts demonstrated a significantly delayed SG disassembling response at all time points compared to the controls (Fig 4.15B, $p<0.001$). At 150 minutes post stress release G287S mutant fibroblasts were observed to retain SGs (5-8%, $p<0.05$). A321V mutant fibroblasts also showed a significant delay in recovery compared to the controls at 15-90 minutes post-stress release (Fig 4.15C, $p<0.05$). However the A321V fibroblasts followed a similar rate of SG disassembly compared to the controls and this pattern differed from that of G287S mutant fibroblasts. By 120 minutes post stress release A321V mutant fibroblasts showed no difference to the control (Fig 4.15C). Although statistics could not be analysed for M337V mutant fibroblasts as the number of repeats was only two, M337V fibroblasts also showed a delay in SG recovery and the pattern observed in SG disassembly was different to the other two mutants in that between 30 and 90 minutes post-stress release the SG disassembly plateaus.

Table 4.1 Time delay in mTDP-43 fibroblasts to recover from stress: Stress granule (SG) disassembly as a readout

	Proportion of cells with SGs at 45min stress (time point A)	Time taken for 50% of the cells at time point A to disassemble SG during recovery (minutes)	Time delay to recover in mutant cells compared to the controls (minutes)
Control1	60	15	-
Control 2	62	15	-
Control 3	58	20	-
G287S	80	60	43
M337V	70	90	73
A321V	76	45	28

We also analysed the time taken by the fibroblasts to disassemble SGs to or below 50% of the proportion of the fibroblasts which developed SGs at 45 minutes of stress (time point A). We noted that compared to the controls TDP-43 mutants recorded delays from 28 minutes in A321V mutants to 73 minutes in the M337V mutant fibroblasts (Table 4.1). This data also supports that TDP-43 mutations delay the fibroblasts from stress recovery. Further studies are necessary to understand this phenomenon. The differences amongst the 3 TDP-43 mutants in the SG disassembly in fibroblasts upon stress release can be appreciated in Figure 4.15E.

A Control fibroblasts

% Cells with stress granules

- Average
- Control 1
- Control 2
- Control 3

Stress and stress recovery process (R)

B G287S mutant fibroblasts

% Cells with stress granules

- Control
- G287S

Stress and stress recovery process (R)

C A321V mutant

% Cells with stress granules

- Control
- A321V

Stress and stress recovery process (R)

D M337V mutant

% Cells with stress granules

- Control
- M337V

Stress and stress recovery process (R)

185

E

Mutant TDP-43 vs Control fibroblasts

Figure 4.15. TDP-43 mutant fibroblasts demonstrate hypersensitivity to arsenite treatment and delay in SG disassembly compared to the control fibroblasts. A) At 30 minutes post stress, only about 35-40% of the control fibroblasts showed SG formation. A maximum SG assembly was seen at 45 minutes of treatment with Arsenite (just under 60% of control fibroblasts). 60 minutes post stress removal more than 90% of the control fibroblasts have disassembled SGs. Hardly any control fibroblasts showed SGs at 120 min post stress removal. **B)** G287S mutant fibroblasts demonstrated a significantly robust response to arsenite stress at all time points compared to controls in SGs assembly. SG disassembly was significantly delayed in G287S cells even at 120 minutes post stress release. **C)** A321V fibroblasts also demonstrate a similar SG assembly and disassembly response, although the overall response is not as robust as G287S mutant fibroblasts. **D)** M337V fibroblasts followed a similar pattern to control fibroblasts in SG assembly but the disassembly process was delayed, n=2 therefore could not statistically analyse. **E)** Amongst the mutant fibroblasts there appears to be an inter-mutant variation in recovering from the stress. The A321V mutant recovered the earliest compared to the other two mutants. * $p<0.05$, ** $p<0.001$, *** $p<0.0001$. paired *t* test was performed for each time point comparing controls vs relevant mutant. At least one hundred cells counted per cover slip per experimental repeat (average and SD of at least three experiments were plotted except ofr M337V cells (n=2)).

186

4.9 Entities formed in response to sodium arsenite are stress granules and SG formation can be inhibited by co-treatment with cycloheximide

To confirm that the HUR positive punctate lesions formed in response to arsenite treatment are stress granules, the fibroblasts were treated with cycloheximide. Cycloheximide treatment arrests translation and thereby makes the translational machinery and its components, which are essential for the formation of SGs, unavailable for the formation of SGs in response to arsenite or other stress granule inducers (Quaresma et al., 2009). As described above, when exposed to arsenite and thapsigargin, HUR positive stress granules formed in both control and G287S TDP-43 mutant fibroblasts (Fig 4.16 Controls: A-C and Mutants: F-H). Consistent with published data, pre-treatment of fibroblasts with 10µg/µl of cycloheximide resulted in complete abrogation of HUR positive SG formation when exposed to arsenite, in both controls and the mutants (Fig 4.16 E and J). These data confirm that the HUR positive punctate lesions are indeed SGs.
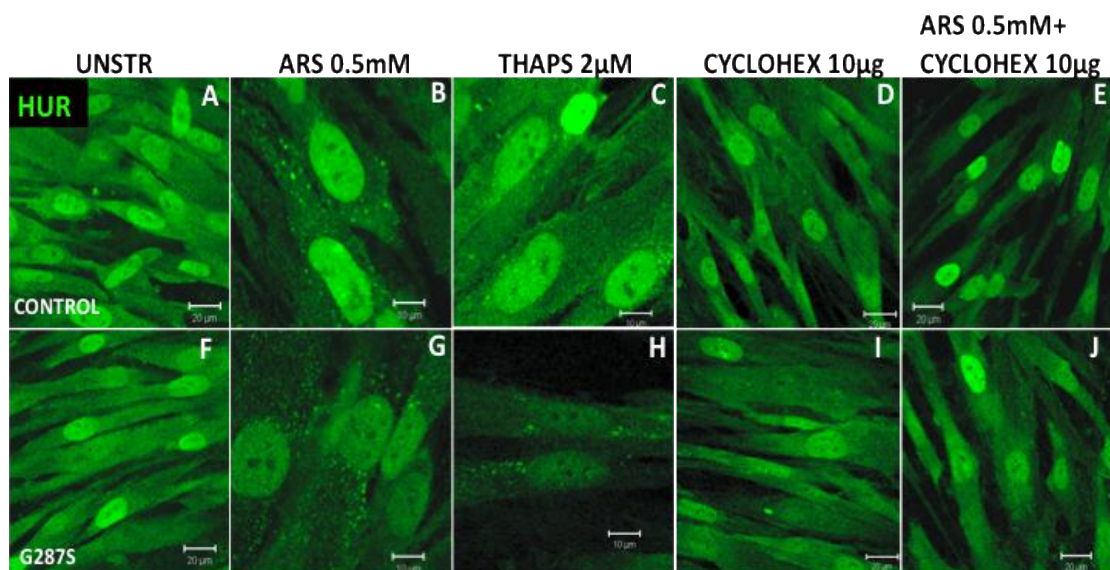
Figure 4.16. Arsenite and thapsigargin induced HUR positive punctate lesion are stress granules (SGs) as they are abolished by pre-treatment with cycloheximide, confirming these cytoplasmic entities are indeed SGs. A-E) Control fibroblasts. **(A)** Unstressed control fibroblasts. SG formation in response to Arsenite **(B)** and Thapsigargin **(C)** treatment. **(D)** Treatment with Cycloheximide 10µg/µl did not produce abnormality in HUR staining. E) Pre-treatment of fibroblasts with cycloheximide abrogates the formation of HUR positive cytoplasmic punctate lesions confirming that these punctate lesions are stress granules. **F-J)** Similar results were observed with mutant (G287S) mutant fibroblasts. Mouse monoclonal antibody against HUR, 1:1000, Scale bar 10 or 20µm as indicated on the figure.

4.10 The difference in stress granule response between the control group and the mutant TDP-43 fibroblasts is independent of survival of cells following treatment with arsenite

We studied the amount of cell death following arsenite treatment and we used the MTT assay to assess the cell death as used by various other groups to assess the cell death in fibroblasts following treatment with cytotoxic material (Arechabala et al., 1999). We studied all 3 controls and an additional control fibroblast line as well as the three TDP-43 mutant fibroblast cell lines (A321V, M337V, G287S). We did not see a statistically different increase in mortality in any of the groups. There was about 20-25% increase in the cell death across all the group following arsenite treatment, suggesting that differences observed amongst control and TDP-43 mutant fibroblast lines in handling aresenite induced stress could not be due to differences in their survival post exposure to arsenite (Fig 4.17).
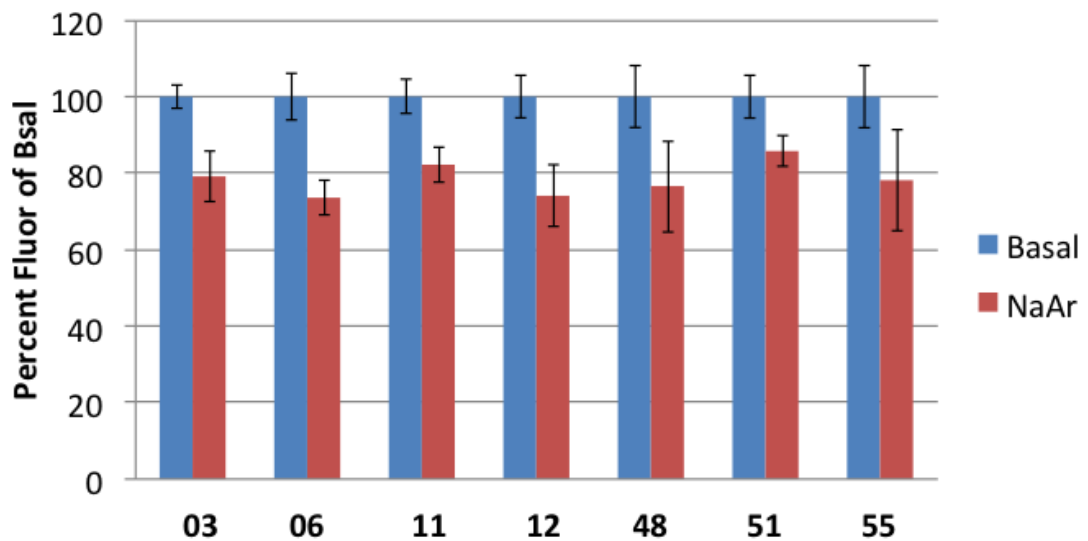
Figure 4.17. No difference in cell survival between mutants and controls noted in response to arsenite treatment. Assessed by MTT assay. Basal level survival is indicated in blue whilst arsenite treated cell survival is indicated in red. We studied 4 different controls (3, 6, 11 and 12) and compared with the three TDP-43 mutant fibroblast lines: A321V (pt48), M337V (pt51) and G287S (pt55)**.** There was 20-25% increase in cell death following treatment with arsenite across all groups, mutant or control. Y axis- percentage fluorescence when corrected for basal level fluorescence.

4.11   No obvious difference in endogenous TDP-43 localisation in fibroblasts from sporadic ALS cases (sALS) and healthy controls.

We compared the categories of endogenous TDP-43 staining in fibroblasts from three control and three sporadic ALS cases (sALS). We did not see a statistically significant difference in the pattern of nuclear staining of endogenous TDP-43 staining in the sporadic ALS cases when compared to the age matched controls (>85% of the cells were saturated with TDP-43 in the nuclei in both control and sALS case) (Fig 4.18 A-C). However the sALS cases showed prominent cytoplasmic staining for endogenous TDP-43 compared to the control fibroblasts (Fig 4.18 D and G). A biochemical analysis of cytoplasmic and nuclear fractions could confirm or refute the prominence of the cytoplasmic staining of endogenous TDP-43 in the sALS cases compared to the controls.
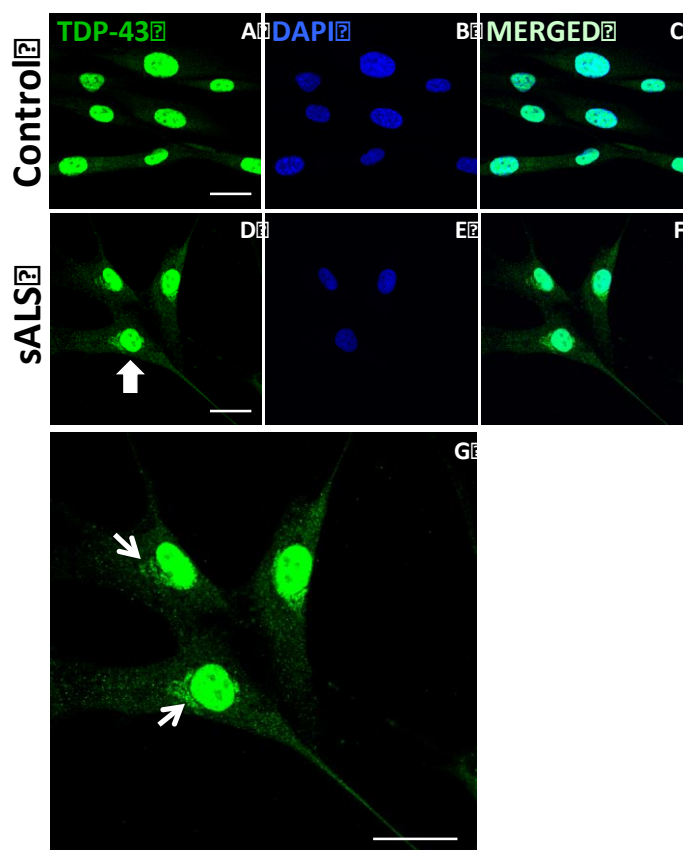
Figure 4.18 Endogenous nuclear TDP-43 was similar between control and sporadic ALS (sALS) fibroblasts but peri-nuclear staining pattern was different in sALS case. Unstressed fibroblasts from age and gender matched control **(A-C)** and sALS case **(D-F)** showed similar nuclear TDP-43 staining pattern. **G)** However cytoplasmic staining for endogenous TDP-43 was prominent in the sALS case (arrow). (Solid arrow indicated the cell that has been digitally enlarged). Scale bar 40µm. Green fluorescence is endogenous TDP-43. Scale bar 50µm.

4.12 More GEM bodies are found in G287S TDP-43 mutant but not in M337V mutant fibroblasts

TDP-43 is a nuclear protein, which participates in a variety of RNA metabolism related functions (Ito, 2012). GEM bodies are RNA related foci in the nucleus, which is abbreviated for Gemini of Cajal bodies. Cajal bodies are not only seen in rapidly proliferating cells or metabolically active cells such as motor neurons, and are functionally involved in recycling and biogenesis of splicing factors (Charroux et al., 2000). A recent study reported that TDP-43 overexpression resulted in increased distribution of SMN associated GEM bodies in the motor neuron nuclei of the mice over-expressing TDP-43. Furthermore knockdown of TDP-43 resulted in lower number of SMN associated GEM bodies in motor neurons (Shan et al., 2010). Significant alteration in TDP-43 levels can affect many RNA and protein targets of TDP-43. We studied the number of SMN positive GEM bodies in fibroblasts with physiological levels of mutant TDP-43. We studied M337V and G287S TDP-43 for the frequency of GEM bodies. G287S mutant fibroblasts showed a higher number of SMN positive GEM bodies compared to the control and M337V mutant fibroblasts (Fig 4.19, J-L and M, p<0.001) highlighting again the differences between different TDP-43 mutations. However M337V mutant cells had significantly higher number of GEM bodies compares to the cells from control 3 (p<0.01)(Fig 4.19, M). Although a previous study demonstrated that increase levels of TDP-43 expression is associated with an increased number of GEMs (Shan et al., 2010), our data indicate that even at physiological levels of TDP-43, mutant TDP-43 (G287S) is associated with elevation of SMN positive GEMs in the nuclei.

Figure 4.19 G287S mutant fibroblasts have higher number of SMN positive GEM bodies. A-F) Control fibroblasts. Digitally enlarged fibroblast demonstrates GEM bodies in a control fibroblast (Empty arrow). The number of GEMs in a control fibroblast varied between 1-2. **G-I)** M337V mutant fibroblasts also have 1-2 GEMs in the nuclei. **J-L)** G287S mutant fibroblasts showed multiple GEMs. Digitally enlarged nucleus demonstrates the multiple GEMs in a mutant fibroblast (arrow). **M)** G287S mutant fibroblasts harbour significantly more GEMs compared to M337V and control fibroblasts (p<0.001) (One way ANOVA Bonferroni multiple column comparison test). Four random optical fields at X63 magnification were selected for counting, in three experimental repeats amounting to approximately 100-120 cells. Scale bar 50μm. Green fluorescence is endogenous SMN.
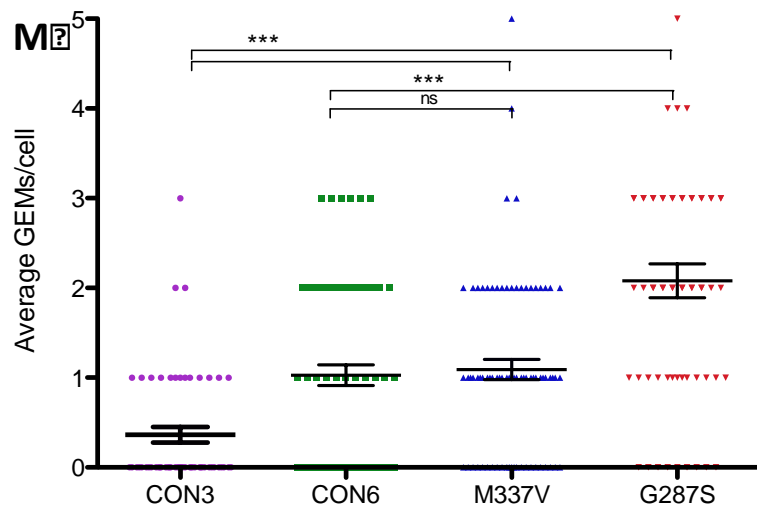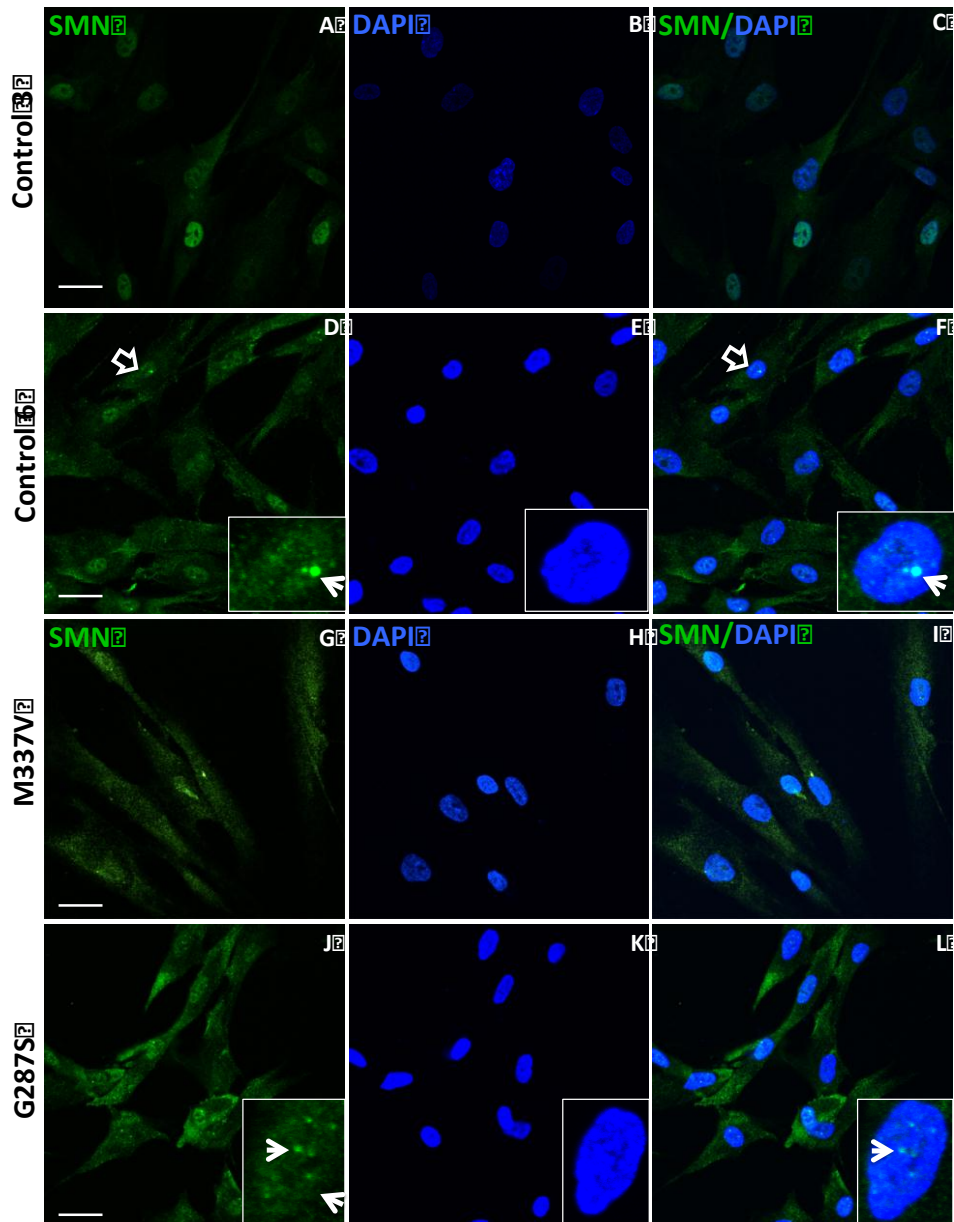
4.13 Discussion

Mis-localisation of TDP-43

It still remains an enigma as to how autosomal dominant mutations in TDP-43 contribute to neuronal dysfunction and ultimately results in neuronal cell death. Mis-localisation of TDP-43 to the cytoplasm from the nucleus is considered an important feature consistent with TDP-43 proteinopathy. Based on the microscopy, our study shows that fibroblasts from the mutant TDP-43 cases show varying degrees of cytoplasmic mis-localisation and associated nuclear loss of TDP-43 compared to the control cell lines. It is conceivable that this observation is secondary to the dominant mutation in the *TARDBP* gene, which expresses physiological levels of mutant TDP-43, in contrast to artificial over-expression of a protein above physiological levels. Studies assessing the half-life of wtTDP-43 and three different disease associated mutant TDP-43 (Q331K, M337V, G289S) have shown that mutant TDP-43 has a longer half-life (24-48 hours vs 12 hours for wtTDP-43) (Ling et al., 2010). These findings have also been confirmed in a primary fibroblast cell line harbouring a disease associated mutation, G289S, suggesting that mutant TDP-43 is more stable (Ling et al., 2010). It is conceivable that an aggregation prone protein like TDP-43, becomes more stable due to dominant mutations, and thereby enters a cascade of prion like aggregation (Udan and Baloh, 2011). Furthermore mutant TDP-43 has also been shown to interact with other proteins and RNA binding proteins, such as FUS/TLS via its C-terminal region. Therefore it is plausible that mutant TDP-43 via its abnormal stability and altered nature perturbs the normal functions of proteins which are important for nuclear exportation, which ultimately results in loss of nuclear TDP-43 and its cytoplasmic mis-localisation. Furthermore prolonged stability of mutant TDP-43 can expose itself to aberrant post-translational modifications such as phosphorylation (Liachko et al., 2010, Brady et al., 2011), ubiquitination (Dammer et al., 2012) and SUMOylation (Seyfried et al., 2010) reported in previous studies. It is possible that loss of TDP-43 from the nucleus could provoke impairment of essential RNA modulating processes of TDP-43. Over a period of time as the mutant TDP-43 stabilises in the cytoplasm and promotes aggregation, more TDP-43 would be lost from the nucleus until a critical point is reached when nuclear and cellular functions reliant on TDP-43 would be jeopardised whilst increasing the vulnerability of the affected cells to environmental factors. Thus, our findings

are consistent with the notion that loss of function of important nuclear role of TDP-43 as a mechanism for neuronal dysfunction in TDP-43 mutations. Cytoplasmic aggregation of mutant TDP-43 could be an epiphenomenon as a result of increased stability. It has been shown in transgenic mouse models that cytoplasmic aggregation is not essential to confer the neurotoxicity of disease-associated mutations (Wegorzewska et al., 2009, Janssens et al., 2013). However, the A315T disease associated mutation does not affect major nuclear functions of TDP-43 such as regulation of splicing i.e. alternative splicing dependent on TDP-43 such as Cystic fibrosis trans membrane conductance regulator (CFTR) exon 09 splicing suppression, which argues against a loss of nuclear function for some mutations in TDP-43 (Guo et al., 2011).

Phosphorylated TDP-43

Phosphorylation of TDP-43 at S409/410 is a highly consistent feature of TDP-43 proteinopathy in MND and FTLD cases (Hasegawa et al., 2008a, Inukai et al., 2008) and is considered pathological (Neumann et al., 2006). We observed a fine punctate pattern of distribution of phosphorylated TDP-43 in the nuclei of the control fibroblasts which is reminiscent of the distribution of nuclear paraspeckle proteins such as RBM14, NONO and PSF. The nuclear paraspeckle proteins are said to be involved in nuclear functions such as pre-mRNA splicing, alternative splicing, transcriptional regulation etc (Sun et al., 2013) (O'Leary et al., 2013, Shi et al., 2013). These proteins have previously been shown to co-localise in the nucleus with full length as well as the 35kDa fragment of TDP-43 (Dammer et al., 2012). The co-localisation of TDP-43 with paraspeckle proteins, particularly RBM14 and NonO, was not complete (Dammer et al., 2012) suggesting that nuclear speckle like localisation of phosphorylated TDP-43 could very well represent co-localisation with paraspeckle proteins. Further studies co-labeling the control fibroblasts with phosphorylated TDP-43 and markers of paraspeckle protein could clarify this hypothesis. The three controls studied showed very occasional cytoplasmic phospho-TDP-43 aggregation (Fig 4.3 and 4.4 J) compared to the TDP-43 mutants. Studies using antibodies against multiple phosphorylation prone epitopes of TDP-43 showed that phosphorylated TDP-43 is largely absent from the nuclei of neurons from control brains (Hasegawa et al., 2008a) We also observed that the speckled phospho-TDP-43 distribution was pronounced in the nuclei of mutant TDP-43 fibroblasts and furthermore the mutant fibroblasts showed greater

cytoplasmic phospho-TDP-43 staining in keeping with the previous studies done on ALS and FTLD postmortem cases (Neumann et al., 2009, Arai et al., 2010). It is possible that phosphorylation promotes oligomerisation and fibrillation of TDP-43 and perhaps indirectly or directly contributes to alteration of the function of TDP-43 and its interactions with RNA and protein binding partners of TDP-43 (Hasegawa et al., 2008a). Amongst the three mutants the M337V mutant contained the highest amount of cytoplasmic phospho-TDP-43 (Fig 4.4). Although postmortem studies have demonstrated that the phosphorylated TDP-43 lesion load is associated with pathogenesis, mouse models over-expressing M337V mutant TDP-43 have not supported this phenomenon and suggested that phosphorylated ubiquitinated inclusion formation is not a prerequisite for disease pathogenesis. Furthermore, wtTDP-43 over-expressing mice also had phospho-TDP-43, although the levels were significantly less than the mutant TDP-43 mice (Janssens et al., 2013). Our data suggest that at physiological levels of expression of mutant TDP-43 in patient derived fibroblasts, another major feature of TDP-43 proteinopathy- is observed *i.e.* phosphorylation. A C.elegans model demonstrated that phosphorylation of TDP-43 is important for directing mutant TDP-43 associated toxicity (Liachko et al., 2010). In contrast, a drosophila model of TDP-43 C-terminal fragment expression showed that phosphorylation has a protective effect against cytoplasmic aggregation (Li et al., 2011). Although the G287S TDP-43 mutation creates an additional phosphorylation prone epitope, phosphorylated TDP-43 lesion load was lowest in G287S fibroblasts (Fig 4.4 D-F, J) compared to M337V and A321V mutations suggesting that G287S mutant fibroblasts could have an enhanced 'aggregated protein removal' cleanup mechanism *e.g.* the ubiquitin-proteasome system or that this clean up mechanism is suboptimal in M337V and A321V mutants.

P62 staining

Pathological processes of MND and FTLD have been shown to occur in non motor neuronal tissues such as the hippocampus and the cerebellum (King et al., 2011). p62 is a ubiquitin binding protein and promotes degradation of polyubiquitinated proteins via the ubiquitin-proteasome system or autophagy (Moscat et al., 2007, Seibenhener et al., 2007). We observed a significant cytoplasmic phospho-TDP-43 in the mutant TDP-43 fibroblasts suggestive of possible cytoplasmic accumulation,

keeping in with the observations of cytoplasmic aggregations of TDP-43 in postmortem brain and spinal cords of ALS cases. Therefore we hypothesised that fibroblasts from TDP-43 mutant ALS cases might also demonstrate a pathological feature observed in neurodegeneration such as ubiquitinated protein aggregation. Although p62 expression and ubiquitin staining are not synonymous as deposition of p62 could occur earlier in the neurodegenerative process compared to ubiquitin (Kuusisto et al., 2003). Therefore we used a mouse p62 antibody to study p62 staining in the fibroblasts. We demonstrated that TDP-43 mutant fibroblasts carry a significantly higher p62 positive lesion load than the control fibroblasts and amongst different TDP-43 mutations the p62 lesion load changes significantly, suggesting that each mutation needs to be studied individually as the underlying mechanism/s could be affected by the properties of the individual mutations such as its propensity for post-translational modifications like phosphorylation; effect on the secondary structure organisation and functional modulations such as the ability of the mutant protein to interact or not with its RNA and protein binding partners. Functional multi-vesicular body (MVB) formation is essential for the efficient autophagic degradation of TDP-43 and its clearance (Filimonenko et al., 2007). We know that over-expression of TDP-43 and co- chaperone ubiquilin-1 enhances TDP-43 delivery to the autophagasome system ((Kim et al., 2009). TDP-43 is found in rimmed vacuoles of inclusion body myositis (IBM) in which condition a disruption in the autophagic pathway has been well described (Kusters et al., 2009). Therefore it is plausible that the autophagasome might be an intra-cellular compartment in which TDP-43 is degraded. Therefore disruption to the autophagy pathway could result in accumulation of phosphorylated TDP-43. It is possible that in the mutant TDP-43 fibroblasts a degree of autophagasomal pathway disruption is occurring as the proportion of cells with cytoplasmic phosphorylated TDP-43 is greater in the mutant TDP-43 cells compared to that of controls (Fig 4.4). In addition, G287S mutant fibroblasts had the highest amount of p62 staining, whilst M337V mutants had the least p62 staining amongst the three mutants (Fig 4.4J). This observation is interesting in that it appears as if the phospho-TDP-43 staining pattern is inversely correlated with the p62 lesion load. This suggests that activation of the ubiquitin proteasome system/autophagy pathway may help to clear phospho-TDP-43 prior to aggregation in G287S fibroblasts offering a possible protective role. M337V and A321V fibroblasts may

harbour a relatively inefficient autophagy pathway. In support of this hypothesis is the study, which shows inhibition of the p62 pathway, can result in increased accumulation of TDP-43/phosphorylated TDP-43 (Brady et al., 2011). A second insult such as an exogenous stress could overwhelm the UPS/autophagy system which then would lead to an accumulation of the C-terminally phosphorylated TDP-43 in the cytoplasm which in turn initiates aggregation of TDP-43 and subsequent transfer of nuclear TDP-43 to the cytoplasm (Winton et al., 2008a, Watanabe et al., 2013). Therefore we subjected control and mutant fibroblasts to exogenous stress to assess if a second insult (the first insult being the presence of mutant TDP-43) would result in mis-localisation of endogenous TDP-43.

Exogenous stress and endogenous TDP-43 localisation

Aggregation of neurocytoplasmic inclusions (NCI) of disease-characterised proteins is a hallmark of several neurodegenerative conditions. TDP-43 is recognised as a significant contributor to NCI in ALS cases. Post mortem examination of brains and spinal cords from ALS and FTLD patients have demonstrated that several stress granule associated proteins are recognised as components of the TDP-43 (Liu-Yesucevitz et al., 2010) or FUS positive NCI (Bentmann et al., 2012). These findings are not entirely surprising as in several other neurodegenerative conditions disease associated proteins such as tau, ataxin, SMN and angiogenin have been shown to co-localise with SGs or modulate SG dynamics (Wolozin, 2012). We observed endogenous TDP-43 localisation to cytoplasmic inclusions in HEK cells in response to sorbitol treatment and these inclusions also co-localised with the stress granule protein TIAR. However, we did not observe endogenous TDP-43 co-localisation with TIAR positive SGs following exposure to other exogenous stressors such as arsenite, H_2O_2 and menadione. We hypothesised that having physiological levels of mutant TDP-43 in the patient derived fibroblasts would allow us to study differences in the localisation pattern of endogenous mutant TDP-43 in comparison to wtTDP-43 in the control cells. However, we only observed cytoplasmic localisation of endogenous mutant TDP-43 in response to sorbitol but not with arsenite. wtTDP-43 co-localises with the SG nucleating protein TIAR in response to an endoplasmic reticulum stressor – thapsigargin. Taken together, these data suggest that fibroblasts and HEK cell lines do not produce cytoplasmic inclusions positive for endogenous TDP-43 when treated with acute stressors like arsenite although TIAR positive SGs are formed

readily. A possible explanation is that the SG marker HUR or TIAR localisation to the stress granules in response to exogenous stress is a global event in the cells, whilst TDP-43 co-localisation only occurs in a subset of SGs. Another explanation is that TDP-43 recruitment to SGs is a prolonged and slow process in fibroblasts and HEK cells. Several different cell models have shown endogenous and over-expressed TDP-43 recruitment to SGs in response to arsenite treatment, although these models have not recapitulated the key features of TDP-43 proteinopathy. Moreover we think that it is important to ensure whichever model is used to study SG dynamics that this model also accurately represents features of the TDP-43 proteinopathy related to ALS. We have clearly demonstrated that the mutant TDP-43 fibroblasts show broad features of TDP-43 proteinopathy including nuclear clearing, phosphorylation of TDP-43, and aggregation of p62.

It is important to highlight at this point that we did not simultaneously use a phosphorylation dependent TDP-43 antibody to assess for pathological TDP-43 as both the phosphorylation dependent TDP-43 antibody and antibodies to SG markers TIAR and HUR were raised in mouse. An assessment of phospho-TDP-43 lesions in stressed and non stressed control and mutant fibroblasts with or without SG marker staining would be a future experiment to perform. Interestingly we observed that a greater proportion of G287S mutant fibroblasts formed SGs at 30 minutes of treatment with arsenite compared to A321V, M337V mutants and controls (Fig 4.11 Q). Therefore we hypothesised that stress granule assembly and disassembly dynamics could be different amongst the TDP-43 mutant fibroblasts and between mutants and control fibroblasts.

Mutant TDP-43 alters stress granule dynamics

To assess the dynamics of stress granule assembly and disassembly, we used HUR as a marker that would indicate accurately the distribution of stress granules, as HUR expression is independent of HUR-TDP-43 interactions (McDonald et al., 2011). TDP-43 has been shown to modulate RNA levels of stress granule nucleating proteins such as TIA1 and TIAR but not HUR (McDonald et al., 2011). Several studies have reported the recruitment of endogenous TDP-43 to SGs upon arsenite stress, which we were not able to demonstrate in a robust fashion. The reasons for these observed differences could be inherent to the fibroblast cell model and also that most studies used TIA-1 as the stress granule marker whereas we used both TIAR and HUR as stress granule markers. Therefore we were unable

to use TDP-43 localisation to SGs to differentiate between mutant TDP-43 and wtTDP-43 effects on SG related TDP-43 function.

McDonald et al (2011) demonstrated that siRNA knock down of endogenous TDP-43 resulted in changes in the mRNA levels of stress granule related proteins G3BP (down-regulated), TIA-1 (up-regulated), TIAR (up-regulated –not significant) whilst HUR mRNA levels were unchanged (McDonald et al., 2011). Although TDP-43 has been shown to be non-essential for stress granule formation, previous studies have demonstrated that knockdown of TDP-43 resulted in a suboptimal stress granule response in HeLa cells when treated with arsenite (McDonald et al., 2011). These findings are somewhat different to our findings in that TDP-43 mutant fibroblasts showed an enhanced stress granule formation response to arsenite compared to the controls. Furthermore upon stress release the SGs persisted for a significantly longer period compared to the control situation (Fig 4.14E). This difference between the SG dynamics described by McDonald et al (2011) and our findings could be due to gross alteration in cellular RNA related TDP-43 interactions when endogenous TDP-43 is knocked down, compared to physiological levels of dysfunctional disease associated mutated TDP-43. Although all three mutant lines (A321V, M337V and G287S) demonstrated a similar pattern of stress granule dynamics compared to the controls, there were variations amongst the three TDP-43 mutant fibroblast cell lines in their stress granule response to arsenite treatment. G287S fibroblasts had the most robust SG assembly response and the most delayed SG disassembly dynamics. In support of the differences in SG dynamics we observed in the fibroblasts carrying different mutations in TDP-43 is the study in lymphoblastoid cell lines from disease associated TDP-43 mutations D169G showed significantly greater SG response compared to R361S cells. This difference was thought to be secondary to lower levels of G3BP SG associated protein (McDonald et al., 2011).

Mechanisms important in TDP-43 ALS and SG dynamics and implications for ALS

Studies have suggested a role for stress kinases such as JNK and p38 in ALS (Zhu et al., 2003, Veglianese et al., 2006). A chronic stress model using paraquat demonstrated that JNK can modulate TDP-43 localisation to SGs (Meyerowitz et al., 2011). hnRNPA1, which belongs to the family of hnRNPs like TDP-43, is

phosphorylated by p38, inducing hnRNPA1 localisation to SGs (Shimada et al., 2009). It has been reported that inhibition of ERK leads to increased TDP-43 aggregation. Furthermore ERK also aggregates in stressed cells as well as in tissues obtained from ALS cases (Ayala et al., 2011a). Whilst TDP-43 is not essential for SG formation, it is possible that phosphorylation of specific hnRNP in response to a stress can modulate its interaction with TDP-43, thus deciding the fate of TDP-43-stress granule association. Furthermore McDonald et al 2011 suggested that TDP-43 modulated the levels of stress granule nucleating proteins such as TIA-1 and G3BP (McDonald et al., 2011). The development of neurodegenerative conditions is thought to reflect prolonged cumulative damage predisposed to by a combination of genetic and environmental influences. Neuronal cells depend on precise control of the internal milieu so its very important not to have a maladaptive state of heightened stress levels. Therefore if genetic factors predispose to prolonged accumulation of stress granules in response to exogenous stress, one would hypothesise that over a long period of time the neurons would be at risk of damage due to entrapment of vital mRNAs, hnRNPs and cellular components in the SGs or similar cytoplasmic aggregations for longer than necessary periods of time after the stress has passed.

We conclude that mutant TDP-43 alters RNA related cellular functions. In support of this statement we demonstrate a significant change in stress granule assembly and disassembly dynamics in response to exogenous stress in the presence of mutations in the C-terminal end of TDP-43. Furthermore we demonstrated that SMN associated GEM bodies, which are nuclear foci of RNA related functions, are altered compared to controls in association with certain TDP-43 mutations (Fig 4.19). Taken together, these observations support the notion of using ALS patients' derived fibroblasts as a platform to study mutant TDP-43 related TDP-43 proteinopathy. Furthermore studies on stress signaling cascades and phosphorylation of tau in Alzheimer's dementia have successfully used skin fibroblasts from cases with presenilin-1 mutations, setting up a precedence for other neurodegenerative conditions to use fibroblasts to model disease related mechanisms (Mendonsa et al., 2009). We did observe a difference in endogenous TDP-43 localisation in the fibroblasts from a single sporadic ALS case suggesting the potential to extend the use of fibroblasts to study ALS related mechanisms in the larger group of sporadic ALS. Moreover a recent publication by

Mead et al (2013) confirms that fibroblasts from ALS cases can be used successfully in drug screening (Mead et al., 2013). The role of different kinases, which would modify the fate of interactions amongst hnRNPs and TDP-43 to modulate SG dynamics, highlights potential therapeutic targets for multiple compound screening to identify small molecules capable of modifying SG dynamics in favour of improving motor neuronal health. Finally one of the limitations in our study is that we only had one cell line per mutation in TDP-43 and ideally we would like to study at least three different patient cell lines per mutation ideally age and sex matched.

Chapter 05:

The effects of transient knock-down of the zebrafish homologues of *TARDBP: tardbp and tardbpl* in zebrafish embryos

5.1   Introduction

The presence of neuro-cytoplasmic inclusions is a characteristic feature of several neurodegenerative conditions. The disease causing proteins in some of the neurodegenerative conditions were discovered many years ago, for example tau in Alzheimer's dementia, and alpha-synuclein containing Lewy bodies in dementia with parkinsonism. However in ALS/MND although the neuro-cytoplasmic aggregations were a recognised feature, a common disease related protein was not discovered until recently. The seminal discoveries of associations of TDP-43 in ALS and front temporal lobe dementia with ubiquitinated inclusions (FTLD-U) and more recently, Fused in sarcoma 1 (FUS1) in ALS and FTLD-U have raised hope of a novel patho-mechanistic pathway for the investigation of ALS and FTLD-U related selective neuronal vulnerability and for a therapeutic breakthrough. Although ALS due to mutations in *SOD1* is associated with SOD1 accumulation, SOD1 accumulation is not a shared feature amongst non- SOD1 mutation related ALS. However, most disease models of ALS in the last two decades have been based on the SOD1 model. Although the SOD1 model has provided vital insights into the pathophysiology of ALS, a significant therapeutic breakthrough has not yet materialised.

In relation to ALS associated with *TARDBP* mutations and sporadic ALS, it is still unclear if the TDP-43 positive inclusions are merely a pathological marker or whether mis-localisation and aggregation contribute to the disease process. Confirming the disease causative nature of the dysfunctional TDP-43 is the numerous reports of ALS associated mutations in *TARDBP.* TDP-43, similar to FUS1 and other hnRNPs, has multiple functions such as splicing and transcription regulation, RNA metabolism, RNA transport, miRNA processing and various protein interactions and has an established role as a protein important for RNA processing. However, the processes involved in TDP-43 accumulation in neuro-

cytoplasmic aggregations and the mechanisms by which TDP-43 exerts its pathological effects have not been established. To help understand the pathological effects of TDP-43, it is important to gain information about its normal function in both *in vivo* and *in vitro* models. Zebrafish represents an excellent disease model because of it's optical translucency, high fecundity and external development coupled with its use in high throughput drug screening (Bandmann and Burton, 2010). Precedence in using zebrafish as an *in vivo* platform to study mechanisms involved in motor system dysfunction has already been set (Kasher et al., 2009, Ciura et al., 2013, McGown et al., 2013). It is still unclear if the dysfunctional TDP-43 causes motor neuron death via toxic gain of function and/or a loss of function. Zebrafish is an excellent disease model to study loss of function phenomena through transient knockdown of targeted genes using morpholino oligonucleotides (AMO). In this chapter the results of the transient knockdown of *tardbp* and *tardbp*l in WT zebrafish embryos are discussed.

5.2   Identification and confirmation of zebrafish othologues of TDP-43: Tardbp and Tardbpl using genome browsing tools

A BLAST search of the human TDP-43 (ENSG00000120948) c.DNA sequence against the zebrafish genome (version 9) identified two putative zebrafish orthologues of human *TARDBP*. The first homologue is *tardbp*, on chromosome 6 (ENSG0000040031), which encodes a 412 amino acid protein. The second orthologue identified is *tardbp* like (*tardbpl*) (ENSG00000004452) on chromosome 23, which is predicted to encode a shorter protein with 303 amino acids. Analysis of the amino acid sequences of the zebrafish orthologues of TDP-43 revealed that the important functional domains of TDP-43 such as nuclear localisation signal (NLS), RNA recognising motif 1 and 2 (RRM1 and RRM2) and part of the glycine rich domain (GRD) are represented within Tardbp and Tardbpl (Figure 5.1).

5.3 Zebrafish TDP-43 orthologues are highly conserved across species

Alignment of the amino acid sequence of the two zebrafish orthologues of TDP-43, Tardbp and Tardbpl along with TDP-43 and using clustalW analysis suggests significant identity amongst the three proteins (Figure 5.1). Tardbp is 412 amino acids

```
Zebrafish_tardbp    MAEMYIRVAEEENEEPMEIPSEDDGTVLLSTVSAQFPGACGLRFRSPVSQCMRGVRLVDG 60
Zebrafish_tardbpl   MTECYIRVAEDENEEPMEIPSEEDGTVLLSTVAAQFPGACGLRYRSPVSQCMRGVRLVEG 60
Human_TDP-43        -MSEYIRVTEDENDEPIEIPSEDDGTVLLSTVTAQFPGACGLRYRNPVSQCMRGVRLVEG 59
                     . ****:*:**:**:*****:********:*:********:*.************:*

                                              NLS                       RRM1
Zebrafish_tardbp    ILHAPENGWGNLVYVVNYPKETVLPDNKRKMDEIDASSATKIKRGDQKTSDLIVLGLPWK 120
Zebrafish_tardbpl   VLHAPEADWGNLVYVVNYPKD-----NKRKMDEMDAASAVKIKRGIQKTSDLIVLGLPWK 115
Human_TDP-43        ILHAPDAGWGNLVYVVNYPKD-----NKRKMDETDASSAVKVKRAVQKTSDLIVLGLPWK 114
                    :****: .************:        ******* **:**.*:**. **********

Zebrafish_tardbp    TSEQDLKDYFGTFGEVIMVQVKRDVKTGNSKGFGFVRFGDWETQSKVMTQRHMIDGRWCD 180
Zebrafish_tardbpl   TTEQDLKDYFGTFGEVIMVQVKRDAKSGNSKGFGFVRFTDYETQIKVMSQRHMIDGRWCD 175
Human_TDP-43        TTEQDLKEYFSTFGEVLMVQVKKDLKTGHSKGFGFVRFTEYETQVKVMSQRHMIDGRWCD 174
                    *:*****:**.*****:*****:*  *:*:********** ::*** ***:**********

                                                   RRM2
Zebrafish_tardbp    CKLPNSK-----QGIDEPMRSRKVFVGRCTEDMTADELRQFFMQYGEVTDVFIPKPFRAF 235
Zebrafish_tardbpl   CKLPNSKYFLEQAGPDEPMRSRKVFVGRCTEDMTADELRQFFMQYGEVTDVFIPKPFRAF 235
Human_TDP-43        CKLPNSK-----QSQDEPLRSRKVFVGRCTEDMTEDELREFFSQYGDVMDVFIPKPFRAF 229
                    *******      ***:************** **** :** ***:* ***********

                                                                GRD
Zebrafish_tardbp    AFVTFADDQVAAALCGEDLIIKGVSVHISNAEPKHNNTRQMMERA---GRFGNGFGGQGF 292
Zebrafish_tardbpl   AFVTFADDQVAQSLCGEDLIIKGTSVHISNAEPKHNNIHHLFS------------NF 280
Human_TDP-43        AFVTFADDQIAQSLCGEDLIIKGISVHISNAEPKHNSNRQLERSGRFGGNPGGFGNQGGF 289
                    *********:* :********** ************ .  ::: .          .*

Zebrafish_tardbp    AGSRSNMGGGGGGSSSSLGN---FGNFNLNPAMMAAAQAALQSSWGMMGMLA--QQNQSGT 348
Zebrafish_tardbpl   PGR-----------SPSLA-----------AMFERSQYQFPSSHV-------------- 303
Human_TDP-43        GNSRGGGAGLGNNQGSNMGGGMNFGAFSINPAMMAAAQAALQSSWGMMGMLASQQNQSGP 349
                    .              ...:.            **: :* : **

Zebrafish_tardbp    SGTSTSGTSSSRDQAQTYSSANSNY--GSSSAALGWGTGSNSGAASAGFNSSFGSSMESK 406
Zebrafish_tardbpl   ------------------------------------------------------------
Human_TDP-43        SGNNQNQGNMQREPNQAFGSGNNSYSGSNSGAAIGWGSASNAGSGS-GFNGGFGSSMDSK 408

NLS - Nuclear Localisation Signal

Zebrafish_tardbp    SSGWGM 412
Zebrafish_tardbpl   ------              RRM1/2- RNA Recognising Motif 1/2
Human_TDP-43        SSGWGM 414

GRD- Glycine Rich Domain
```

Figure 5.1 Alignment of amino acid sequences of zebrafish Tardbp and Tardbpl with human TDP-43 using Clustal W software. TDP-43 is 414 amino acids long whilst tardbp and tardbpl are 412 and 303 amino acids in length respectively. NLS- nuclear localisation signal and RRM1/2-RNA recognsingising motif 1 and 2 are conserved between the two species. The GRD (Glycine rich domain) and the rest of the C- terminal residues are similar between Tardbp and TDP-43 but different in tardbpl as it is lacking the C- terminal residues of TDP-43. Tardbp is 74% identical to TDP-43 whilst Tardbpl is only 54% identical. Asterisks (*) denote identical residues across the species, colons (:) indicate similar residues and dots (.) indicate somewhat similar residues.

of which 74% are identical to that of the human TDP-43. The second orthologue Tardbp like (Tardbpl) is a shorter protein with 303 amino acids, of which 54% are identical to the human TDP-43 (Figure 5.1). When comparing the important domains and motifs of TDP-43, the identity with TDP-43 increases. Thus the two homologues share 100% amino acid identity in the nuclear localisation signal and 81% identity in the RNA recognition motif 1 (RRM1) and 94% similar to that of hTDP-43. The residues in the RRM2 are 85% identical (92% similar) amongst TDP-43, Tardbp and Tardbpl emphasising the evolutionary conservation of the N-terminal region. However, only 25% of the residues in the C-terminal end (glycine rich domain) are identical (48% similar) amongst the three proteins. The Tardbpl protein lacks a large portion of the C-terminal glycine rich domain. We confirmed the predicted *tardbp* and *tardbpl* sequences by amplifying the reverse transcribed zebrafish c.DNA and sequencing using primers specific for *tardbp* and *tardbpl*.

5.4 Zebrafish Tardbp and Tardbpl expression

Given the homology between human and zebrafish proteins, we used the human TDP-43 antibody raised against the first 260 amino acids of the human TDP-43 n-terminus (h.TDP-43 Ab1) to detect zebrafish Tardbp.

5.4.1 Expression of *tardbp* and *tardbpl* mRNA at different developmental stages of WT zebrafish embryos

tardbp and *tardbpl* specific primers (Table 5.1) were used to amplify the gene specific c.DNA synthesised using pre-mRNA from RNA extracted from zebrafish embryos at 0.5hpf to 120hpf. The RT-PCR products from gene specific amplifications were run on electrophoretic agarose gels separately for *tardbp* and *tardbpl* and demonstrate that *tardbp* and *tardbpl* are expressed from very early stages of zebrafish development (Fig 5.2A-B). Expression of *tardbp/tardbpl* in the early stages of embryological development suggests that both mRNAs for *tardbp* and *tardbpl* are maternally expressed which indicates that both genes have essential functions in the early developmental stages in zebrafish embryos.
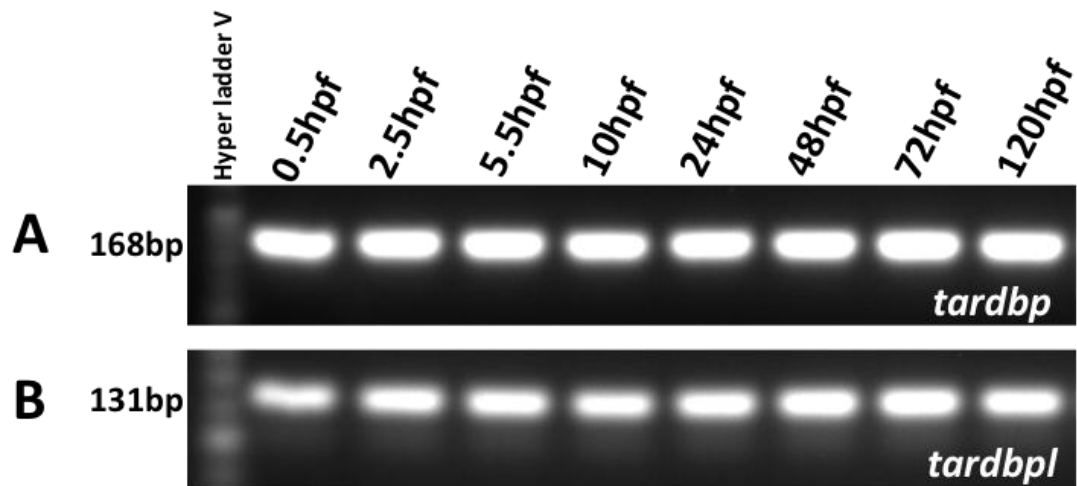
Figure 5.2 Expression of *tardbp* and *tardbpl* mRNA in WT zebrafish embryos at different stages of development. A) *tardbp* specific primers were used to amplify cDNA from 0.5hpf to 120hpf embryos. *tardbp* is expressed throughout including the very early stages of development. B) *tardbpl* specific primers used to amplify the reverse transcribed mRNA also show expression of *tardbpl* similar to *tardbp*. Both Tardbp and Tardbpl are expressed early in development suggesting maternally transmitted mRNA expression. The product sizes were similar to those predicted by the primer select programme used to design the primers. hpf (hours post fertilisation, bp (base pairs). 168 and 131 are respective product lengths for the primer pairs used for *tardbp* and *tardbpl* RT-PCR.

Table 5.1 Primers used in amplification of *tardbp and tardbpl* RT-PCR	
Primer name and location	**5'→3'**
***tardbp*-forward-5UTR**	CTG GAT CCA TGG CCG AGA TGT ACA TTC GAG TTG
***tardbp* -reverse-(exon 2)**	ACG AAT TCT TAC ATA CCC CAC CCC GAT GAC TTG 3
***tardbpl*- forward--(exon 5)**	GCATTCGGTGTAATCATGACG
***tardbpl* – reverse-3UTR**	ATACTCTGATATGTGGGCATACTGA

Immunofluorescence of whole- mount zebrafish embryos at 36hpf was performed with a h.TDP-43 Ab1 which is raised against the N-terminus of TDP-43 and is predicted to detect both Tardbp and Tardbpl, and an anti-Islet1 antibody which stains motor neurons and Rohon Beard neurons. The whole mount zebrafish immunofluorescent stains suggest that TDP-43 orthologues, Tardbp and Tardbpl are ubiquitously expressed in the zebrafish embryos (Fig 5.3A-B). TDP-43 in zebrafish also co-localises with islet1 antibody stain indicating that Tardbp and Tardbpl are expressed in the neuronal nuclei (Fig 5.3D and G) and are predominantly expressed in the nucleus (Fig 5.3E-G) in keeping with what is observed in human tissues.

5.4.2 Expression of TDP-43 ortholgues in WT zebrafish embryos is ubiquitous
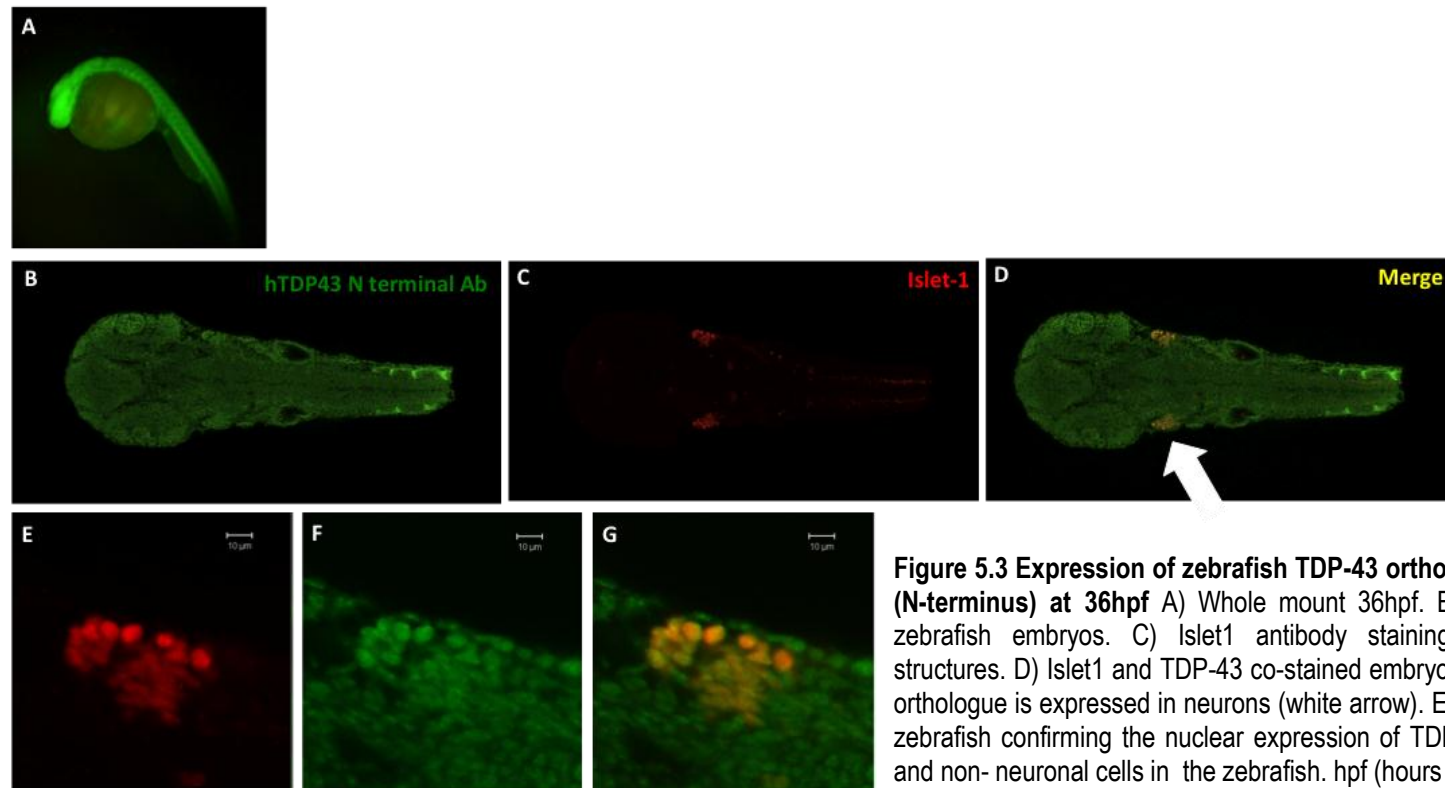
Figure 5.3 Expression of zebrafish TDP-43 orthologues using h.TDP-43 Ab1 (N-terminus) at 36hpf A) Whole mount 36hpf. B) Dorsal view of the rostral zebrafish embryos. C) Islet1 antibody staining to demonstrate neuronal structures. D) Islet1 and TDP-43 co-stained embryos demonstrating that TDP-43 orthologue is expressed in neurons (white arrow). E-G) Trigeminal nucleus of the zebrafish confirming the nuclear expression of TDP-43 orthologues in neuronal and non- neuronal cells in the zebrafish. hpf (hours post fertilisation)

5.4.3 Expression of Tardbp and Tardbpl at protein level detected by immuno-blotting
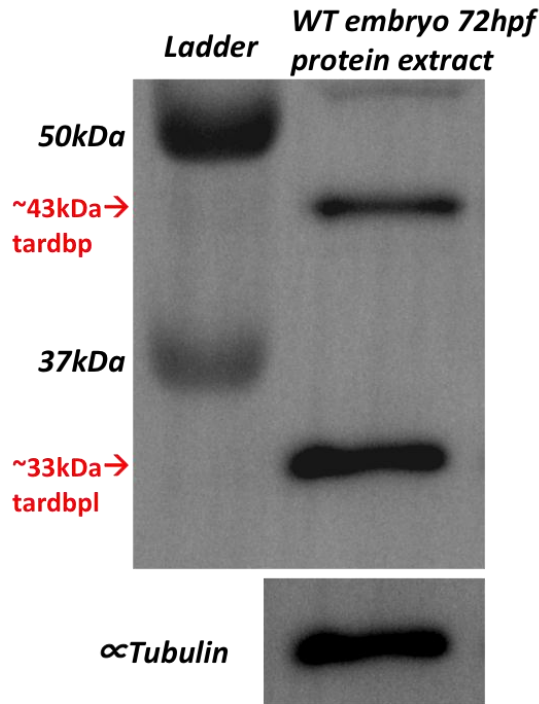
Figure 5.4 Immunoblotting of 72hpf zebrafish total protein extracts using h.TDP-43 Ab1. Western blot of protein extracts from 72hpf zebrafish embryos probed by h.TDP-43 Ab1 demonstrates the presence of both Tardbp and Tardbpl at the predicted molecular weights of 43kDa and 33kDa respectively. Loading control was alpha tubulin.

.

We calculated the predicted molecular weight of Tardbp and Tardbpl by processing the amino acid sequence of Tardbp and Tardbpl proteins using a protein prediction software (expacy.com). The predicted molecular weight for Tardbp is ~43kDa and Tardbpl is ~33kDa. Protein extracts obtained from 72hpf WT zebrafish embryos when probed with h.TDP-43 Ab1 detected both Tardbp (at 43kDa) and Tardbpl (at ~33kDa) on immunoblotting. We also noted that there were several other non-specific bands detected on western blotting making the immuno-fluorescent staining using h.TDP-43 Ab1 difficult to interpret (Please note that this figure is part of Figure 6.9 from chapter 6, used in this chapter to illustrate the molecular weights of TDP-43 zebrafish orthologues). We also know that 33kDa band is not a breakdown product of the higher 43kDa Tardbp band, as morpholino knockdown of *tardbpl* obliterates the 33kDa band (refer Figure 5.15).

5.4.4 Identification of antibodies h.TDP-43 Ab1 and h.TDP-43 Ab2

The antibodies used to detect TDP-43 were obtained from Protein Tech. Initially h.TDP-43 Ab1 (Catalogue number 10782-2-AP) was marketed. A few months later the Protein Tech company produced a second antibody, which we called h.TDP-43 Ab2 (Catalogue number 12892-1-AP). Interestingly the antigen epitopes used for the two antibodies were different. The first 260aa of the TDP-43 protein were used for generation h.TDP-43 Ab1, therefore h.TDP-43 Ab1 detects the *N-term*inus of the TDP-43 protein and *N-term*inal fragments. The last 154aa of the *C-termin*us was used to generate the h.TDP-43 Ab2 which therefore detects up the *C-termin*al end of the TDP-43 and *C-termin*al fragments (Figure 5.5) (http://www.ptglab.com/Products/Search.aspx?key=tdp-43). Discovering the two antibodies h.TDP-43 Ab1 and h.TDP-43 Ab2 helped us to identify Tardbp and Tardbpl separately. The h.TDP-43 Ab1 detects both Tardbp and Tardbpl (Figure 5.4 and Figure 5.5). The h.TDP-43 Ab2 detects **only** Tardbp and does not detect Tardbpl as the Tardbpl lacks the majority of the *C-termin*al amino acids, which are conserved to a greater extent between zebrafish Tardbp and human TDP-43. h.TDP-43 Ab2 detected the expression of Tardbp in the zebrafish at different stages of development and also in various tissues of the adult zebrafish at 1 year of age (See chapter 6, Figure 6.6). In the adult zebrafish the Tardbp orthologue was expressed mainly in the brain, spinal cord and the eye. When Tardbp expression was knocked down in the zebrafish, the corresponding Tardbp signal disappears (See chapter 6) suggesting that the ~43kDa band h.TDP-43 Ab2 detects is indeed specific for Tardbp. Therefore the h.TDP-43 Ab2 can be used as a tool to detect the loss of Tardbp.

```
CLUSTAL 2.1 multiple sequence alignment
```
Amino acid sequence detected by h.TDP.43 Ab1
is highlighted in yellow

```
tardbp    MAEMYIRVAEEENEEPMEIPSEDDGTVLLSTVSAQFPGACGLRFRSPVSQCMRGVRLVDG 60
tardbpl   MTECYIRVAEDENEEPMEIPSEEDGTVLLSTVAAQFPGACGLRYRSPVSQCMRGVRLVEG 60
          *:*  ******:**********:**********:*********:**************:*

tardbp    ILHAPENGWGNLVYVVNYPKETVLPDNKRKMDEIDASSATKIKRGDQKTSDLIVLGLPWK 120
tardbpl   VLHAPEADWGNLVYVVNYPKD-----NKRKMDEMDAASAVKIKRGIQKTSDLIVLGLPWK 115
          :***** .***********:      ******:**:**.***** **************

tardbp    TSEQDLKDYFGTFGEVIMVQVKRDVKTGNSKGFGFVRFGDWETQSKVMTQRHMIDGRWCD 180
tardbpl   TTEQDLKDYFGTFGEVIMVQVKRDAKSGNSKGFGFVRFTDYETQIKVMSQRHMIDGRWCD 175
          *:**********************.*:********** .*:*** ***:***********

tardbp    CKLPNSK-----QGIDEPMRSRKVFVGRCTEDMTADELRQFFMQYGEVTDVFIPKPFRAF 235
tardbpl   CKLPNSKYFLEQAGPDEPMRSRKVFVGRCTEDMTADELRQFFMQYGEVTDVFIPKPFRAF 235
          *******     * **********************************************

tardbp    AFVTFADDQVAAALCGEDLIIKGVSVHISNAEPKHNNTRQMMERAGRFGNGFGGQGFAGS 295
tardbpl   AFVTFADDQVAQSLCGEDLIIKGTSVHISNAEPKHNNIHHLFS------------NFPGR 283
          ***********  :**********.*************  ::::.          .*.*

tardbp    RSNMGGGGGGSSSSLGNFGNFNLNPAMMAAAQAALQSSWGMMGMLAQQNQSGTSGTSTSG 355
tardbpl   -----------SPSLA---------AMFERSQYQFPSSHV-------------------- 303
                     *.**.          **:  :*  :  **

tardbp    TSSSRDQAQTYSSANSNYGSSSAALGWGTGSNSGAASAGFNSSFGSSMESKSSGWGM 412
tardbpl   --------------------------------------------------------
```

Amino acid sequence detected by h.TDP-43 Ab2 is
highlighted in green

Figure 5.5 Multiple sequence alignment of Tardbp and Tardbpl with h.TDP-43 Ab1 and 2 binding sites. h.TDP-43 Ab1 is raised against the 1-260aa sequences of TDP-43 (highlighted in yellow). Tardbp and Tardbpl share greater identity towards the n-terminus. Therefore both Tardbp and Tardbpl are detected by h.TDP-43 Ab1. However towards the *C-terminu*s, Tardbpl is lacking most of the *C-termina*l amino acids present in the glycine rich domain of Tardbp. Therefore the h.TDP-43 Ab2 which is raised against the last 154aa (260 to 414aa, (highlighted in green) of TDP-43 binds to Tardbp but not Tardbpl. Clustal W 2.1 multiple molecule alignment software was used.

5.4.5 An antisense morpholino oligonucleotide (AMO) targeting the ATG site of *tardbp* reduces *tardbp* expression in zebrafish embryos

A translation blocking AMO was used to knockdown *tardbp* in WT AB zebrafish. During dose titration experiments, microinjection of 2.5ng of the translation blocking AMO resulted in substantial effect on the embryo survival. Higher dose, 5ng, of *tardbp* ATG AMO with knockdown of *p53* resulted in greater death and severe morphological abnormalities amongst the embryos (Figure 5.6). The 0.8ng dose did not alter the

survival of the embryos. Therefore for all experiments with *tardbp* knock down, 2.5ng of the translation blocking AMO was used. 2.5ng of translation blocking AMO is able to knockdown *tardbp* at 36hpf as shown in the western blot, probed with h.TDP-43 Ab2 (Fig 5.7) and provided confidence that *tardbp* translation blocking AMO was specific. The relevant ~43kDa band was unaltered in the control AMO injected embryos and in the uninjected control embryos (Fig 5.7).
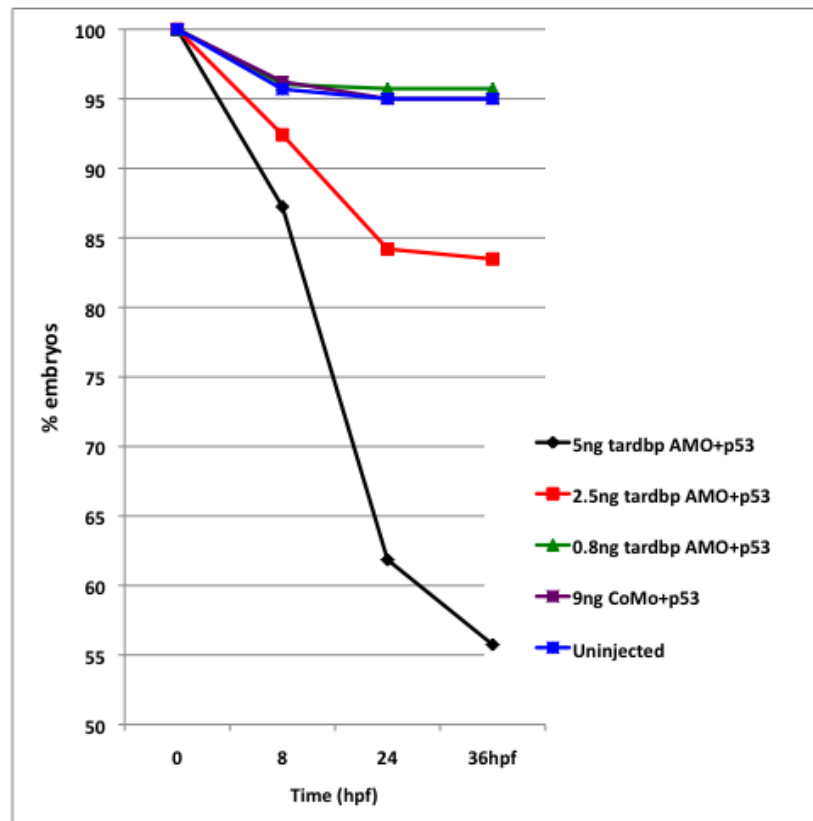
Figure 5.6 Survival of embryos injected with *AMO-tardbp*^{ATG} .
AMO-tardbp^{ATG} 5ng injected embryos rapidly died over the following 36hrs and only 55% of the embryos were alive at 36hpf (p<0.001). Whereas more than 84% of the embryos injected with 2.5ng and 95% of the 0.8ng of *AMO-tardbp*^{ATG} injected group survived at 36hpf. 0.8ng of *AMO-tardbp*^{ATG} , 9ng of CoMo and uninjected groups were similar in survival rates. One way ANOVA, Bonferroni multiple column comparison used.
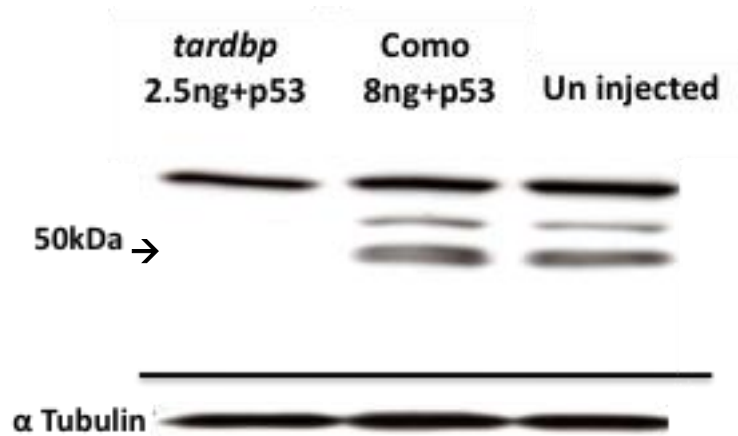
Figure 5.7 *tardbp* knockdown with 2.5ng of *AMO-tardbp^ATG* . Protein extracts from 2.5ng *AMO-tardbp^ATG* , 8ng of CoMo and uninjected embryos immunoblotted with h.TDP-43 Ab2 (which detects the C-terminal end of Tardbp). ~43kDa band (just under the 50kDa marker) indicated by → arrowhead was completely abolished by 2.5ng of *AMO-tardbp^ATG*. The Tardbp band was unaltered in the CoMo and uninjected groups. Therefore the *AMO-tardbp^ATG* appears to knock down tardbp in the zebrafish embryos. Protein extracts were obtained at 36hpf following microinjection of the AMO.

5.4.6   AMO knock down of *tardbp* results in a motor phenotype with reduced survival

TDP-43 has been shown to be essential for embryogenesis in mice (Wu et al., Kraemer et al., 2010, Wu et al., 2010). In keeping with the above studies the embryos injected with 5ng of *AMO-tardbp^ATG* had reduced survival compared to that of 2.5ng injected embryos. As injection of 2.5ng of AMO resulted in longer survival, this dose was used for observation of phenotype. Knockdown of *tardbp* resulted in a dorsal curling of the tail of the embryos at 36hpf when compared to the Control AMO injected embryos (Fig 5.8A & 5.8B). The number of embryos with curly tails was significantly raised in *tardbp* knockdown embryos compared to both control AMO injected and uninjected embryos (p<0.0001) (Fig 5.8C). *AMO-tardbp^ATG* mediated *tardbp* knockdown also resulted in hindbrain cloudiness (Fig 5.9B). AMO microinjection could result in non-specific

neuronal damage especially in the hindbrain region, which can be rescued by concurrent AMO knockdown of *p53* (Robu et al., 2007). Co- injection with p53 AMO improved the hindbrain cloudiness, however the knockdown of *p53* only partially rescued the curly tail phenotype (p<0.001) produced by *tardbp* knockdown compared to the controls (p<0.0001) (Fig 5.8C).
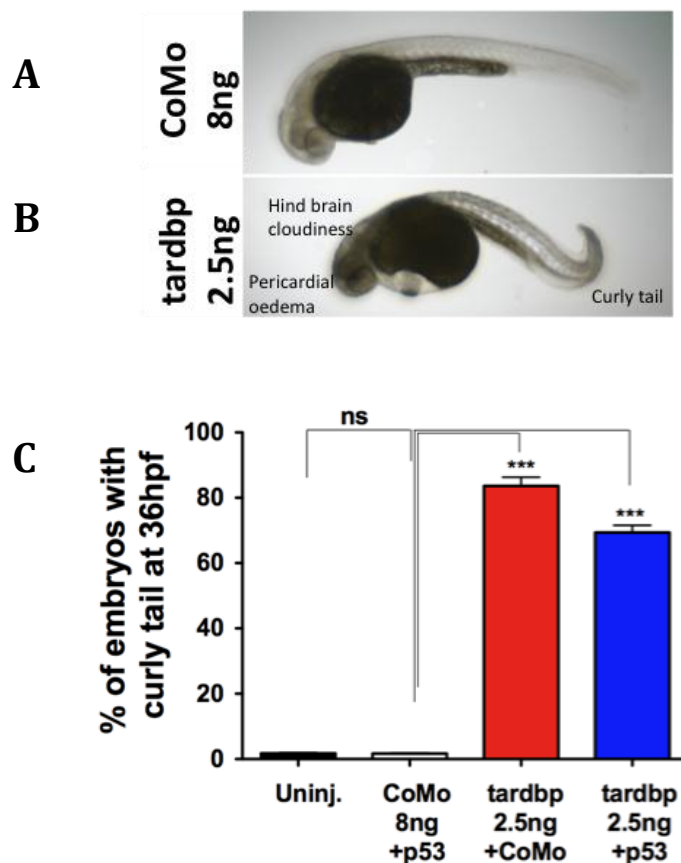
Figure 5.8 Transient *tardbp* knockdown with *AMO-tardbp^ATG* causes a motor phenotype. A) Injection of CoMo 8ng caused no obvious motor phenotype. B) *tardbp* ATG AMO 2.5ng injection caused a curly tail phenotype. *tardbp* ATG AMO injection without p53 causes pericardial oedema and hindbrain cloudiness, effects which are considered to be off target effects. C) No curly tail forms were noted in the CoMo and uninjected controls. A significantly higher proportion of embryos injected with t *tardbp* ATG AMO 2.5ng and 2.5ng+p53 injected groups developed a curly tail phenotype (p<0.0001). Co- injection with p53 AMO (*AMO-tardbp^ATG+p53*) partially rescued the curly up tail phenotype (*AMO-tardbp^ATG+p53* vs *AMO-tardbp^ATG,* p<0.01. Statistical method-Oneway ANOVA with Kruskal-Wallis test and Dunn's multiple comparison tests were used. (*** is equivalent to p<0.0001)

5.4.7 Axonal path finding defects are seen in *tardbp* knockdown embryos

Loss of TDP-43 in the *Drosophila melanogaster* has been shown to disrupt the architecture of motor axons (Feiguin et al., 2009). In order to determine if knockdown of *tardbp* affected axonal outgrowth of spinal motor axons in zebrafish, one-cell stage wild type embryos were microinjected with either 2.5ng of *tardbp* translation blocking

A – Defective axonal lengthening   B - Abnormal axonal branching
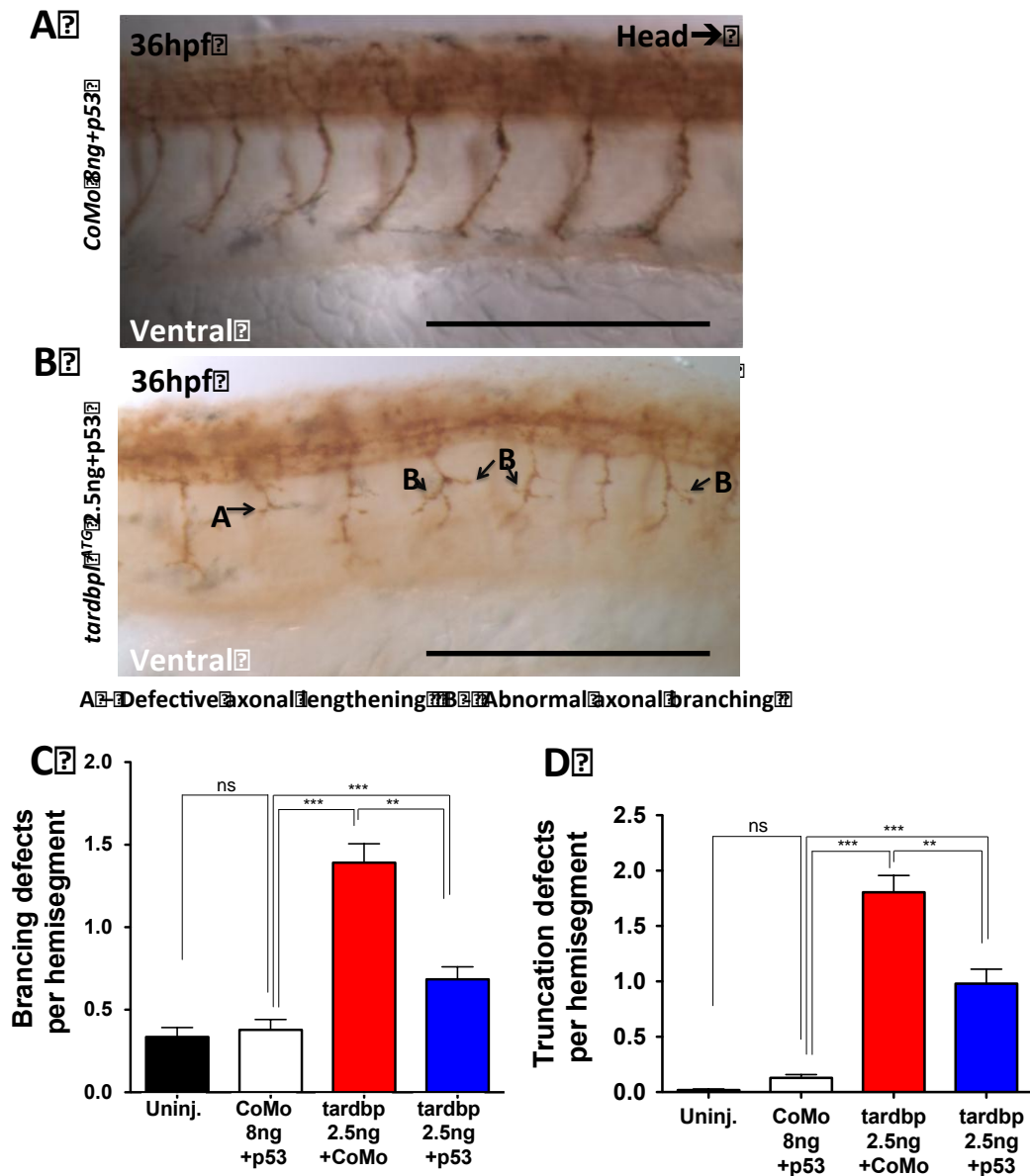
Figure 5.9 Transient *tardbp* knockdown with *AMO-tardbp*^ATG causes axonal out growth defects. Ten axons per hemisection of each embryo counted for axonal defects to compute a score out of 10.A) Lateral views of the whole mount embryos (*AMO-control*) stained with znp1 mouse monoclonal antibody (mAb) at 36hpf. B) Representative znp1 mAb staining of *AMO-tardbp*^ATG+p53 injected embryos at 36hpf with truncated (A→) and abnormally branched (B→) axons. C) The average number of axons with branching defects and D) Abnormal truncation defects per hemi- segment significantly increased in the *AMO-tardbp*^ATG (p<0.0001) and *AMO-tardbp*^ATG+p53 (p<0.001) groups compared to the *AMO-control* and uninjected groups. Co-injection with p53 could only partially rescue the axonal path finding defects (p<0.001). ns= not significant. One way ANOVA with Kruskal-Wallis test and Dunn's multiple comparison post test correction were applied. (*** is equivalent to p<0.0001, ** is equivalent to 0.01). Scale bar 150μm.

AMO with and without p53 or with the standard control AMO. The overall axonal architecture of the differentiating spinal motor neurons was studied by znp-1 immunostaining at 36hpf. The number of axonal defects (prematurely truncated and/or abnormally branched axons) were counted per hemi segment and expressed as a score out of 10 (figure 5.9A and 5.9B).

tardbp knockdown significantly increased the number of axons with axonal growth arrests leading to premature truncation at 36hpf when compared to the control AMO injected embryos and the uninjected control embryos ($p < 0.0001$) (Figure 5.9D). Although simultaneous AMO knockdown of p53 partially rescued the premature axonal truncation defects ($p < 0.0001$), this was still significantly abnormal compared to the controls ($p < 0.0001$) (Fig 5.9D). The loss of *tardbp* also resulted in an increase in the number of axons with abnormal branching ($p < 0.0001$) despite the partial rescue by AMO knockdown of *p53* ($p < 0.001$) (Fig 5.9C). The control AMO injected embryos had no increase in the axonal branching defects compared to the uninjected embryos (Fig 5.9C).

5.4.8 Knockdown of *tardbp* results in loss of motor neurons

Tardbp expression was ubiquitous (Fig 5.3). Therefore to investigate if the knockdown of *tardbp* had a specific effect on motor neuron development we studied the differentiation of motor neurons in the spinal cord of 36hpf embryos microinjected with *AMO-tardbp^{ATG}*. The injected embryos were immunostained with monoclonal antibody to Islet-1, which is a nuclear transcription factor specific to the nuclei of the motor neurons and Rohon Beard sensory neurons. The number of motor neurons counted per hemi- segment of injected embryos at 36hpf was reduced by 65% in the *tardbp* knockdown embryos ($p < 0.0001$) (Fig 5.10 A-C). Interestingly the Rohon-Beard neurons were also reduced by 20% ($p < 0.0001$) with the loss of tardbp (Fig 5.10 B-D).
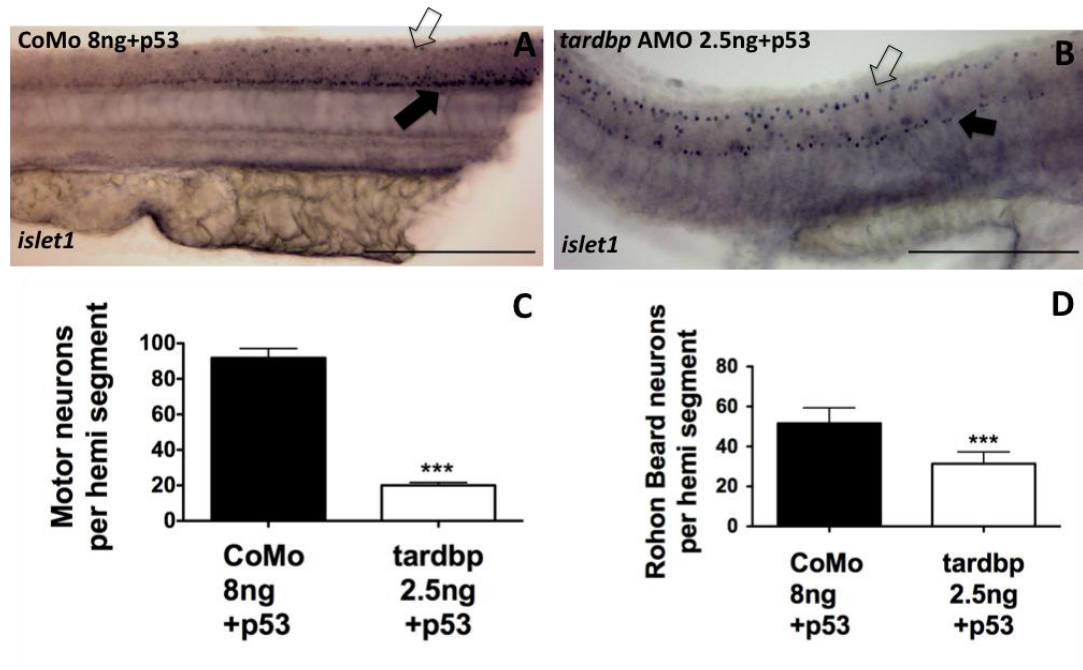
Figure 5.10 Loss of *tardbp* resulted in loss of motor neurons and Rohon Beard neurons. Lateral views of the whole mounted embryos labeled with Islet1 mAb to stain for neuronal cells in (A) *AMO-control and* (B) *AMO-tardbp^{ATG}+p53*. (C) Significant loss of motor neurons (solid black arrow) per hemi-segment was noted in the *AMO-tardbp^{ATG}+p53* group compared to *AMO-control* group (p<0.0001). Effect of loss of tardbp was not specific to motor neurons as Rohon Beard neurons (empty black arrow) were also reduced (p<0.0001). Statistical method- unpaired t test for non-parametric data. Scale bar 200µm.

5.4.9 *tardbpl* splice interfering AMO injection

We observed a significant motor phenotype in the zebrafish embryos associated with *AMO-tardbp^{ATG}* mediated loss of *tardbp* in keeping with findings of Tardbp knockout in mouse studies (Kraemer et al., 2010) and TBPH knockdown in drosophila (Fiesel et al., 2009). Kabashi et al's (2010) data in transient zebrafish *tardbp* knockdown produced similar effects (Kabashi et al., 2010b) to our findings although they did not use p53 knockdown, to counteract the off target effects of AMO. We designed a splice interfering AMO against exon three of *tardbp* to assess if the phenotype obtained using a translation blocking AMO is reproducible with a splice interfering AMO. The number of nucleotides in exon 3 of *tardbp* is not divisible by three. Therefore interfering with exon 3 splicing is expected to result in either exon 3 skipping or intron 3-4 inclusion and is therefore predicted to result in a frame-shift of the open reading frame of *tardbp* (Fig 5.11A). A frame-shift in *tardbp* is predicted to result in a premature stop codon and a prematurely truncated Tardbp protein.

5.4.9.1 tardbpl splice interfering AMO-1 injection (TDPS1)(tardbp^{Spl} AMO)

As described before a range of concentrations (0.8-16ng) of TDPS1 AMO (*tardbp^{Spl}* AMO) was injected into 0hpf WT zebrafish embryos. The embryos however developed into normal zebrafish larvae and demonstrated no curly tail phenotype. There was no excess death amongst the TDPS1 (*tardbp^{Spl}* AMO) injected embryos compared to those injected with control AMO or uninjected groups. The highest dose of 16ng of TDPS1 (*tardbp^{Spl}* AMO) injected embryos were phenotypically similar to those injected with 16ng of control AMO. To assess if the splice interfering AMO was effective in disrupting splicing we performed RT PCR on RNA extracted at 30hpf from the zebrafish embryos injected with a range of TDPS1 (*tardbp^{Spl}* AMO) and primers specific for the *tardbp* mRNA sequence. We used two different sets of primers to detect the splice variant. We could not detect a lower molecular weight product to suggest a splice inhibited (Exon 3 skipped) product on RT PCR suggesting that exon 3 was not excluded. Splice interfering could result in random splicing events such as inclusion of an intron i.e. Intron 3-4. Therefore we exposed the agarose gel longer to detect a higher molecular weight product at around 700bp in length (Fig 5.11C), which increased in intensity in a dose dependent manner. The lower TDPS1 (*tardbp^{Spl}* AMO) doses and the control AMO and un-injected controls did not have the ~700bp product on the RT PCR. The intron 3-4 of *tarbp* is 190bp in length. The product length of the primer set 3 is 492. Therefore it was clear that instead of exon 3 skipping, TDPS1 (*tardbp^{Spl}* AMO) caused intron inclusion. Nevertheless TDPS1 AMO (*tardbp^{Spl}* AMO) did not produce a phenotype. We have previously shown that *tardbp* is maternally expressed as we detect *tardbp* mRNA as early as 30min post fertilisation. Splice targeting AMO would not interfere with mature mRNA transmitted via the oocyte, therefore it is plausible that TDPS1 AMO (*tardbp^{Spl}* AMO) did not produce a phenotype as maternally expressed *tardbp* mRNA rescued the phenotype associated with TDPS1 AMO (*tardbp^{Spl}* AMO) knockdown. However it was also noticeable that the efficiency of splice interference of TDPS1 AMO was poor (Fig 5.11B-C) as there were large amounts of normally spliced *tardbp.*
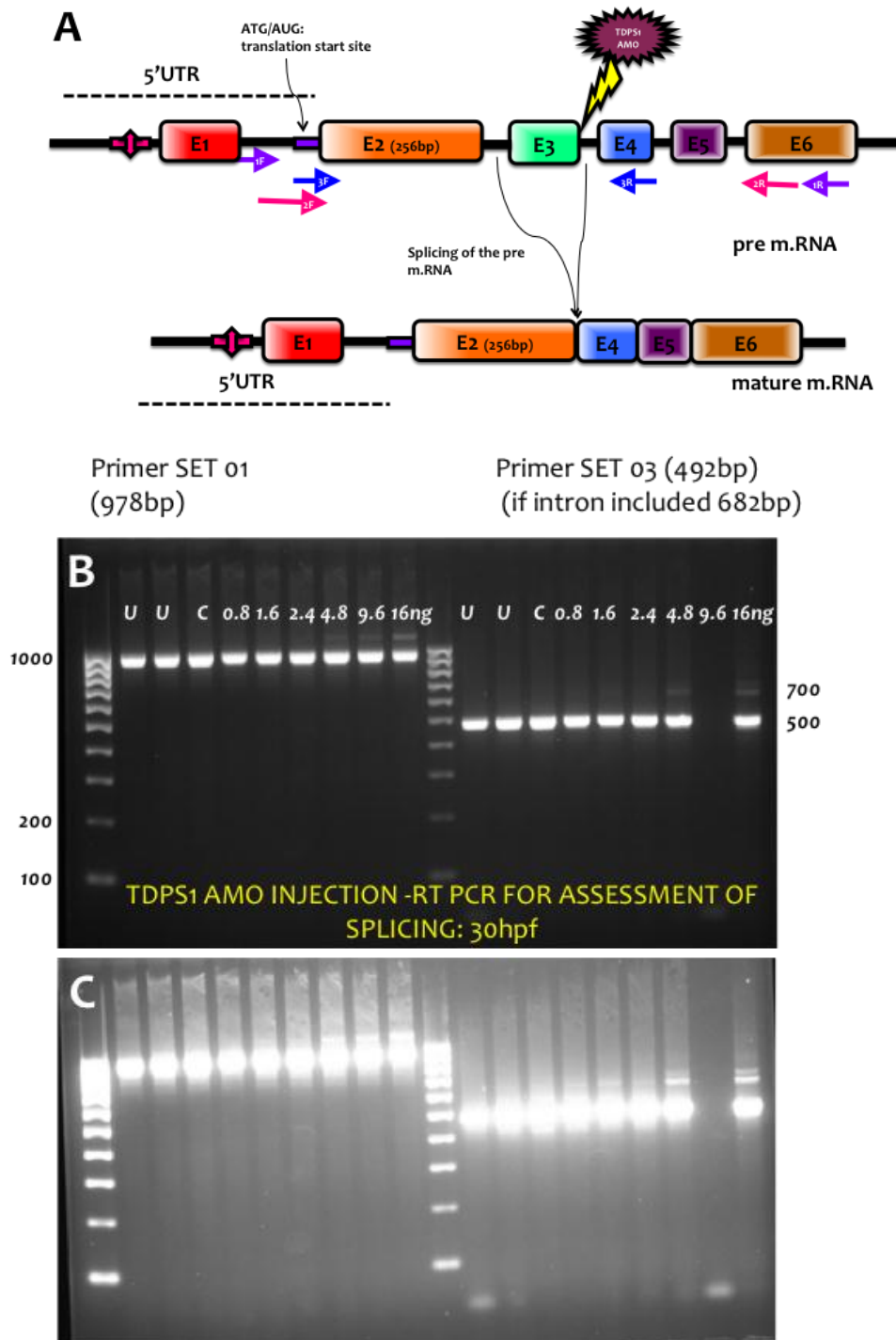
Figure 5.11 Generation of a cryptic splice site by AMO injection-TDPS1 ($tardbp^{Sp1}$ AMO)

(A) Schematic diagram of *tardbp* pre- mRNA as a result of transcription. Pre-mRNA will have exons and intronic regions (Black line between exons). Under normal circumstances pre-mRNA will mature as a mature mRNA when the introns are spliced out. At this point ribosomal subunits will attach to the ribosomal initiation complex and work along the mRNA via the translational initiation site. Splice site targeted AMO (maroon) blocks the conventional splice site. This can result in a splice variant as depicted by joined arrows. B) RT-PCR products from amplification of cDNA synthesised from RNA extracted from U (un-injected), C (control AMO injected) and embryos injected with 0.8-16ng of TDPS1 AMO ($tardbp^{Sp1}$ AMO). RT-PCR amplification done using two sets of primers. A shorter PCR product indicating exon skipping is not seen (492bp is expected as the normal variant PCR product). However, a higher molecular weight PCR product seen ~700bp indicating intron retention (682bp). C) Higher exposure of the agarose gel enhances visualisation of the longer PCR product as a result of the intron retention. This effect appears dose dependent and is not seen in control injected/uninjected groups.

5.4.9.2 tardbpl splice interfering AMO-2 injection - tardbp^{SpII} AMO (TDPS2)

We designed a second splice morpholino *tardbp*^{SpII} AMO (TDPS2) which interferes with the splicing of exon 2 which harbours the translation initiation site of the *tardbp* gene. We were aware that maternally expressed mature *tardbp* mRNA might rescue the phenotype caused by *tardbp*^{SpII} AMO (TDPS2). However our aim was to obtain a demonstrable splice interference (exon 2 skipping) (Figure 5.12A). A range of doses (0.8-16ng) of *tardbp*^{SpII} AMO was injected into single cell zebrafish embryos. Embryos were then raised until 5dpf to observe for a motor phenotype. However even the highest dose of *tardbp*^{SpII} AMO 16ng injected embryos survived till 5dpf. To confirm the splicing interference we designed three sets of primers to amplify c.DNA generated from RNA extracted at 30hpf from the TDPS2 (*tardbp*^{SpII} AMO) injected embryos. The exon 2 of *tardbp* is 256bp in length. When exon two is spliced out it should produce a product length 256bp shorter (Fig 5.12B). RT PCR using three different sets of primer as indicated on Fig 5.12A demonstrated effective splicing interference with the *tardbp*^{SpII} AMO (Fig 5.12C) although there was no obvious macroscopic difference between control AMO and *tardbp*^{SpII} AMO injected embryos. The control AMO injected and the un-injected controls did not show splicing interference noted in the *tardbp*^{SpII} AMO injected embryos. Furthermore splicing interference noted on RT PCR was dose dependent (Fig 5.12C)

Therefore embryos injected with 16ng of *tardbp*^{SpII} AMO were raised up to 36hpf and fixed for znp-1 staining to detect any microscopic phenotypes of axonal out growth defects (Fig 5.13A). Interestingly there was no significant difference in the axonal defects amongst *tardbp*^{SpII} AMO 16ng, CoMo 16ng and uninjected groups (Fig 5.13B) suggesting that while *tardbp*^{SpII} AMO causes significant splice interference, it does not cause a motor neuronal phenotype probably secondary to rescue effect by maternally transmitted *tardbp* mRNA or an alternative molecular mechanism compensating for the loss of *tardbp*. An experiment to assess if *tardbp*^{SpII} AMO injection results in Tardbp knockdown could confirm the possibility of a compensatory mechanism rescuing the *tardbp*^{SpII} AMO injected embryos (We have not performed this experiment).
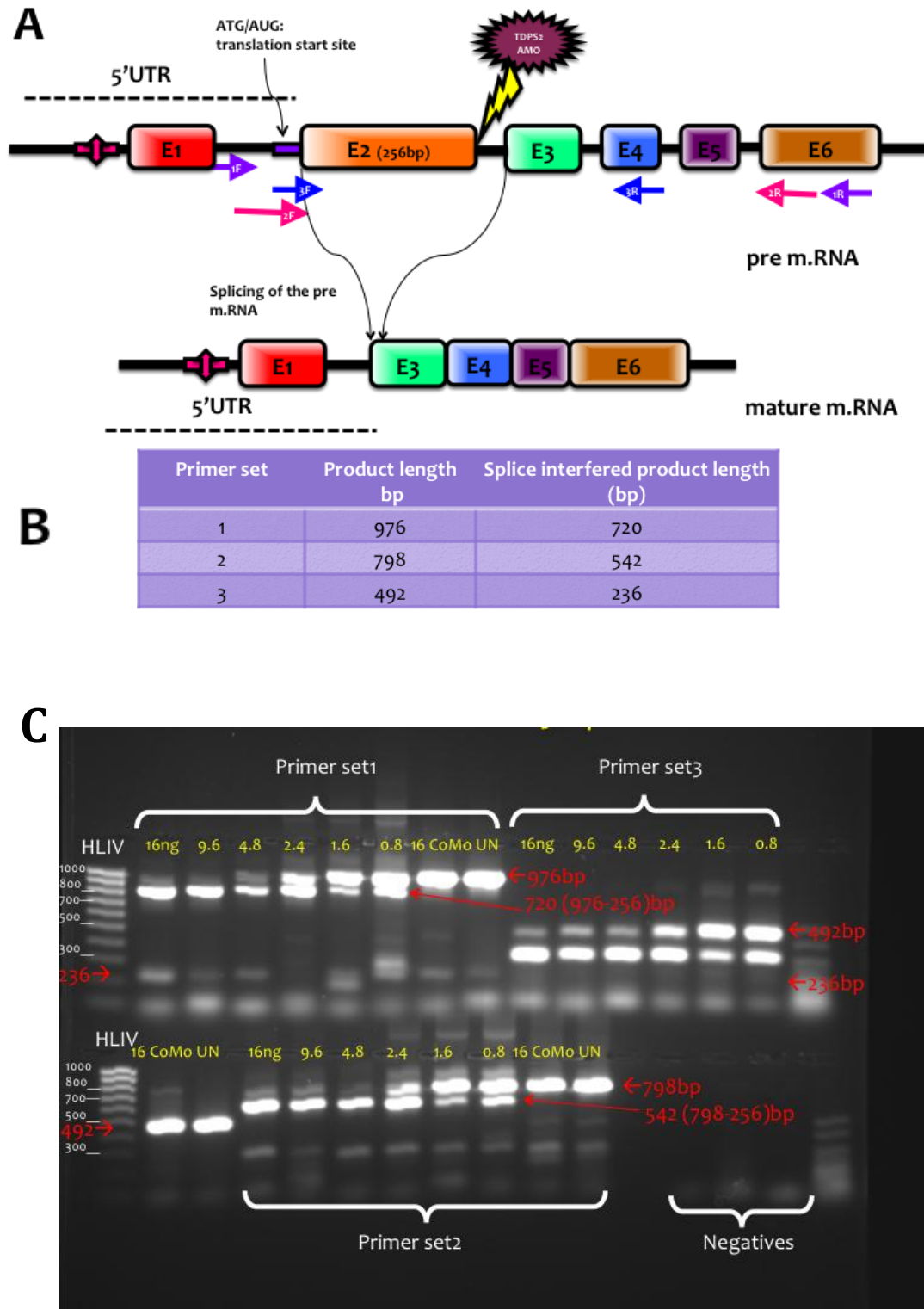
Figure 5.12 Generation of an alternative exon skipping splice site *tardbp* AMO (TDPS2) (*tardbp^Spll* AMO).
A) Schematic diagram demonstrates the binding site of the second splice interfering AMO of *tardbp*, TDPS2 (*tardbp^Spll* AMO). Successful splice interference should lead to skipping of exon two of tardbp which harbours the translation initiation site, ATG. B) Three sets of primers were designed to detect the splicing interference by TDPS2 (*tardbp^Spll* AMO). The table indicates the expected length of the splice altered PCR products for each primer set. C) RT-PCR products from amplification of cDNA synthesised from RNA extracted from UN (uninjected), CoMo (control AMO injected) and embryos injected with 0.8-16ng of TDPS2 (*tardbp^Spll* AMO). RT-PCR products clearly demonstrate effective splice interference of *tardbp* by TDPS2 (*tardbp^Spll* AMO) in a dose dependent manner. Splice interference is captured by all three sets of primers where in product length is reduced by the length of the exon 2 (256bp). In red are the expected product lengths in base pairs (bp), length of the products when exon 2 is spliced out. CoMo injected and uninjected embryos show no evidence of abnormal

219
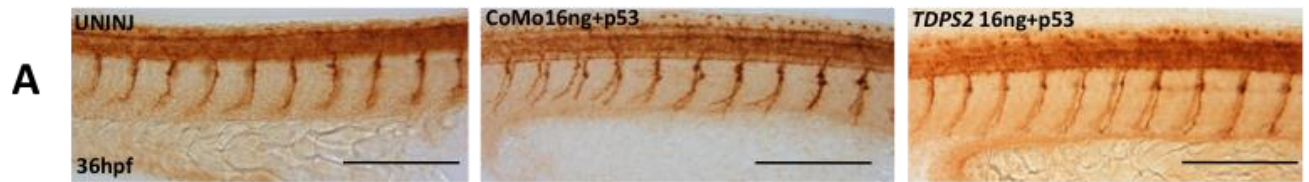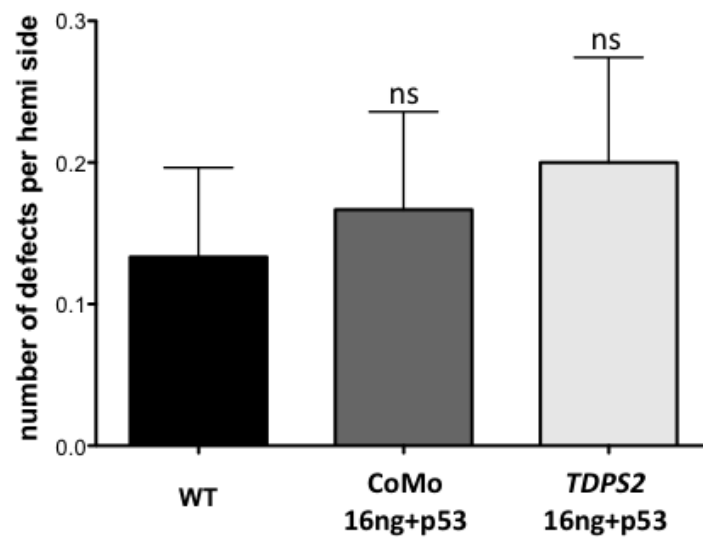
Figure 5.13 TDPS2 (*tardbp^Spll* AMO**) splice interfering AMO does not cause a motor neuron disease like phenotype** A) znp-1 staining of the axonal architecture of un-injected, CoMo 16ng and *tardbp^Spll* AMO 16ng injected embryos at 36hpf showed no axonal defects at highest dose of AMO injection. B) Quantification of axonal defects showed no statistical significance in the axonal defects. One way ANOVA, Kruskall Wallis test with Dunn's multiple comparison tests were used. ns= $p > 0.05$. Scale bar 100µm.

5.4.10 tardbpl knockdown does not lead to a significant phenotype at 48hrs

To investigate if the second orthologue of TDP-43 (Tardbpl) had a direct role in spinal motor neuron integrity, we designed an AMO to block the translation initiation site (ATG) of *tardbpl.* Embryos injected with a range of doses ranging from 2.5-16ng, were observed for up to 48hpf. The embryos injected with the maximum dose of *tardbpl* AMO (16ng) were morphologically indistinguishable from those injected with control AMO at 48hpf (Fig 5.14A). Znp-1 staining was carried out to see if the changes seen with *tardbp* knockdown could be reproduced by *tardbpl* knockdown. However there was no associated increase in the axonal path finding defects with *tardbpl* knockdown (Fig 5.14B) despite achieving significant *tardbpl* knock down ($p < 0.0001$) at protein level (Fig 5.15).
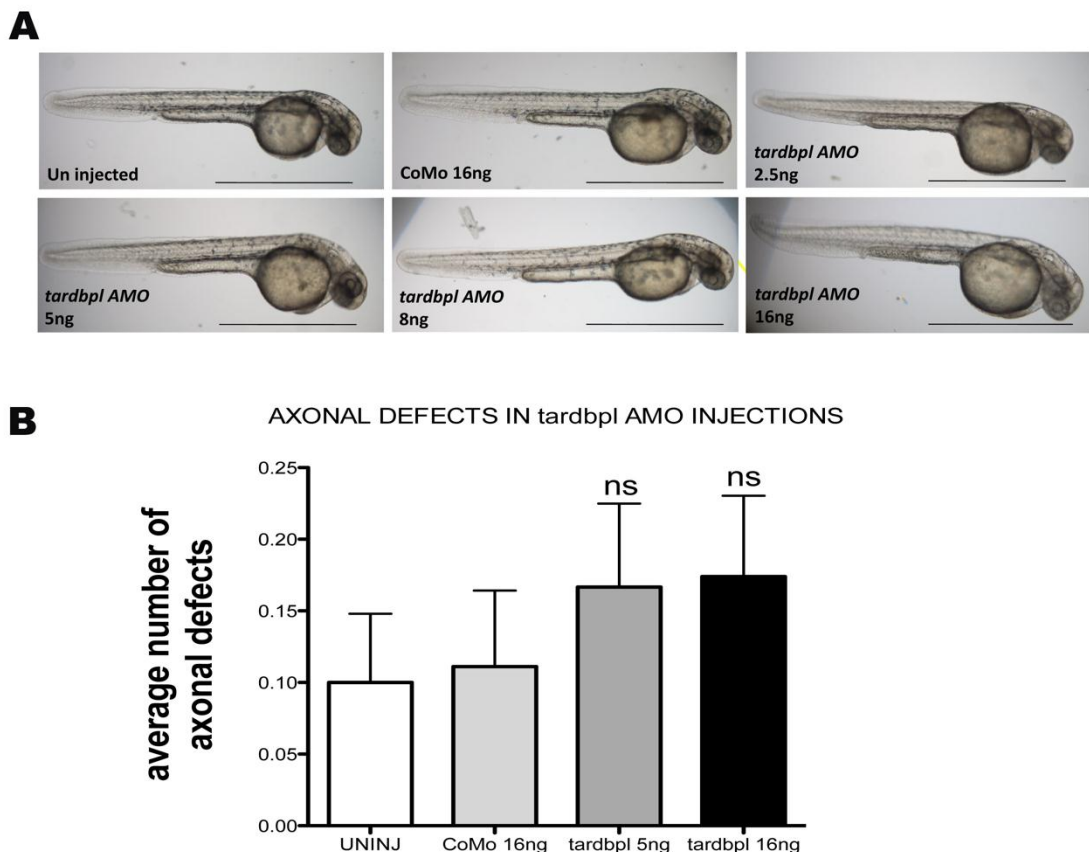
Fig 5.14 AMO knockdown of *tardbpl* in WT zebrafish embryos
(A) Uninjected, AMO-Control injected and *AMO-tardbpl^{ATG} with p53 (AMO-tardbpl^{ATG} +p53)* ranging from 2.5-16ng. There was no macroscopic difference in the phenotype between the CoMo and 16ng of *AMO-tardbpl^{ATG}* injected groups at 48hpf. B) Axonal architecture was studied using znp-1 staining and quantified as described before. There was no statistical significance between uninjected, CoMo and *AMO-tardbpl^{ATG}* injected groups. Statistical method- One way ANOVA, Kruskall Wallis test with Dunn's multiple comparison tests were used. ns= $p > 0.05$. Scale bar
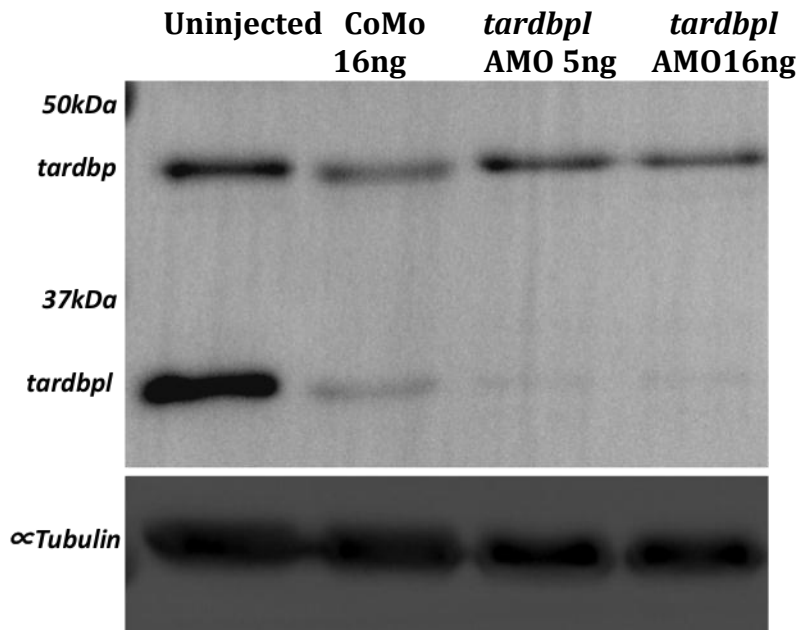
Fig 5.15 Effects of *AMO-tardbpl*^ATG^ knockdown of zebrafish *tardbpl*. Uninjected, AMO-Control injected and *AMO-tardbpl*^ATG^ with p53 (*AMO-tardbpl*^ATG^ +p53), 5ng and 16ng were injected. *AMO-tardbpl*^ATG^ does knockdown tardbpl (~33kDa) when compared to the CoMo injected group. Alpha tubulin was used as the loading control. This immunoblot confirms that *AMO-tardbpl*^ATG^ knocks down *tardbpl*, but the embryos do not develop a phenotype possibly secondary to a molecular mechanism which rescues the loss of *tardbpl* phenotype or may be a non essential gene.

5.4.11 tardbpl knockdown leads to up regulation of tardbp expression

Total protein lysates were obtained from embryos injected with a range of concentrations of *tardbpl* AMO and were subjected to further probing with h.TDP-43 Ab2. We observed that the ~43kDa band representative of Tardbp was significantly enhanced in a dose dependent manner compared to the control AMO injected group (Fig 5.16A). Quantitative analysis showed increased *tardbp* expression compared to the CoMo injected group (($p<0.02$). Taken together it appears that the *tardbpl* knockdown results in an up regulation of Tardbp expression.
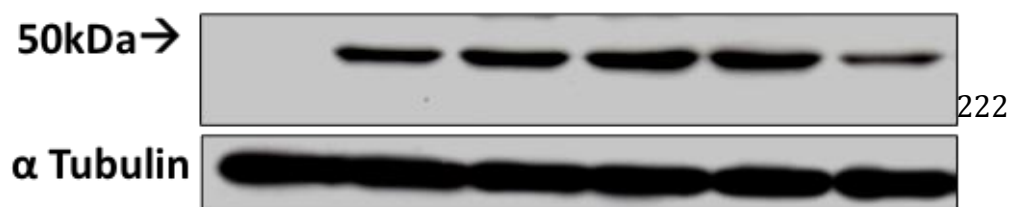
B
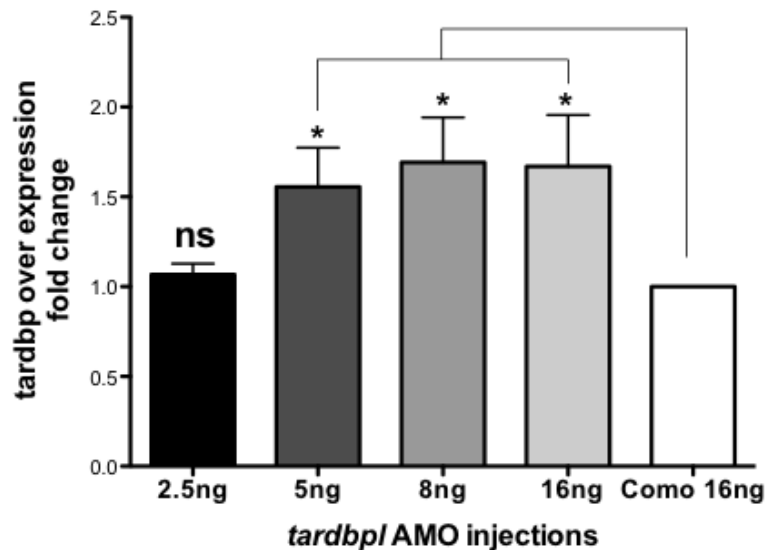
Fig 5.16 *AMO-tardbpl^ATG* **knockdown of zebrafish** *tardbpl* **results in an upregulation of Tardbp expression**. A) h.TDP-43 Ab2 was used to probe the immunoblot prepared with 2.5ng of *AMO-tardbp^ATG* followed by 2.5ng-16ng of *AMO-tardbpl^ATG* and AMO-Control injected embryos. The ~43kDa band indicating Tardbp is abolished in the first lane from the left in *AMO-tardbp^ATG* injected embryos. Ist lane is a positive control for Tardbp. *AMO-tardbpl ^ATG* injection results in a dose dependent increase in Tardbp expression. The CoMo injected group showed no change in Tardbp expression. Alpha tubulin was used as the loading control. This immunoblot confirms that *AMO-tardbpl^ATG* knocks down Tardbpl but the embryos do not develop a phenotype probably secondary to a molecular mechanism which rescues the loss of Tardbpl phenotype. B) Densitometric analysis of the immunoblot demonstrates elevation of Tardbp expression when Tarbpl is knocked down. One way ANOVA with Kruskall Wallis and Dunn's Multiple comparison test to compare all groups was used. * $p < 0.02$, ns= not significant

5.5 Discussion

We have set out to investigate the importance of TDP-43 orthologues in the zebrafish *in vivo* model due to its many advantages. In the body of work described in this chapter, we investigated the role of Tardbp and Tardbpl in zebrafish development. Our data demonstrate that knock-down of Tardbp results in a motor

neuron like disease pattern, loss of motor neurons, axonal path finding abnormalities and reduced survival, in the zebrafish. As shown by the immunofluorescence studies, TDP-43 orthologues are ubiquitously expressed during zebrafish development. Thus, knock-down of Tardbp during embryonic development could affect other cell groups as well as motor neurons, resulting in a severe phenotype. It is also unclear at this stage as to why *AMO-tardbp^{ATG}* produced a phenotype but the splice interfering AMO (*tardbp^{SplI}* AMO) injection was not associated with a phenotype. It is plausible that significant off target effects of *AMO-tardbp^{ATG}* is responsible for the phenotype observed although we have taken the necessary precautions to minimise the off-target effects of AMO by co-injection of p53 AMO. It is also possible that maternal expression of *tardbp* mRNA rescues the *tardbp* splice interfering AMO phenotype.

In keeping with our data are the Drosophila TDP-43 orthologue, TBPH knock down and the mouse TDP-43 knock down studies, which resulted in an early embryonic death. TDP-43, like its paralogue hnRNP-A1 has many recognised functions in the cell (Buratti and Baralle, 2010a). The RNA processing functions, including the regulation of transcription and translation of several genes such as CFTR, APO II, SMN, SP-10 and HDAC 6 have been well described (Chapter 1). Therefore, it is also plausible that TDP-43 regulates its own function. Supporting this is our observation that during the knock down of Tardbpl an up-regulation of Tardbp was observed. Taken together, zebrafish TDP-43 orthologues: Tardbp and Tardbpl appear to regulate each other. The published sequence on ensembl.org for Tardbpl does not have a glycine rich domain and part of the C-terminus of TDP-43, which might explain the relatively severe phenotype when Tardbp is knocked down. While this work was being undertaken, Kabashi et al 2010 reported similar data to our study investigating the effects of Tardbp knock down in zebrafish, except regarding Tardbpl, which they reported, has no function (Kabashi, 2010). In order to generate either a loss of function or toxic gain of function model of TDP-43 in fish it is important to find out if the TDP-43 orthologues in zebrafish have a similar role in the zebrafish as it has in the human. In targeted disruption of mouse TDP-43, the heterozygote mutants did not develop progressive neurodegeneration and nor did the level of mouse TDP-43 decrease; suggesting that the TDP-43 level was tightly regulated (Kraemer et al., 2010, Sephton et al., 2010). Taken together, it is evident that Tardbpl, while perhaps less important than Tardbp, has some

function in the zebrafish. The loss of Tardbpl appears to be compensated to a great extent by up regulation of Tardbp.

Kabashi et al 2010 did not investigate the role of concomitant knock down of p53 and *tardbp* (Kabashi, 2010). The co- injection of *tardbp* AMO along with p53 partially rescued the phenotype associated with translational blocking tardbp AMO, and this phenomenon of knockdown of p53 by co-injection of p53 AMO along with targeted gene is well described (Robu et al., 2007). p53 is a tumour suppressor protein, which regulates the cell cycle by protecting against damage to DNA. Activation of p53 results in its conformational change, accumulation of p53 in the cell and an increase in its activity as a transcription factor. This could either result in cell cycle arrest to allow repair of the damaged DNA or apoptosis of the targeted cell (Meek, 2009). Therefore AMO injection could either result in p53 activation due to the stress of AMO injection or there might be a direct interaction between Tardbp and p53 . Tardbp could have an inhibitory regulatory effect on p53, which may be removed when Tardbp is knocked down. It is less likely that p53 is activated by the stress of AMO injection, as control AMO injection did not result in an abnormal phenotype to suggest p53 activation. TDP-43 is known to participate in the regulation of the transcription of several genes, therefore it is plausible to hypothesise that Tardbp may have a regulatory effect on p53 activation. Still the relative functions of Tardbp and Tardbpl remain to be investigated further.

Some evidence from both *in vitro* and *in vivo* models has interrogated whether TDP-43 related ALS is due to a toxic gain of function or a loss of physiological function. Injection of Q331K or M337V TDP-43 mutant constructs into the chick embryo resulted in developmental defects and enhanced apoptosis (Sreedharan et al., 2008) whilst the Q331K mutation has been shown to have a greater propensity to form aggregates (Johnson et al., 2009) suggesting a possible role of toxic gain of function. However, studies in a Drosophila model of ALS, where the impaired locomotive phenotype of drosophila generated by the drosophila TDP-43 orthologue TBPH gene suppression either by chromosomal deletion or the RNA interference method, was rescued by injection of human TDP-43 (Feiguin et al., 2009), suggested a loss of function role for TDP-43. Supporting this theory are the findings from the TDP-43 transgenic mouse model over- expressing the human

TDP-43 A315T mutation, where loss of nuclear TDP-43 is seen in the surviving motor neurons of the mice at late stages of disease (Turner et al., 2008). The loss of TDP-43 from the nucleus could potentially affect the normal RNA processing function of the TDP-43. Cytoplasmic aggregation of disease related proteins of neurodegenerative diseases are postulated to cause a toxic gain of function. The analysis of the brain and cerebellar tissues obtained from TDP-43 A315T PrP transgenic mice did not show TDP-43 positive cytoplasmic aggregation formation (Turner et al., 2008) as seen in human cases, suggesting that dysfunctional TDP-43 can exert its deleterious effects independent of the formation of cytoplasmic aggregates. This further supports the notion of a loss of function mechanism for mutant TDP-43. It is still possible that the transgenic protein could precipitate the endogenous mouse TDP-43 or produce a soluble TDP-43 fragment that drives the disease process, which might on the other hand indicate a toxic gain of function. The knock- down of mouse TDP-43 resulted in embryonic lethality (Kraemer et al., 2010, Wu et al., 2010) whilst knock down of the drosophila TDP-43 orthologue resulted in similar embryonic lethality suggesting that TDP-43 is an essential molecule in early development and that it is tightly regulated from the early stages of embryogenesis. Arguing against the loss of function mechanism are the dominantly inherited disease associated mutations in TDP-43, the A315T transgenic mouse model and the WT TDP-43 transgenic mouse model which demonstrate some of the ALS/ FTLD-U related pathology and disease progression (Wils et al., 2010).

Chapter 06:

Stable *tardbp* mutant

6.1 Introduction

Association of mutations in the *TARDBP* gene with familial amyotrophic lateral sclerosis (ALS) has confirmed the role of TDP-43 in ALS pathogenesis. Most of the mutations of the *TARDBP* gene are located in the glycine rich *C-termin*al domain. It is unclear to date if the 'loss of function' of the vital nuclear functions of TDP-43 or its toxic accumulation in the cytoplasm or in the nucleus or both, are responsible for the subsequent neuronal death. Various studies on cellular and animal models of TDP-43 function have shown that both over- expression of WT TDP-43 and the knockdown of the same is toxic to cells or the organism as much as over-expression of mutant TDP-43. Recently Kabashi et al (2010) showed that transient knockdown of the zebrafish orthologue of TDP-43, Tardbp, causes a motor phenotype and associated neuronal defects supporting a loss of function mechanism. The results described in chapter 5, did confirm some of the Kabashi et al 2010 findings, but we could not be certain if there was an off target effect from the AMO, although during our study we co-injected p53 AMO to control for some of the known off target effects.

It is widely believed that a stable mutant would overcome the limitations of the transient knockdown of genes. There are several methods for developing a stable mutant. One commonly used method is targeted induced local lesions in the genome (TILLING) wherein adult zebrafish are mutagenised following exposure to ethylnitrosurea (ENU) containing water (Moens et al., 2008). These F0 adult fish are out-crossed to generate the F1 founder fish that potentially carry a high degree of mutations in their genome. These fish can be fin-clipped to form a DNA library. Alternatively sperm can be obtained and frozen to generate a sperm library. Either DNA or sperm libraries could be used to screen for mutations in genes of interest by TILLING which uses PCR to amplify the disease related exons of targeted genes for mutation screening (Figure 6.1). Once a mutation in a gene of interest is identified,
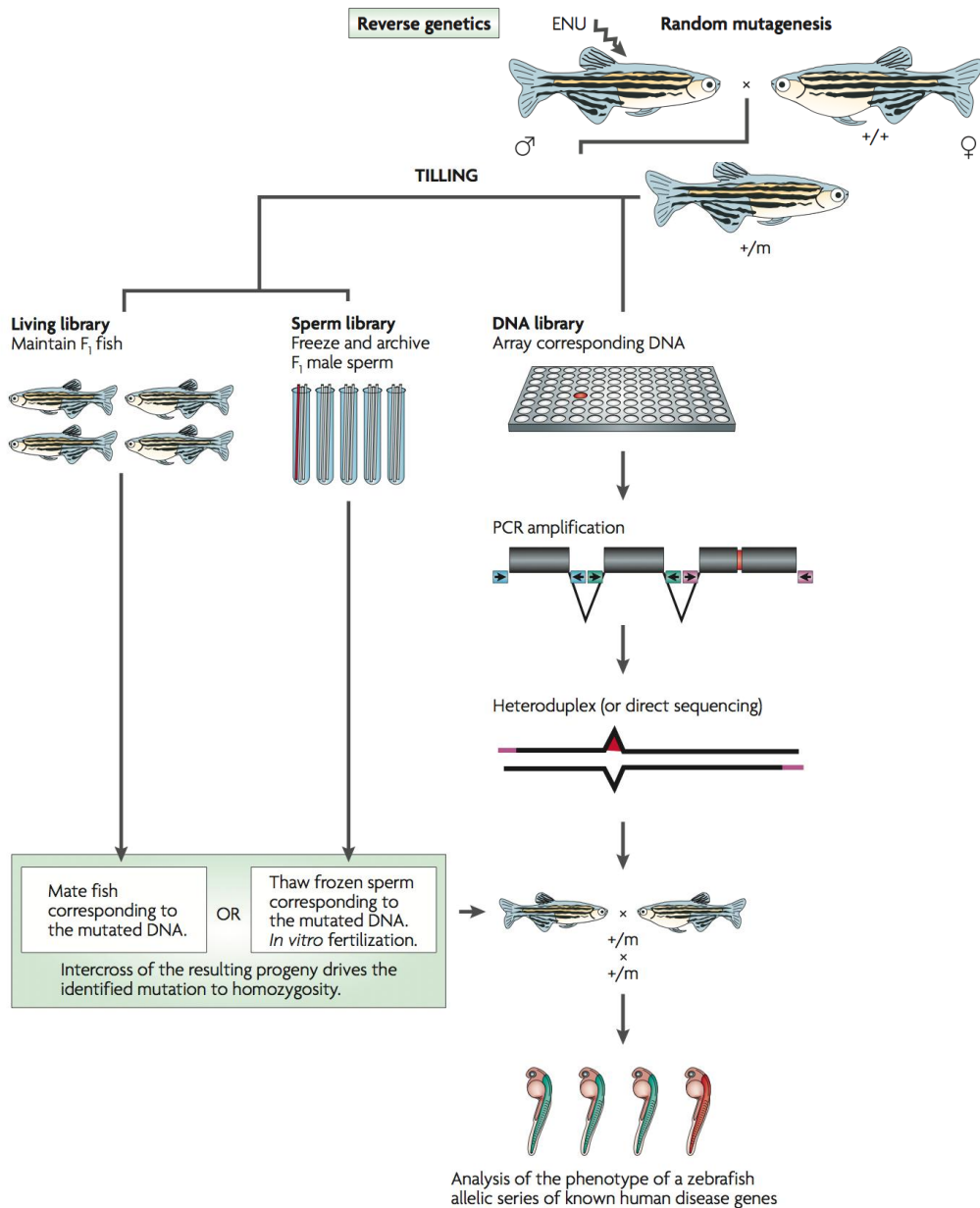
Figure 6.1 Important steps in targeting induced local lesions in the genomes (TILLING) to generate a mutant zebrafish. The adult zebrafish are exposed to 0.3nM ENU to mutagenise their spermatogonia. Mutagenised fish are then bred with wild type female fish to generate the F1 progeny. These F1 progency then are allowed to grow til adulthood when they are finclipped to form a TILLING library and/or sperm frozen for *in vitro* fertilisation in future. The library is then subjected to targeted gene screening, heteroduplex screening methods or whole genome sequencing (WGS) to identify relevant mutation/s. Fish harbouring mutation/s (+/m) are then out bred with wild type fish to reduce the effects of non phenotypic mutations (Stern and Zon, 2003). Adapted from (Lieschke and Currie, 2007).

the F1 fish are out-crossed to obtain an F2 generation of heterozygous fish. Similar out-crossings over 6 generations are then undertaken and heterozygotes thus identified are believed to reduce the risk of the non-causative mutations caused by ENU . We utilised this reverse genetics approach as it is efficient. Our collaborator's Prof Cecilia Moens laboratory in Seattle has established TILLING process and had identified a *tardbp* mutation in the F1 zebrafish.

Our aim was to obtain a zebrafish with a premature truncating mutation in the *tardbp* gene, therefore in the homozygous state one could expect the loss of the full length Tardbp protein, thus generating a stable Tardbp null zebrafish model. So far one ALS associated premature truncation mutation in the *TARDBP* gene has been described. Solski et al 2012 described c.1158_1159delAT; c.1158_1159insCACCAACC insertion-deletion in the glycine rich domain of the TDP-43 protein. The fibroblasts from the affected patients showed relative nuclear clearing under induced exogenous stress, with cytoplasmic accumulation of TDP-43 in keeping with what is observed in the neuropathology of TDP-43 proteinopathies. (Solski et al., 2012). Stable knockdown of Tardbp in other model systems have not been viable. Complete loss of Tardbp in the Drosophila model resulted in lethality at the second instar stage (Fiesel et al., 2009, 2010). Furthermore, knockout of Tardbp in mice caused early lethality around the blastocyst implantation stage of embryogenesis (Sephton et al., 2010, Wu et al., 2010), complicating the analysis of the role of Tardbp in vertebrate neuronal development and function. As discussed before the advantages of the zebrafish as a disease model allows us to overcome some of these limitations.

6.2   Generation of zebrafish *tardbp*^{fh301/+} mutant

As AMO injection can only knockdown *tardbp* transiently, we used ENU mutagenesis to generate a stable *tardbp* mutant. Mutation screening identified several point mutations as indicated by the black dots (Fig 6.2A). However, we were only able to obtain the c.660C>A mutant (Red dot on Fig 6.2A) from the frozen down sperm of the adult zebrafish exposed to ENU mutagenesis. The mutation results in a premature stop codon, p.Y220X which truncates the 413aa protein midway through its second RNA binding domain (Fig 6.2B). Protein

parameter   prediction   software   (http://web.expasy.org/cgi-bin/protparam/protparam) predicts a molecular weight of the premature truncated protein at ~24kDa and also predicts it to be unstable (instability index of 50.83 which suggests significantly unstable molecule highly likely to under go premature decay). This mutant *tardbp* allele is called fh_301 allele. Therefore from here on zebrafish heterozygous and homozygous to the mutation are indicated as *tardbp*$^{fh301/+}$ and *tardbp*$^{fh301/fh301}$ respectively.
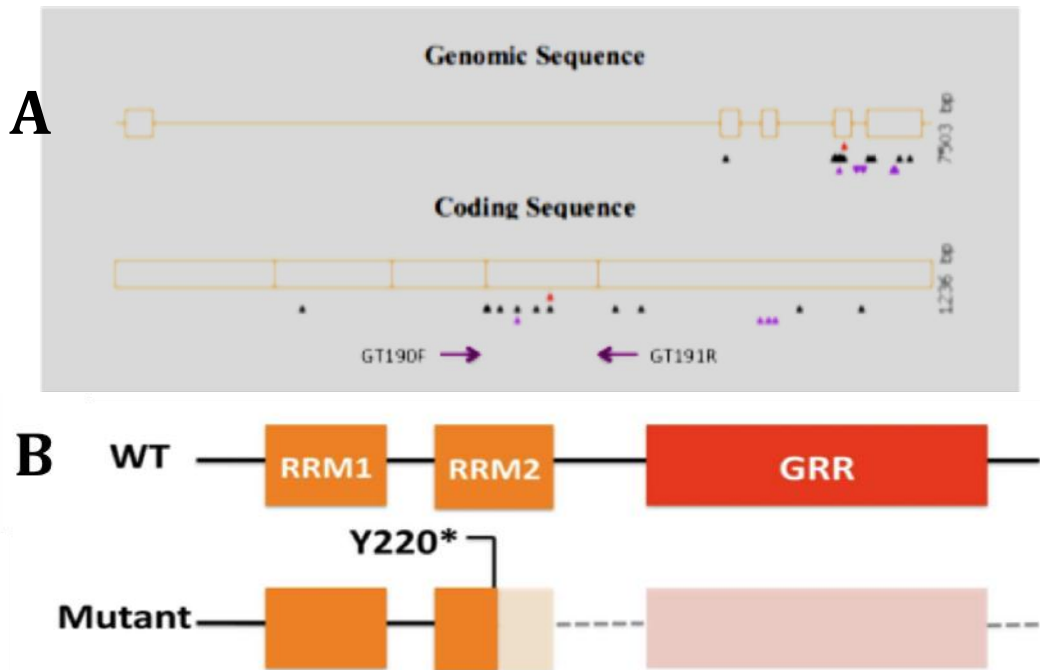
Figure 6.2 The *tardbp* fh301 mutant (*tardbp*$^{fh301/+}$) zebrafish generated by TILLING . A) Identified mutations in the zebrafish tardbp gene indicated in black and purple triangles in the genomic sequence and the coding sequence B) The c.660 C>A mutation results in a premature truncation mutation at the 220 amino acid (aa) residue (Threonine) in the RRM2 domain. (RRM1&2 -RNA recognition motif 1 and 2. GRR- Glycine rich region)
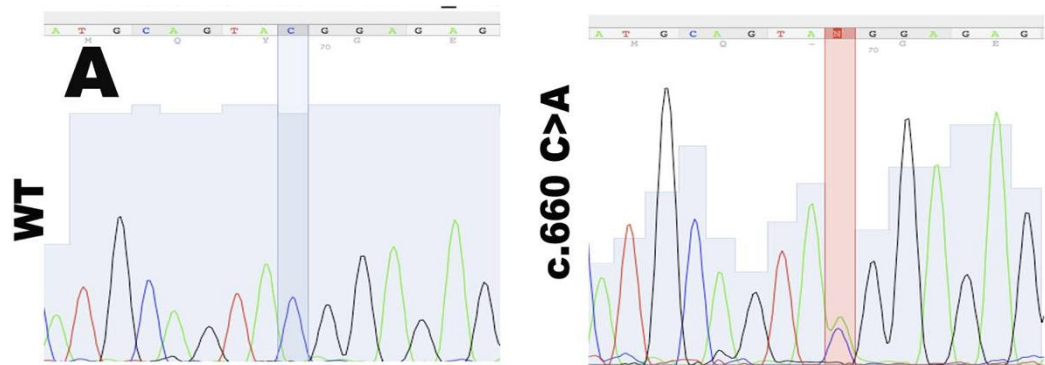
Figure 6.3 The c.660 C>A missense in frame mutation which is named *tardbp* fh301 mutant allele. A) Through mutation screening of a zebrafish ENU mutagenesis library, a c.660 C>A missense in frame mutation in *tardbp* was detected.

When we processed the nucleotide sequence of the mutant allele using the New England BioLabs software tool (http://tools.neb.com/NEBcutter2) we identified that the single nucleotide change from cytosine to adenine, c.660 C>A (Fig 6.3A) results in a loss of restriction enzyme digest sites of CviQI and RsaI (Figure 6.3A and B). This interruption of the CviQI restriction digest enzyme site was exploited to identify the genotype of the mutant zebrafish as depicted in the Figure 6.4C.

c.660 C>A allele

A

C

B **WT allele**
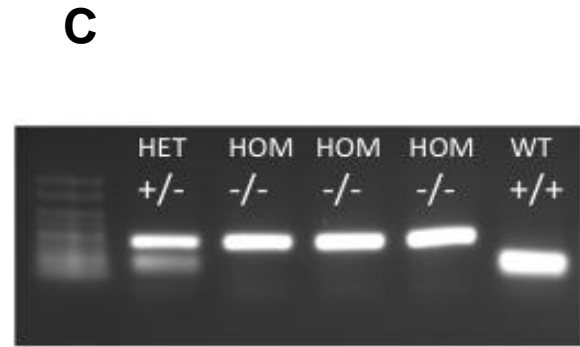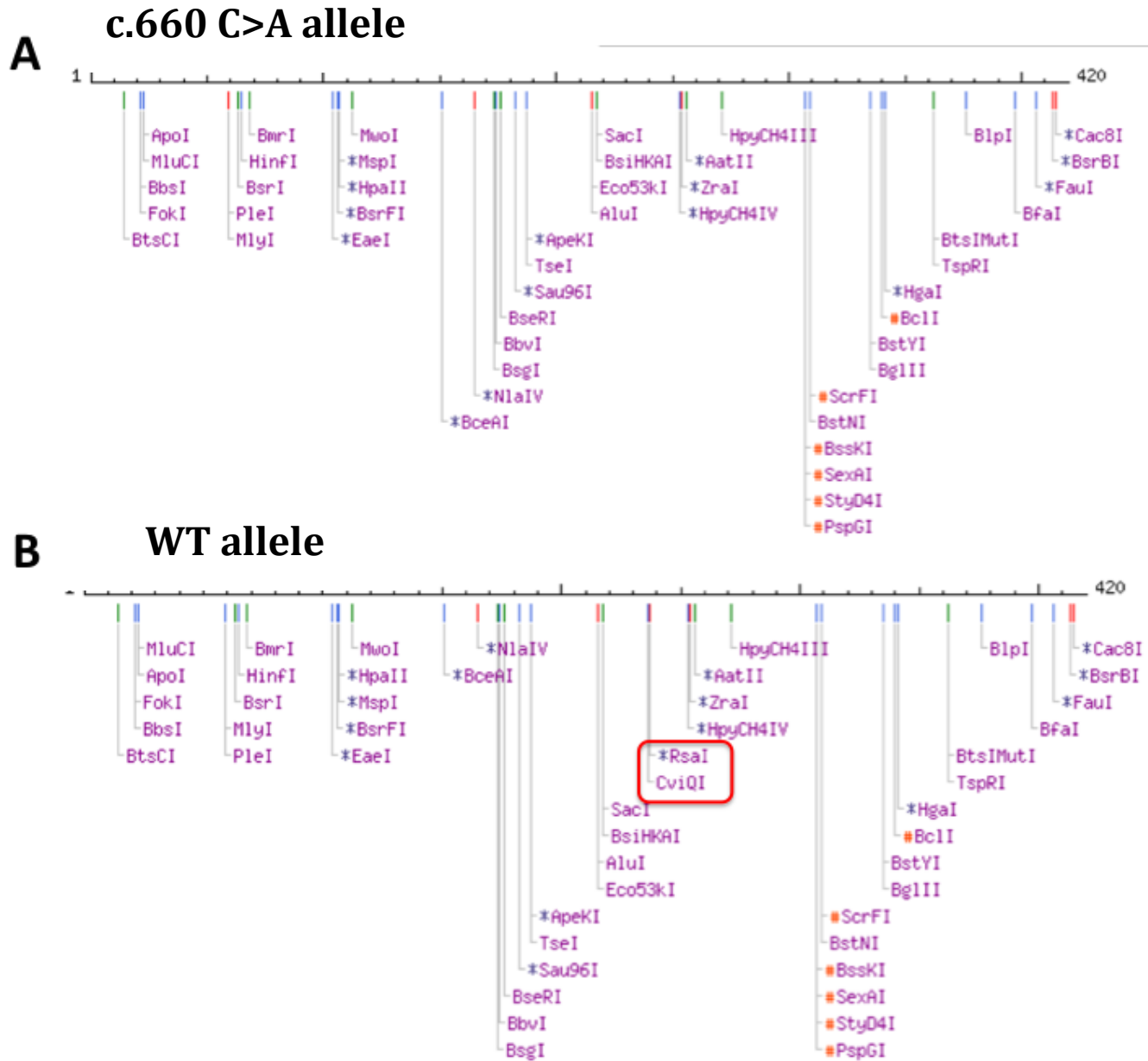
Figure 6.4 c.660 C>A results in a loss of CViQ1 restriction digest enzyme site. A & B) NEB cutter software prediction result of the loss of CviQI and RsaI restriction enzyme sites. C) PCR products from genomic DNA amplified using *tardbp* specific primers to amplify the targeted DNA to detect the above mutations. PCR products digested with CviQI results in digest products when run on an agarose gel with a pattern by which the genotype of the siblings from a tardbp heterozygous zebrafish incross can be easily identified. Circle indicates the the position of the CviQI and RsaI enzyme sites. HOM (*tardbp$^{fh301/fh301}$*). HET (*tardbp$^{fh301/+}$*). WT (*tardbp$^{+/+}$*).

6.3 The tardbp null *tardbp*^{fh301/fh301} (Homozygous) mutant is adult viable

Heterozygous *tardbp*^{fh301/+} animals were indistinguishable from their wild-type siblings. After repeated out-crossing, (F5) *tardbp*^{fh301/+} heterozygotes were selected and in-crossed to generate homozygous *tardbp* mutants (*tardbp*^{fh301/fh301}). Interestingly, the expected Mendelian ratios for a heterozygous (*tardbp*^{fh301/+}) in-cross were observed at 3 months indicating that the homozygous (*tardbp*^{fh301/fh301}) fish survived at the same rate as the *tardbp*^{+/+} and *tardbp*^{fh301/+} siblings. The mean weights and standard length of each adult F5 zebrafish were recorded at the time of fin clipping for genotyping. *tardbp*^{fh301/fh301} zebrafish were shorter in length ($p < 0.0001$) (Fig 6.5A) and lighter in mass ($p < 0.0001$) (Figure 5.5B) when compared to *tardbp*^{+/+} siblings.
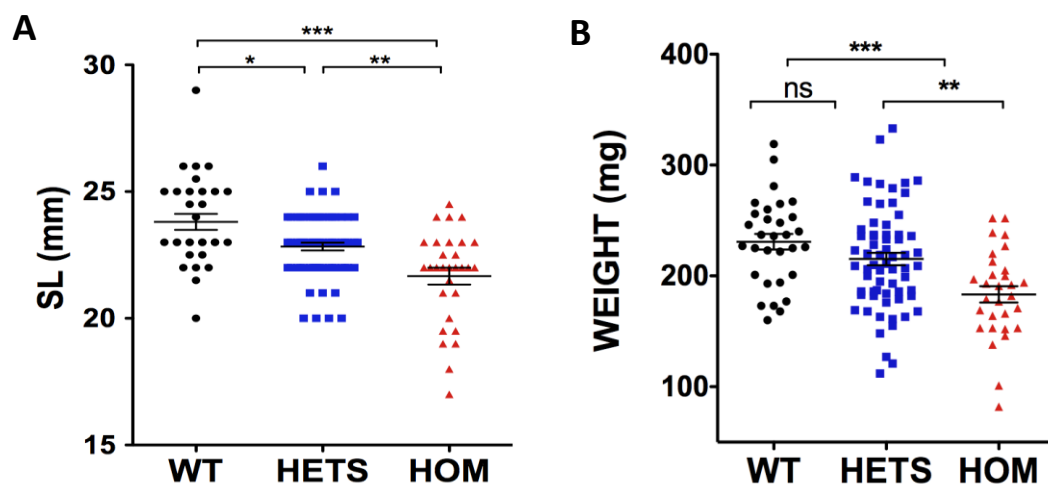
Figure 6.5 Siblings from the *tardbp*^{fh301/+} heterozygote in-cross have subtle phenotypic differences. A) Fry from a *tardbp*^{fh301/+} heterozygous in cross at F5 generation were fin clipped at 6 months of age to identify the genotype. The weights were significantly different between *tardbp*^{+/+} and *tardbp*^{fh301/fh301} (230mg, SD± 39 vs 183mg, SD± 40, $p < 0.0001$) and *tardbp*^{fh301/+} (215mg, SD± 46, $p < 0.001$). There was no significant weight difference between *tardbp*^{fh301/+} and *tardbp*^{+/+} ($p > 0.05$). B) Measurement of Standard Length revealed significant differences between *tardbp*^{+/+} (23.81mm, SD±1.76), *tardbp*^{fh301/+} (22.83mm, SD±1.26) and *tardbp*^{fh301/fh301} (21.67mm, SD± 1.84)(* $p < 0.01$, ** $p < 0.001$, ***$p < 0.0001$).

6.4 Tardbp expression in the homozygous ($tardbp^{fh301/fh301}$) zebrasfish

To study the Tardbp protein expression in the homozygous ($tardbp^{fh301/fh301}$) and their WT siblings, we dissected tissues from three 6 month old $tardbp^{fh301/fh301}$ and three $tardb^{+/+}$ zebrafish and obtained whole cell lysates of brain, eyes, muscle, heart, gills and liver for immunoblotting using the h.TDP-43 Ab2 (recognizes the *C-termin*us which is conserved between the TDP-43 and Tardbp). The $tardbp^{fh301/fh301}$ zebrafish tissues have undetectable levels of full-length functional Tardbp when compared to tardbp$^{+/+}$ tissue (Figure 6.6).
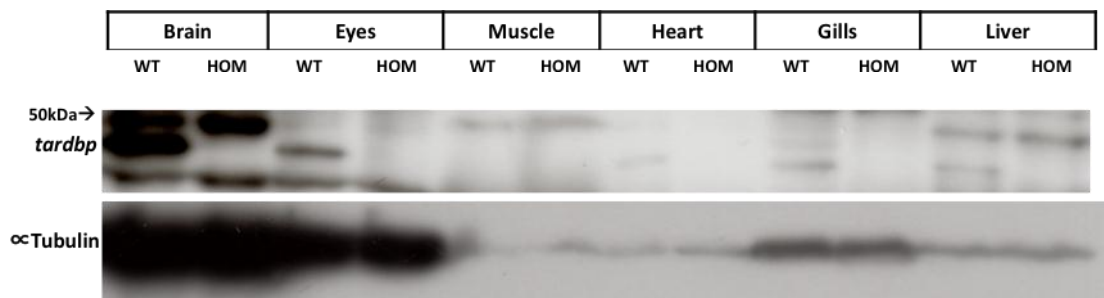
Figure 6.6 Full-length Tardbp protein is absent from homozygous mutant zebrafish ($tardbp^{fh301/fh301}$). An immunoblot probed with h.TDP-43 Ab2 (which binds to the *C-termin*us of TDP-43) demonstrates loss of Tardbp from all tissues in a 6 month old adult homozygous mutant zebrafish ($tardbp^{fh301/fh301}$). h.TDP-43 Ab2 is specific to Tardbp and does not detect Tardbpl.

Protein parameter prediction software (http://web.expasy.org/cgi-bin/protparam/protparam) predicts a molecular weight of the premature truncated protein at ~25kDa and also predicts the protein to be unstable (instability index of 50.83). In keeping with the above predictions and the h.TDP-43 Ab1 which detects the N- terminal fragment of TDP-43 does not show an increase in the 25kDa fragment in the $tardbp^{fh301/fh301}$ fish compared to the WT littermates (Fig 6.7). The above findings confirm that the premature truncation of Tardbp due to the Y220X mutation results in nonsense mediated decay of Tardbp. Therefore the $tardbp^{fh301/fh301}$ (homozygous) fish are 'Tardbp null'.

Brain		Eyes		Muscle		Heart		Gills		Liver	
WT	HOM	WT	HOM	WT	HOM	WT	HOM	WT	HOM	WT	HOM

50→
#

37→

25→

α Tubulin
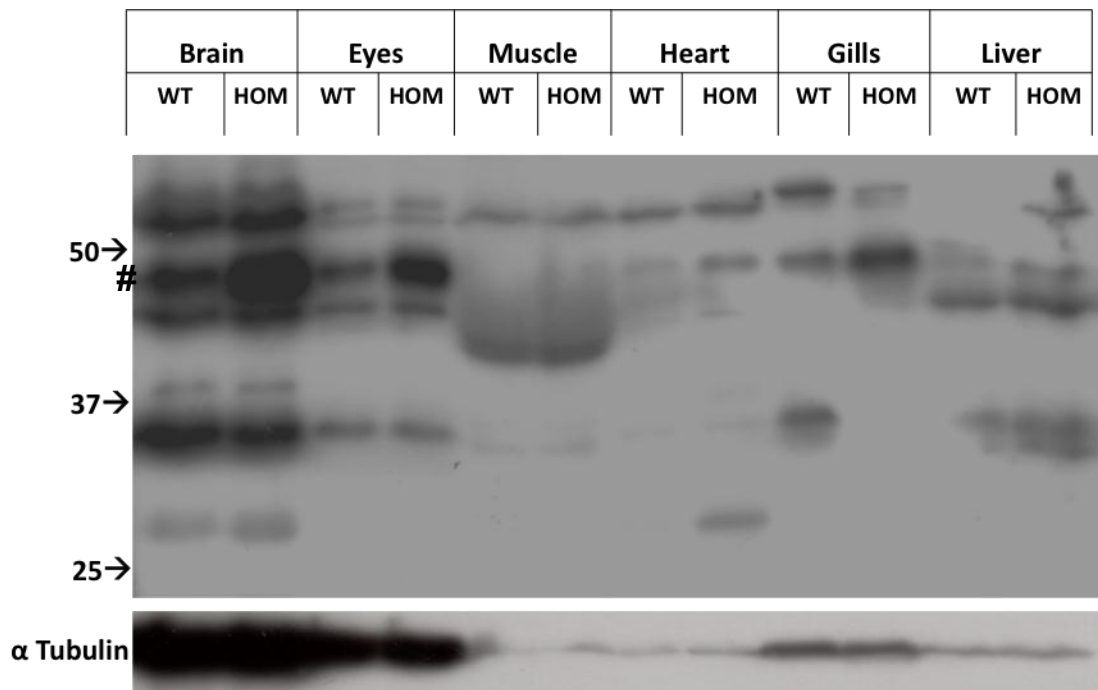
Figure 6.7 Western blot of tissues from 6 month old adult *tardbp*[fh301 /fh301] **zebrafish**. Compared to the *tardbp*^{+/+}, *tardbp*[fh301 /fh301] embryos have an over expressed signal at approximately 43 kDa molecular weight indicated by #. This relative over-expression of a protein similar to the molecular weight of Tardbp is present in all the tested tissues of *tardbp*[fh301 /fh301] adult zebrafish. There is no evidence of a 25kDa Tardbp truncated fragment in the *tardbp*[fh301/fh301] mutant fish. The antibody used is h.TDP-43 Ab1 which binds to the *N-term*inus of TDP-43.

6.5   Up regulation of Tardbpl full length protein (Tardbpl-FL) in the *tardbp* mutant zebrafish

TDP-43 is a tightly regulated protein, which is essential for DNA and RNA related nuclear functions, including the regulation of splicing (Buratti and Baralle, 2001, 2008). TDP-43 has also been shown to autoregulate its own protein level via the C-terminal end of the protein (reviewed by (Budini and Buratti, 2011). It has been reported that loss of TDP-43 in the early embryological stages is either lethal or causes significant motor deficits in mice and drosophila. Therefore it was unclear why our Tardbp mutant zebrafish survived until adulthood with apparently preserved motor function. Furthermore, as we observed, an up- regulation of Tardbp when Tardbpl was knocked down (Chapter 5), we hypothesised that a similar regulatory loop might be activated in the absence of Tardbp, by the up-regulation of Tardbpl.
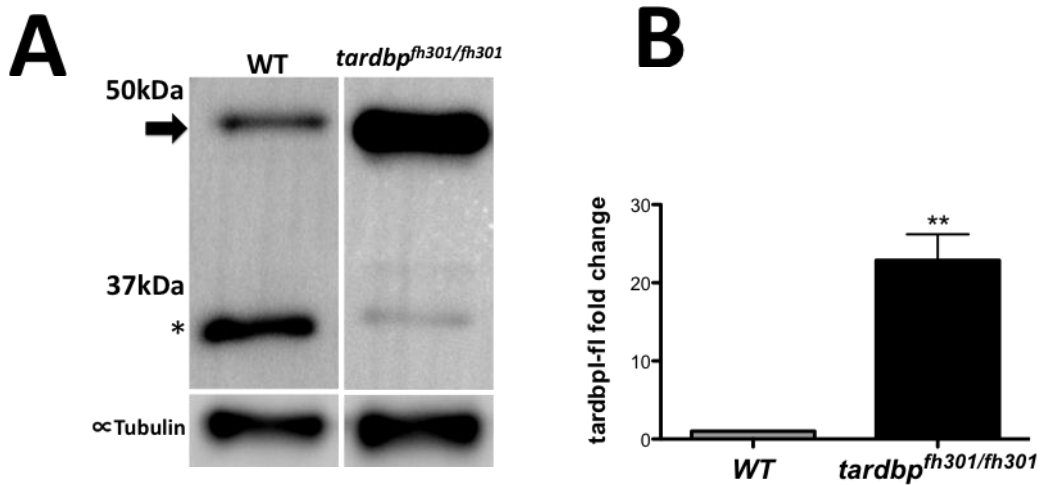
Figure 6.8 Compensatory over-expression of Tardbpl-FL in the Tardbpl null zebrafish embryos at 48hpf (A)Western blot of WT and *tardbp$^{fh301/fh301}$* embryos at 48hpf, probed with h.TDP-43 Ab1, demonstrating relative over expression of Tardbpl-FL (solid black arrow) and the reduction in Tardbpl expression in the *tardbp$^{fh301/fh301}$* mutant zebrafish (asterisk). (B) Densitometric analysis of the westernblots demonstrating the 25 fold over-expression of the ~43kDa band in the HOMs compared to the WT. Western blots carried out using h.TDP-43 Ab1 against the N-terminus which recognizes both Tardbp and Tardbpl/Tardbpl-FL proteins. ** p<0.01

Both Tardbp and Tardbpl share greater identity in the N-terminal end and we have shown that the h.TDP-43 Ab1 can detect both Tardbp and Tardbpl. We probed homogenates of various tissues from tardbp$^{+/+}$ and *tardbp$^{fh301/fh301}$* adult zebrafish. with h.TDP-43 Ab1 (Fig. 6.7). Interestingly, instead of an absent ~43kDa band we observed a 25 fold increase in the signal of the ~43kDa band in the *tardbp$^{fh301/fh301}$* fish when compared to the tardbp$^{+/+}$ littermates. This observation was the same at 48hpf (whole cell extract from embryos) (Fig 6.8) (p<0.001). A band at 33kDa suggestive of Tardbpl was detected in both tardbp$^{+/+}$ and *tardbp$^{fh301/fh301}$* fish, suggesting that the absence of Tardbp results in either an activation of a novel transcript, which shares similar molecular and structural characteristics to that of *tardbp* or that *tardbpl* under goes alternative splicing to generate a novel full-length tardbpl protein. Supporting this statement is the reduction in the expression of Tardbpl (33kDa band) in the *tardbp$^{fh301/fh301}$* compared to WT control embryos. Based on the findings of ensembl

genome browser, zebrafish has only two TDP-43 homologues. Therefore we hypothesised that the enhanced ~43kDa signal in *tardbp^{fh301/fh301}* lysates is due to a regulatory loop involving tardbpl.

6.6 Knockdown of Tardbpl using *AMO tardbpl^{ATG}* abolishes the compensatory rise in ~43kDa band, tardbpl-FL, in the HOMs

To confirm the findings described above, we designed an experiment to knockdown *tardbpl* expression in *tardbp^{fh301/fh301}* embryos obtained from an in cross of *tardbp^{fh301/fh301}* fish using *AMO tardbpl^{ATG}*. Proteins extracted from the Tardbp null embryos microinjected with *AMO tardbpl^{ATG}* at 48hpf and were probed with h.TDP-43 Ab1. Interestingly near complete (with 5ng of *AMO tardbpl^{ATG}*) and complete (with 16ng of *AMO tardbpl^{ATG}*) knockdown of the newly identified 43kDa protein was noted compared to the control AMO injected embryos (p<0.0001) (Fig 6.9). The reduction of the Tardbpl signal at 33kDa, following *AMO tardbpl^{ATG}* injection (Fig 6.9¥) further confirms that *AMO tardbpl^{ATG}* is specific to the *tardbpl* ATG site and the novel transcript shares a similar nucleotide structure at least at the translation initiation site with that of *tardbpl*. Therefore we named this protein as Tardbp full length (Tardbpl-FL).

6.7 *tardbp* and *tardbpl/tardbpl-FL* double knockouts have reduced survival and develop a severe motor phenotype

An experiment to knockdown *tardbpl/tardbpl-FL* in the homozygous *tardbp^{fh301/fh301}* embryos, obtained from homozygous in cross to overcome the possibility of maternal expression of *tardbp* was designed. A curly tail phenotype was observed as early as 32hpf (p<0.0001), when complete knock down of *tardbpl/tardbpl-FL* was achieved with 16ng of *AMO tardbpl^{ATG}* in *tardbp^{fh301/fh301}* embryos (Fig 6.10H) compared to the WT (Fig 6.10D) . Although injection of 5ng of *AMO tardbpl^{ATG}* into *tardbp^{fh301/fh301}* embryos resulted in near complete knock down of *tardbpl* and *tardbpl-FL*, and the embryos developed a less severe curly tail (p<0.0001)(Fig 6.10G), the phenotype progressively worsened with time (Fig 6.11). Complete knockdown of tardbpl/tardbpl-FL in the tardbp null embryos resulted in significantly reduced survival (all double knockout embryos died by 10dpf) (p<0.0001) (Fig 6.12) compared to those injected with control AMO. Although low dose (5ng *AMO tardbpl^{ATG}*) injected

group survived 6 days longer than the high dose *AMO tardbpl[ATG]* injected group (16ng), all embryos were sacrificed due to the inability to feed and distress by 16dpf, compared to the controls (Fig 6.12). The double knockouts had a significantly reduced escape response (p<0.0001) demonstrating a motor behavioural defect at 5 dpf caused by loss of both Tardbp and Tardbpl/Tardbpl-FL (Fig 6.13).
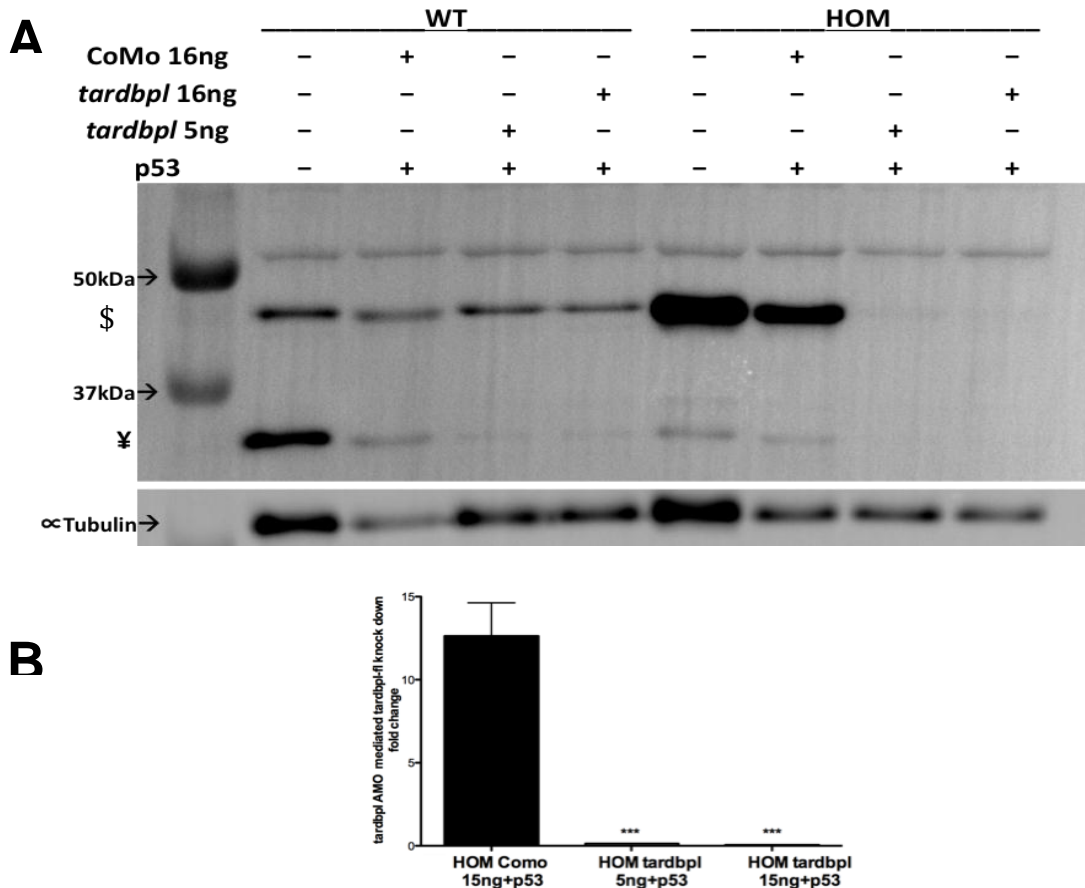
Figure 6.9 The *tardbp[fh301/fh301]* null phenotype is rescued by over- expression of a tardbpl full-length protein (tardbpl-FL). (A) Western blot of tissues from 6 month old adult *tardbp[fh301 /fh301]* zebrafish using h.TDP-43 Ab1 which binds to the N-terminus of TDP-43. Compared to the *tardbp^{+/+}*, *tardbp[fh301 /fh301]* embryos have an over expressed signal at approximately 43 kDa molecular weight indicated by $. This relative over-expression of a protein similar to the molecular weight of tardbp is present in all the tested tissues of *tardbp[fh301 /fh301]* adult zebrafish. (B) *AMO-tardbpl[ATG]* injection into *tardbp[fh301/fh301]* fish resulted in near complete (5ng) and complete (16ng) knockdown of tardbpl-FL over expression, and tardbpl (~33kDa - indicated by ¥) suggesting that *tardbpl* and *tardbpl-FL* share a similar translational initiation region. *** p<0.0001
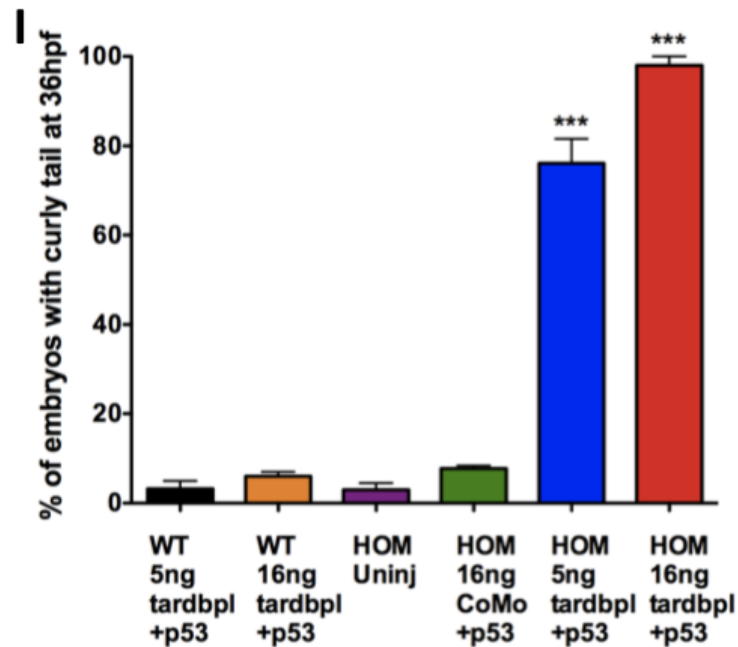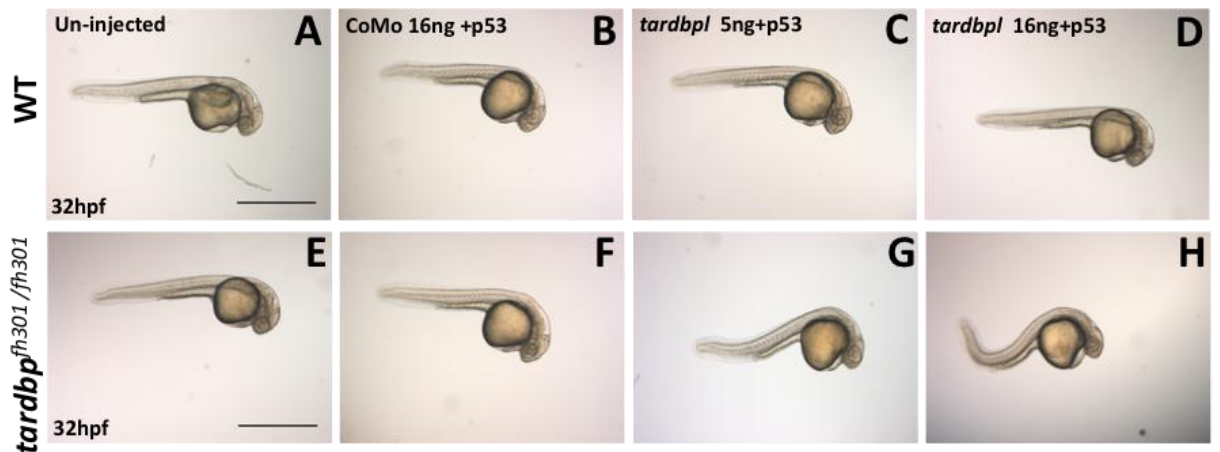
Figure 6.10 Effects of tardbpl knockdown in WT and *tardbp* null zebrafish embryos. (A-D) Uninjected, AMO-Control injected and *AMO-tardbpl^{ATG} with p53 (AMO-tardbpl^{ATG} +p53)* groups of WT (*tardbp$^{+/+}$*) embryos were morphologically normal when compared to *AMO-tardbpl^{ATG} with p53* injected HOM (*tardbp$^{fh301\ /fh301}$* embryos) zebrafish (E-H) which develop a curly tail phenotype at 32hpf. Complete knockdown of tardbpl results in almost 100% curly tail phenotype (*** signifies p<0.0001), whereas tardbpl knockdown in WT embryos developed no significant curly tail phenotype compared to control AMO injected embryos (I) at 32hpf. Scale bar 500μm.
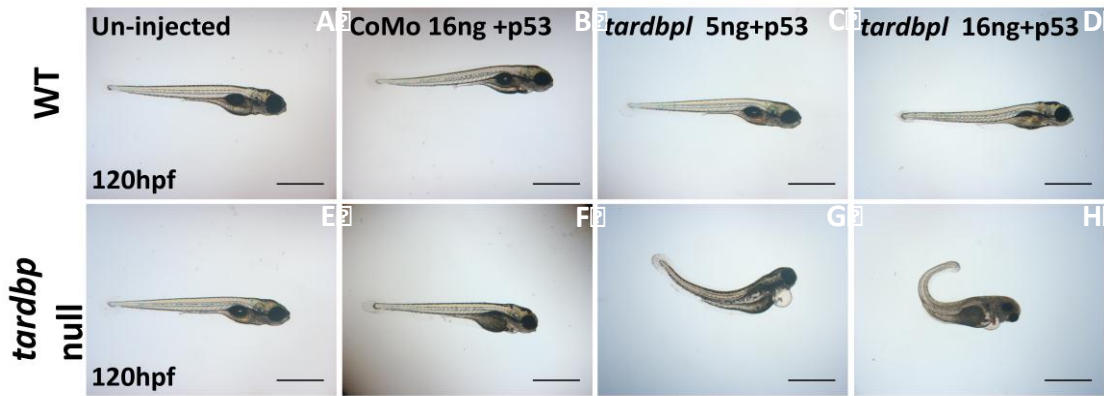
Figure 6.11 AMO knockdown of *tardbpl* in WT and *tardbp^(fh301/fh301)* **zebrafish embryos at day 5 (120hpf)**
(A)Uninjected, (B) AMO-Control injected and (C-D) *AMO-tardbpl^(ATG) with p53 (AMO-tardbpl^(ATG) +p53)* groups of
WT (*tardbp^(+/+)*) embryos were morphologically normal at 120 hours post fertilisation. (G-H) However
tardbpl/tardbpl-FL knockdown in the *tardbp^(fh301/fh301)* embryos (double knockouts) with *AMO-tardbpl^(ATG) + p53 AMO*
developed a severe curly tail phenotype at 120 hours post fertilisation (hpf). Scale bar 500μm.
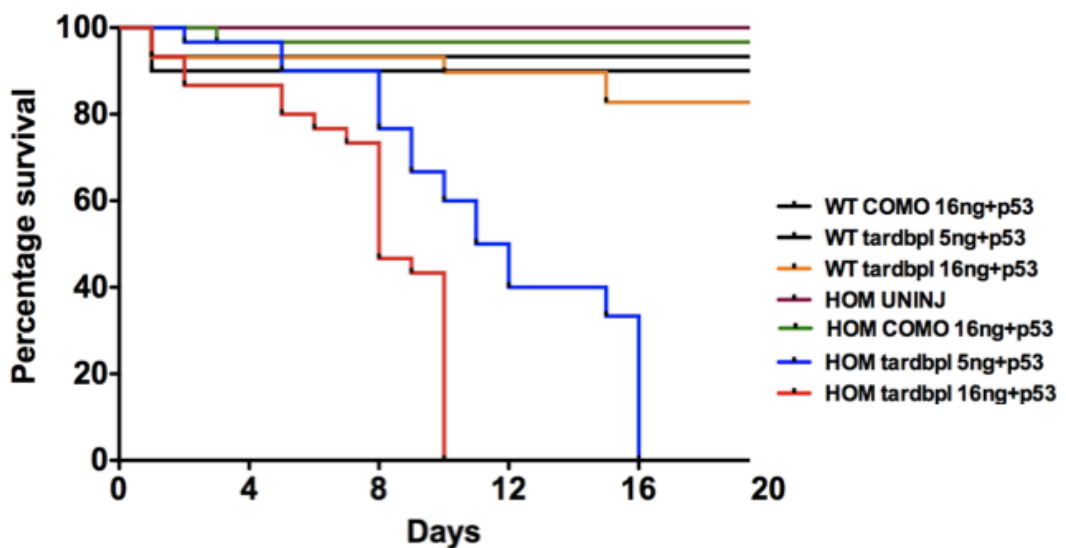
Figure 6.12 *tardbpl* knockdown reduces survival in the HOM. Double knockout of *tardbp*
and *tardbpl/ tardbpl-FL* significantly reduces survival of *tardbp^(fh301 /fh301)* embryos to 10dpf (16ng)
and 16dpf (5ng). Both Kaplan Meir curves are statistically significant compared to the AMO-
Control+p53 injected group (p<0.001).
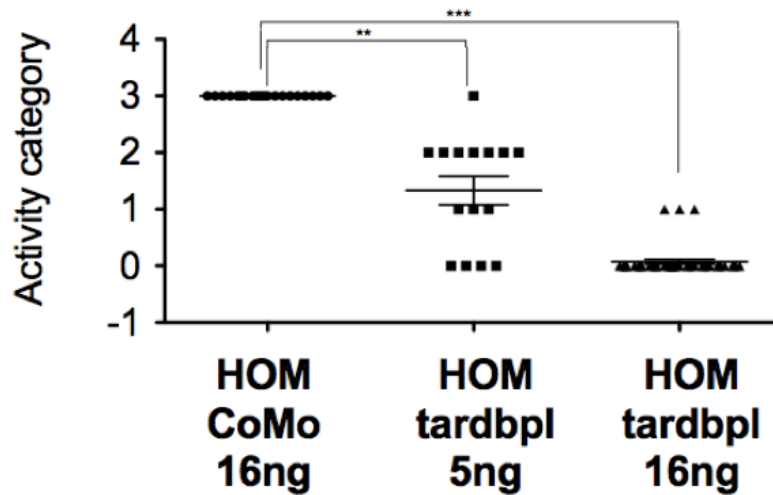
Figure 6.13 Escape response in Tardbp and Tardbpl/Tardbpl-FL knockouts at 5dpf. The double knockout zebrafish also had a significantly reduced escape response (p<0.001) demonstrating a motor behavioural defect caused by loss of both tardbp and tardbpl/tardbpl-FL. *** p<0.001, ** p<0.01

6.8 Loss of *tardbp* and *tardbpl-FL* results in significant axonal path finding defects

Knockdown of *tardbp* has been shown to result in axonal growth defects in zebrafish by others (Kabashi, 2010). It is well established that mutations in the *TARDBP* gene are associated with ALS and are therefore deleterious to motor neurons. However there was no significant difference in the motor defects between $tardbp^{fh301/fh301}$ and tardbp$^{+/+}$ littermates at 36hpf compared to uninjected embryos (Fig. 6.14A-C) and the *AMO-control* injected groups (Fig 6.14D-F). Therefore we analysed the axonal defects when both *tardbp* and *tardbpl* are knocked down. Interestingly, *tardbpl-FL* knock down in Tardbp null ($tardbp^{fh301/fh301}$) embryos resulted in complete arrest of axonal outgrowth at 36hpf with *AMO tardbpl^{ATG}* 16ng (p<0.001). A less severe axonal path finding defect was observed with a lower dose (5ng, p<0.01) of *AMO tardbpl^{ATG}* (Fig 6.14G-N) (in excess of what was observed with tardbp AMO injections to knockdown *tardbp* in WT zebrafish (Chapter 5). Taken together these findings confirm that *tardbpl* is a functionally important gene in the absence of Tarbdp and is able to compensate for the loss of *tardbp*. The significant axonal defects observed at 32hpf in the double knockout embryos, evolve to presynaptic axonal defects at 14days post fertilisation as

241

WT

tardbp$_{Y220*}$ -/-

Un injected

CoMo 16ng+p53

tardbpl AMO 5ng+p53

tardbpl AMO 16ng+p53

A

B

C

D

E

F

G

H

I

J

K

L

M

N

ns

ns

**

***

242
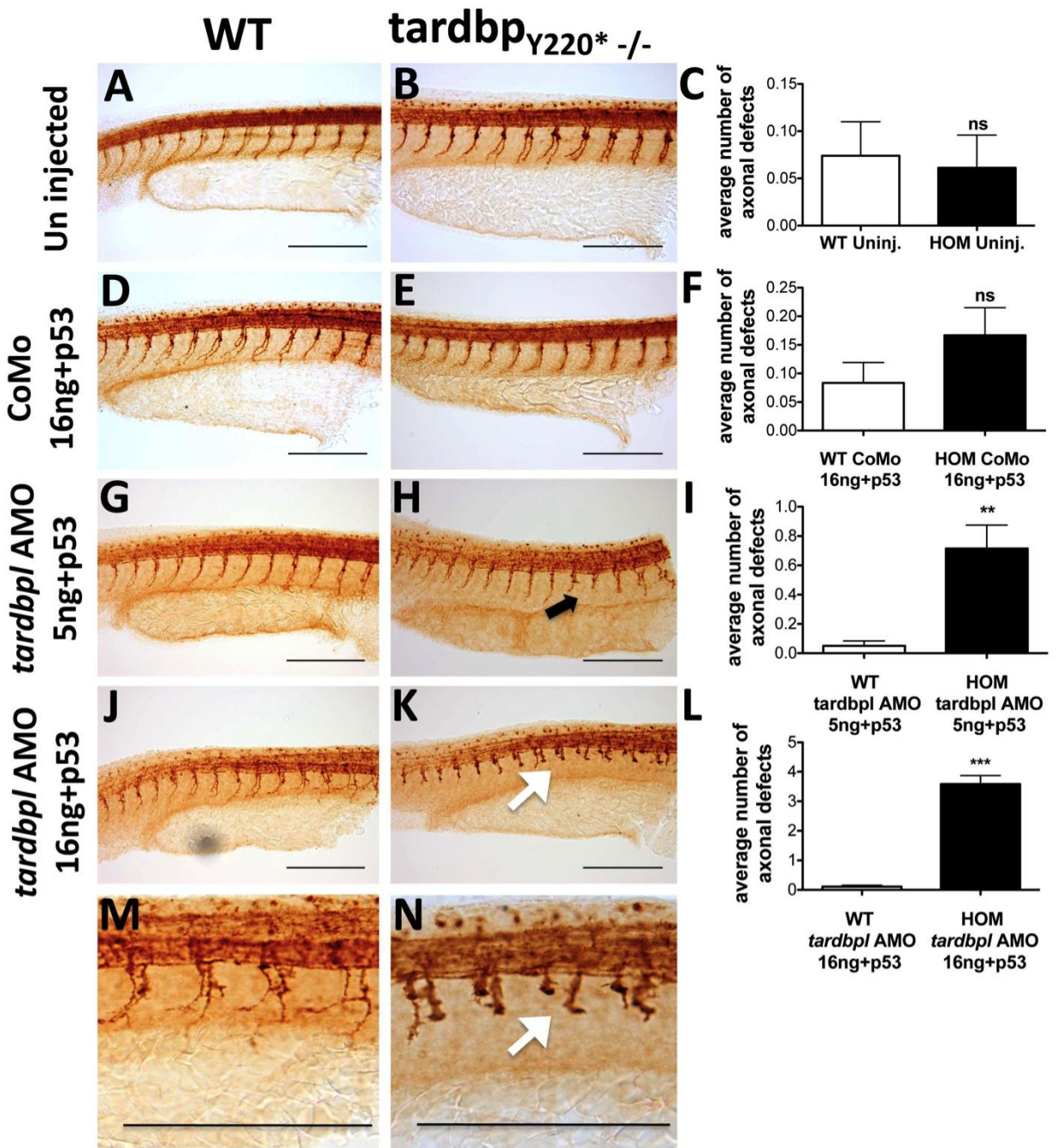
Figure 6.14 Motor axons are abnormal in Tardbpl-FL knocked down *tardbp*[fh301 /fh301]**embryos at 36hpf.** Lateral views of the whole mounted *tardbp*^{+/+}and *tardbp*[fh301 /fh301]embryos stained with Znp-1 to detect axons. (A-C) Uninjected *tardbp*[+/+](WT) and *tardbp*[fh301/fh301] do not show a significant difference in axonal defects similar to *AMO-control (CoMo)* injected groups (D-F). (G-I) Partial knockdown of *tardbpl-FL* with *AMO-tardbpl*[ATG] *+p53* results in a significant rise in the axonal defects in the *tardbp*[fh301 /fh301]mutant zebrafish(p<0.001). (J) Normal motor axons in tardbp^{+/+}injected with *AMO-tardbpl*[ATG] *16ng*. (K) Complete knockdown of *tardbpl-FL* in *the tardbp*[fh301 /fh301]resulted in severe axonal outgrowth defects with complete arrest of axons at the horizontal myoseptum, (p<0.0001)(L). (M&N) Enlarged sections of J&K demonstrating severe axonal out growth defects in the double knockout (tardbp and tardbpl) embryos. Black arrow points at an infrequent axonal truncation defect (low dose *AMO-tardbpl*[ATG]) whilst white arrows indicate numerous axonal out growth defects (high dose *AMO-tardbpl*[ATG]). Scale bar 200µm.

depicted by neuromuscular junction staining. This is only an observation of a single experiment and requires further repeats to confirm the true association. From the available NMJ staining of several different double knockout embryos it was apparent that there is a loss of presynaptic marker (SV2) staining in the double knockouts (Figure 6.15). We did not observe a difference in NMJ staining in *tardbp*[fh301/fh301] and tardbp^{+/+} siblings.
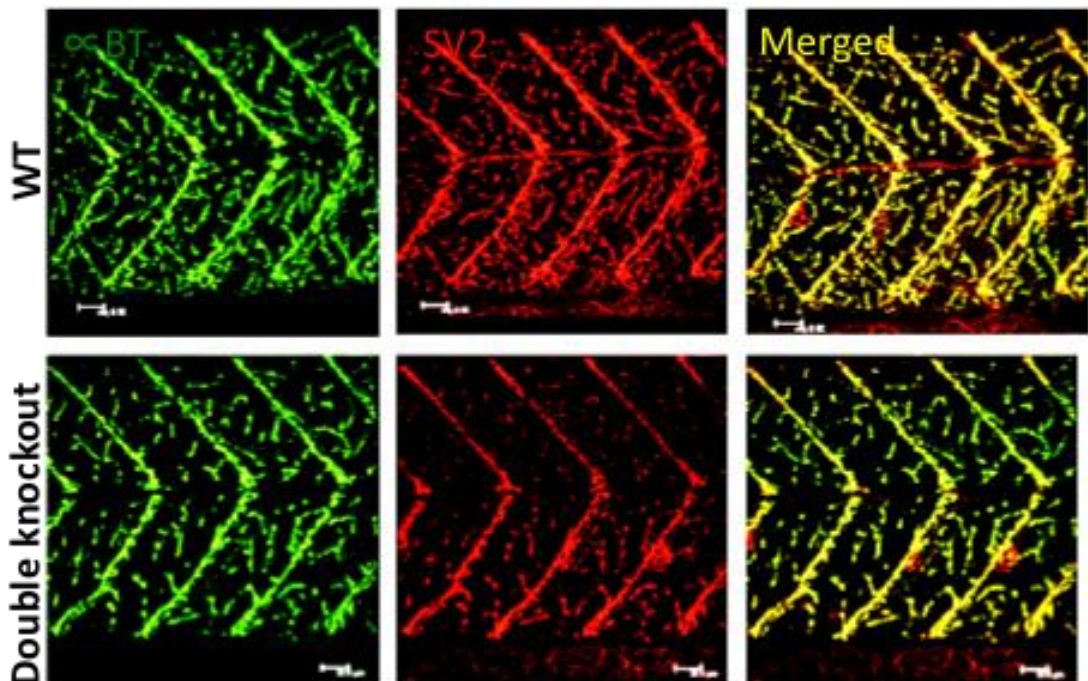
Figure 6.15 Neuro-muscular junction (NMJ) staining at 14dpf in the *tardbp/tardbpl* **knockout zebrafish show a loss of pre-synaptic markers.** Compared to the WT (upper three panels) the double knockout (bottom three panels) demonstrate marked loss of the pre-synaptic marker (SV2). The post synaptic marker used was alpha bungaratoxin. Pictures obtained by confocal microscopy.

6.9   *tardbpl-FL* is the newly identified alternatively spliced *tardbpl* transcript

The basal levels of Tardbp and Tardbpl differ in the *tardbp^(+/+)* and *tardbp^(fh301/fh301)* zebrafish. In *tardbp^(fh301/fh301)* animals the compensatory over-expression of *tardbp-FL* is associated with a reduction in 33kDa Tardbpl levels, which indicated to us the possibility of an alternative-splicing event involving *tardbpl*. We speculated that

this potential alternative-splicing event might give rise to *tardbpl-FL* (Fig 6.16). Theoretically *tardbpl-FL* should have significant identity at nucleotide level in the translation initiation site with *tardbpl* as *AMO tardbpl^(ATG)* is able to knockdown *tardbpl-FL* and *tardbpl*. Therefore we re-examined the TDP-43 orthologues of zebrafish. Using BLAST, the *tardbpl* sequence (ENSDARG00000004452) was used for ascertaining the intron/exon boundaries. The intron/exon boundaries for *tardbpl* and cDNA sequence for Genbank predicted *tardbpl* was manually computed to obtain an open reading frame, from which a theoretical amino acid sequence was generated. This analysis resulted in the discovery of a newly identified isoform of the Tardbpl protein with 398 amino acids, which we called Tardbpl-FL.

Further analysis of *tardbpl* intron exon boundaries and alignment with *tardbpl-FL* sequence was undertaken, which led us to the identification of an intronic sequence between exon 5 and 6 of *tardbpl*, which is able to code for the missing amino acids of Tardbpl (Fig 6.16). Furthermore within this intronic region we also identified a stop codon. It is therefore plausible that *tardbpl-FL* is a consequence of an alternative-splicing event, which results in an inclusion of intron 5-6 of *tardbpl*. This intron contains the necessary coding for the essential C-terminal amino acids. We also identified a UGUGU motif near the splice donor site of exon 6 in *tardbpl* gene (Fig 6.16). Although this motif is not a canonical high affinity RNA binding site of TDP-43, it has the elements for interacting with TDP-43 during splicing (Ayala et al., 2006), suggesting that Tardbp could potentially promote the splicing event which results in exclusion of the intron 5-6 of *tardbpl* by binding to the UGUGU site. So, in the absence of tardbp this inhibitory loop is abolished, and results in an alternative-splicing event where by intron 5-6 is included to generate *tardbpl-FL*. As *tardbpl-FL* encodes a 398aa protein it is able to rescue the Tardbp null phenotype. Furthermore in the 3'UTR of the *tardbpl*

transcript we found a canonical TDP-43 high affinity binding site -(GU)$_6$ via which TDP-43 has been shown to inhibit expression of target mRNAs (Ayala et al., 2011b). Taken together, we demonstrate that Tardbpl plays an important role in the regulation of the optimal level of zebrafish Tardbp function that is vital for the zebrafish development and neuronal health. An alteration of the optimal Tardbp level results in changes in the interaction of Tardbp with its RNA targets in an attempt to restore the status quo. In the case of the Tardbp null zebrafish, the predicted alternative splicing event results in alternative splicing of *tardbpl* giving rise to *tardbpl-FL*.
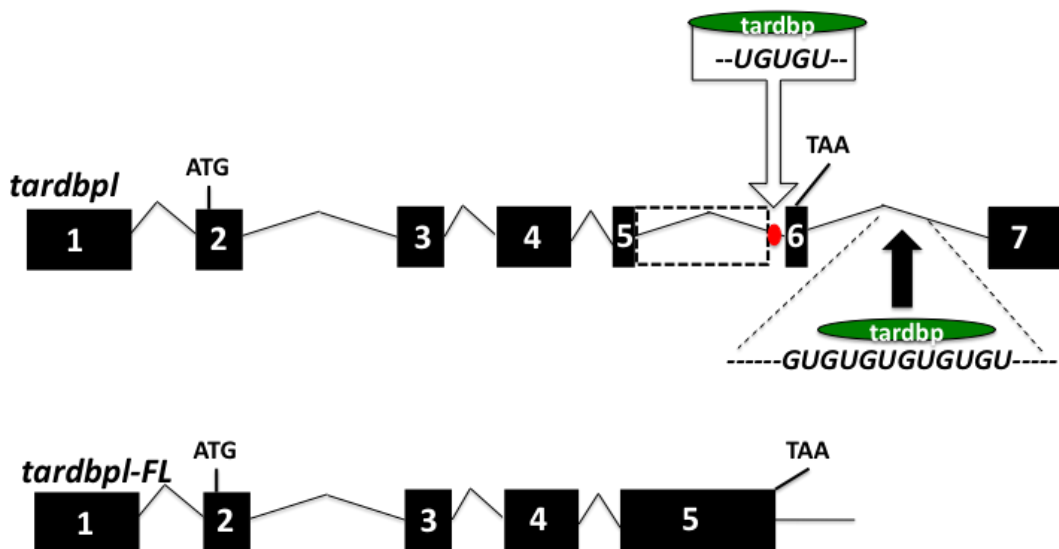
Figure 6.16 Alternative splice event of *tardbpl* gives rise to *tardbpl-FL*, which rescues tardbp[fh301/fh301] **null phenotype.** Intron 5-6 of the *tardbpl* (ENSDART00000027255) on chromosome 23 contains a coding sequence, which potentially could give rise to a longer Tardbpl protein (Tardbpl-FL). In the intron 5-6 is a TDP-43 binding site depicted by ~*UGUGU*~. There is also a canonical high affinity TDP-43 binding site -(GU)$_6$ in what might be the 3'UTR region of *tardbpl-FL* via which tardbp could potentially suppress the *tardbpl-FL* mRNA. (Bottom diagram) Predicted alternative splicing event, which results in inclusion of intron 5-6 creating *tardbpl-FL*.

6.10   RT-qPCR confirms that in the *tardbp*[fh301/fh301]   *tardbpl-FL* is over-expressed at the expense of Tardbpl, at RNA level, indicating an auto-regulatory alternative splicing event

We performed RT-qPCR using transcript specific primers designed across exon-exon boundaries to quantify the relative abundance of the two splice isoforms of

tardbpl. An internal primer set (Table 6.1) was designed to cross the exon 2-3 boundary in the 5' end of *tardbpl,* which is common to both isoforms. cDNA amplified using the RNA extracted from both *tardbp⁺/⁺* and *tardbp^{fh301/fh301}* embryos showed that in the *tardbp^{fh301/fh301}* embryos *tardbpl-FL* is over-expressed by as much as 2.4 fold (ΔΔ CT, WT-HOM *tardbp^{fh301/fh301}* 1.27), whilst *tardbpl* expression is reduced by 0.8 fold ((ΔΔ CT, WT-HOM *tardbp^{fh301/fh301}* -0.21) (Fig 6.17A-C). These data confirm the alternative splicing event involving *tardbpl.* Furthermore when the amino acid sequences of Tardbp and Tardbp-FL were aligned, we noticed that Tardbpl-FL has lost 8 glycine residues from the GRD (Fig 6.18). This observation might explain the relatively benign nature of *de novo* 20 fold over-expression of Tardbpl-FL protein, compared to the toxicity of over-expression of TDP-43 seen in *in vivo* and *in vitro* studies (Ash et al., 2010, Igaz et al., 2011) and also may explain why *tardbpl-FL* cannot alter its own splicing. Interestingly we also observed that when amplified using the target PCR primers on RT-qPCR products, *tardbpl-FL* RNA is present even at an early stage of embryonic development in both *tardbp⁺/⁺* and *tardbp^{fh301/fh301}* embryos (Figure 6.19).

Table 6.1 Primers used in characterisation of *tardbpl and tardbpl-FL* and in RT-qPCR	
Primer name and location	**5'→3'**
1 **TDPL-F-1-5UTR**	AAATTACTTGTTTTGTGCACATTCG
2 **TDPL-F-2-ATG SPAN**	GCATTCGGTGTAATCATGACG
3 **TDPL-R-1-TAG SPAN (exon 5)**	CCCTACATTCCCCAACTGG
4 **TDPL-R-2-3UTR**	ATACTCTGATATGTGGGCATACTGA
5 **TDPL-R-EXON3**	AGTTTGCAGTCGCACCATC
6 **TDPL-F-EXON3**	GAGTGGAAATTCCAAAGGATTC
Primer 6+3= primer set 1	*tardbpl-FL-* C-terminus (reverse primer in the spliced intron)
Primer 2+4= primer set 2	*tardbpl-* C-terminus
Primer 1+5 = primer set 3	Internal control for both *tardbpl* and *tarbpl-fl*

6.17 Quantification of splice variants of *tardbpl* by RT-qPCR primer sets and critical threshold calculation.

A) Primer set 1 was designed to specifically identify *tardbpl-FL* exon-exon boundaries. Primer set 3 was designed as an internal control to detect exon 1-2 of *tardbpl, which* is identical for *tardbpl-FL*. Amplification curves show a ΔCT value of 1.74 between WT and HOMS and a $\Delta\Delta$CT value of 1.27. Primer dimers are non-significant. B) Primer set specifically identifies *tardbpl*. Forward primer of primer set 2 is common to both *tardbpl* and *tardbpl-FL*. However reverse primer of primer set 2 is specific for *tardbpl* and it sits on exon 5-6 boundary of *tardbpl*. Amplification curves show no impact from primer dimers and a $\Delta\Delta$CT of -0.21 for WT-HOM. C) The expression of *tardbpl* and *tardbpl-FL* specific primers were corrected for by internal control (primer set 3) and a house keeping gene eIF4$\propto$.

tardbpl-FL

Primer set 1 (1), Primer set 3 (3)

$WT_{CT} - HOM_{CT} = \Delta CT = 1.74$

$\Delta\Delta CT = 1.27$

tardbpl

Primer set 2 (2), Primer set 3 (3)

$WT_{CT} - HOM_{CT} = \Delta\Delta CT = -0.21$

$WT_{CT} - HOM_{CT} = \Delta CT = 0.47$

A

B

C

Primer set 1 = *tardbpl-FL*
Primer set 2 = *tardbpl*
Primer set 3 = internal control
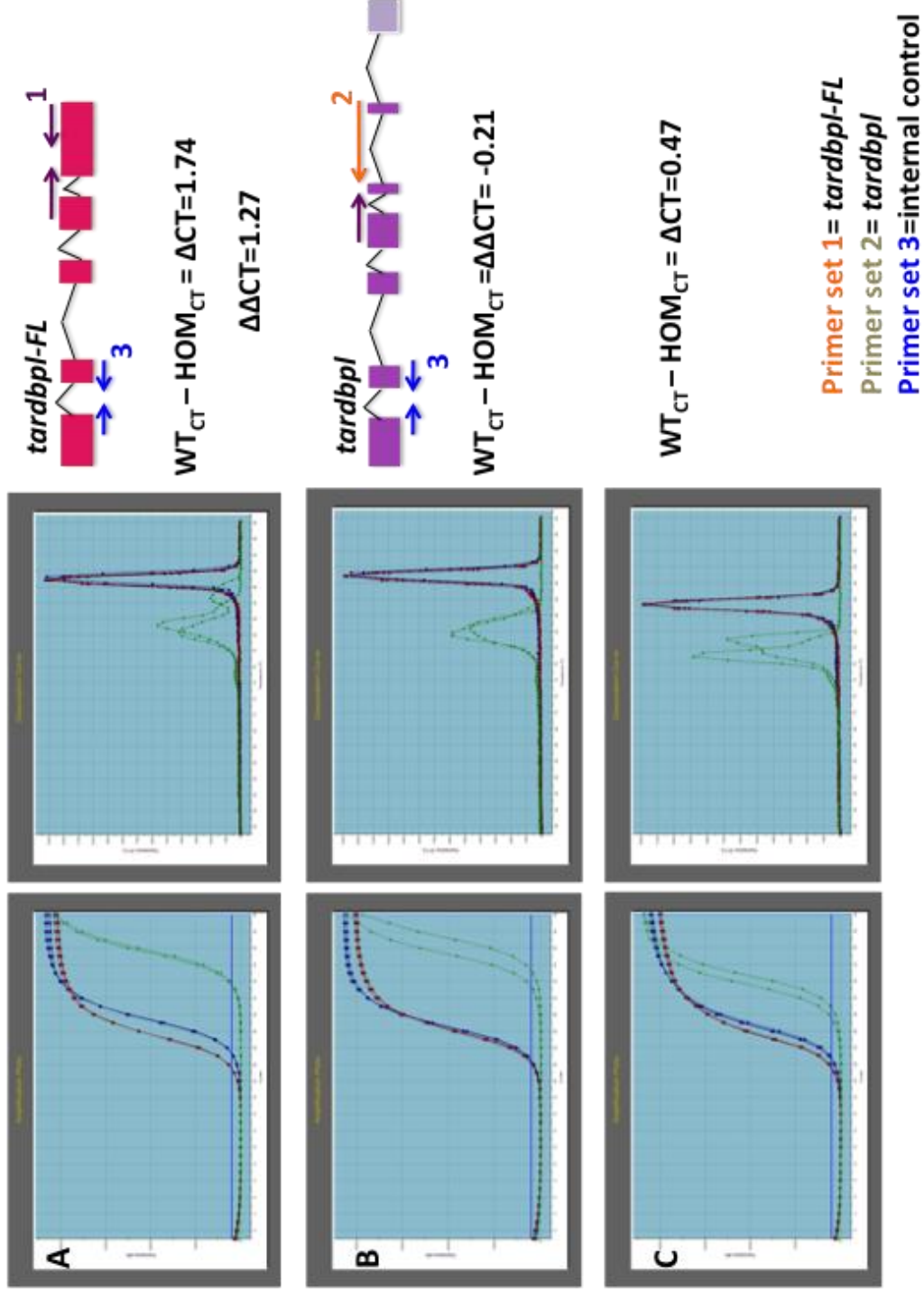
```
CLUSTAL 2.1 multiple sequence alignment


Danio_tardbp        MAEMYIRVAEEENEEPMEIPSEDDGTVLLSTVSAQFPGACGLRFRSPVSQCMRGVRLVDG 60
Danio_tardbpl-FL    MTECYIRVAEDENEEPMEIPSEEDGTVLLSTVAAQFPGACGLRYRSPVSQCMRGVRLVEG 60
                    *:* *****:***********:*********:**********:************* :*

Danio_tardbp        ILHAPENGWGNLVYVVNYPKETVLPDNKRKMDEIDASSATKIKRGDQKTSDLIVLGLPWK 120
Danio_tardbpl-FL    VLHAPEADWGNLVYVVNYPKD-----NKRKMDEMDAASAVKIKRGIQKTSDLIVLGLPWK 115
                    :***** .************:      *******:**:**.***** *************

Danio_tardbp        TSEQDLKDYFGTFGEVIMVQVKRDVKTGNSKGFGFVRFGDWETQSKVMTQRHMIDGRWCD 180
Danio_tardbpl-FL    TTEQDLKDYFGTFGEVIMVQVKRDAKSGNSKGFGFVRFTDYETQIKVMSQRHMIDGRWCD 175
                    *:*********************.*:**********:**  *:*** ***:*********

Danio_tardbp        CKLPNSKQGIDEPMRSRKVFVGRCTEDMTADELRQFFMQYGEVTDVFIPKPFRAFAFVTF 240
Danio_tardbpl-FL    CKLPNSKAGPDEPMRSRKVFVGRCTEDMTADELRQFFMQYGEVTDVFIPKPFRAFAFVTF 235
                    ******* * **************************************************

Danio_tardbp        ADDQVAAALCGEDLIIKGVSVHISNAEPKHNNTRQMMERAGRFGNGFGGQGFAGSRSNMG 300
Danio_tardbpl-FL    ADDQVAQSLCGEDLIIKGTSVHISNAEPKHNNSRQMMDR-GRFG-GYGGQGFGSSRS--- 290
                    ****** :**********.************:****:* **** *:*****..***

Danio_tardbp        GGGGGSSSSLGNFGNFNLNPAMMAAAQAALQSSWGMMGMLA-QQNQSGTSGTSTSGTSSS 359
Danio_tardbpl-FL    ------PNSNVNFGALNLNPAMMAAAQAALQSSWGMMGMLANQQNQTPASGTNPSGQSGS 344
                    ..*   *** :********************** ****: :***..** *.*

Danio_tardbp        RDQAQTYSSANSNYGS-SSAALGWGTGSNSGAASAGFNSSFGSSMESKSSGWGM 412
Danio_tardbpl-FL    RDQTQNYSASSNNYNAGSSAALGWGAGTNS-AAAGGFNSSFGSSMETKSS-WGM 396
                    ***:*.**::..**.: ********:*:** **:.***********:*** ***
```

Figure 6.18 ClustalW2 alignment of the Tardbp and predicted Tardbpl-FL amino acid sequences. Both the N and the C-termini are highly conserved. Tardbpl-FL is missing nine amino acids from the GRD, of which six are glycine residues (Highlighted in grey).
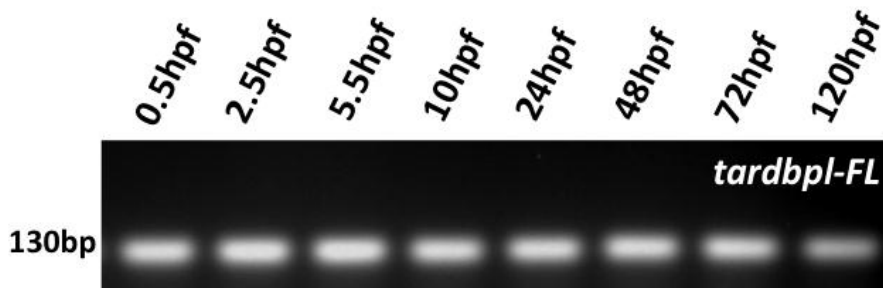
Figure 6.19 RT-qPCR products amplified using targeted PCR primers for *tardbpl-FL*. Agarose gel showing that *tardbpl-FL* RNA is expressed from an early stage of development in the *tardbp*[fh301/fh301] mutants.

6.11 Curly tail motor phenotype associated with *tardbp*[ATG] AMO injection is likely to be caused by a p53 pathway independent, off target effect.

It was puzzling to discover that *tardbp*[fh301/fh301] fish survived till adulthood with no obvious motor phenotype. We have shown that full-length Tardbp null phenotype is rescued by the over-expression of Tardbpl-FL protein. We also have shown that

249

obliteration of *tardbpl* and thus *tardbpl-FL* translation initiation results in a severe motor phenotype and reduced survival in the *tardbp^{fh301/fh301}* but not in *tardbp^{+/+}* siblings (Figure 6.11 and 6.12). Therefore we undertook to investigate the reasons why a transient *tardbp* knockdown model in the zebrafish by Kabashi et al 2010 and later by us (Chapter 5) resulted in a severe motor phenotype and was not rescued by a similar rescue mechanism like Tardbpl-FL up-regulation in *tardbp^{fh301/fh301}* (Kabashi, 2010). One hypothesis to explain this was that of 'off target effects' of *tardbp^{ATG}* AMO could result in a phenotype via activation of *p53* as Kabashi et al did not co-inject anti *p53* ^{ATG} AMO. Therefore when we transiently knocked down *tardbp* using AMO we co-injected embryos with anti *p53* AMO as per Robu et al guidelines (Robu et al., 2007). Although we observed a statistically significant improvement in the curly tail phenotype with co- injection of *tardbp^{ATG}* and *p53* AMO, still the motor phenotype was significantly abnormal compared to the controls (Chapter 5). A second hypothesis to explain the discrepancy between transient and stable knockdown of Tardbp was that an acute knockdown of a gene *tardbp*)may result in rapid changes in the protein levels causing a phenotype due to lack of time for adaptation, whereas in the *tardbp^{fh301/fh301}* mutants have undergone a degree of adaptation from the maternally transmitted tardbp at the point of generation of the F6. Another hypothesis was that the *tardbp^{ATG}* AMO could potentially knockdown both Tardbpl and Tardbpl-FL proteins. To test all three hypotheses we designed an experiment to co-inject *tardbp^{ATG}* AMO with *p53* AMO into both *tardbp^{fh301/fh301}* and *tardbp^{+/+}* embryos.

Immunoblot from protein extracts obtained from various injection categories when probed with h.TDP-43 Ab2 (N-terminus) as depicted in figure 6.20A control AMO injected *tardbp^{+/+}* (WT) controls demonstrate Tardbl-FL (⚲) and Tardbpl expression appears more than that of Tardbp) (lane 1 Fig 6.20A). The *tardbp^{+/+}* embryos when injected with *tardbp^{ATG}* AMO showed an up regulation of the ~43kDa band despite the knockdown of Tardbp (Fig 6.20B, h.TDP-43 Ab1 immunoblot). This band is at the same height as the Tardbpl-FL band in *tardbp^{fh301/fh301}* control AMO injected group (Fig 6.20A, lane 3). Injection of *tardbp^{ATG}* AMO into *tardbp^{fh301/fh301}* embryos did not change the Tardbpl or Tardbpl-FL band pattern when corrected for loading (Fig 6.20A, lane 4 and Fig 5.19C alpha tubulin loading control). These results indicate that *tardbp^{ATG}* AMO does not alter Tardbpl/Tardbpl-FL protein levels.

Phenotype analysis showed that *tardbp^ATG* AMO injection into *tardbp^+/+* (Fig 6.21E) and *tardbp^fh301/fh301* embryos (Fig 6.21F) result in a curly tail phenotype, suggesting the possibility of off- target effects of *tardbp^ATG* AMO despite co-injection with p53. This result also nullifies the theory that acute knockdown of *tardbp* by AMO was a less adaptable condition compared to *tardbp^fh301/fh301* (homozygous) siblings of a heterozygous-heterozygous in cross where maternal transmission of *tardbp* mRNA is expected to allow the HOMs (*tardbp^fh301/fh301*) to gradually rescue the *tardbp^fh301/fh301* Tardbp null mutants from developing a motor phenotype.

We also injected *tardbp^+/+* and *tardbp^fh301/fh301* embryos with a splice disrupting AMO against *tardbp* gene (*tardbp^SpII* AMO). In chapter 5 we have shown that although *tardbp^SpII* AMO disrupts splicing of *tardbp*,(Figure 5.14) it does not result in a motor phenotype. Therefore we injected *tardbp^SpII* AMO into HOM and WT siblings and demonstrated that these embryos were morphologically normal (Fig 6.21G-H) despite injecting a higher dose at which almost completely abolishes the WT *tardbp* splice isoform (Fig 6.21I) . A phenotype was observed only in relation to *tardbp^ATG* AMO injection where either into WT or HOM embryos, but same observation was not made with *tardbp^SpII* AMO (Fig 6.21J). Taken together these results indicate that the *tardbp^ATG* AMO obtained from genetools.com (similar in sequence to the *tardbp^ATG* AMO sequence published by Kabashi and colleagues) produces a curly tail phenotype when injected in to both WT and HOM zebrafish embryos, suggests p53 dependent and independent off target effects of the *tardbp^ATG* AMO.
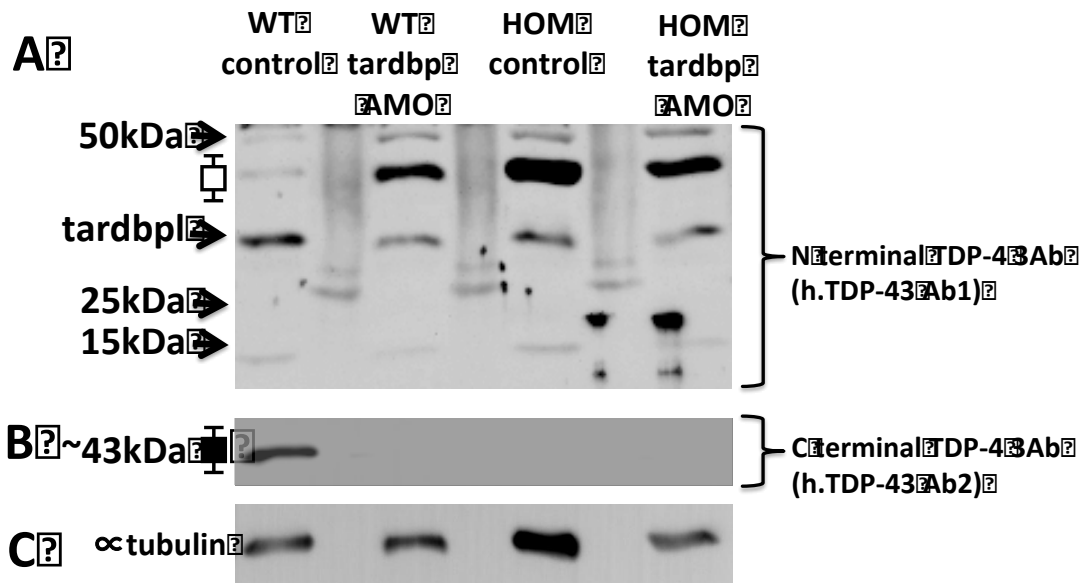
Figure 6.20 Knockdown of *tardbp* using *tardbp^ATG* AMO +*p53* in WT and homogygous mutant embryos does not knockdown the Tardbpl-FL protein. A) N-terminal TDP-43 Ab immunoblot. Lane 1 demonstrates the relative proportions of Tardbpl and Tardbp in the WT embryos. Lane 2 demonstrates that Tardbp knockdown in the WT embryos causes up-regulation of Tardbpl-FL ⊡. Lane 3 Control AMO injected homozygous embryos (HOM controls) have massively upregulated Tardbpl-FL levels. Homozygous embryos injected with *tardbp^ATG* AMO also show unaltered levels of tardbpl-FL. B) Complete tardbp knockdown or absence is demonstrated by the C-terminal TDP-43 Ab ▮. C) Alpha tubulin loading control.

WT — A — CoMo+p53 — 8ng

tardbp^*fh301/fh301* — B — CoMo+p53 — 8ng

WT — C — CoMo+p53 — 16ng

tardbp^*fh301/fh301* — D — CoMo+p53 — 16ng

E — tardbp ATG+p53 — 2.5ng

F — tardbp ATG+p53 — 2.5ng

G — tardbp splice.II+p53 — 16ng

H — tardbp splice.II+p53 — 16ng

Control AMO+p53

ATG or Splice AMO+p53
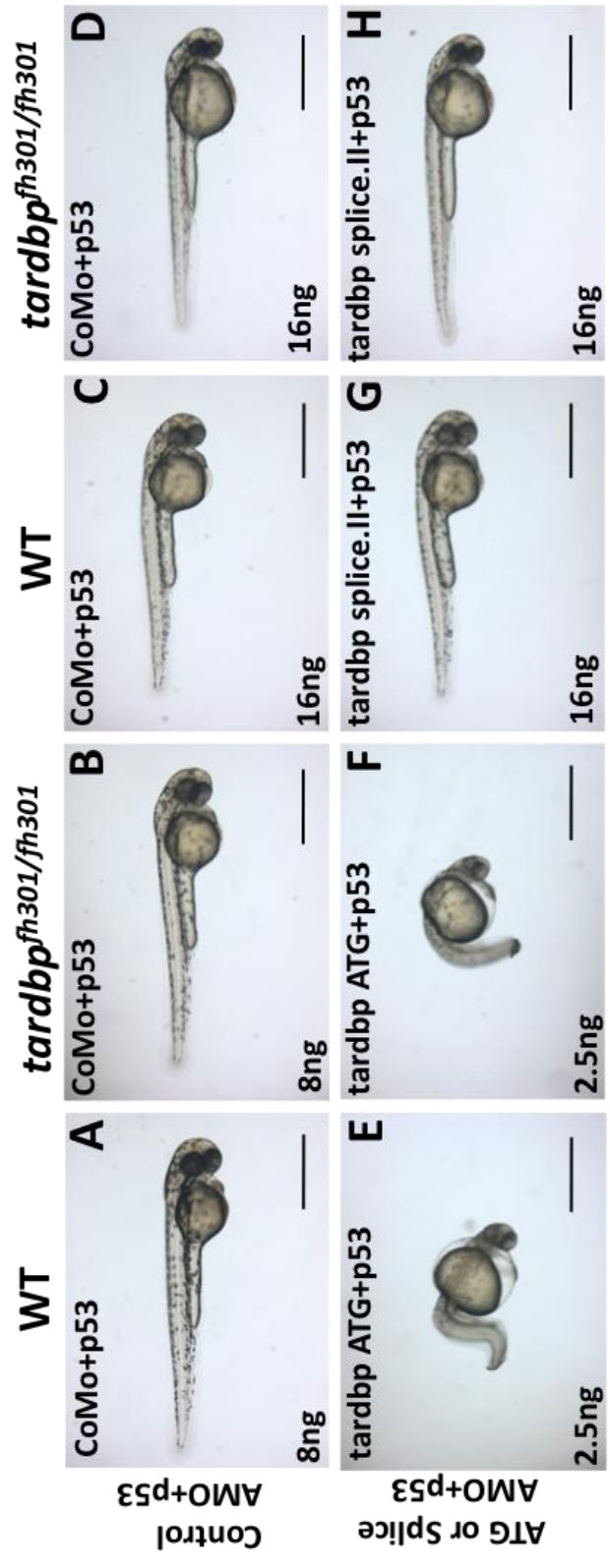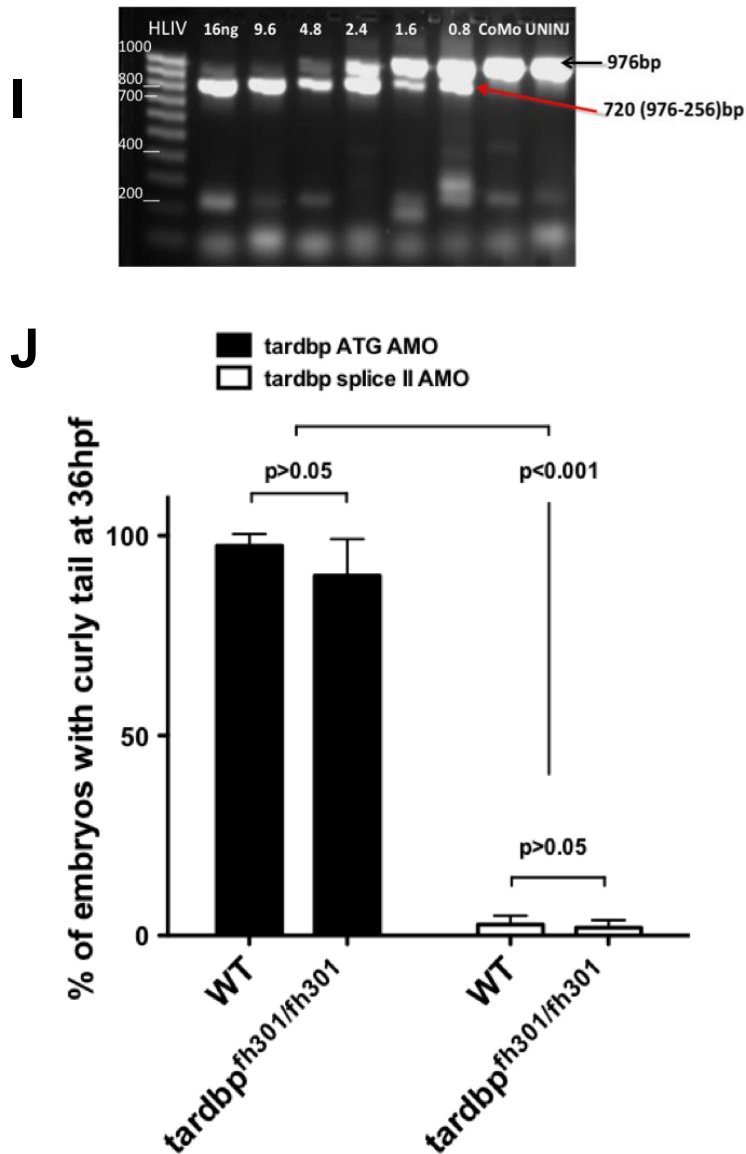
Figure 6.21 Injection of splice blocking morpholino II (*tardbp^{SpII}* AMO) does not cause abnormal embryonic development in *tardbp$^{+/+}$* (WT) or *tardbp$^{fh301/fh301}$* (Homozygous/HOM) embryos. WT and HOM embryos were injected with either *tardbp* translation blocking AMO (*tardbp^{ATG}* AMO) or *tardbp* splice blocking AMO (*tardbp^{SpII}* AMO). WT and HOM embryos injected with control AMO (A, B), 2.5 ng of *tardbp^{ATG}* AMO (E,F), 16ng of control AMO (C,D) or 16 ng of *tardbp^{SpII}* AMO (G,H). The *tardbp^{ATG}* AMO injected embryos showed severe embryonic malformations in both WT (*tardbp$^{+/+}$*) and HOMs (*tardbp$^{fh301/fh301}$*), while *tardbp^{SpII}* AMO injected embryos (WT and HOMs) appeared phenotypically similar. (I) RT-PCR of RNA obtained from embryos injected with 16 ng of control AMO or varying doses (0.8, 16, 2.4, 4.8, 9.6, or 16 ng) of *tardbp^{SpII}* AMO. A dose dependent reduction in the wild type *tardbp* splice isoform (976bp) is observed and the highest dose shows an almost complete lack of the wildtype *tardbp* splice isoform. The new splice isoform is detected as a 720 base pair fragment on the gel.(J) Post AMO injection phenotype analysis shows a significant curly tail phenotype in the *tardbp* ^{ATG} AMO injected WT and HOMs, whereas *tardbp^{SpII}* AMO injected embryos produced no phenotype in either WT nor HOMs embryos.

6.12 Discussion

TDP-43 is one of the key proteins involved in the pathogenesis of FTLD-U and ALS (Sendtner, 2011). The importance of TDP-43 related pathology in ALS and FTLD-U has been reinforced by the recent discovery showing that TDP-43 pathology predominates in ALS and FTLD cases with an intronic hexanucleotide repeat expansion in *C9ORF72*, which accounts for up to 50% of fALS and 7-10% of sALS cases (Dejesus-Hernandez et al., 2011, Renton et al., 2011, Cooper-Knock et al., 2012). Aggregate formation with C-terminus truncated and hyperphosphorylated TDP-43 is observed in pathological brain samples (Neumann et al., 2006) whilst full length TDP-43 aggregates are seen in the spinal cord (Igaz et al., 2008) of ALS and FTLD-U cases, suggesting a toxic gain of abnormal function of TDP-43 in disease (Hasegawa et al., 2011). However, a dramatic redistribution of nuclear TDP-43 to the cytoplasm of surviving motor neurons in pathological samples has been consistently observed. Analysis of postmortem brain and spinal cord samples has also revealed that cells with cytoplasmic inclusions positive for TDP-43 show depletion of nuclear TDP-43 (Neumann et al., 2006). This reduction of normal nuclear expression of TDP-43 may cause a loss of normal nuclear function, with potential adverse effects on vital nuclear functions such as transcription and post transcriptional regulation of gene expression, including alternative splicing (Buratti and Baralle, 2010b) . Therefore a strong case exists to investigate the loss of nuclear function as a possible mechanism of TDP-43 related pathology.

Here we describe the first stable mutant TDP-43 (Tardbp) zebrafish model of ALS. Furthermore we show that the loss of full length Tardbp in the *tardbp^{fh301/fh301}* animals leads to enhanced alternative splicing of *tardbpl* to generate a novel transcript *tardbpl-FL*, indicating the existence of a newly identified regulatory loop that controls Tardbp levels in zebrafish. In addition, we demonstrate that knockdown of both *tardbp* and *tardbpl-FL* leads to severe defects in motor neuronal development, therefore establishing a vital role for Tardbp in zebrafish development. This provides a novel, tractable vertebrate model for the analysis of the morphological and biochemical consequences of Tardbp loss of function.

The loss of TDP-43 has been shown to cause embryonic lethality in mice (Kraemer et al., 2010) and in fruit-fly (Fiesel et al., 2010). Studies *in vitro* showed that TDP-43 knockdown in a neuronal cell line using small interfering RNA (siRNA)

resulted in neurite out growth defects, increased cell death (Iguchi et al., 2009) and increased apoptosis, together with defective cell proliferation (Ayala et al., 2008a). Additionally, in zebrafish, morpholino-mediated transient knockdown of *tardbp* was shown to produce a severe impairment of motor axon growth and development (Kabashi et al 2010).

Thus, it was surprising to observe normal Mendelian ratios maintained amongst homozygous (*tardbp^{fh301/fh301}*), heterozygous (*tardbp^{fh301/+}*) and WT (*tardbp^{+/+}*) zebrafish generated from a heterozygous (*tardbp^{fh301/+}*) in cross, and survival of homozygous mutant (*tardbp^{fh301/fh301}*) animals to adulthood, in contrast to the phenotype observed in *tardbp* null mice. Our findings suggest that the compensatory role played by the *tardbpl* locus allows *tardbp* mutants (*tardbp^{fh301/fh301}*) to have sufficient Tardbpl-FL levels to allow normal development. However, an earlier study in zebrafish using *tardbp* and *tardbp^{ATG}* AMO indicated that *tardbp* is a functional gene, whereas *tardbpl* is non-functional, based on the lack of a phenotype in the *tardbpl* morphants. We also observed that knockdown of the *tardbpl* gene using a *tardbpl* AMO did not cause any phenotype in wild type zebrafish, indicating that the 33kDa Tardbpl isoform is likely to be non-functional. However, on closer examination of the *tardbpl* locus, we identified the possibility that the *tardbpl* gene might be able to encode a full length Tardbpl protein (Tardbpl-FL). Interestingly, suppression of the alternatively spliced product of the *tardbpl* locus, *tardbpl-FL,* in the *tardbp^{fh301/fh301}* mutant zebrafish is lethal, and these findings support the critical role played by *tardbp* and *tardbpl-FL* expression in normal development.

It is not surprising that our results contrast somewhat with the findings of Kabashi *et al* who used a purely morpholino-based approach to explore the function of *tardbp* and *tardbpl* (Kabashi *et al,* 2010). They observed that antisense morpholino-mediated knockdown of *tardbp* produced severe deficits in axonal growth and development, while they saw no obvious function for the *tardbpl* locus. Using the same morpholinos utilised in the Kabashi study, we also observed that AMO knockdown of *tardbp* using the translation blocking AMO produced severely defective embryos when injected in both WT and the tardbp^{fh301} mutants (Fig 6.21 bottom panel E, F). However, even when we used the highest dose of a splice blocking AMO, that completely eliminated the WT splice form of tardbp (Fig 6.21I), we saw that the embryos were apparently normal (Fig 6.21, Bottom panel G,H).

Thus, we believe that the translation blocking AMO experiments may have some off- target mediated effects that could have contributed to the observed phenotype. Therefore, it remained unclear whether depletion of Tardbp produced embryonic lethality in zebrafish.

Using a stable *tardbp* null mutant zebrafish generated by the TILLING process we observed that complete knockdown of Tardbpl/Tardbpl-FL in *tardbp*$^{fh301/fh301}$ zebrafish produced severe axonal defects and reduced survival, but in addition we identified a crucial role for the *tardbpl* locus in regulating Tardbp levels. Unlike in the scenario occurring with transient knockdown, germ- line knockout of *tardbp* caused an induction of the novel isoform (*tardbp-FL*) that was able to rescue the loss of *tardbp* function. While, the AMO studies suggested that the *tardbpl* locus might be non-functional, using the Y220X mutant we were able to assign a compensatory function for this locus, through the generation of Tardbpl-FL. Although morpholino (AMO) based approaches have in general been useful for the characterisation of gene function, here we present a scenario where generation of a stable mutant but not the AMO approach was useful in identifying the function of a duplicated gene. This highlights one potential pitfall of using purely morpholino- based approaches to study gene function and indicates that a combined approach may add value in many circumstances. Our data suggest that sole reliance on AMO gene knock-down may occasionally allow the roles of auto- and cross- regulatory genes to be missed and the functions of genes with similar or redundant functions to be obscured.

It is noteworthy that humans also have two *TARDBP* genes; one is located on chromosome 1p36.22 (*TARDBP*) while the other is a pseudogene located on chromosome 20p12.3 (*TARDBPP1*). The *tardbp* gene in zebrafish is located on chromosome 6 and the *tardbpl* gene is located on chromosome 23. Zebrafish and humans appear to share ancestral chromosomes (Woods et al., 2005). We compared the synteny map of the *tardbp* and *tardbpl* loci in zebrafish with those of the human gene and the pseudogene, and found partial conservation of synteny in both cases. However, genes around the zebrafish *tardbp* locus were less rearranged compared to those at the *tardbpl* locus (Figure 6.22). The zebrafish chromosome 23 is extensively recombined and relevant genes are distributed amongst many other chromosomes in humans (such as 1,2,6,12,20 and X), with a component on chromosome 20, where the human *TARDBPP1* gene is located. Thus, it is likely that

'*tardbpl*' in humans underwent recombination events that could have potentially led to the loss of functional *tardbpl* and the creation of the *TARDBPP1* pseudogene.

Human homologenes	Danio Ch 6-tardbp locus	Human homologenes	Danio Ch 23-tardbpl locus
MITF:3p14.2-p14.1	mitfa	CHIA: 1p13.2	Zgc:65788
FOXP1:3p14.1	foxp1b	HSD17B10: xp11.2	hsd17b10
PROK2:3p13	prok2	RPL10: Xq28	rpl10
RYBP:3p13	rybpb	BGN: Xq28	bgnb
PPP4R2:3p13	ppp4r2b	TNNC2: 20q12-q13.11	tnnc2
EPHα2:1p36	epha2	SLC2A1: 1p34.2	slc2a1a
RBP7:1p36.22	rbp7b	CLCNKB:1p36	clcnkb
APITD1:1p36.22	zgc:194319	ADA: 20p13.2	ada
TARDBP:1p36.22	tardbp	PTGES3: 12q13.3	ptges3a
STAU1:20q13.1	stau1	WNT1: 12q13	wnt1
PADI2:1p36.13	zgc:66317	LMBR1L: 12q13.12	lmbr1l
SYCP1:1p13.12	sycp1	TARDBPP1:20p12.3	tardbpl
SLC5A8:12q23.1	slc58al	PIK3CD:1p36.2	pik3cd
NGF:1p13.1	ngf	UTS2: 1p36	uts2a
RAB22A:20q13.32	rab22a	TBPL1:6q22.1-q22.3	tbpl
VAPB:20q13.33	vapb	ALDH8A1: 6q23.2	aldh8a1
NPEPL1:20q13.32	npepl1		
CTSZ:20q13.32	ctsz		
TH1L:20q13	th1l		
AHCY:20cen-q13.1	ahcy		
ERGIC3:20pter-q12	ergic3		
PIGU:20q11.22	pigu		

Figure 6.22 Synteny map of zebrafish *tardbp* (Chromosome 6) and *tarbpl* (Chromosome 23) loci with human orthologues. The genes in zebrafish chromosome 6 and 23 near the *tardbp* and *tardbpl* loci were mapped to human chromosome locations and plotted. Genes around *tardbp* on zebrafish chromosome 6 appear to be grouped together with fewer recombinations as compared to the chromosome 23 *tardbpl* locus. Genes coloured similarly are located on the same chromosome.

It is of interest to question what selection pressure enabled the maintenance of functional *tardbp* and *tardbp-FL* genes in zebrafish. One interesting clue suggesting divergent roles for Tardbp and Tardbpl-FL, is the phenotype of the *tardbp^{fh301/fh301}* mutants. We observed that despite the up-regulation of *tardbpl-FL* in the *tardbp^{fh301/fh301}* mutant zebrafish, the mutants were smaller in size compared to WT (Figure 6.5), which indicates that Tardbp and Tardbpl/Tardbpl-FL may have, both functionally overlapping and distinct roles in zebrafish development and in adult life. The small body phenotype of *tardbp^{fh301/fh301}* animals suggests that Tardbp may play a critical role in growth regulation, which is not fully compensated by the up-regulation of *tardbpl-FL* expression in the mutants. In keeping with this are the

findings from conditional postnatal knockout of *Tardbp* in mice which showed that these mice develop loss of body weight and down regulation of Tbc1d1, increased expression of which is associated with obesity (Chiang et al., 2010). Thus, the specialised role played by *tardbp* as compared to *tardbpl* may have been important in maintaining the two genes during evolution. As we do not yet have a stable *tardbpl* mutant, we do not yet know what specific role *tardbpl-FL* may play in zebrafish development.

Up-regulation of *tardbpl-FL* expression by alternative splicing of the *tardbpl* locus in the *tardbp*$^{fh301/fh301}$ mutants is interesting. The generation of the *tardbpl-FL* transcript occurs by the inclusion of intron 5 of *tardbpl*, which is able to code for the additional C- terminal amino acids generating an almost full-length Tardbp-like protein. This intron contains a UGUGU motif near the splice donor site of exon 6. Additionally, another canonical high affinity TDP-43 binding site -$(GU)_6$ is located in the 3'UTR region of the *tardbp* and *tardbpl-FL* transcripts. Although the UGUGU motif is not a canonical high affinity RNA binding site of TDP-43, it has the elements required for interacting with TDP-43 during splicing (Ayala et al., 2006), suggesting that Tardbp could potentially regulate the *tardbpl/tardbpl-FL* splicing process. This phenomenon is illustrated in the report describing the alternative splicing of the splice regulatory factor SC35. SC35 promotes alternative splicing of its terminal exon by binding to the intronic low affinity sequence, which has UGUG repeats. TDP-43 inhibits this exon skipping by competing with SC35 for the low affinity binding sites (Dreumont et al., 2010). Furthermore the canonical high affinity TDP-43 binding site -$(GU)_6$ in the 3'UTR region of *tardbp* and *tardbpl-FL* could also potentially play a role in suppression of the *tardbpl-FL* mRNA splicing. Hence, it is likely that in the absence of tardbp, a tardbp- induced inhibitory loop is abolished, which in turn results in alternative splicing of *tardbpl* where intron 5-6 is retained to generate *tardbpl-FL* and results in a 20 fold up regulation of Tardbpl-FL protein levels in the *tardbp*$^{fh301/fh301}$ mutants. Taken together these results predict an *in vivo* autoregulatory model involving Tardbp and *tardbpl/tardbpl-FL* in keeping with the auto-regulatory mechanism/s hypothesised for TDP-43 (Buratti and Baralle, 2011b).

One interesting aspect of the up-regulation of tardbpl-FL expression is that it is unable to completely rescue the loss of Tardbp despite the high homology between Tardbp and Tardbpl-FL. Tardbpl-FL lacks nine residues from the glycine

rich domain (GRD) of which six are glycine residues. This observation might explain three other findings. Firstly, in *tardbp* null zebrafish, the tardbpl-FL protein level is increased by 20 fold. Perhaps this massive compensatory elevation of Tardbp-FL may explain the absence of an overt phenotype in the *tardbp*^*fh301/fh301*^zebrafish. Secondly, given the high homology between *tardbpl-FL* and *tardbp*, one would expect *tardbpl-FL* to auto-regulate itself by inducing alternative splicing to promote skipping of intronic exon 5 to generate *tardbpl*. However *tardbpl-FL* appears to fail to regulate its own splicing efficiently, resulting in a massive 20-fold up-regulation of the tardbpl-FL protein. Thirdly, an observation from TDP-43 over-expression *in vitro* and *in vivo* models is that over-expression of full length WT, mutant TDP-43 or C-terminal fragments of TDP-43 are all toxic and lethal (Xu et al., 2010). The toxicity of over-expression of exogenous TDP-43 even at relatively low levels in transgenic rodents (Swarup et al., 2011b, a) is not observed in the *tardbp*^*fh301/fh301*^ null zebrafish with compensatory 20 fold increase in the Tardbpl-FL protein level. Therefore it is plausible that the glycine residues which are missing from the GRD of the Tardbpl-FL (Figure 6.18 shaded in grey) are indeed important for maintaining maximum efficiency of the function of TDP-43, as well as mediating TDP-43 over- expression related toxicity.

Taken together, our data describe for the first time, a critical role for *tardbp* and *tardbpl* in zebrafish development. We show that *tardbp* is critical in the regulation of body size as over-expression of Tardbpl-FL in the *tardbp*^*fh301/fh301*^ mutants is unable to rectify this deficit. However, increased *tardbp-FL* expression in *tardbp*^*fh301/fh301*^ mutants is able to partially compensate for the early developmental role of *tardbp*. The complete knockdown of *tardbp* and *tardbpl-FL* results in severely abnormal neuronal development and concurrent embryonic lethality, demonstrating a critical role for Tardbp or Tardbpl-FL in embryonic neurodevelopment. The uncovering of a newly identified regulatory loop between *tardbp* and *tardbpl* and the discovery of *tardbpl-FL* in zebrafish will allow us to use the double knockdown zebrafish model to study disease mechanisms and neuroprotective strategies and to better understand human ALS associated with *TARDBP* mutations.

Chapter 07:

Overall discussion

7.1 Introduction

Multifunctional TDP-43 is described as one of the major components of the ubiquitinated neurocytoplasmic aggregations observed in the pathological samples of ALS/MND cases with or without FTLD. The presence of aggregated proteins is a well-established facet of neurodegenerative conditions. TDP-43 positive ubiquitinated-protein aggregates in non-SOD1 related ALS are a consistent observation. Whether aggregated TDP-43 confers a toxic effect on neuronal health and drives the disease process, or represents an epiphenomenon or indeed a marker of processes protecting the surviving neurons from the harm of toxic misfolded proteins, is open for debate. However, it is well established that mutations in the TARDBP gene encoding TDP-43 are associated with ALS and FTLD. TDP-43 proteinopathy encompasses a range of neurodegenerative disorders including sporadic and familial ALS, FTLD, corticobasal degeneration, and progressive supranuclear palsy. TDP-43 has been implicated in multiple RNA processing functions such as transcription, splicing, translation, RNA-transport, stress granule formation, and miRNA processing. The discovery of RNA binding and processing proteins like TDP-43, FUS and the recent discovery of C9ORF72 intronic hexanucleotide expansion in ALS cases has highlighted the importance of RNA processing in ALS pathogenesis. The discovery of the association of dysfunction of TDP-43, FUS and C9ORF72 with ALS has been paradigm changing and the focus of many studies only on pathophysiological mechanisms and models related to SOD1, has now shifted to proteins with RNA-related functional importance such as TDP-43, FUS and C9ORF72. Furthermore, over-expression of TDP-43 or knockdown of the TDP-43 orthologue in mice, rats, fruit fly, zebrafish and *C.elegans* results in motor neuronal dysfunction. It still remains uncertain whether dysfunctional TDP-43 causes motor neuron degeneration by a gain of toxic function, loss of function or both mechanisms.

7.2 Has over-expression of WT or mutant TDP-43 in animal models contributed to the understanding of TDP-43 function?

In cases with ALS and FTLD the total TDP-43 level is 2.5 fold greater than in those who are normal ((Cairns et al., 2007, Gitcho et al., 2009). This fact, along with the tradition of over-expression of mutant genes in animal models to study mutations in genes associated with human diseases, have led to the generation of several animal models to gain insights into mechanisms of TDP-43-related ALS, since the discovery of the association of TDP-43 with ALS/FTLD in 2006. Transgenic mouse and rat models generated using different promoters to target expression patterns (ubiquitous or CNS only) and timings (throughout life or expression at a certain developmental period) have resulted in inconsistent features of TDP proteinopathy.

Several *in vitro* and *in vivo* models have been set up to study the toxic gain of function mechanisms of TDP-43-related ALS by over-expression of mutant and wild type TDP-43. Interestingly not only mutant TDP-43 but also WT-TDP-43 over-expression resulted in an ALS like phenotype in rodent models. Although clinical manifestations of motor neuronal dysfunction were observed, the formation of neurocytoplasmic inclusions or aggregations, cytoplasmic mis-localisation, C-terminal truncation and phosphorylated TDP-43 accumulation were not observed in a consistent pattern in all the models generated. Over -expression of the human M337V mutation under the human endogenous promoter in the rat, did however, produce clinical and biochemical phenotypes of ALS (Zhou et al., 2010). Cytoplasmic mis-localisation and alteration of DNA/RNA-related functions appeared to be relatively more consistent than other biochemical features, suggesting that loss of function of nuclear TDP-43 could be a major contributor to the pathogenesis ALS. The most important contribution from the over-expression rodent models informs us that cytoplasmic aggregation; C-terminal truncation and phosphorylation are not essential for motor neuron degeneration related to dysfunctional TDP-43. Furthermore, mutant or wild type TDP-43 is toxic to neurons when over- expressed. Drosophila models over-expressing full length wtTDP-43 demonstrated aggregate formation, whilst none of the full length mutant TDP-43 resulted in aggregate formation, supporting the notion that aggregate formation is not essential for neurodegeneration to occur (Estes et al., 2011).

7.3 Is loss of function of nuclear TDP-43 important for neurodegeneration in TDP-43 related ALS?

Studying loss of TDP-43 function is reasonable in an animal model to directly observe affected genes and relate this information to the human disease. Knockdown models of TDP-43 in mice, drosophila and zebrafish have informed us that TDP-43 is essential for development and neuronal health. Conditional knockout mice did not develop an ALS like phenotype, but demonstrated abnormalities of body fat metabolism (Chiang et al., 2010). Targeted depletion of TDP-43 in the spinal cord resulted in an ALS-like phenotype and formation of ubiquitinated protein aggregates (Wu et al., 2012, Saxena et al., 2013). Overexpression rodent models of TDP-43 showed loss of endogenous TDP-43 from the neuronal nuclei (Wegorzewska et al., 2009, Tsai et al., 2010, Wils et al., 2010, Igaz et al., 2011, Swarup et al., 2011a) suggesting that once TDP-43 starts mis-localising to the cytoplasm, it causes a whirlpool effect and drags physiological nuclear TDP-43 out of the nucleus. It is well established that TDP-43 is vital for several nuclear functions including regulation of transcription and RNA splicing. Therefore loss of nuclear TDP-43 could result in neuronal dysfunction. Taken together, it appears that maintenance of endogenous physiological levels of wild type TDP-43 is essential for neuronal health and disturbance of this finely controlled expression could result in neurotoxicity.

It may not be possible to study accurately the effects of disease related mutations of a protein like TDP-43, which has tens of thousands of RNA targets in both exonic and intronic regions, in a model that is genetically distant from that of humans. In such a model, it is also nearly impossible to decipher the effects of over-expression of mutant or wild type TDP-43. Zebrafish models generated by our team using TILLING mutagenesis or by others by genome wide editing with zinc finger endonucleases demonstrated that tardbp knockdown is insufficient to generate a motor phenotype, as an auto-regulatory process rescues the loss of tardbp motor phenotype. This demonstrates that complex RNA regulatory mechanisms are either switched on or off when the physiological level of TDP-43 is altered artificially. Animal models have clearly demonstrated that TDP-43 is an essential protein at all stages of life. Most knockdown models show reduced survival at the embryonic stage and loss of motor neurons when knocked down

conditionally at later stages of life. Over-expression models have informed us that perturbation of the TDP-43 level, whether WT or mutant is also unfavourable for normal neuronal function. Despite regular publications of new TDP-43 animal models, there is still considerable debate about the exact pathophysiological features of TDP-43 proteinopathy and we still do not understand the pathophysiological mechanisms of disease-related mutations or the neuronal dysfunction occurring in the presence of the aggregation of non -mutant TDP-43. Taken together, it appears that the focus should be on investigating ALS and related mechanisms using a human model such as patient -derived cell lines and post-mortem CND tissue.

It is important to find out if the predominant feature associated with either sporadic ALS or *TARDBP*-related fALS is gain of function or loss of function as this will help in the identification of therapeutic targets for neuroprotection. Potential therapeutic measures involved in addressing loss of function mechanisms would be external delivery and expression of target molecules/TDP-43 into the neurons so that functional physiological TDP-43 levels can be maintained above a critical threshold. This could potentially be achieved by either inhibiting mis-localisation and aggregation in the cytoplasmic inclusions or enhancing the solubilisation of aggregated TDP-43. Should the major pathogenic mechanism be a gain of toxic function, theoretically, an agent to inhibit the mutant protein/disease-causing fragment of the molecule could be generated.

7.4 Is it reasonable to use animal models to study TDP-43-related ALS?

Humans and rodents are evolutionarily divergent and other non-mammalian species and non-vertebrates are even further divergent. Through evolution the genomes have undergone vast changes and the evolutionary forces, which worked on introns, were different from those applied to exons. Therefore the genetic distances between rodents and humans with regards to intronic sequences are vast. Polymenidou et al (2011) identified more than 39,000 RNA binding sites of TDP-43 in the mouse genome in a RNA cross linking, high- throughput sequencing and immunoprecipitation study (Wegorzewska and Baloh, 2010, Polymenidou et al., 2011). Interestingly most pre-mRNA targets of TDP-43 contained long introns with TDP-43 binding sites. Whilst it is the scope of another detailed study to

compare the relative conservation of these intronic TDP-43 binding sites across species, it is conceivable that intronic RNA sequences are significantly variable between two evolutionarily close species such as mouse and the rat, with even greater variability between rodents and humans. Therefore to study pathophysiological mechanisms related to ALS of an RNA binding protein like TDP-43 with thousands of targets in intronic non-coding regions, in a non-primate model, would be extremely challenging. This is at least in part, reflected in the relative paucity of new information gathered from 32 different mammalian and 71 non- mammalian TDP-43 animal models (transgenic, TILLING mutagenesis, zinc finger endonuclease, mutagenised and knockout models) published to date. These studies have not so far extended our knowledge beyond what we already know about TDP-43 and its function from cellular models and from the study of human cases. Furthermore, although loss of TDP-43 from the nucleus and cytoplasmic aggregate formation is noted in motor neurons from ALS and FTLD cases, only 4% of the ALS cases have mutations in the *TARDBP* gene. In addition, the study of TDP-43 and its disease-causing mechanisms requires physiological levels of mutant or wild type TDP-43 to prevent artifactual changes in the disease model.

We know that knockdown of TDP-43 in mice, drosophila and zebrafish models is embryonic lethal (Kraemer et al., 2010, Sephton et al., 2010, Hewamadduma et al., 2013) and over-expression of either wild type or mutant TDP-43 is also toxic in cellular and animal models (Ayala et al., 2011b, Igaz et al., 2011). Moreover, we have demonstrated in an *in vivo* zebrafish model that physiological expression of a loss of function mutation results in a loss of a negative feedback loop which activates expression of an alternative mRNA (Hewamadduma et al., 2013). Studies from other groups have also supported the concept that TDP-43 autoregulates its own mRNA levels to optimise the levels of intracellular TDP-43 (Ayala et al., 2011b). Taken together, it appears challenging to generate an animal model of dysfunctional TDP-43. We know that a sporadic form of disease afflicts about 90% of ALS and FTLD cases indicating that complex genetic and environmental factors operate upstream of TDP-43 during disease initiation and subsequent progression. As such, it is nearly impossible to model the sporadic form of ALS in an animal or in an *in vitro* cell model. Therefore, we believe that models based on patient derived tissues such as fibroblasts and

lymphoblastoid cell lines, can overcome some of the potentially huge pitfalls inherent in animal models.

7.5 Are patient-derived fibroblasts sufficiently robust as a cell model to interrogate TDP-43-related ALS ?

Limitations in artificially modifying the physiological levels of TDP-43, mutant or wild type, pose many challenges when it comes to interpretation of the results from such animal or cell models. Patient-derived cell lines such as fibroblasts have a greater advantage in that TDP-43 levels are physiological. Although fibroblasts unlike neurons, can undergo multiple cell divisions, our studies have demonstrated that fibroblasts derived from ALS cases with TDP-43 mutations exhibit features of TDP-43 proteinopathy such as relative nuclear clearing, hyperphophorylated aggregated cytoplasmic and nuclear TDP-43 and p62 positive aggregates, which are observed in motor neurons from pathological brain and spinal cord samples (Neumann, 2009). Furthermore, we have shown that RNA metabolism dynamics are impaired in mutant TDP-43 fibroblasts when compared to controls in studies investigating assembly and disassembly of stress granules in fibroblasts in response to exogenous stress and in studies analysing the expression of gene splicing variations (Merdzhanova et al., 2010).

Living motor neurons derived from induced pluripotent stem cells (iPSC) are considered to provide an ideal platform to model wild type and mutant TDP-43, which is closest to the living motor neurons of an affected patient. iPSCs derived from patients with fALS associated with TDP-43 mutations like Q343R, M337V and G298S have demonstrated decreased cell survival and defective neurite out growth (Bilican et al., 2012, Egawa et al., 2012) indicating motor neuron dysfunction. Furthermore, others have demonstrated hyperphosphorylated TDP-43 aggregates similar to our observations in patient-derived fibroblasts harbouring M337V, G287S and A321V *TARDBP* mutations (Egawa et al., 2012). Interestingly a report from Burkhardt *et al* also described hyperphosphorylated TDP-43 aggregate formation in the cytoplasm of motor neurons derived from iPSCs from sALS cases (Burkhardt et al., 2013) suggesting that motor neurons derived from iPS cells potentially could form an excellent platform to study TDP-43 related motor neuronal dysfunction in both sALS and fALS cases. However, we are aware of significant challenges the iPSC system poses,

such as significant variability amongst the clones obtained from a single patient, effects on so-called epigenetic memory which can be lost during reprogramming (Burkhardt et al., 2013) and high costs associated with generation of iPSCs. Furthermore, significantly low throughput of successfully generated iPSCs is in the order of 0.01-0.1%, suggesting the need for precision control of timing and balancing the absolute levels of expression levels of the reprogramming genes (Knippenberg et al., 2013). The use of transcription factors to reprogramme the original somatic cell can result in integration, which can lead to insertion of mutations in the target cell's genome. Fibroblasts provide an excellent platform to study the sporadic form of ALS, which is considered to have non-mutant but dysfunctional TDP-43. Sporadic ALS is considered to be a manifestation of complex genetic, epigenetic and environmental factors. It is plausible that iPSCs derived from patient fibroblasts could lose vital epigenetic memory during reprogramming and as such it is logical to believe that iPSCs might not be ideal to model sporadic ALS. On the other hand, the use of novel techniques such as employing polyarginine anchors to channel certain proteins into the cells without causing any genetic alterations, called piPS cells (protein-induced pluripotent stem cells) could potentially provide living motor neurons harbouring the exact genetic make up and the epigenetic memory of the original donor tissues/fibroblasts .

7.6 How do stress granules fit in with the neurodegenerative process in TDP-43-related ALS?

Eukaryotic cells have adapted well to face environmental stress, wherein during stress the cells preserve energy and resources by temporarily shutting down the untranslated mRNA and the associated RNA binding proteins and directing them into dynamic cytoplasmic entities called stress granules. This enables the cell to direct its resources to cell survival and recovery once the stress has passed (Anderson and Kedersha, 2008). Several different RNA binding proteins are traditionally used as SG marker proteins, such as TIA1, TIAR, staufen, G3BP, HuR1, hnRNPA1 etc. Interestingly, most of these RNA binding proteins, in addition to a RNA recognition motif (RRM), also have a prion-like domain which enables them to aggregate rapidly and this feature is of vital importance in facing cellular stress and the formation of SGs where rapid aggregation of translational factors and pre-mRNA molecules is required(Kim et al., 2013). Furthermore, both TDP-43 and FUS

have RNA recognition motifs and prion-like domains. The TDP-43 prion-like domain is predicted to be in the C-terminus between amino acids 277-414, whilst FUS has a prion-like domain in the N-terminus between amino acids 1-239. Interestingly, mutations in the key SG marker protein TIA1 have been linked with neurodegenerative conditions like Welander distal myopathy and mutations in hnRNPA1 and hnRNPA2/B1 protein are associated with a complex form of ALS associated with inclusion body myositis, Paget's disease, and fronto temporal dementia (IBMPFD/ALS) (Kim et al., 2013, Kuijpers et al., 2013). Furthermore, displaced hnRNPA3, an RNA binding protein with prion-like domain, was found in aggregates in pathological samples of cases with C9orf72 hexanucleotide expansion associated FTLD (Mori et al., 2013). ALS-related proteins, TDP-43 and FUS have been reported to colocalise with SG binding proteins such as TIA1, TIAR and HUR (McDonald et al., 2011, Vance et al., 2013). Moreover, our studies demonstrate that fibroblasts harbouring mutant TDP-43 take an abnormally long time to disassemble the SGs after the stress has passed. In keeping with these findings, one study showed that SGs formed in response to 'chronic stress' in a background of dysfunctional TDP-43, do not appear to disassemble (Parker et al., 2012). Several studies investigating pathological brain and spinal cord samples from ALS cases have demonstrated that some intra-neuronal TDP-43 positive aggregates indeed co-localise with certain SG marker proteins such as TIA1 and TIAR (Liu-Yesucevitz et al., 2010). Although TDP-43 does not appear to be essential for SG assembly, some studies have shown that knockdown of TDP-43 can affect the size of SGs (McDonald et al., 2011). FUS has also been shown to co-localise with SGs and this effect is heightened by ALS- related mutations (Bosco et al., 2010b). Taken together, a body of evidence is now demonstrating that stress granules and their dynamics are likely to play an important role in ALS and FTLD associated neurodegeneration.

7.7 How dysfunctional TDP-43 might contribute to neurodegeneration by modulating RNA function involved in stress granule dynamics: an hypothesis

In computational modeling TDP-43 and many other proteins have been shown to possess a prion-like domain in the C-terminus (Bucheli et al., 2014). Furthermore, in heat shock experiments TDP-43 has been shown to aggregate in the nucleus in a

prion-like domain (Q/N rich domain in the C-terminus) dependent manner modulated by various chaperones like hsp40 and hsp70 (Wood, 2013). Prion-like domain and RNA binding domains are said to be common features of many RNA binding proteins that take part in SG formation in response to environmental stress (Kawaguchi-Niida et al., 2013). TDP-43 shares many of these features in its molecular structure. Under physiological conditions, when cells are subjected to stress, RNA binding proteins can rapidly herd their RNA targets and the RNA binding molecules they interact with, into temporary cytoplasmic entities *i.e.* stress granules (SG) making the optimal use of their 'prion like domains'. TDP-43, like these RNA binding proteins, which are important in SG formation, is equipped with a prion- like domain and RRMs to modulate SG formation until the stress has passed. Under physiological conditions this prion-like state is reversible and as such when the stress has passed SGs can disassemble releasing the mRNA and RNA binding proteins so the translational process can resume (Figure 8.1 stage 1). The exact mechanisms responsible for SG disassembly is not known. SGs have been likened to liquid and gel-like states, which are reversible. However, these states can subsequently evolve into multiple conformational states and at its most stable format can form self-templating oligomers, which subsequently could lead to non-reversible aggregate formation (Fernandez et al., 2013, Bresch et al., 2014, Song et al., 2014). It is known that mutant TDP-43 is more stable than its wild-type counterpart and most of the mutations of TDP-43 are located in the C-terminal region. Alteration of TDP-43 function or structure could be the first 'hit' which then subsequently alters its prion-like behaviour and promotes self assembly and/ or delayed disassembly once oligomerised into transient fluid or gel-like non membranous formations i.e. stress granules, following a 'second hit' such as cellular stress (Figure 8.1 Stage 2). Once initiated, dysfunctional TDP-43 may self-assemble at a rate, which could be kept under check by the ubiquitin proteasome system, which clears misfolded proteins. In the presence of mutations of TDP-43, uncontrolled self -assembly of TDP-43, which is sufficient to cause aggregation of either nuclear or cytoplasmic TDP-43 eventually results in loss of functional nuclear TDP-43 (loss of function model) and/or localisation to SGs with alteration in their properties such as delaying disassembly. The results from our studies (Chapter 5) and others have clearly demonstrated that cells carrying mutant TDP-

43 exhibit an altered SG response to acute stress (Liu-Yesucevitz et al., 2010, McDonald et al., 2011) (Gain of function model).
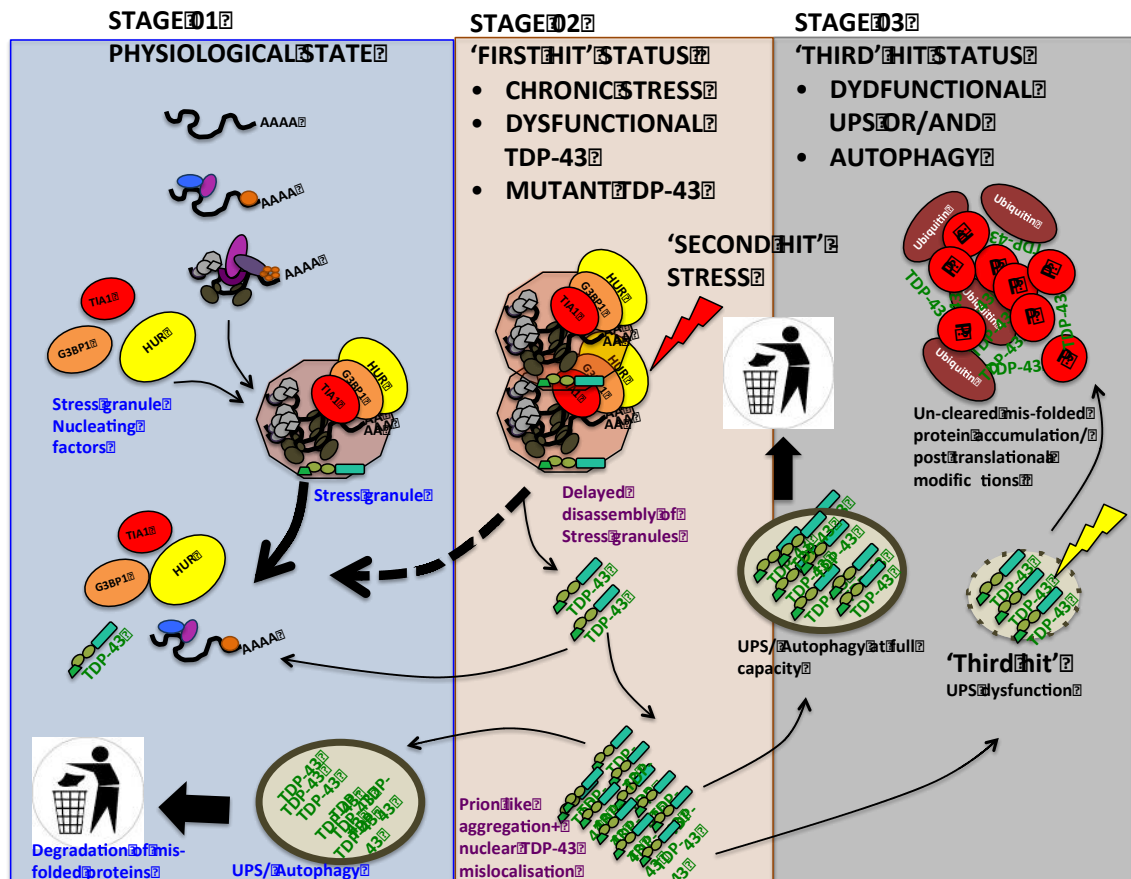
Figure 7.1 Triple hit hypothesis involving stress granule (SG) formation during neurodegeneration
Stage 01- Physiological states during which stress granules assemble and disassemble.
Stage 02- Dysfunctional/mutant TDP-43 as a 'first hit' in interfering with normal SG formation and function. Impaired SG formation and delayed disassembly could lead to a self-templating protein aggregation process and the propensity to behave in a prion-like manner. However effective ubiquitin-proteasome system (UPS) and/or autophagy can overcome this potential threat. Persistent chronic stress can predispose to and/or cause dysfunctional TDP-43-like RNA binding proteins to aggregate more robustly.
Stage 03- Dysfunctional UPS/autophagy system can exacerbate the self-templating prion-like aggregation leading to toxic aggregation and neuronal death.

In support of this phenomenon are the findings from studies on another ALS-related protein called FUS (Fused in sarcoma -1 protein), which also harbours a prion-like domain. Disease associated mutations of FUS tend to result in cytoplasmic mis-localisation and abnormal SG dynamics (Bosco et al., 2010a, Bresch et al., 2014). Perhaps a 'third hit' is necessary in the case of wild-type TDP-

43 related neurodegeneration, wherein a dysfunctional ubiquitin-proteasome system unable to cope with aggregated misfolded proteins combined with chronic exogenous stress which potentially can lead to persistent TDP-43 positive aggregate formation (Parker et al., 2012).   This eventually could result in precipitation of nuclear proteins like TDP-43 and other RNA binding proteins important for RNA metabolism and vital cellular functions, into these aggregates. Once initiated this self-perpetuating prion-like aggregation then results in premature cellular death (Figure 8.1, stage 3).

An emerging concept is the cell to cell propagation of neuro-cytoplasmic aggregates from one brain/spinal cord region to other anatomically linked regions like a 'bush fire' from the onset to the progression of the disease process in many neurodegenerative conditions (Zhou et al., 2013, Bame et al., 2014). Therefore, it is plausible that these aggregated proteins then behave like prions and spread to neighbouring neurons. Furthermore, it is also possible that *de novo* nucleation of protein aggregates can occur in anatomically distant locations which then spread out to neurons local to the initial site. Taken together, it is plausible that dysfunctional TDP-43 associated alteration of SG dynamics could contribute to neurodegeneration in both gain of function and loss of function mechanisms.

7.8. Future work

7.8.1 Patient derived cell lines

We have demonstrated by immunocytochemistry the relative loss of nuclear TDP-43 in the ALS related mutant TDP-43 fibroblasts compared to controls. Studies from the pathological tissues have shown that overall TDP-43 levels in TDP-43 mutants' tissues are greater than that of the controls suggesting greater stability of mutant TDP-43, potentially rendering it more susceptible to post-translational modifications leading downstream to aggregation (Ling et al., 2010). Therefore further studies assessing whole cell extracts and cytoplasmic and nuclear fractions extracted from all three mutant TDP-43 fibroblasts and the controls need to be immunoblotted with both phosphorylation independent and dependent antibodies to confirm the observations made using immunocytochemistry. Similar studies should also be carried out on arsenite treated and untreated cells to assess the generation of C-terminal fragmentation of TDP-43, phosphorylation and

ubiquitination of endogenous wtTDP-43 and mutant TDP-43. We also need to obtain more cell lines for each mutant TDP-43 fibroblast cell line to increase the accuracy and the repeatability of the findings.

We hypothesised that over expression of TDP-43 is toxic to HEK293T cells and this needs to be directly measured in an objective measure such as using an MTT assay.

Endogenous TDP-43, detected by a phosphorylation independent antibody, did not co-localise with SG nucleating proteins such as TIAR and HUR, when fibroblasts were treated with arsenite. Therefore it would be interesting to see if phosphorylation-dependent TDP-43 would co-localise in a different pattern i.e. into stress granules, to non phosphorylated TDP-43 upon stress. A current limitation in our patient derived cell lines is that we need to increase the number of cell lines per TDP-43 mutation.

We have identified nuclear TDP-43 localisation and the intensity and dynamics of SG assembly and disassembly as readouts that differentiate mutant TDP-43 from control fibroblasts. Therefore we could utilise these parameters in identifying agent/s that can alter the above readouts favourably to identify small molecules from screening drug libraries and in the identification of therapeutic agents capable of ameliorating TDP-43 related neurodegeneration. Furthermore we also plan to study formation of SG in an *in vivo* model such as zebrafish.

7.8.2 Mutant zebrafish *tardbp* $^{fh301/fh301}$

Further characterisation of the *tardbp* $^{fh301/fh301}$ needs to be undertaken. Mutations in TARDBP are also associated with FTLD in addition to ALS (Table 1.2). Furthermore nearly 50% of ALS cases demonstrate features of FTLD upon psychometric analysis. Therefore it is conceivable that mutant fish could develop behavioural traits despite an apparent rescue by *tardbpl-FL.* We also need to perform immunohistochemistry and immunofluorescence of mutant zebrafish to assess cellular/sub-cellular distribution of *tardbpl-FL*. We can also use the mutant and wtTDP-43 constructs used for over-expression in HEK293T cells to assess if double knockout zebrafish can be rescued by injection of mTDP-43 or wtTDP-43 mRNA. Furthermore confirmation of the NMJ defects of Tardbp and Tardbpl-Tardbpl-FL double knockout embryos, by analysing NMJ staining of more embryos.

Generation of a *tardbp* transgenic zebrafish model with the heat shock promoter to induce TDP-43, need to be generated, a motor phenotype if present could be utilised to screen for small molecule libraries. The principle for which is already established in our lab (Ramesh et al, ongoing work on *SOD1* mutant zebrafish).

Outputs and achievements during the MRC Clinical Training Fellowship

Prizes

Prize for one of the best two platform presentations titled **-** *Role of REEP1 in Hereditary spastic paraparesis,* at The South Yorkshire and Humber deanery ACF conference, 2010

Publications

- **Hewamadduma**, C.A., Allen, A., Higginbottom, A., Grierson, A., Shaw, P. Fibroblasts from patients with ALS associated with mutations in TARDBP gene as model of TDP-43 proteinopathy. *Human molecular genetics* (2014) (Manuscript in preparation).

- Highley JR, Kirby J, Jansweijer JA, Webb PS, **Hewamadduma**, C. A., Heath PR, Higginbottom A, Raman R, Ferraiuolo L, Cooper-Knock J, McDermott CJ, Wharton SB, Shaw PJ, Ince PG. Amyotrophic lateral sclerosis-causing TARDBP (TDP-43) mutations cause widespread dysregulation of mRNA splicing in cell lines from human patients. Neuropathol Appl Neurobiol. 2014 Apr 18.

- Morrison, K. E. *et al.* Lithium in patients with amyotrophic lateral sclerosis (LiCALS): a phase 3 multicentre, randomised, double-blind, placebo-controlled trial. *Lancet neurology* 12, 339-345, (2013).

- **Hewamadduma**, C. A. *et al.* Tardbpl splicing rescues motor neuron and axonal development in a mutant tardbp zebrafish. *Human molecular genetics* 22, (2013).

- Al-Chalabi, A. *et al.* Protocol for a double-blind randomised placebo-controlled trial of lithium carbonate in patients with amyotrophic lateral sclerosis (LiCALS) [Eudract number: 2008-006891-31]. *BMC neurology* 11, 111 (2011).

- **Hewamadduma**, C. *et al.* New pedigrees and novel mutation expand the phenotype of REEP1-associated hereditary spastic paraplegia (HSP). *Neurogenetics* 10, 105-110, (2009).

Platform presentation

- *Role of REEP1 in Hereditary spastic paraparesis,* at The South Yorkshire and Humber deanery ACF conference, 2010.

- Tardbpl splicing rescues motor neuron and axonal development in a mutant tardbp zebrafish. *American Association of Neurology (AAN)*, 2012.

Poster presentation

- Fibroblasts as a model to study TDP-43 related RNA modulation and its implications on ALS. Annual research day, University of Sheffield (2012).

- Tardbpl splicing rescues motor neuron and axonal development in a mutant tardbp zebrafish. International zebrafish conference, Edinburgh (2011).

- Altered stress response in ALS associated mutations in *TARDBP*. Association of British neurologists (2010).

References

(1966) The amyotrophic lateral sclerosis of Guam. Med J Aust 2:31.

Abhyankar MM, Urekar C, Reddi PP (2007) A novel CpG-free vertebrate insulator silences the testis-specific SP-10 gene in somatic tissues: role for TDP-43 in insulator function. J Biol Chem 282:36143-36154.

Acharya KK, Govind CK, Shore AN, Stoler MH, Reddi PP (2006) cis-requirement for the maintenance of round spermatid-specific transcription. Dev Biol 295:781-790.

Ahlskog JE, Waring SC, Petersen RC, Esteban-Santillan C, Craig UK, O'Brien PC, Plevak MF, Kurland LT (1998) Olfactory dysfunction in Guamanian ALS, parkinsonism, and dementia. Neurology 51:1672-1677.

Amador-Ortiz C, Lin WL, Ahmed Z, Personett D, Davies P, Duara R, Graff-Radford NR, Hutton ML, Dickson DW (2007) TDP-43 immunoreactivity in hippocampal sclerosis and Alzheimer's disease. Ann Neurol 61:435-445.

Andersen PM (2012) Mutation in C9orf72 changes the boundaries of ALS and FTD. Lancet neurology 11:205-207.

Anderson P, Kedersha N (2002) Visibly stressed: the role of eIF2, TIA-1, and stress granules in protein translation. Cell stress & chaperones 7:213-221.

Anderson P, Kedersha N (2008) Stress granules: the Tao of RNA triage. Trends Biochem Sci 33:141-150.

Anderson P, Kedersha N (2009) Stress granules. Curr Biol 19:R397-398.

Andersson MK, Stahlberg A, Arvidsson Y, Olofsson A, Semb H, Stenman G, Nilsson O, Aman P (2008) The multifunctional FUS, EWS and TAF15 proto-oncoproteins show cell type-specific expression patterns and involvement in cell spreading and stress response. BMC Cell Biol 9:37.

Arai T, Hasegawa M, Akiyama H, Ikeda K, Nonaka T, Mori H, Mann D, Tsuchiya K, Yoshida M, Hashizume Y, Oda T (2006) TDP-43 is a component of ubiquitin-positive tau-negative inclusions in frontotemporal lobar degeneration and amyotrophic lateral sclerosis. Biochem Biophys Res Commun 351:602-611.

Arai T, Hasegawa M, Nonoka T, Kametani F, Yamashita M, Hosokawa M, Niizato K, Tsuchiya K, Kobayashi Z, Ikeda K, Yoshida M, Onaya M, Fujishiro H, Akiyama H (2010) Phosphorylated and cleaved TDP-43 in ALS, FTLD and other neurodegenerative disorders and in cellular models of TDP-43 proteinopathy. Neuropathology 30:170-181.

Arechabala B, Coiffard C, Rivalland P, Coiffard LJ, de Roeck-Holtzhauer Y (1999) Comparison of cytotoxicity of various surfactants tested on normal human fibroblast cultures using the neutral red test, MTT assay and LDH release. Journal of applied toxicology : JAT 19:163-165.

Arnold ES, Ling SC, Huelga SC, Lagier-Tourenne C, Polymenidou M, Ditsworth D, Kordasiewicz HB, McAlonis-Downes M, Platoshyn O, Parone PA, Da Cruz S, Clutario KM, Swing D, Tessarollo L, Marsala M, Shaw CE, Yeo GW, Cleveland DW (2013) ALS-linked TDP-43 mutations produce aberrant RNA splicing and adult-onset motor neuron disease without aggregation or loss of nuclear TDP-43. Proceedings of the National Academy of Sciences of the United States of America 110:E736-745.

Arrasate M, Mitra S, Schweitzer ES, Segal MR, Finkbeiner S (2004) Inclusion body formation reduces levels of mutant huntingtin and the risk of neuronal death. Nature 431:805-810.

Ascherio A (2005) Physical activity and the association with sporadic ALS. Neurology 65:972-973; author reply 972-973.

Ash PE, Zhang YJ, Roberts CM, Saldi T, Hutter H, Buratti E, Petrucelli L, Link CD (2010) Neurotoxic effects of TDP-43 overexpression in C. elegans. Hum Mol Genet 19:3206-3218.

Aulas A, Stabile S, Vande Velde C (2012) Endogenous TDP-43, but not FUS, contributes to stress granule assembly via G3BP. Mol Neurodegener 7:54.

Ayala V, Granado-Serrano AB, Cacabelos D, Naudi A, Ilieva EV, Boada J, Caraballo-Miralles V, Llado J, Ferrer I, Pamplona R, Portero-Otin M (2011a) Cell stress induces TDP-43 pathological changes associated with ERK1/2 dysfunction: implications in ALS. Acta Neuropathol.

Ayala YM, De Conti L, Avendano-Vazquez SE, Dhir A, Romano M, D'Ambrogio A, Tollervey J, Ule J, Baralle M, Buratti E, Baralle FE (2011b) TDP-43 regulates its mRNA levels through a negative feedback loop. EMBO J 30:277-288.

Ayala YM, Misteli T, Baralle FE (2008a) TDP-43 regulates retinoblastoma protein phosphorylation through the repression of cyclin-dependent kinase 6 expression. Proc Natl Acad Sci U S A 105:3785-3789.

Ayala YM, Pagani F, Baralle FE (2006) TDP43 depletion rescues aberrant CFTR exon 9 skipping. FEBS Lett 580:1339-1344.

Ayala YM, Pantano S, D'Ambrogio A, Buratti E, Brindisi A, Marchetti C, Romano M, Baralle FE (2005) Human, Drosophila, and C.elegans TDP43: nucleic acid binding properties and splicing regulatory function. J Mol Biol 348:575-588.

Ayala YM, Zago P, D'Ambrogio A, Xu YF, Petrucelli L, Buratti E, Baralle FE (2008b) Structural determinants of the cellular localization and shuttling of TDP-43. J Cell Sci 121:3778-3785.

Bai Q, Garver JA, Hukriede NA, Burton EA (2007) Generation of a transgenic zebrafish model of Tauopathy using a novel promoter element derived from the zebrafish eno2 gene. Nucleic Acids Res 35:6501-6516.

Baker HF, Ridley RM, Duchen LW, Crow TJ, Bruton CJ (1994) Induction of beta (A4)-amyloid in primates by injection of Alzheimer's disease brain homogenate. Comparison with transmission of spongiform encephalopathy. Mol Neurobiol 8:25-39.

Bame M, Grier RE, Needleman R, Brusilow WS (2014) Amino acids as biomarkers in the SOD1(G93A) mouse model of ALS. Biochimica et biophysica acta 1842:79-87.

Bandmann O, Burton EA (2010) Genetic zebrafish models of neurodegenerative diseases. Neurobiol Dis 40:58-65.

Barber SC, Mead RJ, Shaw PJ (2006) Oxidative stress in ALS: a mechanism of neurodegeneration and a therapeutic target. Biochim Biophys Acta 1762:1051-1067.

Barber SC, Shaw PJ (2010) Oxidative stress in ALS: key role in motor neuron injury and therapeutic target. Free radical biology & medicine 48:629-641.

Barmada SJ, Finkbeiner S (2010) Pathogenic TARDBP mutations in amyotrophic lateral sclerosis and frontotemporal dementia: disease-associated pathways. Rev Neurosci 21:251-272.

Barmada SJ, Skibinski G, Korb E, Rao EJ, Wu JY, Finkbeiner S (2010) Cytoplasmic mislocalization of TDP-43 is toxic to neurons and enhanced by a mutation

associated with familial amyotrophic lateral sclerosis. J Neurosci 30:639-649.

Baumer D, Hilton D, Paine SM, Turner MR, Lowe J, Talbot K, Ansorge O (2010) Juvenile ALS with basophilic inclusions is a FUS proteinopathy with FUS mutations. Neurology 75:611-618.

Beal MF (2000) Mitochondria and the pathogenesis of ALS. Brain 123 (Pt 7):1291-1292.

Beattie CE, Carrel TL, McWhorter ML (2007) Fishing for a mechanism: using zebrafish to understand spinal muscular atrophy. J Child Neurol 22:995-1003.

Beattie CE, Melancon E, Eisen JS (2000) Mutations in the stumpy gene reveal intermediate targets for zebrafish motor axons. Development 127:2653-2662.

Beghi E, Logroscino G, Chio A, Hardiman O, Mitchell D, Swingler R, Traynor BJ (2006) The epidemiology of ALS and the role of population-based registries. Biochim Biophys Acta 1762:1150-1157.

Beleza-Meireles A, Al-Chalabi A (2009) Genetic studies of amyotrophic lateral sclerosis: controversies and perspectives. Amyotroph Lateral Scler 10:1-14.

Benajiba L, Le Ber I, Camuzat A, Lacoste M, Thomas-Anterion C, Couratier P, Legallic S, Salachas F, Hannequin D, Decousus M, Lacomblez L, Guedj E, Golfier V, Camu W, Dubois B, Campion D, Meininger V, Brice A (2009) TARDBP mutations in motoneuron disease with frontotemporal lobar degeneration. Ann Neurol 65:470-473.

Bentmann E, Neumann M, Tahirovic S, Rodde R, Dormann D, Haass C (2012) Requirements for stress granule recruitment of fused in sarcoma (FUS) and TAR DNA-binding protein of 43 kDa (TDP-43). J Biol Chem 287:23079-23094.

Biamonti G, Ruggiu M, Saccone S, Della Valle G, Riva S (1994) Two homologous genes, originated by duplication, encode the human hnRNP proteins A2 and A1. Nucleic Acids Res 22:1996-2002.

Biamonti G, Vourc'h C (2010) Nuclear stress bodies. Cold Spring Harbor perspectives in biology 2:a000695.

Bilican B, Serio A, Barmada SJ, Nishimura AL, Sullivan GJ, Carrasco M, Phatnani HP, Puddifoot CA, Story D, Fletcher J, Park IH, Friedman BA, Daley GQ, Wyllie DJ, Hardingham GE, Wilmut I, Finkbeiner S, Maniatis T, Shaw CE, Chandran S (2012) Mutant induced pluripotent stem cell lines recapitulate aspects of TDP-43 proteinopathies and reveal cell-specific vulnerability. Proc Natl Acad Sci U S A 109:5803-5808.

Blackburn D, Sargsyan S, Monk PN, Shaw PJ (2009) Astrocyte function and role in motor neuron disease: a future therapeutic target? Glia 57:1251-1264.

Bolognani F, Perrone-Bizzozero NI (2008) RNA-protein interactions and control of mRNA stability in neurons. J Neurosci Res 86:481-489.

Bonvicini F, Vinceti M, Marcello N, Rodolfi R, Rinaldi M (2008) The epidemiology of amyotrophic lateral sclerosis in Reggio Emilia, Italy. Amyotroph Lateral Scler 9:350-353.

Borden LA, Maxfield FR, Goldman JE, Shelanski ML (1992) Resting [Ca2+]i and [Ca2+]i transients are similar in fibroblasts from normal and Alzheimer's donors. Neurobiology of aging 13:33-38.

Borroni B, Archetti S, Del Bo R, Papetti A, Buratti E, Bonvicini C, Agosti C, Cosseddu M, Turla M, Di Lorenzo D, Pietro Comi G, Gennarelli M, Padovani A (2010)

TARDBP mutations in frontotemporal lobar degeneration: frequency, clinical features, and disease course. Rejuvenation Res 13:509-517.

Borroni B, Bonvicini C, Alberici A, Buratti E, Agosti C, Archetti S, Papetti A, Stuani C, Di Luca M, Gennarelli M, Padovani A (2009) Mutation within TARDBP leads to frontotemporal dementia without motor neuron disease. Hum Mutat 30:E974-983.

Bosco DA, Lemay N, Ko HK, Zhou H, Burke C, Kwiatkowski TJ, Jr., Sapp P, McKenna-Yasek D, Brown RH, Jr., Hayward LJ (2010a) Mutant FUS proteins that cause amyotrophic lateral sclerosis incorporate into stress granules. Human molecular genetics 19:4160-4175.

Bosco DA, Lemay N, Ko HK, Zhou H, Burke C, Kwiatkowski TJ, Jr., Sapp P, McKenna-Yasek D, Brown RH, Jr., Hayward LJ (2010b) Mutant FUS proteins that cause amyotrophic lateral sclerosis incorporate into stress granules. Hum Mol Genet 19:4160-4175.

Bose JK, Wang IF, Hung L, Tarn WY, Shen CK (2008) TDP-43 overexpression enhances exon 7 inclusion during the survival of motor neuron pre-mRNA splicing. J Biol Chem 283:28852-28859.

Braak H, Rub U, Gai WP, Del Tredici K (2003) Idiopathic Parkinson's disease: possible routes by which vulnerable neuronal types may be subject to neuroinvasion by an unknown pathogen. Journal of neural transmission 110:517-536.

Brady OA, Meng P, Zheng Y, Mao Y, Hu F (2011) Regulation of TDP-43 aggregation by phosphorylation and p62/SQSTM1. J Neurochem 116:248-259.

Bresch S, Delmont E, Soriani MH, Desnuelle C (2014) [Electrodiagnostic criteria for early diagnosis of bulbar-onset ALS: a comparison of El Escorial, revised El Escorial and Awaji algorithm]. Revue neurologique 170:134-139.

Brettschneider J, Libon DJ, Toledo JB, Xie SX, McCluskey L, Elman L, Geser F, Lee VM, Grossman M, Trojanowski JQ (2012) Microglial activation and TDP-43 pathology correlate with executive dysfunction in amyotrophic lateral sclerosis. Acta Neuropathol 123:395-407.

Brody JA, Chen KM (1968) Recent studies of amyotrophic lateral sclerosis and parkinsonism-dementia on Guam. Proc Aust Assoc Neurol 5:331-334.

Brooks BR (1994) El Escorial World Federation of Neurology criteria for the diagnosis of amyotrophic lateral sclerosis. Subcommittee on Motor Neuron Diseases/Amyotrophic Lateral Sclerosis of the World Federation of Neurology Research Group on Neuromuscular Diseases and the El Escorial "Clinical limits of amyotrophic lateral sclerosis" workshop contributors. J Neurol Sci 124 Suppl:96-107.

Brooks BR (1996) Clinical epidemiology of amyotrophic lateral sclerosis. Neurol Clin 14:399-420.

Brooks BR, Miller RG, Swash M, Munsat TL (2000) El Escorial revisited: revised criteria for the diagnosis of amyotrophic lateral sclerosis. Amyotroph Lateral Scler Other Motor Neuron Disord 1:293-299.

Bucheli M, Andino A, Montalvo M, Cruz J, Atassi N, Berry J, Salameh J (2014) Amyotrophic lateral sclerosis: analysis of ALS cases in a predominantly admixed population of Ecuador. Amyotrophic lateral sclerosis & frontotemporal degeneration 15:106-113.

Budini M, Buratti E (2011) TDP-43 Autoregulation: Implications for Disease. J Mol Neurosci.

Buratti E, Baralle D (2010a) Novel roles of U1 snRNP in alternative splicing regulation. RNA Biol 7:412-419.

Buratti E, Baralle FE (2001) Characterization and functional implications of the RNA binding properties of nuclear factor TDP-43, a novel splicing regulator of CFTR exon 9. J Biol Chem 276:36337-36343.

Buratti E, Baralle FE (2008) Multiple roles of TDP-43 in gene expression, splicing regulation, and human disease. Front Biosci 13:867-878.

Buratti E, Baralle FE (2009) The molecular links between TDP-43 dysfunction and neurodegeneration. Adv Genet 66:1-34.

Buratti E, Baralle FE (2010b) The multiple roles of TDP-43 in pre-mRNA processing and gene expression regulation. RNA Biol 7:420-429.

Buratti E, Baralle FE (2011a) TDP-43: New aspects of autoregulation mechanisms in RNA binding proteins and their connection with human disease. FEBS J.

Buratti E, Baralle FE (2011b) TDP-43: new aspects of autoregulation mechanisms in RNA binding proteins and their connection with human disease. FEBS J 278:3530-3538.

Buratti E, Brindisi A, Giombi M, Tisminetzky S, Ayala YM, Baralle FE (2005) TDP-43 binds heterogeneous nuclear ribonucleoprotein A/B through its C-terminal tail: an important region for the inhibition of cystic fibrosis transmembrane conductance regulator exon 9 splicing. J Biol Chem 280:37572-37584.

Buratti E, Dork T, Zuccato E, Pagani F, Romano M, Baralle FE (2001) Nuclear factor TDP-43 and SR proteins promote in vitro and in vivo CFTR exon 9 skipping. EMBO J 20:1774-1784.

Burkhardt MF, Martinez FJ, Wright S, Ramos C, Volfson D, Mason M, Garnes J, Dang V, Lievers J, Shoukat-Mumtaz U, Martinez R, Gai H, Blake R, Vaisberg E, Grskovic M, Johnson C, Irion S, Bright J, Cooper B, Nguyen L, Griswold-Prenner I, Javaherian A (2013) A cellular model for sporadic ALS using patient-derived induced pluripotent stem cells. Molecular and cellular neurosciences 56C:355-364.

Caccamo A, Majumder S, Oddo S (2011) Cognitive Decline Is Typical of Frontotemporal Lobar Degeneration in Transgenic Mice Expressing the 25-kDa C-Terminal Fragment of TDP-43. Am J Pathol.

Cairns NJ, Neumann M, Bigio EH, Holm IE, Troost D, Hatanpaa KJ, Foong C, White CL, 3rd, Schneider JA, Kretzschmar HA, Carter D, Taylor-Reinwald L, Paulsmeyer K, Strider J, Gitcho M, Goate AM, Morris JC, Mishra M, Kwong LK, Stieber A, Xu Y, Forman MS, Trojanowski JQ, Lee VM, Mackenzie IR (2007) TDP-43 in familial and sporadic frontotemporal lobar degeneration with ubiquitin inclusions. Am J Pathol 171:227-240.

Cannon A, Yang B, Knight J, Farnham IM, Zhang Y, Wuertzer CA, D'Alton S, Lin WL, Castanedes-Casey M, Rousseau L, Scott B, Jurasic M, Howard J, Yu X, Bailey R, Sarkisian MR, Dickson DW, Petrucelli L, Lewis J (2012) Neuronal sensitivity to TDP-43 overexpression is dependent on timing of induction. Acta Neuropathol 123:807-823.

Caputo C, Bolanos P (2008) Effect of mitochondria poisoning by FCCP on Ca2+ signaling in mouse skeletal muscle fibers. Pflugers Archiv : European journal of physiology 455:733-743.

Casafont I, Bengoechea R, Tapia O, Berciano MT, Lafarga M (2009) TDP-43 localizes in mRNA transcription and processing sites in mammalian neurons. J Struct Biol 167:235-241.

Charcot JM JA (1869) Deux cas d'atrophie musculaire progressive avec le`sions de la substancegrise et des faisceaux antero-late`raux de la moelle epinie`re. Arch Physiol Neurol Pathol 2:744.

Charroux B, Pellizzoni L, Perkinson RA, Yong J, Shevchenko A, Mann M, Dreyfuss G (2000) Gemin4. A novel component of the SMN complex that is found in both gems and nucleoli. J Cell Biol 148:1177-1186.

Chen YZ, Bennett CL, Huynh HM, Blair IP, Puls I, Irobi J, Dierick I, Abel A, Kennerson ML, Rabin BA, Nicholson GA, Auer-Grumbach M, Wagner K, De Jonghe P, Griffin JW, Fischbeck KH, Timmerman V, Cornblath DR, Chance PF (2004) DNA/RNA helicase gene mutations in a form of juvenile amyotrophic lateral sclerosis (ALS4). Am J Hum Genet 74:1128-1135.

Chiang HH, Andersen PM, Tysnes OB, Gredal O, Christensen PB, Graff C (2012) Novel TARDBP mutations in Nordic ALS patients. J Hum Genet 57:316-319.

Chiang PM, Ling J, Jeong YH, Price DL, Aja SM, Wong PC (2010) Deletion of TDP-43 down-regulates Tbc1d1, a gene linked to obesity, and alters body fat metabolism. Proc Natl Acad Sci U S A 107:16320-16324.

Chio A, Traynor BJ, Lombardo F, Fimognari M, Calvo A, Ghiglione P, Mutani R, Restagno G (2008) Prevalence of SOD1 mutations in the Italian ALS population. Neurology 70:533-537.

Christians ES, Yan LJ, Benjamin IJ (2002) Heat shock factor 1 and heat shock proteins: Critical partners in protection against acute cell injury. Critical care medicine 30:S43-S50.

Ciura S, Lattante S, Le Ber I, Latouche M, Tostivint H, Brice A, Kabashi E (2013) Loss of function of C9orf72 causes motor deficits in a zebrafish model of amyotrophic lateral sclerosis. Annals of neurology 74:180-187.

Cobianchi F, Biamonti G, Maconi M, Riva S (1994) Human hnRNP protein A1: a model polypeptide for a structural and genetic investigation of a broad family of RNA binding proteins. Genetica 94:101-114.

Collins LJ, Penny D (2009) The RNA infrastructure: dark matter of the eukaryotic cell? Trends Genet 25:120-128.

Colombrita C, Zennaro E, Fallini C, Weber M, Sommacal A, Buratti E, Silani V, Ratti A (2009) TDP-43 is recruited to stress granules in conditions of oxidative insult. J Neurochem 111:1051-1061.

Cookson MR, Ince PG, Shaw PJ (1998) Peroxynitrite and hydrogen peroxide induced cell death in the NSC34 neuroblastoma x spinal cord cell line: role of poly (ADP-ribose) polymerase. Journal of neurochemistry 70:501-508.

Cooper-Knock J, Hewitt C, Highley JR, Brockington A, Milano A, Man S, Martindale J, Hartley J, Walsh T, Gelsthorpe C, Baxter L, Forster G, Fox M, Bury J, Mok K, McDermott CJ, Traynor BJ, Kirby J, Wharton SB, Ince PG, Hardy J, Shaw PJ (2012) Clinico-pathological features in amyotrophic lateral sclerosis with expansions in C9ORF72. Brain 135:751-764.

Corrado L, Del Bo R, Castellotti B, Ratti A, Cereda C, Penco S, Soraru G, Carlomagno Y, Ghezzi S, Pensato V, Colombrita C, Gagliardi S, Cozzi L, Orsetti V, Mancuso M, Siciliano G, Mazzini L, Comi GP, Gellera C, Ceroni M, D'Alfonso S, Silani V (2009a) Mutations of FUS Gene in Sporadic Amyotrophic Lateral Sclerosis. J Med Genet.

Corrado L, Ratti A, Gellera C, Buratti E, Castellotti B, Carlomagno Y, Ticozzi N, Mazzini L, Testa L, Taroni F, Baralle FE, Silani V, D'Alfonso S (2009b) High frequency of TARDBP gene mutations in Italian patients with amyotrophic lateral sclerosis. Hum Mutat 30:688-694.

Corrado L, Ratti A, Gellera C, Buratti E, Castellotti B, Carlomagno Y, Ticozzi N, Mazzini L, Testa L, Taroni F, Baralle FE, Silani V, D'Alfonso S (2009c) High frequency of TARDBP gene mutations in Italian patients with amyotrophic lateral sclerosis. Human mutation 30:688-694.

Criddle DN, Gillies S, Baumgartner-Wilson HK, Jaffar M, Chinje EC, Passmore S, Chvanov M, Barrow S, Gerasimenko OV, Tepikin AV, Sutton R, Petersen OH (2006) Menadione-induced reactive oxygen species generation via redox cycling promotes apoptosis of murine pancreatic acinar cells. The Journal of biological chemistry 281:40485-40492.

D'Ambrogio A, Buratti E, Stuani C, Guarnaccia C, Romano M, Ayala YM, Baralle FE (2009) Functional mapping of the interaction between TDP-43 and hnRNP A2 in vivo. Nucleic Acids Res 37:4116-4126.

Da Costa MM, Allen CE, Higginbottom A, Ramesh T, Shaw PJ, McDermott CJ (2014) A new zebrafish model produced by TILLING of SOD1-related amyotrophic lateral sclerosis replicates key features of the disease and represents a tool for in vivo therapeutic screening. Disease models & mechanisms 7:73-81.

Dammer EB, Fallini C, Gozal YM, Duong DM, Rossoll W, Xu P, Lah JJ, Levey AI, Peng J, Bassell GJ, Seyfried NT (2012) Coaggregation of RNA-binding proteins in a model of TDP-43 proteinopathy with selective RGG motif methylation and a role for RRM1 ubiquitination. PLoS One 7:e38658.

Daoud H, Valdmanis PN, Kabashi E, Dion P, Dupre N, Camu W, Meininger V, Rouleau GA (2009) Contribution of TARDBP mutations to sporadic amyotrophic lateral sclerosis. J Med Genet 46:112-114.

De Marco G, Lupino E, Calvo A, Moglia C, Buccinna B, Grifoni S, Ramondetti C, Lomartire A, Rinaudo MT, Piccinini M, Giordana MT, Chio A (2011) Cytoplasmic accumulation of TDP-43 in circulating lymphomonocytes of ALS patients with and without TARDBP mutations. Acta neuropathologica 121:611-622.

Dejesus-Hernandez M, Mackenzie IR, Boeve BF, Boxer AL, Baker M, Rutherford NJ, Nicholson AM, Finch NA, Flynn H, Adamson J, Kouri N, Wojtas A, Sengdy P, Hsiung GY, Karydas A, Seeley WW, Josephs KA, Coppola G, Geschwind DH, Wszolek ZK, Feldman H, Knopman DS, Petersen RC, Miller BL, Dickson DW, Boylan KB, Graff-Radford NR, Rademakers R (2011) Expanded GGGGCC Hexanucleotide Repeat in Noncoding Region of C9ORF72 Causes Chromosome 9p-Linked FTD and ALS. Neuron 72:245-256.

Del Bo R, Ghezzi S, Corti S, Pandolfo M, Ranieri M, Santoro D, Ghione I, Prelle A, Orsetti V, Mancuso M, Soraru G, Briani C, Angelini C, Siciliano G, Bresolin N, Comi GP (2009) TARDBP (TDP-43) sequence analysis in patients with familial and sporadic ALS: identification of two novel mutations. Eur J Neurol 16:727-732.

Dewey CM, Cenik B, Sephton CF, Dries DR, Mayer P, 3rd, Good SK, Johnson BA, Herz J, Yu G (2011) TDP-43 is directed to stress granules by sorbitol, a novel physiological osmotic and oxidative stressor. Mol Cell Biol 31:1098-1108.

Dewey CM, Cenik B, Sephton CF, Johnson BA, Herz J, Yu G (2012) TDP-43 aggregation in neurodegeneration: are stress granules the key? Brain Res 1462:16-25.

Diaper DC, Adachi Y, Lazarou L, Greenstein M, Simoes FA, Di Domenico A, Solomon DA, Lowe S, Alsubaie R, Cheng D, Buckley S, Humphrey DM, Shaw CE, Hirth F (2013) Drosophila TDP-43 dysfunction in glia and muscle cells cause cytological and behavioural phenotypes that characterize ALS and FTLD. Human molecular genetics.

Dimos JT, Rodolfa KT, Niakan KK, Weisenthal LM, Mitsumoto H, Chung W, Croft GF, Saphier G, Leibel R, Goland R, Wichterle H, Henderson CE, Eggan K (2008) Induced pluripotent stem cells generated from patients with ALS can be differentiated into motor neurons. Science 321:1218-1221.

Dion PA, Daoud H, Rouleau GA (2009) Genetics of motor neuron disorders: new insights into pathogenic mechanisms. Nat Rev Genet 10:769-782.

Dreumont N, Hardy S, Behm-Ansmant I, Kister L, Branlant C, Stevenin J, Bourgeois CF (2010) Antagonistic factors control the unproductive splicing of SC35 terminal intron. Nucleic Acids Res 38:1353-1366.

Dubnau J, Chiang AS, Grady L, Barditch J, Gossweiler S, McNeil J, Smith P, Buldoc F, Scott R, Certa U, Broger C, Tully T (2003) The staufen/pumilio pathway is involved in Drosophila long-term memory. Curr Biol 13:286-296.

Egawa N, Kitaoka S, Tsukita K, Naitoh M, Takahashi K, Yamamoto T, Adachi F, Kondo T, Okita K, Asaka I, Aoi T, Watanabe A, Yamada Y, Morizane A, Takahashi J, Ayaki T, Ito H, Yoshikawa K, Yamawaki S, Suzuki S, Watanabe D, Hioki H, Kaneko T, Makioka K, Okamoto K, Takuma H, Tamaoka A, Hasegawa K, Nonaka T, Hasegawa M, Kawata A, Yoshida M, Nakahata T, Takahashi R, Marchetto MC, Gage FH, Yamanaka S, Inoue H (2012) Drug screening for ALS using patient-specific induced pluripotent stem cells. Science translational medicine 4:145ra104.

Elvira G, Wasiak S, Blandford V, Tong XK, Serrano A, Fan X, del Rayo Sanchez-Carbente M, Servant F, Bell AW, Boismenu D, Lacaille JC, McPherson PS, DesGroseillers L, Sossin WS (2006) Characterization of an RNA granule from developing brain. Mol Cell Proteomics 5:635-651.

Estes PS, Boehringer A, Zwick R, Tang JE, Grigsby B, Zarnescu DC (2011) Wild-type and A315T mutant TDP-43 exert differential neurotoxicity in a Drosophila model of ALS. Hum Mol Genet.

Evdokimidis I, Constantinidis TS, Gourtzelidis P, Smyrnis N, Zalonis I, Zis PV, Andreadou E, Papageorgiou C (2002) Frontal lobe dysfunction in amyotrophic lateral sclerosis. J Neurol Sci 195:25-33.

Eymery A, Callanan M, Vourc'h C (2009) The secret message of heterochromatin: new insights into the mechanisms and function of centromeric and pericentric repeat sequence transcription. The International journal of developmental biology 53:259-268.

Farrar MA, Johnston HM, Grattan-Smith P, Turner A, Kiernan MC (2009) Spinal muscular atrophy: molecular mechanisms. Curr Mol Med 9:851-862.

Feiguin F, Godena VK, Romano G, D'Ambrogio A, Klima R, Baralle FE (2009) Depletion of TDP-43 affects Drosophila motoneurons terminal synapsis and locomotive behavior. FEBS Lett 583:1586-1592.

Fernandez C, Pilar Callao M, Larrechi MS (2013) UV-visible-DAD and 1H-NMR spectroscopy data fusion for studying the photodegradation process of azo-dyes using MCR-ALS. Talanta 117:75-80.

Ferraiuolo L, Kirby J, Grierson AJ, Sendtner M, Shaw PJ (2011) Molecular pathways of motor neuron injury in amyotrophic lateral sclerosis. Nat Rev Neurol 7:616-630.

Fiesel FC, Schurr C, Weber SS, Kahle PJ (2011) TDP-43 knockdown impairs neurite outgrowth dependent on its target histone deacetylase 6. Mol Neurodegener 6:64.

Fiesel FC, Voigt A, Weber SS, Van den Haute C, Waldenmaier A, Gorner K, Walter M, Anderson ML, Kern JV, Rasse TM, Schmidt T, Springer W, Kirchner R, Bonin M, Neumann M, Baekelandt V, Alunni-Fabbroni M, Schulz JB, Kahle PJ (2009) Knockdown of transactive response DNA-binding protein (TDP-43) downregulates histone deacetylase 6. EMBO J.

Fiesel FC, Voigt A, Weber SS, Van den Haute C, Waldenmaier A, Gorner K, Walter M, Anderson ML, Kern JV, Rasse TM, Schmidt T, Springer W, Kirchner R, Bonin

M, Neumann M, Baekelandt V, Alunni-Fabbroni M, Schulz JB, Kahle PJ (2010) Knockdown of transactive response DNA-binding protein (TDP-43) downregulates histone deacetylase 6. EMBO J 29:209-221.

Figley MD, Gitler AD (2013) Yeast genetic screen reveals novel therapeutic strategy for ALS. Rare diseases 1:e24420.

Filimonenko M, Stuffers S, Raiborg C, Yamamoto A, Malerod L, Fisher EM, Isaacs A, Brech A, Stenmark H, Simonsen A (2007) Functional multivesicular bodies are required for autophagic clearance of protein aggregates associated with neurodegenerative disease. J Cell Biol 179:485-500.

Fillman C, Lykke-Andersen J (2005) RNA decapping inside and outside of processing bodies. Curr Opin Cell Biol 17:326-331.

Flanders KC, Ren RF, Lippa CF (1998) Transforming growth factor-betas in neurodegenerative disease. Prog Neurobiol 54:71-85.

Flinn L, Mortiboys H, Volkmann K, Koster RW, Ingham PW, Bandmann O (2009) Complex I deficiency and dopaminergic neuronal cell loss in parkin-deficient zebrafish (Danio rerio). Brain 132:1613-1623.

Forbes JM, Coughlan MT, Cooper ME (2008) Oxidative stress as a major culprit in kidney disease in diabetes. Diabetes 57:1446-1454.

Fuentealba RA, Udan M, Bell S, Wegorzewska I, Shao J, Diamond MI, Weihl CC, Baloh RH (2010) Interaction with polyglutamine aggregates reveals a Q/N-rich domain in TDP-43. J Biol Chem 285:26304-26314.

Fujita Y, Ikeda M, Yanagisawa T, Senoo Y, Okamoto K (2011) Different clinical and neuropathologic phenotypes of familial ALS with A315E TARDBP mutation. Neurology 77:1427-1431.

Gallone S, Giordana MT, Scarpini E, Rainero I, Rubino E, Fenoglio P, Galimberti D, Grifoni S, Venturelli E, Acutis PL, Peletto S, Maniaci MG, Ferrero P, Zotta M, Pinessi L (2009) Absence of TARDBP gene mutations in an italian series of patients with frontotemporal lobar degeneration. Dement Geriatr Cogn Disord 28:239-243.

Gandhi S, Wood-Kaczmar A, Yao Z, Plun-Favreau H, Deas E, Klupsch K, Downward J, Latchman DS, Tabrizi SJ, Wood NW, Duchen MR, Abramov AY (2009) PINK1-associated Parkinson's disease is caused by neuronal vulnerability to calcium-induced cell death. Molecular cell 33:627-638.

Gao X, Xu Z (2008) Mechanisms of action of angiogenin. Acta Biochim Biophys Sin (Shanghai) 40:619-624.

Gates RE (1991) Elimination of interfering substances in the presence of detergent in the bicinchoninic acid protein assay. Anal Biochem 196:290-295.

Geiss-Friedlander R, Melchior F (2007) Concepts in sumoylation: a decade on. Nat Rev Mol Cell Biol 8:947-956.

Gelpi E, van der Zee J, Turon Estrada A, Van Broeckhoven C, Sanchez-Valle R (2014) TARDBP mutation p.Ile383Val associated with semantic dementia and complex proteinopathy. Neuropathology and applied neurobiology 40:225-230.

Gendron TF, Josephs KA, Petrucelli L (2010) Review: transactive response DNA-binding protein 43 (TDP-43): mechanisms of neurodegeneration. Neuropathol Appl Neurobiol 36:97-112.

Gendron TF, Rademakers R, Petrucelli L (2013) TARDBP mutation analysis in TDP-43 proteinopathies and deciphering the toxicity of mutant TDP-43. Journal of Alzheimer's disease : JAD 33 Suppl 1:S35-45.

Gibson GE, Peterson C (1987) Calcium and the aging nervous system. Neurobiology of aging 8:329-343.

Gijselinck I, Sleegers K, Engelborghs S, Robberecht W, Martin JJ, Vandenberghe R, Sciot R, Dermaut B, Goossens D, van der Zee J, De Pooter T, Del-Favero J, Santens P, De Jonghe P, De Deyn PP, Van Broeckhoven C, Cruts M (2009) Neuronal inclusion protein TDP-43 has no primary genetic role in FTD and ALS. Neurobiol Aging 30:1329-1331.

Gitcho MA, Baloh RH, Chakraverty S, Mayo K, Norton JB, Levitch D, Hatanpaa KJ, White CL, 3rd, Bigio EH, Caselli R, Baker M, Al-Lozi MT, Morris JC, Pestronk A, Rademakers R, Goate AM, Cairns NJ (2008) TDP-43 A315T mutation in familial motor neuron disease. Ann Neurol 63:535-538.

Gitcho MA, Strider J, Carter D, Taylor-Reinwald L, Forman MS, Goate AM, Cairns NJ (2009) VCP mutations causing frontotemporal lobar degeneration disrupt localization of TDP-43 and induce cell death. J Biol Chem 284:12384-12398.

Glisovic T, Bachorik JL, Yong J, Dreyfuss G (2008) RNA-binding proteins and post-transcriptional gene regulation. FEBS letters 582:1977-1986.

Goedert M (2001) The significance of tau and alpha-synuclein inclusions in neurodegenerative diseases. Curr Opin Genet Dev 11:343-351.

Golebiowski F, Matic I, Tatham MH, Cole C, Yin Y, Nakamura A, Cox J, Barton GJ, Mann M, Hay RT (2009) System-wide changes to SUMO modifications in response to heat shock. Sci Signal 2:ra24.

Gregory JM, Barros TP, Meehan S, Dobson CM, Luheshi LM (2012) The aggregation and neurotoxicity of TDP-43 and its ALS-associated 25 kDa fragment are differentially affected by molecular chaperones in Drosophila. PLoS One 7:e31899.

Gregory RI, Yan KP, Amuthan G, Chendrimada T, Doratotaj B, Cooch N, Shiekhattar R (2004) The Microprocessor complex mediates the genesis of microRNAs. Nature 432:235-240.

Grohmann K, Schuelke M, Diers A, Hoffmann K, Lucke B, Adams C, Bertini E, Leonhardt-Horti H, Muntoni F, Ouvrier R, Pfeufer A, Rossi R, Van Maldergem L, Wilmshurst JM, Wienker TF, Sendtner M, Rudnik-Schoneborn S, Zerres K, Hubner C (2001) Mutations in the gene encoding immunoglobulin mu-binding protein 2 cause spinal muscular atrophy with respiratory distress type 1. Nat Genet 29:75-77.

Gros-Louis F, Kriz J, Kabashi E, McDearmid J, Millecamps S, Urushitani M, Lin L, Dion P, Zhu Q, Drapeau P, Julien JP, Rouleau GA (2008) Als2 mRNA splicing variants detected in KO mice rescue severe motor dysfunction phenotype in Als2 knock-down zebrafish. Hum Mol Genet 17:2691-2702.

Gros-Louis F, Lariviere R, Gowing G, Laurent S, Camu W, Bouchard JP, Meininger V, Rouleau GA, Julien JP (2004) A frameshift deletion in peripherin gene associated with amyotrophic lateral sclerosis. J Biol Chem 279:45951-45956.

Grunewald A, Voges L, Rakovic A, Kasten M, Vandebona H, Hemmelmann C, Lohmann K, Orolicki S, Ramirez A, Schapira AH, Pramstaller PP, Sue CM, Klein C (2010) Mutant Parkin impairs mitochondrial function and morphology in human fibroblasts. PLoS One 5:e12962.

Grunwald DJ, Eisen JS (2002) Headwaters of the zebrafish -- emergence of a new model vertebrate. Nat Rev Genet 3:717-724.

Guerreiro RJ, Schymick JC, Crews C, Singleton A, Hardy J, Traynor BJ (2008) TDP-43 is not a common cause of sporadic amyotrophic lateral sclerosis. PLoS One 3:e2450.

Guo W, Chen Y, Zhou X, Kar A, Ray P, Chen X, Rao EJ, Yang M, Ye H, Zhu L, Liu J, Xu M, Yang Y, Wang C, Zhang D, Bigio EH, Mesulam M, Shen Y, Xu Q, Fushimi K,

Wu JY (2011) An ALS-associated mutation affecting TDP-43 enhances protein aggregation, fibril formation and neurotoxicity. Nat Struct Mol Biol 18:822-830.

Gurney ME (1997) Transgenic animal models of familial amyotrophic lateral sclerosis. J Neurol 244 Suppl 2:S15-20.

Haass C, Selkoe DJ (2007) Soluble protein oligomers in neurodegeneration: lessons from the Alzheimer's amyloid beta-peptide. Nat Rev Mol Cell Biol 8:101-112.

Habelhah H, Shah K, Huang L, Ostareck-Lederer A, Burlingame AL, Shokat KM, Hentze MW, Ronai Z (2001) ERK phosphorylation drives cytoplasmic accumulation of hnRNP-K and inhibition of mRNA translation. Nat Cell Biol 3:325-330.

Hanson KA, Kim SH, Wassarman DA, Tibbetts RS (2010) Ubiquilin modifies TDP-43 toxicity in a Drosophila model of amyotrophic lateral sclerosis (ALS). J Biol Chem 285:11068-11072.

Harwood CA, McDermott CJ, Shaw PJ (2009) Physical activity as an exogenous risk factor in motor neuron disease (MND): a review of the evidence. Amyotroph Lateral Scler 10:191-204.

Hasegawa M, Arai T, Akiyama H, Nonaka T, Mori H, Hashimoto T, Yamazaki M, Oyanagi K (2007) TDP-43 is deposited in the Guam parkinsonism-dementia complex brains. Brain 130:1386-1394.

Hasegawa M, Arai T, Nonaka T, Kametani F, Yoshida M, Hashizume Y, Beach TG, Buratti E, Baralle F, Morita M, Nakano I, Oda T, Tsuchiya K, Akiyama H (2008a) Phosphorylated TDP-43 in frontotemporal lobar degeneration and amyotrophic lateral sclerosis. Ann Neurol 64:60-70.

Hasegawa M, Arai T, Nonaka T, Kametani F, Yoshida M, Hashizume Y, Beach TG, Morita M, Nakano I, Oda T, Tsuchiya K, Akiyama H (2008b) [Significance of the TDP-43 deposition in FTLD-U and ALS]. Rinsho Shinkeigaku 48:994-997.

Hasegawa M, Nonaka T, Tsuji H, Tamaoka A, Yamashita M, Kametani F, Yoshida M, Arai T, Akiyama H (2011) Molecular dissection of TDP-43 proteinopathies. J Mol Neurosci 45:480-485.

Hatzipetros T, Bogdanik LP, Tassinari VR, Kidd JD, Moreno AJ, Davis C, Osborne M, Austin A, Vieira FG, Lutz C, Perrin S (2014) C57BL/6J congenic Prp-TDP43A315T mice develop progressive neurodegeneration in the myenteric plexus of the colon without exhibiting key features of ALS. Brain Res 1584:59-72.

Hay RT (2005) SUMO: a history of modification. Mol Cell 18:1-12.

Hayflick L, Moorhead PS (1961) The serial cultivation of human diploid cell strains. Experimental cell research 25:585-621.

Hazelett DJ, Chang JC, Lakeland DL, Morton DB (2012) Comparison of parallel high-throughput RNA sequencing between knockout of TDP-43 and its overexpression reveals primarily nonreciprocal and nonoverlapping gene expression changes in the central nervous system of Drosophila. G3 (Bethesda) 2:789-802.

Henkel JS, Beers DR, Zhao W, Appel SH (2009) Microglia in ALS: The Good, The Bad, and The Resting. J Neuroimmune Pharmacol.

Henshall TL, Tucker B, Lumsden AL, Nornes S, Lardelli MT, Richards RI (2009) Selective neuronal requirement for huntingtin in the developing zebrafish. Hum Mol Genet 18:4830-4842.

Herdewyn S, Cirillo C, Van Den Bosch L, Robberecht W, Vanden Berghe P, Van Damme P (2014) Prevention of intestinal obstruction reveals progressive neurodegeneration in mutant TDP-43 (A315T) mice. Mol Neurodegener 9:24.

Herman AM, Khandelwal PJ, Rebeck GW, Moussa CE (2012) Wild type TDP-43 induces neuro-inflammation and alters APP metabolism in lentiviral gene transfer models. Exp Neurol 235:297-305.

Hewamadduma CA, Grierson AJ, Ma TP, Pan L, Moens CB, Ingham PW, Ramesh T, Shaw PJ (2013) Tardbpl splicing rescues motor neuron and axonal development in a mutant tardbp zebrafish. Human molecular genetics 22:2376-2386.

Hillel AD, Miller R (1989) Bulbar amyotrophic lateral sclerosis: patterns of progression and clinical management. Head Neck 11:51-59.

Hirokawa N (2006) mRNA transport in dendrites: RNA granules, motors, and tracks. J Neurosci 26:7139-7142.

Huang C, Tong J, Bi F, Zhou H, Xia XG (2012a) Mutant TDP-43 in motor neurons promotes the onset and progression of ALS in rats. J Clin Invest 122:107-118.

Huang HM, Martins R, Gandy S, Etcheberrigaray R, Ito E, Alkon DL, Blass J, Gibson G (1994) Use of cultured fibroblasts in elucidating the pathophysiology and diagnosis of Alzheimer's disease. Annals of the New York Academy of Sciences 747:225-244.

Huang R, Fang DF, Ma MY, Guo XY, Zhao B, Zeng Y, Zhou D, Yang Y, Shang HF (2012b) TARDBP gene mutations among Chinese patients with sporadic amyotrophic lateral sclerosis. Neurobiol Aging 33:1015 e1011-1016.

Igaz LM, Kwong LK, Chen-Plotkin A, Winton MJ, Unger TL, Xu Y, Neumann M, Trojanowski JQ, Lee VM (2009) Expression of TDP-43 C-terminal Fragments in Vitro Recapitulates Pathological Features of TDP-43 Proteinopathies. J Biol Chem 284:8516-8524.

Igaz LM, Kwong LK, Lee EB, Chen-Plotkin A, Swanson E, Unger T, Malunda J, Xu Y, Winton MJ, Trojanowski JQ, Lee VM (2011) Dysregulation of the ALS-associated gene TDP-43 leads to neuronal death and degeneration in mice. J Clin Invest 121:726-738.

Igaz LM, Kwong LK, Xu Y, Truax AC, Uryu K, Neumann M, Clark CM, Elman LB, Miller BL, Grossman M, McCluskey LF, Trojanowski JQ, Lee VM (2008) Enrichment of C-terminal fragments in TAR DNA-binding protein-43 cytoplasmic inclusions in brain but not in spinal cord of frontotemporal lobar degeneration and amyotrophic lateral sclerosis. Am J Pathol 173:182-194.

Iguchi Y, Katsuno M, Niwa J, Yamada S, Sone J, Waza M, Adachi H, Tanaka F, Nagata K, Arimura N, Watanabe T, Kaibuchi K, Sobue G (2009) TDP-43 depletion induces neuronal cell damage through dysregulation of Rho family GTPases. J Biol Chem 284:22059-22066.

Iida A, Kamei T, Sano M, Oshima S, Tokuda T, Nakamura Y, Ikegawa S (2012) Large-scale screening of TARDBP mutation in amyotrophic lateral sclerosis in Japanese. Neurobiology of aging 33:786-790.

Ince PG, Evans J, Knopp M, Forster G, Hamdalla HH, Wharton SB, Shaw PJ (2003) Corticospinal tract degeneration in the progressive muscular atrophy variant of ALS. Neurology 60:1252-1258.

Ince PG, Lowe J, Shaw PJ (1998) Amyotrophic lateral sclerosis: current issues in classification, pathogenesis and molecular pathology. Neuropathol Appl Neurobiol 24:104-117.

Inukai Y, Nonaka T, Arai T, Yoshida M, Hashizume Y, Beach TG, Buratti E, Baralle FE, Akiyama H, Hisanaga S, Hasegawa M (2008) Abnormal phosphorylation of Ser409/410 of TDP-43 in FTLD-U and ALS. FEBS Lett 582:2899-2904.

Ito D (2012) Conjoint pathological cascades mediated by RNA-binding proteins, TDP-43, FUS and Ataxin-2. Rinsho Shinkeigaku 52:1221-1223.

Janssens J, Wils H, Kleinberger G, Joris G, Cuijt I, Ceuterick-de Groote C, Van Broeckhoven C, Kumar-Singh S (2013) Overexpression of ALS-Associated p.M337V Human TDP-43 in Mice Worsens Disease Features Compared to Wild-type Human TDP-43 Mice. Molecular neurobiology 48:22-35.

Jin P, Alisch RS, Warren ST (2004) RNA and microRNAs in fragile X mental retardation. Nat Cell Biol 6:1048-1053.

Johnson BS, McCaffery JM, Lindquist S, Gitler AD (2008) A yeast TDP-43 proteinopathy model: Exploring the molecular determinants of TDP-43 aggregation and cellular toxicity. Proc Natl Acad Sci U S A 105:6439-6444.

Johnson BS, Snead D, Lee JJ, McCaffery JM, Shorter J, Gitler AD (2009) TDP-43 is intrinsically aggregation-prone, and amyotrophic lateral sclerosis-linked mutations accelerate aggregation and increase toxicity. J Biol Chem 284:20329-20339.

Julien JP, Kriz J (2006) Transgenic mouse models of amyotrophic lateral sclerosis. Biochim Biophys Acta 1762:1013-1024.

Kabashi E (2010) Gain and loss of function of ALS related mutations of TARDBP (TDP-43) cause motor deficits in vivo. Human molecular genetics 19:671-683.

Kabashi E, Daoud H, Riviere JB, Valdmanis PN, Bourgouin P, Provencher P, Pourcher E, Dion P, Dupre N, Rouleau GA (2009) No TARDBP mutations in a French Canadian population of patients with Parkinson disease. Arch Neurol 66:281-282.

Kabashi E, Lin L, Tradewell ML, Dion PA, Bercier V, Bourgouin P, Rochefort D, Bel Hadj S, Durham HD, Vande Velde C, Rouleau GA, Drapeau P (2010a) Gain and loss of function of ALS-related mutations of TARDBP (TDP-43) cause motor deficits in vivo. Human molecular genetics 19:671-683.

Kabashi E, Lin L, Tradewell ML, Dion PA, Bercier V, Bourgouin P, Rochefort D, Bel Hadj S, Durham HD, Vande Velde C, Rouleau GA, Drapeau P (2010b) Gain and loss of function of ALS-related mutations of TARDBP (TDP-43) cause motor deficits in vivo. Hum Mol Genet 19:671-683.

Kabashi E, Valdmanis PN, Dion P, Spiegelman D, McConkey BJ, Vande Velde C, Bouchard JP, Lacomblez L, Pochigaeva K, Salachas F, Pradat PF, Camu W, Meininger V, Dupre N, Rouleau GA (2008) TARDBP mutations in individuals with sporadic and familial amyotrophic lateral sclerosis. Nat Genet 40:572-574.

Kamada M, Maruyama H, Tanaka E, Morino H, Wate R, Ito H, Kusaka H, Kawano Y, Miki T, Nodera H, Izumi Y, Kaji R, Kawakami H (2009) Screening for TARDBP mutations in Japanese familial amyotrophic lateral sclerosis. J Neurol Sci 284:69-71.

Kametani F, Nonaka T, Suzuki T, Arai T, Dohmae N, Akiyama H, Hasegawa M (2009) Identification of casein kinase-1 phosphorylation sites on TDP-43. Biochem Biophys Res Commun 382:405-409.

Kane MD, Lipinski WJ, Callahan MJ, Bian F, Durham RA, Schwarz RD, Roher AE, Walker LC (2000) Evidence for seeding of beta -amyloid by intracerebral infusion of Alzheimer brain extracts in beta -amyloid precursor protein-transgenic mice. J Neurosci 20:3606-3611.

Kasher PR, De Vos KJ, Wharton SB, Manser C, Bennett EJ, Bingley M, Wood JD, Milner R, McDermott CJ, Miller CC, Shaw PJ, Grierson AJ (2009) Direct evidence for axonal transport defects in a novel mouse model of mutant spastin-induced hereditary spastic paraplegia (HSP) and human HSP patients. Journal of neurochemistry 110:34-44.

Kawaguchi-Niida M, Yamamoto T, Kato Y, Inose Y, Shibata N (2013) MCP-1/CCR2 signaling-mediated astrocytosis is accelerated in a transgenic mouse model of SOD1-mutated familial ALS. Acta neuropathologica communications 1:21.

Kawakami K, Shima A, Kawakami N (2000) Identification of a functional transposase of the Tol2 element, an Ac-like element from the Japanese medaka fish, and its transposition in the zebrafish germ lineage. Proc Natl Acad Sci U S A 97:11403-11408.

Kawamoto Y, Akiguchi I, Fujimura H, Shirakashi Y, Honjo Y, Sakoda S (2005) 14-3-3 proteins in Lewy body-like hyaline inclusions in a patient with familial amyotrophic lateral sclerosis with a two-base pair deletion in the Cu/Zn superoxide dismutase (SOD1) gene. Acta Neuropathol 110:203-204.

Kedersha N, Anderson P (2007) Mammalian stress granules and processing bodies. Methods Enzymol 431:61-81.

Kedersha N, Stoecklin G, Ayodele M, Yacono P, Lykke-Andersen J, Fritzler MJ, Scheuner D, Kaufman RJ, Golan DE, Anderson P (2005) Stress granules and processing bodies are dynamically linked sites of mRNP remodeling. The Journal of cell biology 169:871-884.

Kieran D, Woods I, Villunger A, Strasser A, Prehn JH (2007) Deletion of the BH3-only protein puma protects motoneurons from ER stress-induced apoptosis and delays motoneuron loss in ALS mice. Proc Natl Acad Sci U S A 104:20606-20611.

Kiledjian M, Dreyfuss G (1992) Primary structure and binding activity of the hnRNP U protein: binding RNA through RGG box. EMBO J 11:2655-2664.

Kim HJ, Kim NC, Wang YD, Scarborough EA, Moore J, Diaz Z, MacLea KS, Freibaum B, Li S, Molliex A, Kanagaraj AP, Carter R, Boylan KB, Wojtas AM, Rademakers R, Pinkus JL, Greenberg SA, Trojanowski JQ, Traynor BJ, Smith BN, Topp S, Gkazi AS, Miller J, Shaw CE, Kottlors M, Kirschner J, Pestronk A, Li YR, Ford AF, Gitler AD, Benatar M, King OD, Kimonis VE, Ross ED, Weihl CC, Shorter J, Taylor JP (2013) Mutations in prion-like domains in hnRNPA2B1 and hnRNPA1 cause multisystem proteinopathy and ALS. Nature 495:467-473.

Kim SH, Shi Y, Hanson KA, Williams LM, Sakasai R, Bowler MJ, Tibbetts RS (2009) Potentiation of amyotrophic lateral sclerosis (ALS)-associated TDP-43 aggregation by the proteasome-targeting factor, ubiquilin 1. J Biol Chem 284:8083-8092.

King A, Maekawa S, Bodi I, Troakes C, Al-Sarraj S (2011) Ubiquitinated, p62 immunopositive cerebellar cortical neuronal inclusions are evident across the spectrum of TDP-43 proteinopathies but are only rarely additionally immunopositive for phosphorylation-dependent TDP-43. Neuropathology 31:239-249.

Kirby J, Goodall EF, Smith W, Highley JR, Masanzu R, Hartley JA, Hibberd R, Hollinger HC, Wharton SB, Morrison KE, Ince PG, McDermott CJ, Shaw PJ

(2009) Broad clinical phenotypes associated with TAR-DNA binding protein (TARDBP) mutations in amyotrophic lateral sclerosis. Neurogenetics.

Knippenberg S, Sipos J, Thau-Habermann N, Korner S, Rath KJ, Dengler R, Petri S (2013) Altered expression of DJ-1 and PINK1 in sporadic ALS and in the SOD1(G93A) ALS mouse model. Journal of neuropathology and experimental neurology 72:1052-1061.

Kraemer BC, Schuck T, Wheeler JM, Robinson LC, Trojanowski JQ, Lee VM, Schellenberg GD (2010) Loss of murine TDP-43 disrupts motor function and plays an essential role in embryogenesis. Acta Neuropathol 119:409-419.

Krecic AM, Swanson MS (1999) hnRNP complexes: composition, structure, and function. Curr Opin Cell Biol 11:363-371.

Krivickas LS (2003) Amyotrophic lateral sclerosis and other motor neuron diseases. Phys Med Rehabil Clin N Am 14:327-345.

Kuhnlein P, Sperfeld AD, Vanmassenhove B, Van Deerlin V, Lee VM, Trojanowski JQ, Kretzschmar HA, Ludolph AC, Neumann M (2008) Two German kindreds with familial amyotrophic lateral sclerosis due to TARDBP mutations. Arch Neurol 65:1185-1189.

Kuijpers M, van Dis V, Haasdijk ED, Harterink M, Vocking K, Post JA, Scheper W, Hoogenraad CC, Jaarsma D (2013) Amyotrophic lateral sclerosis (ALS)-associated VAPB-P56S inclusions represent an ER quality control compartment. Acta neuropathologica communications 1:24.

Kumar S, Rezaei-Ghaleh N, Terwel D, Thal DR, Richard M, Hoch M, Mc Donald JM, Wullner U, Glebov K, Heneka MT, Walsh DM, Zweckstetter M, Walter J (2011) Extracellular phosphorylation of the amyloid beta-peptide promotes formation of toxic aggregates during the pathogenesis of Alzheimer's disease. The EMBO journal 30:2255-2265.

Kusters B, van Hoeve BJ, Schelhaas HJ, Ter Laak H, van Engelen BG, Lammens M (2009) TDP-43 accumulation is common in myopathies with rimmed vacuoles. Acta Neuropathol 117:209-211.

Kuusisto E, Parkkinen L, Alafuzoff I (2003) Morphogenesis of Lewy bodies: dissimilar incorporation of alpha-synuclein, ubiquitin, and p62. Journal of neuropathology and experimental neurology 62:1241-1253.

Kuzuhara S (2007) [ALS-parkinsonism-dementia complex of the Kii peninsula of Japan (Muro disease). Historical review, epidemiology and concept]. Rinsho Shinkeigaku 47:962-965.

Kwiatkowski TJ, Jr., Bosco DA, Leclerc AL, Tamrazian E, Vanderburg CR, Russ C, Davis A, Gilchrist J, Kasarskis EJ, Munsat T, Valdmanis P, Rouleau GA, Hosler BA, Cortelli P, de Jong PJ, Yoshinaga Y, Haines JL, Pericak-Vance MA, Yan J, Ticozzi N, Siddique T, McKenna-Yasek D, Sapp PC, Horvitz HR, Landers JE, Brown RH, Jr. (2009) Mutations in the FUS/TLS gene on chromosome 16 cause familial amyotrophic lateral sclerosis. Science 323:1205-1208.

Lagier-Tourenne C, Cleveland DW (2009) Rethinking ALS: the FUS about TDP-43. Cell 136:1001-1004.

Lee EB, Lee VM, Trojanowski JQ, Neumann M (2008) TDP-43 immunoreactivity in anoxic, ischemic and neoplastic lesions of the central nervous system. Acta Neuropathol 115:305-311.

Lee WC, Xue ZX, Melese T (1991) The NSR1 gene encodes a protein that specifically binds nuclear localization sequences and has two RNA recognition motifs. The Journal of cell biology 113:1-12.

Lemmens R, Race V, Hersmus N, Matthijs G, Van Den Bosch L, Van Damme P, Dubois B, Boonen S, Goris A, Robberecht W (2009) TDP-43 M311V mutation in familial amyotrophic lateral sclerosis. J Neurol Neurosurg Psychiatry 80:354-355.

Li HY, Yeh PA, Chiu HC, Tang CY, Tu BP (2011) Hyperphosphorylation as a defense mechanism to reduce TDP-43 aggregation. PLoS One 6:e23075.

Li Y, Ray P, Rao EJ, Shi C, Guo W, Chen X, Woodruff EA, 3rd, Fushimi K, Wu JY (2010) A Drosophila model for TDP-43 proteinopathy. Proc Natl Acad Sci U S A 107:3169-3174.

Liachko NF, Guthrie CR, Kraemer BC (2010) Phosphorylation promotes neurotoxicity in a Caenorhabditis elegans model of TDP-43 proteinopathy. J Neurosci 30:16208-16219.

Lieschke GJ, Currie PD (2007) Animal models of human disease: zebrafish swim into view. Nature reviews Genetics 8:353-367.

Lin AC, Holt CE (2008) Function and regulation of local axonal translation. Curr Opin Neurobiol 18:60-68.

Ling SC, Albuquerque CP, Han JS, Lagier-Tourenne C, Tokunaga S, Zhou H, Cleveland DW (2010) ALS-associated mutations in TDP-43 increase its stability and promote TDP-43 complexes with FUS/TLS. Proc Natl Acad Sci U S A 107:13318-13323.

Liscic RM, Grinberg LT, Zidar J, Gitcho MA, Cairns NJ (2008) ALS and FTLD: two faces of TDP-43 proteinopathy. Eur J Neurol 15:772-780.

Liu-Yesucevitz L, Bilgutay A, Zhang YJ, Vanderwyde T, Citro A, Mehta T, Zaarur N, McKee A, Bowser R, Sherman M, Petrucelli L, Wolozin B (2010) Tar DNA binding protein-43 (TDP-43) associates with stress granules: analysis of cultured cells and pathological brain tissue. PLoS One 5:e13250.

Logroscino G, Traynor BJ, Hardiman O, Chio A, Couratier P, Mitchell JD, Swingler RJ, Beghi E (2008) Descriptive epidemiology of amyotrophic lateral sclerosis: new evidence and unsolved issues. J Neurol Neurosurg Psychiatry 79:6-11.

Lomen-Hoerth C, Anderson T, Miller B (2002) The overlap of amyotrophic lateral sclerosis and frontotemporal dementia. Neurology 59:1077-1079.

Longstreth WT, Nelson LM, Koepsell TD, van Belle G (1991) Hypotheses to explain the association between vigorous physical activity and amyotrophic lateral sclerosis. Med Hypotheses 34:144-148.

Lu Y, Ferris J, Gao FB (2009) Frontotemporal dementia and amyotrophic lateral sclerosis-associated disease protein TDP-43 promotes dendritic branching. Mol Brain 2:30.

Ma AS, Moran-Jones K, Shan J, Munro TP, Snee MJ, Hoek KS, Smith R (2002) Heterogeneous nuclear ribonucleoprotein A3, a novel RNA trafficking response element-binding protein. J Biol Chem 277:18010-18020.

Mackenzie IR, Bigio EH, Ince PG, Geser F, Neumann M, Cairns NJ, Kwong LK, Forman MS, Ravits J, Stewart H, Eisen A, McClusky L, Kretzschmar HA, Monoranu CM, Highley JR, Kirby J, Siddique T, Shaw PJ, Lee VM, Trojanowski JQ (2007) Pathological TDP-43 distinguishes sporadic amyotrophic lateral sclerosis from amyotrophic lateral sclerosis with SOD1 mutations. Ann Neurol 61:427-434.

Mackenzie IR, Feldman H (2004) Neuronal intranuclear inclusions distinguish familial FTD-MND type from sporadic cases. Dement Geriatr Cogn Disord 17:333-336.

Mackenzie IR, Rademakers R (2007) The molecular genetics and neuropathology of frontotemporal lobar degeneration: recent developments. Neurogenetics 8:237-248.

Maekawa S, Leigh PN, King A, Jones E, Steele JC, Bodi I, Shaw CE, Hortobagyi T, Al-Sarraj S (2009) TDP-43 is consistently co-localized with ubiquitinated inclusions in sporadic and Guam amyotrophic lateral sclerosis but not in familial amyotrophic lateral sclerosis with and without SOD1 mutations. Neuropathology.

Mah AL, Perry G, Smith MA, Monteiro MJ (2000) Identification of ubiquilin, a novel presenilin interactor that increases presenilin protein accumulation. J Cell Biol 151:847-862.

Mahl P, Lutz Y, Puvion E, Fuchs JP (1989) Rapid effect of heat shock on two heterogeneous nuclear ribonucleoprotein-associated antigens in HeLa cells. The Journal of cell biology 109:1921-1935.

Majoor-Krakauer D, Willems PJ, Hofman A (2003) Genetic epidemiology of amyotrophic lateral sclerosis. Clin Genet 63:83-101.

Marc G, Leah R, Ofira E, Oded A, Zohar A, Hanna R (2013) Presymptomatic treatment with acetylcholinesterase antisense oligonucleotides prolongs survival in ALS (G93A-SOD1) mice. BioMed research international 2013:845345.

Marino M, Papa S, Crippa V, Nardo G, Peviani M, Cheroni C, Trolese MC, Lauranzano E, Bonetto V, Poletti A, DeBiasi S, Ferraiuolo L, Shaw PJ, Bendotti C (2014) Differences in protein quality control correlate with phenotype variability in 2 mouse models of familial amyotrophic lateral sclerosis. Neurobiol Aging.

McCallum CM, Comai L, Greene EA, Henikoff S (2000) Targeted screening for induced mutations. Nat Biotechnol 18:455-457.

McDonald KK, Aulas A, Destroismaisons L, Pickles S, Beleac E, Camu W, Rouleau GA, Vande Velde C (2011) TAR DNA-binding protein 43 (TDP-43) regulates stress granule dynamics via differential regulation of G3BP and TIA-1. Hum Mol Genet 20:1400-1410.

McGown A, McDearmid JR, Panagiotaki N, Tong H, Al Mashhadi S, Redhead N, Lyon AN, Beattie CE, Shaw PJ, Ramesh TM (2013) Early interneuron dysfunction in ALS: insights from a mutant sod1 zebrafish model. Annals of neurology 73:246-258.

McWhorter ML, Monani UR, Burghes AH, Beattie CE (2003) Knockdown of the survival motor neuron (Smn) protein in zebrafish causes defects in motor axon outgrowth and pathfinding. J Cell Biol 162:919-931.

Mead RJ, Higginbottom A, Allen SP, Kirby J, Bennett E, Barber SC, Heath PR, Coluccia A, Patel N, Gardner I, Brancale A, Grierson AJ, Shaw PJ (2013) S[+] Apomorphine is a CNS penetrating activator of the Nrf2-ARE pathway with activity in mouse and patient fibroblast models of amyotrophic lateral sclerosis. Free radical biology & medicine 61C:438-452.

Media Relations TA (2013) The ALS Association: Fighting Lou Gehrig disease on multiple fronts. Rare diseases 1:e24910.

Meek DW (2009) Tumour suppression by p53: a role for the DNA damage response? Nat Rev Cancer 9:714-723.

Mendonsa G, Dobrowolska J, Lin A, Vijairania P, Jong YJ, Baenziger NL (2009) Molecular profiling reveals diversity of stress signal transduction cascades in highly penetrant Alzheimer's disease human skin fibroblasts. PLoS One 4:e4655.

Mercado PA, Ayala YM, Romano M, Buratti E, Baralle FE (2005) Depletion of TDP 43 overrides the need for exonic and intronic splicing enhancers in the human apoA-II gene. Nucleic Acids Res 33:6000-6010.

Merdzhanova G, Gout S, Keramidas M, Edmond V, Coll JL, Brambilla C, Brambilla E, Gazzeri S, Eymin B (2010) The transcription factor E2F1 and the SR protein SC35 control the ratio of pro-angiogenic versus antiangiogenic isoforms of vascular endothelial growth factor-A to inhibit neovascularization in vivo. Oncogene 29:5392-5403.

Meyerowitz J, Parker SJ, Vella LJ, Ng DC, Price KA, Liddell JR, Caragounis A, Li QX, Masters CL, Nonaka T, Hasegawa M, Bogoyevitch MA, Kanninen KM, Crouch PJ, White AR (2011) C-Jun N-terminal kinase controls TDP-43 accumulation in stress granules induced by oxidative stress. Mol Neurodegener 6:57.

Miguel L, Frebourg T, Campion D, Lecourtois M (2011) Both cytoplasmic and nuclear accumulations of the protein are neurotoxic in Drosophila models of TDP-43 proteinopathies. Neurobiol Dis 41:398-406.

Millecamps S, Salachas F, Cazeneuve C, Gordon P, Bricka B, Camuzat A, Guillot-Noel L, Russaouen O, Bruneteau G, Pradat PF, Le Forestier N, Vandenberghe N, Danel-Brunaud V, Guy N, Thauvin-Robinet C, Lacomblez L, Couratier P, Hannequin D, Seilhean D, Le Ber I, Corcia P, Camu W, Brice A, Rouleau G, LeGuern E, Meininger V (2010) SOD1, ANG, VAPB, TARDBP, and FUS mutations in familial amyotrophic lateral sclerosis: genotype-phenotype correlations. J Med Genet 47:554-560.

Mishra M, Paunesku T, Woloschak GE, Siddique T, Zhu LJ, Lin S, Greco K, Bigio EH (2007) Gene expression analysis of frontotemporal lobar degeneration of the motor neuron disease type with ubiquitinated inclusions. Acta Neuropathol 114:81-94.

Moens CB, Donn TM, Wolf-Saxon ER, Ma TP (2008) Reverse genetics in zebrafish by TILLING. Briefings in functional genomics & proteomics 7:454-459.

Moisse K, Mepham J, Volkening K, Welch I, Hill T, Strong MJ (2009a) Cytosolic TDP-43 expression following axotomy is associated with caspase 3 activation in NFL-/- mice: support for a role for TDP-43 in the physiological response to neuronal injury. Brain Res 1296:176-186.

Moisse K, Volkening K, Leystra-Lantz C, Welch I, Hill T, Strong MJ (2009b) Divergent patterns of cytosolic TDP-43 and neuronal progranulin expression following axotomy: implications for TDP-43 in the physiological response to neuronal injury. Brain Res 1249:202-211.

Mollet S, Cougot N, Wilczynska A, Dautry F, Kress M, Bertrand E, Weil D (2008) Translationally repressed mRNA transiently cycles through stress granules during stress. Molecular biology of the cell 19:4469-4479.

Monani UR, Lorson CL, Parsons DW, Prior TW, Androphy EJ, Burghes AH, McPherson JD (1999) A single nucleotide difference that alters splicing patterns distinguishes the SMA gene SMN1 from the copy gene SMN2. Hum Mol Genet 8:1177-1183.

Mori K, Weng SM, Arzberger T, May S, Rentzsch K, Kremmer E, Schmid B, Kretzschmar HA, Cruts M, Van Broeckhoven C, Haass C, Edbauer D (2013) The C9orf72 GGGGCC repeat is translated into aggregating dipeptide-repeat proteins in FTLD/ALS. Science 339:1335-1338.

Morimoto RI, Santoro MG (1998) Stress-inducible responses and heat shock proteins: new pharmacologic targets for cytoprotection. Nature biotechnology 16:833-838.

Mortiboys H, Thomas KJ, Koopman WJ, Klaffke S, Abou-Sleiman P, Olpin S, Wood NW, Willems PH, Smeitink JA, Cookson MR, Bandmann O (2008) Mitochondrial function and morphology are impaired in parkin-mutant fibroblasts. Ann Neurol 64:555-565.

Moscat J, Diaz-Meco MT, Wooten MW (2007) Signal integration and diversification through the p62 scaffold protein. Trends in biochemical sciences 32:95-100.

Munch C, Sedlmeier R, Meyer T, Homberg V, Sperfeld AD, Kurt A, Prudlo J, Peraus G, Hanemann CO, Stumm G, Ludolph AC (2004) Point mutations of the p150 subunit of dynactin (DCTN1) gene in ALS. Neurology 63:724-726.

Murphy J, Henry R, Lomen-Hoerth C (2007a) Establishing subtypes of the continuum of frontal lobe impairment in amyotrophic lateral sclerosis. Arch Neurol 64:330-334.

Murphy JM, Henry RG, Langmore S, Kramer JH, Miller BL, Lomen-Hoerth C (2007b) Continuum of frontal lobe impairment in amyotrophic lateral sclerosis. Arch Neurol 64:530-534.

Murray ME, Dejesus-Hernandez M, Rutherford NJ, Baker M, Duara R, Graff-Radford NR, Wszolek ZK, Ferman TJ, Josephs KA, Boylan KB, Rademakers R, Dickson DW (2011) Clinical and neuropathologic heterogeneity of c9FTD/ALS associated with hexanucleotide repeat expansion in C9ORF72. Acta Neuropathol 122:673-690.

Nakamura M, Ito H, Wate R, Nakano S, Hirano A, Kusaka H (2008) Phosphorylated Smad2/3 immunoreactivity in sporadic and familial amyotrophic lateral sclerosis and its mouse model. Acta Neuropathol 115:327-334.

Nakashima-Yasuda H, Uryu K, Robinson J, Xie SX, Hurtig H, Duda JE, Arnold SE, Siderowf A, Grossman M, Leverenz JB, Woltjer R, Lopez OL, Hamilton R, Tsuang DW, Galasko D, Masliah E, Kaye J, Clark CM, Montine TJ, Lee VM, Trojanowski JQ (2007) Co-morbidity of TDP-43 proteinopathy in Lewy body related diseases. Acta Neuropathol 114:221-229.

Nelson LM (1995) Epidemiology of ALS. Clin Neurosci 3:327-331.

Nelson PT, Wang WX, Rajeev BW (2008) MicroRNAs (miRNAs) in neurodegenerative diseases. Brain Pathol 18:130-138.

Neumann M (2009) Molecular Neuropathology of TDP-43 Proteinopathies. Int J Mol Sci 10:232-246.

Neumann M, Kwong LK, Lee EB, Kremmer E, Flatley A, Xu Y, Forman MS, Troost D, Kretzschmar HA, Trojanowski JQ, Lee VM (2009) Phosphorylation of S409/410 of TDP-43 is a consistent feature in all sporadic and familial forms of TDP-43 proteinopathies. Acta Neuropathol 117:137-149.

Neumann M, Kwong LK, Sampathu DM, Trojanowski JQ, Lee VM (2007a) TDP-43 proteinopathy in frontotemporal lobar degeneration and amyotrophic lateral sclerosis: protein misfolding diseases without amyloidosis. Arch Neurol 64:1388-1394.

Neumann M, Mackenzie IR, Cairns NJ, Boyer PJ, Markesbery WR, Smith CD, Taylor JP, Kretzschmar HA, Kimonis VE, Forman MS (2007b) TDP-43 in the ubiquitin pathology of frontotemporal dementia with VCP gene mutations. J Neuropathol Exp Neurol 66:152-157.

Neumann M, Sampathu DM, Kwong LK, Truax AC, Micsenyi MC, Chou TT, Bruce J, Schuck T, Grossman M, Clark CM, McCluskey LF, Miller BL, Masliah E, Mackenzie IR, Feldman H, Feiden W, Kretzschmar HA, Trojanowski JQ, Lee VM (2006) Ubiquitinated TDP-43 in frontotemporal lobar degeneration and amyotrophic lateral sclerosis. Science 314:130-133.

Nishihira Y, Tan CF, Onodera O, Toyoshima Y, Yamada M, Morita T, Nishizawa M, Kakita A, Takahashi H (2008) Sporadic amyotrophic lateral sclerosis: two pathological patterns shown by analysis of distribution of TDP-43-immunoreactive neuronal and glial cytoplasmic inclusions. Acta Neuropathol 116:169-182.

Nishimoto Y, Ito D, Yagi T, Nihei Y, Tsunoda Y, Suzuki N (2009) Characterization of alternative isoforms and inclusion body of the TAR DNA binding protein-43. J Biol Chem.

Nomoto N (2013) [An autopsy case of FTLD-MND with reduced cardiac MIBG update]. Brain and nerve = Shinkei kenkyu no shinpo 65:1205-1213.

Nonaka T, Arai T, Buratti E, Baralle FE, Akiyama H, Hasegawa M (2009a) Phosphorylated and ubiquitinated TDP-43 pathological inclusions in ALS and FTLD-U are recapitulated in SH-SY5Y cells. FEBS Lett 583:394-400.

Nonaka T, Arai T, Hasegawa M (2009b) [The molecular mechanisms of intracellular TDP-43 aggregates]. Brain Nerve 61:1292-1300.

Nonaka T, Kametani F, Arai T, Akiyama H, Hasegawa M (2009c) Truncation and pathogenic mutations facilitate the formation of intracellular aggregates of TDP-43. Hum Mol Genet 18:3353-3364.

O'Leary VB, Ovsepian SV, Bodeker M, Dolly JO (2013) Improved lentiviral transduction of ALS motoneurons in vivo via dual targeting. Molecular pharmaceutics 10:4195-4206.

Okamoto Y, Ihara M, Urushitani M, Yamashita H, Kondo T, Tanigaki A, Oono M, Kawamata J, Ikemoto A, Kawamoto Y, Takahashi R, Ito H (2011) An autopsy case of SOD1-related ALS with TDP-43 positive inclusions. Neurology 77:1993-1995.

Orr HT (2004) Neurodegenerative disease: neuron protection agency. Nature 431:747-748.

Ou SH, Wu F, Harrich D, Garcia-Martinez LF, Gaynor RB (1995) Cloning and characterization of a novel cellular protein, TDP-43, that binds to human immunodeficiency virus type 1 TAR DNA sequence motifs. J Virol 69:3584-3596.

Pamphlett R, Luquin N, McLean C, Jew SK, Adams L (2009) TDP-43 neuropathology is similar in sporadic amyotrophic lateral sclerosis with or without TDP-43 mutations. Neuropathol Appl Neurobiol 35:222-225.

Pang SY, Jiang J, Ma J, Ouyang F (2009) New insight into the oxidation of arsenite by the reaction of zerovalent iron and oxygen. Comment on "pH dependence of Fenton reagent generation and As(III) oxidation and removal by corrosion of zero valent iron in aerated water". Environmental science & technology 43:3978-3979; author reply 3980-3971.

Paquet D, Bhat R, Sydow A, Mandelkow EM, Berg S, Hellberg S, Falting J, Distel M, Koster RW, Schmid B, Haass C (2009) A zebrafish model of tauopathy allows in vivo imaging of neuronal cell death and drug evaluation. J Clin Invest 119:1382-1395.

Parker SJ, Meyerowitz J, James JL, Liddell JR, Crouch PJ, Kanninen KM, White AR (2012) Endogenous TDP-43 localized to stress granules can subsequently form protein aggregates. Neurochem Int 60:415-424.

Parkinson N, Ince PG, Smith MO, Highley R, Skibinski G, Andersen PM, Morrison KE, Pall HS, Hardiman O, Collinge J, Shaw PJ, Fisher EM (2006) ALS phenotypes with mutations in CHMP2B (charged multivesicular body protein 2B). Neurology 67:1074-1077.

Pesiridis GS, Lee VM, Trojanowski JQ (2009) Mutations in TDP-43 link glycine-rich domain functions to amyotrophic lateral sclerosis. Hum Mol Genet 18:R156-162.

Peterson C, Ratan RR, Shelanski ML, Goldman JE (1988) Altered response of fibroblasts from aged and Alzheimer donors to drugs that elevate cytosolic free calcium. Neurobiology of aging 9:261-266.

Polymenidou M, Lagier-Tourenne C, Hutt KR, Huelga SC, Moran J, Liang TY, Ling SC, Sun E, Wancewicz E, Mazur C, Kordasiewicz H, Sedaghat Y, Donohue JP, Shiue L, Bennett CF, Yeo GW, Cleveland DW (2011) Long pre-mRNA depletion and RNA missplicing contribute to neuronal vulnerability from loss of TDP-43. Nat Neurosci 14:459-468.

Pouget J, Azulay JP, Bille-Turc F, Sangla I, Serratrice GT (1995) The diagnosis of amyotrophic lateral sclerosis. Adv Neurol 68:143-152.

Quaresma AJ, Bressan GC, Gava LM, Lanza DC, Ramos CH, Kobarg J (2009) Human hnRNP Q re-localizes to cytoplasmic granules upon PMA, thapsigargin, arsenite and heat-shock treatments. Experimental cell research 315:968-980.

Rakovic A, Grunewald A, Kottwitz J, Bruggemann N, Pramstaller PP, Lohmann K, Klein C (2011) Mutations in PINK1 and Parkin impair ubiquitination of Mitofusins in human fibroblasts. PLoS One 6:e16746.

Ramesh T, Lyon AN, Pineda RH, Wang C, Janssen PM, Canan BD, Burghes AH, Beattie CE (2010) A genetic model of amyotrophic lateral sclerosis in zebrafish displays phenotypic hallmarks of motoneuron disease. Dis Model Mech 3:652-662.

Ratnavalli E, Brayne C, Dawson K, Hodges JR (2002) The prevalence of frontotemporal dementia. Neurology 58:1615-1621.

Reed DM, Brody JA (1975) Amyotrophic lateral sclerosis and parkinsonism-dementia on Guam, 1945-1972. I. Descriptive epidemiology. Am J Epidemiol 101:287-301.

Renton AE, Majounie E, Waite A, Simon-Sanchez J, Rollinson S, Gibbs JR, Schymick JC, Laaksovirta H, van Swieten JC, Myllykangas L, Kalimo H, Paetau A, Abramzon Y, Remes AM, Kaganovich A, Scholz SW, Duckworth J, Ding J, Harmer DW, Hernandez DG, Johnson JO, Mok K, Ryten M, Trabzuni D, Guerreiro RJ, Orrell RW, Neal J, Murray A, Pearson J, Jansen IE, Sondervan D, Seelaar H, Blake D, Young K, Halliwell N, Callister JB, Toulson G, Richardson A, Gerhard A, Snowden J, Mann D, Neary D, Nalls MA, Peuralinna T, Jansson L, Isoviita VM, Kaivorinne AL, Holtta-Vuori M, Ikonen E, Sulkava R, Benatar M, Wuu J, Chio A, Restagno G, Borghero G, Sabatelli M, Heckerman D, Rogaeva E, Zinman L, Rothstein JD, Sendtner M, Drepper C, Eichler EE, Alkan C, Abdullaev Z, Pack SD, Dutra A, Pak E, Hardy J, Singleton A, Williams NM, Heutink P, Pickering-Brown S, Morris HR, Tienari PJ, Traynor BJ (2011) A hexanucleotide repeat expansion in C9ORF72 is the cause of chromosome 9p21-linked ALS-FTD. Neuron 72:257-268.

Renz A, Fackelmayer FO (1996) Purification and molecular cloning of the scaffold attachment factor B (SAF-B), a novel human nuclear protein that specifically binds to S/MAR-DNA. Nucleic acids research 24:843-849.

Ritson GP, Custer SK, Freibaum BD, Guinto JB, Geffel D, Moore J, Tang W, Winton MJ, Neumann M, Trojanowski JQ, Lee VM, Forman MS, Taylor JP (2010) TDP-43 mediates degeneration in a novel Drosophila model of disease caused by mutations in VCP/p97. J Neurosci 30:7729-7739.

Robertson J, Doroudchi MM, Nguyen MD, Durham HD, Strong MJ, Shaw G, Julien JP, Mushynski WE (2003) A neurotoxic peripherin splice variant in a mouse model of ALS. J Cell Biol 160:939-949.

Robu ME, Larson JD, Nasevicius A, Beiraghi S, Brenner C, Farber SA, Ekker SC (2007) p53 activation by knockdown technologies. PLoS Genet 3:e78.

Rollinson S, Snowden JS, Neary D, Morrison KE, Mann DM, Pickering-Brown SM (2007) TDP-43 gene analysis in frontotemporal lobar degeneration. Neurosci Lett 419:1-4.

Roman GC (1996) Neuroepidemiology of amyotrophic lateral sclerosis: clues to aetiology and pathogenesis. J Neurol Neurosurg Psychiatry 61:131-137.

Rowland LP (1993) Babinski and the diagnosis of amyotrophic lateral sclerosis. Ann Neurol 33:108.

Rowland LP (1998) Diagnosis of amyotrophic lateral sclerosis. J Neurol Sci 160 Suppl 1:S6-24.

Rutherford NJ, Zhang YJ, Baker M, Gass JM, Finch NA, Xu YF, Stewart H, Kelley BJ, Kuntz K, Crook RJ, Sreedharan J, Vance C, Sorenson E, Lippa C, Bigio EH, Geschwind DH, Knopman DS, Mitsumoto H, Petersen RC, Cashman NR, Hutton M, Shaw CE, Boylan KB, Boeve B, Graff-Radford NR, Wszolek ZK, Caselli RJ, Dickson DW, Mackenzie IR, Petrucelli L, Rademakers R (2008) Novel mutations in TARDBP (TDP-43) in patients with familial amyotrophic lateral sclerosis. PLoS Genet 4:e1000193.

Sanelli T, Xiao S, Horne P, Bilbao J, Zinman L, Robertson J (2007) Evidence that TDP-43 is not the major ubiquitinated target within the pathological inclusions of amyotrophic lateral sclerosis. J Neuropathol Exp Neurol 66:1147-1153.

Sato T, Takeuchi S, Saito A, Ding W, Bamba H, Matsuura H, Hisa Y, Tooyama I, Urushitani M (2009) Axonal ligation induces transient redistribution of TDP-43 in brainstem motor neurons. Neuroscience.

Savica R, Adeli A, Vemuri P, Knopman DS, Dejesus-Hernandez M, Rademakers R, Fields JA, Whitwell J, Jack CR, Lowe V, Petersen RC, Boeve BF (2012) Characterization of a family with c9FTD/ALS associated with the GGGGCC repeat expansion in C9ORF72. Archives of neurology 69:1164-1169.

Saxena S, Roselli F, Singh K, Leptien K, Julien JP, Gros-Louis F, Caroni P (2013) Neuroprotection through excitability and mTOR required in ALS motoneurons to delay disease and extend survival. Neuron 80:80-96.

Schroer TA, Bingham JB, Gill SR (1996) Actin-related protein 1 and cytoplasmic dynein-based motility - what's the connection? Trends Cell Biol 6:212-215.

Schumacher A, Friedrich P, Diehl-Schmid J, Ibach B, Perneczky R, Eisele T, Vukovich R, Foerstl H, Riemenschneider M (2009) No association of TDP-43 with sporadic frontotemporal dementia. Neurobiol Aging 30:157-159.

Schwab C, Arai T, Hasegawa M, Yu S, McGeer PL (2008) Colocalization of transactivation-responsive DNA-binding protein 43 and huntingtin in inclusions of Huntington disease. J Neuropathol Exp Neurol 67:1159-1165.

Seibenhener ML, Geetha T, Wooten MW (2007) Sequestosome 1/p62--more than just a scaffold. FEBS letters 581:175-179.

Seilhean D, Takahashi J, El Hachimi KH, Fujigasaki H, Lebre AS, Biancalana V, Durr A, Salachas F, Hogenhuis J, de The H, Hauw JJ, Meininger V, Brice A, Duyckaerts C (2004) Amyotrophic lateral sclerosis with neuronal intranuclear protein inclusions. Acta Neuropathol 108:81-87.

Sendtner M (2011) TDP-43: multiple targets, multiple disease mechanisms? Nat Neurosci 14:403-405.

Sephton CF, Good SK, Atkin S, Dewey CM, Mayer P, 3rd, Herz J, Yu G (2010) TDP-43 is a developmentally regulated protein essential for early embryonic development. J Biol Chem 285:6826-6834.

Seyfried NT, Gozal YM, Dammer EB, Xia Q, Duong DM, Cheng D, Lah JJ, Levey AI, Peng J Multiplex SILAC analysis of a cellular TDP-43 proteinopathy model reveals protein inclusions associated with SUMOylation and diverse polyUb chains. Mol Cell Proteomics.

Seyfried NT, Gozal YM, Dammer EB, Xia Q, Duong DM, Cheng D, Lah JJ, Levey AI, Peng J (2010) Multiplex SILAC analysis of a cellular TDP-43 proteinopathy model reveals protein inclusions associated with SUMOylation and diverse polyubiquitin chains. Mol Cell Proteomics 9:705-718.

Shan X, Chiang PM, Price DL, Wong PC (2010) Altered distributions of Gemini of coiled bodies and mitochondria in motor neurons of TDP-43 transgenic mice. Proc Natl Acad Sci U S A 107:16325-16330.

Shan X, Vocadlo D, Krieger C (2009) Mislocalization of TDP-43 in the G93A mutant SOD1 transgenic mouse model of ALS. Neurosci Lett 458:70-74.

Shankaran SS, Capell A, Hruscha AT, Fellerer K, Neumann M, Schmid B, Haass C (2008) Missense mutations in the progranulin gene linked to frontotemporal lobar degeneration with ubiquitin-immunoreactive inclusions reduce progranulin production and secretion. J Biol Chem 283:1744-1753.

Shaw CE, Arechavala-Gomeza V, Al-Chalabi A (2007) Chapter 14 Familial amyotrophic lateral sclerosis. Handb Clin Neurol 82:279-300.

Shaw PJ (2001) Genetic inroads in familial ALS. Nat Genet 29:103-104.

Shaw PJ (2005) Molecular and cellular pathways of neurodegeneration in motor neurone disease. J Neurol Neurosurg Psychiatry 76:1046-1057.

Shaw PJ, Eggett CJ (2000) Molecular factors underlying selective vulnerability of motor neurons to neurodegeneration in amyotrophic lateral sclerosis. J Neurol 247 Suppl 1:I17-27.

Shi P, Gal J, Kwinter DM, Liu X, Zhu H (2009) Mitochondrial dysfunction in amyotrophic lateral sclerosis. Biochim Biophys Acta.

Shi Y, Rhodes NR, Abdolvahabi A, Kohn T, Cook NP, Marti AA, Shaw BF (2013) Deamidation of asparagine to aspartate destabilizes Cu, Zn superoxide dismutase, accelerates fibrillization, and mirrors ALS-linked mutations. Journal of the American Chemical Society 135:15897-15908.

Shimada N, Rios I, Moran H, Sayers B, Hubbard K (2009) p38 MAP kinase-dependent regulation of the expression level and subcellular distribution of heterogeneous nuclear ribonucleoprotein A1 and its involvement in cellular senescence in normal human fibroblasts. RNA biology 6:293-304.

Shodai A, Morimura T, Ido A, Uchida T, Ayaki T, Takahashi R, Kitazawa S, Suzuki S, Shirouzu M, Kigawa T, Muto Y, Yokoyama S, Kitahara R, Ito H, Fujiwara N, Urushitani M (2013) Aberrant assembly of RNA recognition motif 1 links to pathogenic conversion of TAR DNA-binding protein of 43 kDa (TDP-43). The Journal of biological chemistry 288:14886-14905.

Singh OP (2001) Functional diversity of hnRNP proteins. Indian J Biochem Biophys 38:129-134.

Solski JA, Yang S, Nicholson GA, Luquin N, Williams KL, Fernando R, Pamphlett R, Blair IP (2012) A novel TARDBP insertion/deletion mutation in the flail arm variant of amyotrophic lateral sclerosis. Amyotroph Lateral Scler 13:465-470.

Song F, Chiang P, Ravits J, Loeb JA (2014) Activation of microglial neuregulin1 signaling in the corticospinal tracts of ALS patients with upper motor neuron signs. Amyotrophic lateral sclerosis & frontotemporal degeneration 15:77-83.

Sreedharan J, Blair IP, Tripathi VB, Hu X, Vance C, Rogelj B, Ackerley S, Durnall JC, Williams KL, Buratti E, Baralle F, de Belleroche J, Mitchell JD, Leigh PN, Al-Chalabi A, Miller CC, Nicholson G, Shaw CE (2008) TDP-43 mutations in familial and sporadic amyotrophic lateral sclerosis. Science 319:1668-1672.

Stallings NR, Puttaparthi K, Luther CM, Burns DK, Elliott JL (2010) Progressive motor weakness in transgenic mice expressing human TDP-43. Neurobiol Dis 40:404-414.

Stern HM, Zon LI (2003) Cancer genetics and drug discovery in the zebrafish. Nature reviews Cancer 3:533-539.

Strong M, Rosenfeld J (2003) Amyotrophic lateral sclerosis: a review of current concepts. Amyotroph Lateral Scler Other Motor Neuron Disord 4:136-143.

Strong MJ (2008) The syndromes of frontotemporal dysfunction in amyotrophic lateral sclerosis. Amyotroph Lateral Scler 9:323-338.

Strong MJ (2009) The evidence for altered RNA metabolism in amyotrophic lateral sclerosis (ALS). J Neurol Sci.

Strong MJ, Volkening K, Hammond R, Yang W, Strong W, Leystra-Lantz C, Shoesmith C (2007) TDP43 is a human low molecular weight neurofilament (hNFL) mRNA-binding protein. Mol Cell Neurosci 35:320-327.

Subramanian V, Crabtree B, Acharya KR (2008) Human angiogenin is a neuroprotective factor and amyotrophic lateral sclerosis associated angiogenin variants affect neurite extension/pathfinding and survival of motor neurons. Hum Mol Genet 17:130-149.

Sun H, Benardais K, Stanslowsky N, Thau-Habermann N, Hensel N, Huang D, Claus P, Dengler R, Stangel M, Petri S (2013) Therapeutic potential of mesenchymal stromal cells and MSC conditioned medium in Amyotrophic Lateral Sclerosis (ALS)--in vitro evidence from primary motor neuron cultures, NSC-34 cells, astrocytes and microglia. PLoS One 8:e72926.

Suzuki H, Lee K, Matsuoka M (2011) TDP-43-induced Death Is Associated with Altered Regulation of BIM and Bcl-xL and Attenuated by Caspase-mediated TDP-43 Cleavage. J Biol Chem 286:13171-13183.

Swarup V, Phaneuf D, Bareil C, Robertson J, Rouleau GA, Kriz J, Julien JP (2011a) Pathological hallmarks of amyotrophic lateral sclerosis/frontotemporal lobar degeneration in transgenic mice produced with TDP-43 genomic fragments. Brain.

Swarup V, Phaneuf D, Bareil C, Robertson J, Rouleau GA, Kriz J, Julien JP (2011b) Pathological hallmarks of amyotrophic lateral sclerosis/frontotemporal lobar degeneration in transgenic mice produced with TDP-43 genomic fragments. Brain 134:2610-2626.

Talbot K (2002) Motor neurone disease. Postgrad Med J 78:513-519.

Talbot K, Ansorge O (2006) Recent advances in the genetics of amyotrophic lateral sclerosis and frontotemporal dementia: common pathways in neurodegenerative disease. Hum Mol Genet 15 Spec No 2:R182-187.

Tan CF, Eguchi H, Tagawa A, Onodera O, Iwasaki T, Tsujino A, Nishizawa M, Kakita A, Takahashi H (2007) TDP-43 immunoreactivity in neuronal inclusions in familial amyotrophic lateral sclerosis with or without SOD1 gene mutation. Acta Neuropathol 113:535-542.

Tan CF, Kakita A, Piao YS, Kikugawa K, Endo K, Tanaka M, Okamoto K, Takahashi H (2003) Primary lateral sclerosis: a rare upper-motor-predominant form of amyotrophic lateral sclerosis often accompanied by frontotemporal lobar degeneration with ubiquitinated neuronal inclusions? Report of an autopsy case and a review of the literature. Acta Neuropathol 105:615-620.

Tang R, Dodd A, Lai D, McNabb WC, Love DR (2007) Validation of zebrafish (Danio rerio) reference genes for quantitative real-time RT-PCR normalization. Acta Biochim Biophys Sin (Shanghai) 39:384-390.

Tian T, Huang C, Tong J, Yang M, Zhou H, Xia XG (2011) TDP-43 Potentiates Alpha-synuclein Toxicity to Dopaminergic Neurons in Transgenic Mice. Int J Biol Sci 7:234-243.

Ticozzi N, Leclerc AL, van Blitterswijk M, Keagle P, McKenna-Yasek DM, Sapp PC, Silani V, Wills AM, Brown RH, Jr., Landers JE (2009) Mutational analysis of TARDBP in neurodegenerative diseases. Neurobiol Aging.

Traynor BJ, Codd MB, Corr B, Forde C, Frost E, Hardiman O (1999) Incidence and prevalence of ALS in Ireland, 1995-1997: a population-based study. Neurology 52:504-509.

Tsai KJ, Yang CH, Fang YH, Cho KH, Chien WL, Wang WT, Wu TW, Lin CP, Fu WM, Shen CK (2010) Elevated expression of TDP-43 in the forebrain of mice is sufficient to cause neurological and pathological phenotypes mimicking FTLD-U. J Exp Med 207:1661-1673.

Turner BJ, Baumer D, Parkinson NJ, Scaber J, Ansorge O, Talbot K (2008) TDP-43 expression in mouse models of amyotrophic lateral sclerosis and spinal muscular atrophy. BMC Neurosci 9:104.

Udan M, Baloh RH (2011) Implications of the prion-related Q/N domains in TDP-43 and FUS. Prion 5:1-5.

Udan-Johns M, Bengoechea R, Bell S, Shao J, Diamond MI, True HL, Weihl CC, Baloh RH (2013) Prion-like nuclear aggregation of TDP-43 during heat shock is regulated by HSP40/70 chaperones. Human molecular genetics.

Udvadia AJ, Linney E (2003) Windows into development: historic, current, and future perspectives on transgenic zebrafish. Dev Biol 256:1-17.

Vaccaro A, Tauffenberger A, Aggad D, Rouleau G, Drapeau P, Parker JA (2012) Mutant TDP-43 and FUS cause age-dependent paralysis and neurodegeneration in C. elegans. PLoS One 7:e31321.

van Blitterswijk M, Rademakers R, van den Berg LH (2014) Clinical variability and additional mutations in amyotrophic lateral sclerosis patients with p.N352S mutations in TARDBP. Neuropathology and applied neurobiology 40:356-358.

Van Deerlin VM, Leverenz JB, Bekris LM, Bird TD, Yuan W, Elman LB, Clay D, Wood EM, Chen-Plotkin AS, Martinez-Lage M, Steinbart E, McCluskey L, Grossman M, Neumann M, Wu IL, Yang WS, Kalb R, Galasko DR, Montine TJ, Trojanowski JQ, Lee VM, Schellenberg GD, Yu CE (2008) TARDBP mutations in amyotrophic lateral sclerosis with TDP-43 neuropathology: a genetic and histopathological analysis. Lancet Neurol 7:409-416.

van der Graaff MM, de Jong JM, Baas F, de Visser M (2009) Upper motor neuron and extra-motor neuron involvement in amyotrophic lateral sclerosis: a clinical and brain imaging review. Neuromuscul Disord 19:53-58.

van der Houven van Oordt W, Diaz-Meco MT, Lozano J, Krainer AR, Moscat J, Caceres JF (2000) The MKK(3/6)-p38-signaling cascade alters the subcellular distribution of hnRNP A1 and modulates alternative splicing regulation. J Cell Biol 149:307-316.

Vance C, Rogelj B, Hortobagyi T, De Vos KJ, Nishimura AL, Sreedharan J, Hu X, Smith B, Ruddy D, Wright P, Ganesalingam J, Williams KL, Tripathi V, Al-Saraj S, Al-Chalabi A, Leigh PN, Blair IP, Nicholson G, de Belleroche J, Gallo JM, Miller CC, Shaw CE (2009) Mutations in FUS, an RNA processing protein, cause familial amyotrophic lateral sclerosis type 6. Science 323:1208-1211.

Vance C, Scotter EL, Nishimura AL, Troakes C, Mitchell JC, Kathe C, Urwin H, Manser C, Miller CC, Hortobagyi T, Dragunow M, Rogelj B, Shaw CE (2013) ALS mutant FUS disrupts nuclear localization and sequesters wild-type FUS within cytoplasmic stress granules. Human molecular genetics 22:2676-2688.

Veglianese P, Lo Coco D, Bao Cutrona M, Magnoni R, Pennacchini D, Pozzi B, Gowing G, Julien JP, Tortarolo M, Bendotti C (2006) Activation of the p38MAPK cascade is associated with upregulation of TNF alpha receptors in the spinal motor neurons of mouse models of familial ALS. Mol Cell Neurosci 31:218-231.

Vertegaal AC, Ogg SC, Jaffray E, Rodriguez MS, Hay RT, Andersen JS, Mann M, Lamond AI (2004) A proteomic study of SUMO-2 target proteins. J Biol Chem 279:33791-33798.

Vinsant S, Mansfield C, Jimenez-Moreno R, Del Gaizo Moore V, Yoshikawa M, Hampton TG, Prevette D, Caress J, Oppenheim RW, Milligan C (2013) Characterization of early pathogenesis in the SOD1(G93A) mouse model of ALS: part I, background and methods. Brain and behavior 3:335-350.

Voigt A, Herholz D, Fiesel FC, Kaur K, Muller D, Karsten P, Weber SS, Kahle PJ, Marquardt T, Schulz JB (2010) TDP-43-mediated neuron loss in vivo requires RNA-binding activity. PLoS One 5:e12247.

Volkening K, Leystra-Lantz C, Yang W, Jaffee H, Strong MJ (2009) Tar DNA binding protein of 43 kDa (TDP-43), 14-3-3 proteins and copper/zinc superoxide dismutase (SOD1) interact to modulate NFL mRNA stability. Implications for altered RNA processing in amyotrophic lateral sclerosis (ALS). Brain Res.

Vos MJ, Kanon B, Kampinga HH (2009) HSPB7 is a SC35 speckle resident small heat shock protein. Biochimica et biophysica acta 1793:1343-1353.

Wang HY, Wang IF, Bose J, Shen CK (2004) Structural diversity and functional implications of the eukaryotic TDP gene family. Genomics 83:130-139.

Wang IF, Reddy NM, Shen CK (2002) Higher order arrangement of the eukaryotic nuclear bodies. Proc Natl Acad Sci U S A 99:13583-13588.

Wang IF, Wu LS, Chang HY, Shen CK (2008) TDP-43, the signature protein of FTLD-U, is a neuronal activity-responsive factor. J Neurochem 105:797-806.

Wang X, Fan H, Ying Z, Li B, Wang H, Wang G (2009) Degradation of TDP-43 and its pathogenic form by autophagy and the ubiquitin-proteasome system. Neurosci Lett.

Watanabe S, Kaneko K, Yamanaka K (2013) Accelerated disease onset with stabilized familial amyotrophic lateral sclerosis (ALS)-linked mutant TDP-43 proteins. The Journal of biological chemistry 288:3641-3654.

Wegorzewska I, Baloh RH (2010) TDP-43-Based Animal Models of Neurodegeneration: New Insights into ALS Pathology and Pathophysiology. Neurodegener Dis.

Wegorzewska I, Bell S, Cairns NJ, Miller TM, Baloh RH (2009) TDP-43 mutant transgenic mice develop features of ALS and frontotemporal lobar degeneration. Proc Natl Acad Sci U S A.

Weighardt F, Cobianchi F, Cartegni L, Chiodi I, Villa A, Riva S, Biamonti G (1999) A novel hnRNP protein (HAP/SAF-B) enters a subset of hnRNP complexes and relocates in nuclear granules in response to heat shock. Journal of cell science 112 (Pt 10):1465-1476.

Wijesekera LC, Leigh PN (2009) Amyotrophic lateral sclerosis. Orphanet J Rare Dis 4:3.

Williams KL, Durnall JC, Thoeng AD, Warraich ST, Nicholson GA, Blair IP (2009) A novel TARDBP mutation in an Australian amyotrophic lateral sclerosis kindred. J Neurol Neurosurg Psychiatry 80:1286-1288.

Wils H, Kleinberger G, Janssens J, Pereson S, Joris G, Cuijt I, Smits V, Ceuterick-de Groote C, Van Broeckhoven C, Kumar-Singh S (2010) TDP-43 transgenic mice develop spastic paralysis and neuronal inclusions characteristic of ALS and frontotemporal lobar degeneration. Proc Natl Acad Sci U S A 107:3858-3863.

Wilson SM, Datar KV, Paddy MR, Swedlow JR, Swanson MS (1994) Characterization of nuclear polyadenylated RNA-binding proteins in Saccharomyces cerevisiae. The Journal of cell biology 127:1173-1184.

Winton MJ, Igaz LM, Wong MM, Kwong LK, Trojanowski JQ, Lee VM (2008a) Disturbance of nuclear and cytoplasmic TAR DNA-binding protein (TDP-43) induces disease-like redistribution, sequestration, and aggregate formation. J Biol Chem 283:13302-13309.

Winton MJ, Van Deerlin VM, Kwong LK, Yuan W, Wood EM, Yu CE, Schellenberg GD, Rademakers R, Caselli R, Karydas A, Trojanowski JQ, Miller BL, Lee VM (2008b) A90V TDP-43 variant results in the aberrant localization of TDP-43 in vitro. FEBS Lett 582:2252-2256.

Wolozin B (2012) Regulated protein aggregation: stress granules and neurodegeneration. Molecular neurodegeneration 7:56.

Wood H (2013) Neurodegenerative disease: C9orf72 RNA foci--a therapeutic target for ALS and FTD? Nature reviews Neurology 9:659.

Wood JD, Landers JA, Bingley M, McDermott CJ, Thomas-McArthur V, Gleadall LJ, Shaw PJ, Cunliffe VT (2006) The microtubule-severing protein Spastin is essential for axon outgrowth in the zebrafish embryo. Hum Mol Genet 15:2763-2771.

Woods IG, Wilson C, Friedlander B, Chang P, Reyes DK, Nix R, Kelly PD, Chu F, Postlethwait JH, Talbot WS (2005) The zebrafish gene map defines ancestral vertebrate chromosomes. Genome Res 15:1307-1314.

Wu D, Yu W, Kishikawa H, Folkerth RD, Iafrate AJ, Shen Y, Xin W, Sims K, Hu GF (2007) Angiogenin loss-of-function mutations in amyotrophic lateral sclerosis. Ann Neurol 62:609-617.

Wu LS, Cheng WC, Hou SC, Yan YT, Jiang ST, Shen CK TDP-43, a neuro-pathosignature factor, is essential for early mouse embryogenesis. Genesis 48:56-62.

Wu LS, Cheng WC, Hou SC, Yan YT, Jiang ST, Shen CK (2010) TDP-43, a neuro-pathosignature factor, is essential for early mouse embryogenesis. Genesis 48:56-62.

Wu LS, Cheng WC, Shen CK (2012) Targeted depletion of TDP-43 expression in the spinal cord motor neurons leads to the development of amyotrophic lateral sclerosis-like phenotypes in mice. J Biol Chem 287:27335-27344.

Wu LS, Cheng WC, Shen CK (2013) Similar dose-dependence of motor neuron cell death caused by wild type human TDP-43 and mutants with ALS-associated amino acid substitutions. Journal of biomedical science 20:33.

Xiao S, Tjostheim S, Sanelli T, McLean JR, Horne P, Fan Y, Ravits J, Strong MJ, Robertson J (2008) An aggregate-inducing peripherin isoform generated through intron retention is upregulated in amyotrophic lateral sclerosis and associated with disease pathology. J Neurosci 28:1833-1840.

Xiong HL, Wang JY, Sun YM, Wu JJ, Chen Y, Qiao K, Zheng QJ, Zhao GX, Wu ZY Association between novel TARDBP mutations and Chinese patients with amyotrophic lateral sclerosis. BMC Med Genet 11:8.

Xu YF, Gendron TF, Zhang YJ, Lin WL, D'Alton S, Sheng H, Casey MC, Tong J, Knight J, Yu X, Rademakers R, Boylan K, Hutton M, McGowan E, Dickson DW, Lewis J, Petrucelli L (2010) Wild-type human TDP-43 expression causes TDP-43 phosphorylation, mitochondrial aggregation, motor deficits, and early mortality in transgenic mice. J Neurosci 30:10851-10859.

Xu YF, Zhang YJ, Lin WL, Cao X, Stetler C, Dickson DW, Lewis J, Petrucelli L (2011) Expression of mutant TDP-43 induces neuronal dysfunction in transgenic mice. Mol Neurodegener 6:73.

Yamanaka K, Chun SJ, Boillee S, Fujimori-Tonou N, Yamashita H, Gutmann DH, Takahashi R, Misawa H, Cleveland DW (2008) Astrocytes as determinants of disease progression in inherited amyotrophic lateral sclerosis. Nat Neurosci 11:251-253.

Yamashita M, Nonaka T, Hirai S, Miwa A, Okado H, Arai T, Hosokawa M, Akiyama H, Hasegawa M (2014) Distinct pathways leading to TDP-43-induced cellular dysfunctions. Human molecular genetics.

Yang C, Tan W, Whittle C, Qiu L, Cao L, Akbarian S, Xu Z (2010) The C-terminal TDP-43 fragments have a high aggregation propensity and harm neurons by a dominant-negative mechanism. PLoS One 5:e15878.

Yokoseki A, Shiga A, Tan CF, Tagawa A, Kaneko H, Koyama A, Eguchi H, Tsujino A, Ikeuchi T, Kakita A, Okamoto K, Nishizawa M, Takahashi H, Onodera O (2008) TDP-43 mutation in familial amyotrophic lateral sclerosis. Ann Neurol 63:538-542.

Zeitlhofer J (1996) [Clinical aspects of amyotrophic lateral sclerosis]. Wien Med Wochenschr 146:182-185.

Zhang H, Xing L, Rossoll W, Wichterle H, Singer RH, Bassell GJ (2006) Multiprotein complexes of the survival of motor neuron protein SMN with Gemins traffic to neuronal processes and growth cones of motor neurons. J Neurosci 26:8622-8632.

Zhang T, Mullane PC, Periz G, Wang J (2011) TDP-43 neurotoxicity and protein aggregation modulated by heat shock factor and insulin/IGF-1 signaling. Hum Mol Genet 20:1952-1965.

Zhang YJ, Xu YF, Cook C, Gendron TF, Roettges P, Link CD, Lin WL, Tong J, Castanedes-Casey M, Ash P, Gass J, Rangachari V, Buratti E, Baralle F, Golde TE, Dickson DW, Petrucelli L (2009) Aberrant cleavage of TDP-43 enhances aggregation and cellular toxicity. Proc Natl Acad Sci U S A 106:7607-7612.

Zhang YJ, Xu YF, Dickey CA, Buratti E, Baralle F, Bailey R, Pickering-Brown S, Dickson D, Petrucelli L (2007) Progranulin mediates caspase-dependent cleavage of TAR DNA binding protein-43. J Neurosci 27:10530-10534.

Zhao ZH, Chen WZ, Wu ZY, Wang N, Zhao GX, Chen WJ, Murong SX (2009) A novel mutation in the senataxin gene identified in a Chinese patient with sporadic amyotrophic lateral sclerosis. Amyotroph Lateral Scler 10:118-122.

Zhou H, Huang C, Chen H, Wang D, Landel CP, Xia PY, Bowser R, Liu YJ, Xia XG (2010) Transgenic rat model of neurodegeneration caused by mutation in the TDP gene. PLoS Genet 6:e1000887.

Zhou Y, Liu S, Liu G, Ozturk A, Hicks GG (2013) ALS-associated FUS mutations result in compromised FUS alternative splicing and autoregulation. PLoS genetics 9:e1003895.

Zhu X, Perry G, Smith MA (2003) Amyotrophic lateral sclerosis: a novel hypothesis involving a gained 'loss of function' in the JNK/SAPK pathway. Redox Rep 8:129-133.